UNIVERSITY OF CRETE

DEPARTMENT OF PHYSICS

PhD THESIS

Radiation in Ultraplanckian particle collisions

Γιάννης Κωνσταντίνου

Advisor: *Prof.* Θεόδωρος Τομαράς - University of Crete

UNIVERSITY OF CRETE
DEPARTMENT OF PHYSICS

PhD THESIS

Doctor of Philosophy
of
- High energy Physics -

Defended by
ΓΙΑΝΝΗΣ ΚΩΝΣΤΑΝΤΙΝΟΥ

Radiation in ultraplanckian particle collisions

COMMITTEE

Prof.	Θεόδωρος Τομαράς	-	University of Crete
Assoc. Prof.	Αναστάσιος Πέτκου	-	Aristotle University of Thessaloniki
Prof.	Νικόλαος Τσάμης	-	University of Crete
Lecturer	Γεώργιος Κοφινάς	-	University of the Aegean
Assoc. Prof.	Νικόλαος Τούμπας	-	University of Cyprus
Prof.	Ηλίας Κυρίτσης	-	University of Crete
Assistant Prof.	Βασιλική Παυλίδου	-	University of Crete

Date of the defense:
23/10/2014

Περίληψη

Χρησιμοποιούμε μία διαραταχτική μέθοδο για να μελετήσουμε την κλασσική ακτινοβολία πέδησης ενός βαθμωτού πεδίου Φ και ενος διανυσματικού πεδίου που παράγεται κατά την υπερ-σχετικιστική σύγκρουση δύο σωματιδίων με μάζα που αλληλεπιδρούν βαρυτικά. Η σύγκρουση λαμβάνει χώρα σε d μη-συμπαγείς ή τοροειδείς επιπλέον διαστάσεις. Αναλύονται η φασματική και η γωνιακή κατανομή της βαθμωτής και διανυσματικής ακτινοβολίας, ενώ δείχνουμε ότι η ολική ενέργεια ενισχύεται ισχυρά κατά ένα παράγοντα Lorentz γ υψωμένο σε κάποια δύναμη εξαρτώμενη από τον αριθμό των επιπλέον διαστάσεων, d. Δείχνουμε επίσης ότι το τοπικό πλάτος της ακτινοβολίας συμβάλλει καταστροφικά (στις δύο πρώτες υπερ-σχετικιστικές τάξεις) με το μη-τοπικό πλάτος στην περιοχή συχνοτήτων $\gamma/b \lesssim \omega \lesssim \gamma^2/b$, σε όλες τις διαστάσεις.

Η ίδια σκέδαση μελετάται για σωματίδια χωρίς μάζα, προωθημένα στην ταχύτητα του φωτός, σε τέσσερεις επίπεδες διαστάσεις, χρησιμοποιώντας την ίδια ουσιαστικά μέθοδο. Υπολογίζονται οι διορθώσεις στον τανυστή ενέργειας - ορμής και στη μετρική σε κλειστή μορφή. Οι διορθώσεις συμπεριλαβάνουν την ανάδραση της μετρικής κατόπιν της σύγκρουσης. Η συμπερίληψη αυτών των διορθώσεων υπονοεί ότι ο τανυστής ενέργειας - ορμής των συγκρουόμενων σωματιδίων έχει μηδενικό ίχνος πριν και μετά τη σύγκρουση. Τονίζεται η ανάγκη για την εισαγωγή μίας παραμέτρου σύγκρουσης b, ενώ φαίνεται ότι η διαταρακτική προσέγγιση δε λειτουργεί όταν $b = 0$. Επιπλέον συζητάμε την ακτινοβολούμενη ενέργεια υπό μορφή βαρυτικής ακτινοβολίας πέδησης, ενώ μελετάται ένα παράδειγμα σύγκρουσης βαρυτικών κυμάτων.

Abstract

We employ a perturbative scheme to study classical bremsstrahlung of a massless scalar field Φ and a massless vector field in gravity mediated ultra-relativistic collisions with impact parameter b of two massive point particles in the presence of d non-compact or toroidal extra dimensions. The spectral and angular distribution of the scalar and vector radiation are analyzed, while the total radiated energy is found to be *strongly enhanced* by a $d-$dependent power of the Lorentz factor γ. The local radiation amplitude from the accelerated particles is shown to *interfere destructively* (in the first two leading ultra-relativistic orders) with the non-local amplitude in the frequency regime $\gamma/b \lesssim \omega \lesssim \gamma^2/b$ in all dimensions.

The same collision is studied for massless particles boosted to the speed of light in flat four-dimensions using essentially the same perturbative scheme. The corrections to the energy momentum tensor and to the metric are computed to second order and closed form formulas are provided. This includes the back-reaction on the metric after the collision. Including such corrections suggests that the tracelessness of the initial stress tensors of the colliding particles is preserved during and after the collision. The necessity for introducing an impact parameter in the perturbative treatment is highlighted and the breaking of the underlying perturbative approach at $b = 0$ is motivated. In addition, the energy radiated in the form of gravitational bremsstrahlung radiation is discussed while an example from gravitational-waves collision is being studied.

Acknowledgements

I would like to thank my advisor Professor Theodore Tomaras for his guidance throughout my PhD studies. I am also grateful to my collaborators Pavel Spirin and Anastasios Taliotis from which I have learned a lot. Not only did we have an excellent collaboration, but both of them essentially advised me during parts of my thesis. Pavel Spirin has also carefully read my entire thesis and has given me insightful comments. This thesis could not have been completed without his help. I would also like to thank my collaborators Professor Dmitry Gal'tsov and Georgios Kofinas. I am indebted to the faculty members of the Univeristy of Crete. I want to thank my friends at the physics department and especially Ioannis Iatrakis and Christina Psaroudaki, for the fruitful discussions and for their support. Finally I would like to thank my friends and family for their support during all these years.

This work was funded by a scholarship from IKY from October 2010 until October 2013.

Contents

1 Introduction

The General Theory of Relativity was postulated in 1915 by Albert Einstein to explain gravitation. It generalizes the Special Theory of Relativity and Newton's Universal Gravitation law. The Minkowskian metric of Special Relativity becomes a dynamic object. It is no longer flat but becomes curved by energy and matter. Objects move along the geodesics in this curved spacetime, instead of flat spacetime, giving us the illusion that a force is deflecting them from their trajectory.

Since its postulation the theory has accounted for the anomalous precession of the perihelion of Mercury. The eclipse expedition in 1919 led by Arthur Eddington confirmed the deflection of light by the Sun. The gravitational redshift of light was measured in an ingenious experiment by Pound and Rebka in 1959 using the Mössbauer effect. These are the so called classical tests of the General Theory of Relativity.

Modern tests include the measurement of the Shapiro delay. Radar reflections from Mercury and Venus before and after they are eclipsed by the Sun agree with General Relativity. Gravitational lensing has also been one of the modern tests of General Relativity, especially from distant radio sources being lensed by the Sun.

Another prediction of General Relativity that has been confirmed is the existence of Gravitational waves. To date these waves have not been measured directly, however observations of the Hulse-Taylor binary show that the system is losing energy due to gravitational radiation. The amount of energy lost is in agreement with what is predicted by General Relativity.

The years after the appearance of the General Theory of Relativity were marked by attempts to develop a classical unified theory. Such theories would unify classical gravitation and classical electromagnetism. Two of the most important approaches to a classical unified theory were Weyl's gauge theory and Eddington's affine geometry. Of particular interest is Kaluza's extra-dimensional theory.

One of the most intriguing ideas that were postulated in the 20th Century is the existence of extra space dimensions. The idea of theories with extra spatial dimensions was first proposed in 1921 by Theodor Kaluza [2] and refined later by Oskar Klein [3]. The advantage this brought was that it unified the General Theory of Relativity with Maxwell electromagnetism. Though the unification of these two theories was made possible as we will see below, the theory, as postulated by Kaluza and Klein, has several drawbacks and is no longer considered to be of particular interest.

The theory of extra spatial dimensions was revived with the revolution of String theory. The quantum theory of relativistic strings requires the existence of extra spatial dimensions in order to be mathematically consistent [4]. The idea was that these theories would be compactified at the Planck scale, implying that they would not be detectable by any of the current accelerators. In fact they would only be detected by accelerators working at, or near, the Planck scale, something that is far from our reach at the moment.

In 1998, Arkani-Hamed, Dimopoulos and Dvali, proposed the so called ADD model [9]. The model was built so as to solve the hierarchy problem without using supersymmetry ot technicolor. The idea, as we will see in detail, required the existence of large extra dimensions (at the order of a milimeter). The standard model particles are localized on a 3-brane, while gravity would propagate in all dimensions. The weakness of gravity would then be explained by the "dilution" of gravity in the extra-dimensional volume. This theory later received a UV completion by being embdedded in string theory [10].

Another solution to the hierarchy problem was proposed in [13]. In this model the geometry of spacetime is warped. A five-dimensional Anti-de Sitter metric is used. The hierarchy is generated by the gravitational warp factor in the metric. Several other similar models have emerged.

Finally the Universal Extra Dimensions (UED) model allows for some or all the Standard Model (SM) gauge fields to propagate in the extra dimensions. We will see an explicit example of the minimal UED model.

Extra-dimensional models, are not only able to solve the hierarchy problem, but they can also provide a mechanism for generating the hierarchies of the fermion masses [5]. They could also provide a mechanism for the unification of the gauge couplings [6], as well as a way to break supersymmetry [7].

The above extra-dimensional models share a common characteristic, the existence of an increased Planck length, $\lambda_{\rm Pl}$. We will discuss how this length arises in each of the models in the section that follows. If the Planck scale is of the order of 1TeV, the regime of quantum gravity will be accessible to the LHC, which will have centre of mass energy 14TeV. In the next section we also discuss the bounds for each of these models.

1.1 Extra dimensions

1.1.1 Kaluza's Theory

The idea of the existence of extra dimensions, was first seriously proposed by Kaluza [2]. His theory naturally unified Einsteinian Gravity with Maxwell's electromagnetic theory. Kaluza assumed a five-dimensional universe. The metric is then expressed as:

$$d\hat{s}^2 = \hat{g}_{MN}(x^\mu, y)\, dx^M dx^N \,, \tag{1.1.1}$$

where capital indices run from $M = 0, ..., 4$, Greek indices are four-dimensional and run from $\mu = 0, ..., 3$ and y is the extra-dimensional space coordinate. The five-dimensional metric, $\hat{g}_{MN}$ is broken into the following:

$$\hat{g}_{MN} = \begin{pmatrix} g_{\mu\nu} & g_{\mu 4} \\ g_{4\nu} & g_{44} \end{pmatrix} ,$$

where $g_{\mu\nu}$ is the usual, four-dimensional, metric.

Kaluza also assumed the so called cylindrical condition, i.e. that the derivatives of state quantities with respect to the fourth spatial dimension are zero, or at least very small, and thus it is not observed. The Christoffel symbols of the five-dimensional metric are defined as usual,

$$\Gamma_{LMN} = \frac{1}{2}\left(g_{LM,N} + g_{LN,M} - g_{MN,L}\right) .$$

The next step is to write the $g_{4\mu}$ component of the metric as a vector field, A_μ and the g_{44} component as scalar field, ϕ, suggesting what will follow,

$$g_{4\mu} = 2\alpha A_\mu \qquad , \qquad g_{44} = 2\phi \,,$$

the Christoffel symbols now take the form

$$\begin{aligned}\Gamma_{\mu\nu 4} &= \alpha\left(A_{\mu,\nu} - A_{\nu,\mu}\right) = \alpha F_{\mu\nu} \\ \Gamma_{4\mu\nu} &= \alpha\left(A_{\mu,\nu} + A_{\nu,\mu}\right) \\ \Gamma_{44\nu} &= \phi_{,\nu} \,.\end{aligned}$$

The weak field approximation, ie that the metric $\hat{g}_{MN}$ is the five-dimensional Minkowski metric perturbed by a small term, is assumed

$$\hat{g}_{MN} = \eta_{MN} + \hat{h}_{MN}, \tag{1.1.2}$$

where $\hat{h}_{MN} \ll 1$. The Riemann curvature tensor is defined as

$$R^R_{SMN} = \Gamma^R_{NS,M} - \Gamma^R_{MS,N} + \Gamma^R_{ML}\Gamma^L_{NS} - \Gamma^R_{NL}\Gamma^L_{MS} \,,$$

while the Ricci tensor is defined by

$$R_{SN} = R^R_{SRN} \,.$$

In order to produce the field equations the energy momentum tensor is required. In the weak field approximation it reads

$$\hat{T}^{MN} = \hat{\mu}_0 u^{\hat{M}} u^{\hat{N}} \,,$$

we have symbolized the rest mass density with $\hat{\mu}_0$ and the five-velocity as $u^{\hat{M}}$.

We now focus on the field equations, the first, corresponding to four-dimensional gravity will be

$$R_{\mu\nu} = \kappa\left(T_{\mu\nu} - \frac{1}{2}g_{\mu\nu}T\right) \,, \tag{1.1.3}$$

which is identified as the four-dimensional field equation of General Relativity.

On the other hand the following equation corresponds to the electromagnetic field equation

$$-\alpha\partial^\mu F_{\mu\nu} = \mu_0 u_4 u_\nu \,, \tag{1.1.4}$$

where u_4 is the component of the five velocity in the extra dimension and u_ν is the four-velocity. Equation (1.1.4) is identified with Maxwell's equation ie

$$\partial^\mu F_{\mu\nu} = J_\nu = \rho_0 v_\nu \,,$$

and thus receives the following interpretation

$$\rho_0 v_\nu = \frac{\kappa}{\alpha}\mu_0 u_4 u_\nu \,.$$

The electric charge is interpreted as the fifth component of the stress-energy tensor of matter. To do this, one sets $u_\mu \approx v_\mu$ (this is true for small velocities) and defines $\kappa = 2\alpha^2$, thus getting the following

$$\frac{\rho_0}{\mu_0} = 2\alpha u_4 \,,$$

which makes this interpretation apparent.

As we have seen, by simply writing down Einstein's equation's in five dimensions, Kaluza recovered regular four-dimensional General Relativity, Maxwell's electromagnetism and a constant scalar field. This is the reason that extra dimensions seemed so attractive, at least in the beginning.

However, along with the simplicity and elegance of this theory, several problems appeared. (i) Nobody had seen (and has not to date seen) a fifth dimension and the elegance alone is not sufficient to justify the lack of any experimental data, (ii) The cylindrical condition could not be justified in any way, (iii) Although the theory has no problem for macroscopic charged bodies, it does have one for charged elementary particles; the ratio ρ_0/μ_0 is not small and thus neither is u_4. This puts into question whether the theory could be valid for elementary particles.

1.1.2 Klein's Modification

Klein gave a natural explanation for the fact that the fifth dimension is not observed. He proposed that the fifth dimension is compactified and has a circular topology; its coordinate, y, satisfies $y = y + 2\pi R_c$. This space-time is a product of a four-dimensional Minkowski space $M_{1,3}$ and a one-dimensional circle S_1 with radius R_c. If the radius of the circle is sufficiently small, then the extra dimension will not be observable in low energy experiments. Following Kaluza's work, Klein then assumed that g_{44} is constant and identified the other components as:

$$\hat{g}_{44} = \phi \qquad , \qquad \hat{g}_{4\mu} = \varkappa\phi A_\mu \qquad , \qquad \hat{g}_{\mu\nu} = g_{\mu\nu} + \varkappa^2 \phi A_\mu A_\nu \,.$$

This ansatz is then replaced into the five-dimensional metric of (1.1.1), yielding:

$$\hat{g}_{MN} = \phi^{-1/3} \begin{pmatrix} g_{\mu\nu} + \varkappa^2\phi A_\mu A_\nu & \varkappa\phi A_\mu \\ \varkappa\phi A_\nu & \phi \end{pmatrix} . \qquad (1.1.5)$$

We now notice that the scalar field ϕ appears only as a scale parameter in the extra dimension, this is referred to as *the dilaton field*. The metric, $g_{\mu\nu}(x)$ will transform as a tensor under four-dimensional general coordinate transformations, $A_\mu(x)$ as a vector, while ϕ will transform as a scalar.

The five-dimensional Einstein-Hilbert action reads

$$\hat{S} = \frac{1}{2\varkappa_5^2}\int d^5\hat{x}\sqrt{-\hat{g}}\hat{R} \tag{1.1.6}$$

$\varkappa_5$ is the five-dimensional Newton's constant.

This action is invariant under five-dimensional general coordinate transformations;

$$\delta\hat{g}_{MN} = \partial_M\hat{\xi}^R\hat{g}_{RN} + \partial_N\hat{\xi}^R\hat{g}_{RM} + \hat{\xi}^R\partial_R\hat{g}_{MN}\,.$$

Before varying the action to get the field equations, one writes the fields as a Fourier series, since they are periodic in the y coordinate:

$$\begin{aligned} g_{\mu\nu}(x,y) &= \sum_{n=-\infty}^{\infty} g_{\mu\nu n}(x)e^{in\cdot y/R_c} \\ A_\mu(x,y) &= \sum_{n=-\infty}^{\infty} A_{\mu n}(x)e^{in\cdot y/R_c} \\ \phi_(x,y) &= \sum_{n=-\infty}^{\infty} \phi_n(x)e^{in\cdot y/R_c} \end{aligned} \tag{1.1.7}$$

We can now see that the action of (1.1.6) describes a theory with an infinite tower of four-dimensional fields. Also, since the action is invariant under five-dimensional general coordinate transformations and the general coordinate parameter can also be expanded as a Fourier series,

$$\hat{\xi}^M(x,y) = \sum_{n=-\infty}^{n=\infty} \hat{\xi}^M(x)e^{in\cdot y/R_c}\,,$$

the four-dimensional fields will satisfy an infinite number of symmetries.

Variation of the action gives the following equations of motion

$$\begin{aligned} (\Box - \partial^y\partial_y)\, g_{\mu\nu}(x,y) &= \left(\Box + \frac{n^2}{R_c^2}\right) g_{\mu\nu n}\,(x) = 0 \\ (\Box - \partial^y\partial_y)\, A_\mu(x,y) &= \left(\Box + \frac{n^2}{R_c^2}\right) A_{\mu n}\,(x) = 0 \\ (\Box - \partial^y\partial_y)\, \phi(x,y) &= \left(\Box + \frac{n^2}{R_c^2}\right) \phi_n\,(x) = 0 \end{aligned}$$

The metric used is a 5×5 symmetric tensor, giving it 15 degrees of freedom. General covariance imposes an additional 5 gauge fixing conditions, thus reducing the number of degrees of freedom to 10. Gauge transformations also impose 5 gauge fixing conditions, reducing the number of degrees of freedom to its final value, 5.

We now proceed to study the properties of the above fields, starting with the *zero modes*, ie the modes with $n = 0$. We expect these to describe the graviton, photon and dilaton as in the Kaluza theory. Substituting the expanded fields (1.1.7) and the metric (1.1.5) in the five-dimensional action (1.1.6) , one obtains the following reduced action

$$S = \frac{1}{2\varkappa^2} \int d^4x \sqrt{-g} \left(R - \frac{1}{4} \phi^{-1} F_{\mu\nu 0} F_0^{\mu\nu} - \frac{1}{2} \partial_\mu \phi_0 \partial^\mu \phi_0 \right) , \tag{1.1.8}$$

where $\varkappa^2 = \frac{\varkappa_5^2}{2\pi R_c}$. This action is again invariant under general coordinate transformations, were now one should use the zero mode of the coordinate parameter, ξ_0^μ,

$$\begin{aligned} \delta g_{\mu\nu 0} &= \partial_\mu \xi_0^\rho g_{\rho\nu 0} + \partial_\nu \xi_0^\rho g_{\mu\rho 0} + \xi_0^\rho \partial_\rho g_{\mu\nu 0} \\ \delta A_{\mu 0} &= \partial_\mu \xi_0^\rho A_{\rho 0} + \xi_0^\rho \partial_\rho A_{\mu 0} \\ \delta \phi_0 &= \xi_0^\rho \partial_\rho \phi_0 \,. \end{aligned}$$

It is also invariant under the local gauge transformation with parameter ξ_0^4

$$\delta A_{\mu 0} = \partial_\mu \xi_0^4 \,,$$

while it is also globally scale invariant under the transformation

$$\delta A_{\mu 0} = \lambda A_{\mu 0}, \qquad \delta \phi_0 = -\frac{2}{\sqrt{3}} \lambda \,.$$

These fields can be quantized in the normal quantum field theory manner, with vacuum expectation values,

$$\langle g_{\mu\nu} \rangle = \eta_{\mu\nu}, \quad \langle A_\mu \rangle = 0, \quad \langle \phi \rangle = \phi_0 \,. \tag{1.1.9}$$

Thus we see that the vacuum respects the symmetry of the four-dimensional Poincare group $\times \mathcal{R}$. The gravitational field will be massless because of general covariance, the electromagnetic field is massless because of gauge invariance, while the dilaton field is massless since it is the Goldstone boson that appears due to the spontaneous breaking of the global scale invariance. The gauge group $\mathcal{R}$ comes from the $U(1)$ invariance that existed, however the zero modes are not dependent on the fifth dimension.

Before proceeding to the non-zero modes, we note that the four-dimensional massless graviton has two degrees of freedom, as well as the four-dimensional gauge boson, while the real scalar field has one degree, summing up to five degrees of freedom as expected.

We now proceed to consider the non zero-modes. We start by noting that that these modes are no longer globally scale invariant, as this is prohibited by the periodic condition on y. In fact these modes are symmetric to a set of infinite parameter local transformations corresponding to a global algebra with generators

$$P_n^\mu = e^{iny/R_c}\partial^\mu. \qquad M_n^{\mu\nu} = e^{iny/R_c}\left(x^\mu\partial^\nu - x^\nu\partial^\mu\right), \qquad Q_n = ie^{iny/R_c}R_c\partial_y\,.$$

The full, four-dimensional theory obeys this symmetry, however the vacuum of equation (1.1.9), is only symmetric under the Poincare group $\times U(1)$. So the gauge parameters ξ_n^μ and ξ_n^4 are spontaneously broken generators and thus, the non-zero modes, $A_{\mu n}$ and ϕ_n are Goldstone bosons. The two degrees of freedom of each of the Goldstone bosons $A_{\mu n}$ and the one degree of freedom of each of ϕ_n fields will be "eaten" by the fields $g_{\mu\nu n}$, giving it mass. So the $g_{\mu\nu n}$ fields will describe massive spin-2 particles with 5 degrees of freedom [8]. An infinite tower of such particles shall exist with mass, m_n, and charge, q_n, given by:

$$q_n = \sqrt{2}\frac{\varkappa}{R_c}n, \quad m_n = \frac{|n|}{R_c} \tag{1.1.10}$$

To conclude, the Kaluza-Klein theory, once reduced to four dimensions, describes Einstein's Gravity, Maxwell's electromagnetism and an infinite tower of massive, spin-2, charged particles. These will be invisible unless we have enough energy to probe them, so they will be essentially invisible to us. This theory, despite its drawbacks, unifies electromagnetism and gravity and explains the quantization of charge. However as pioneering as this might have been, the model is no longer considered as a viable option. We will be more interested in generalizations of these models.

We will explore some of the most notable extra-dimensional models that are the most interesting for us. Namely the so called ADD model, the Randall-Sundrum model and the Universal Extra Dimensional (UED) model.

1.1.3 ADD model

The ADD model was proposed by Arkani-Hamed, Dimopoulos and Dvali [9] as a way to solve the hierarchy problem. Later on it was embedded in string theory [10], thus giving it a UV completion. This model incorporates both gravity and the Standard Model.

The model assumes a space-time described by $M_{1,3} \times T^d$ for $d \geq 2$. T^d is a d-dimensional compact manifold with volume $V_d \sim R_c^d$. The full, $(4+d)$-dimensional Planck scale is of the same order as the electroweak scale which is the only scale in the theory. The gravitational field propagates in all dimensions, while the fields of the SM are localized on the manifold $M_{3,1}$. This manifold has thickness of m_{EW}^{-1} in the extra dimensions.

The action describing this theory is given by

$$S_{4+d} = -\frac{M^{2+d}_{\text{Pl}(4+d)}}{2(2\pi)^d} \int d^{4+d}x\sqrt{-g}R + \int d^4x\sqrt{-g_{\text{ind}}}\mathcal{L}_{\text{SM}} \tag{1.1.11}$$

where $M_{\text{Pl}(4+d)}$ is the $4+d$-dimensional Planck scale, g_{ind} is the induced metric on the 3-brane where the standard model particles propagate, while $\mathcal{L}$ is the four-dimensional Standard Model Lagrangian. Once the Kaluza-Klein reduction to four dimensions is performed one sees that the zero modes become the massless graviton, d massless $U(1)$ gauge bosons and $d(d+1)/2$ massless scalars. The Kaluza-Klein modes give a tower of massive spin-2 particles, $d-1$ towers of massive spin-1 particles and $d(d-1)/2$ massive spin-0 particles [11]. At low energies, the massive modes will not be excited and thus the action reduces to

$$S_4 = -\frac{M^{2+d}_{\text{Pl}(4+d)}V_d}{2(2\pi)^d} \int d^{4+d}x\sqrt{-g}R + \int d^4x\sqrt{-g_{\text{ind}}}\mathcal{L}_{\text{SM}}\,. \tag{1.1.12}$$

From the above action, one can identify the effective, four-dimensional Planck mass M_{Pl} to be

$$M^2_{\text{Pl}} \sim M^{2+d}_{\text{Pl}(4+d)}R^d_c\,. \tag{1.1.13}$$

The same result can be obtained by assuming two test masses m_1 and m_2, at as small distance between them compared to the radius of the extra dimensions ($r \ll R_c$). The gravitational potential in $(4+d)$ dimensions is given by

$$V(r) \sim \frac{m_1 m_2}{M^{d+2}_{\text{Pl}(4+d)}}\frac{1}{r^{d+1}}\,.$$

However if the distance between the masses is much bigger than the radius of the extra dimensions ($r \gg R_c$), the extra dimensions will no longer be visible and one obtains the usual gravitational potential, with an effective Planck mass:

$$V(r) \sim \frac{m_1 m_2}{M^{d+2}_{\text{Pl}(4+d)}R^d_c}\frac{1}{r}\,.$$

Setting the actual Planck mass, $M_{\text{Pl}(4+d)}$, to be of the order of the electroweak scale m_{EW}, and demanding that the effective Planck mass is the observed value $M_{\text{Pl}} \sim 10^{19}$Gev, one obtains the value of R_c. The $d=1$ scenario is excluded, since then $R_c \sim 10^{13}$cm. This gives deviations from Newton's law within the solar system that have not been measured. However the cases where $d \geq 2$, cannot be ruled out by the current experimental data. In fact the $d=2$ scenario predicts a radius of milimeter scale.

So this model could potentially account for the hierarchy problem. Gravity is essentially diluted in the extra dimensions, while the SM field only live in the 4 dimensions, explaining the apparent difference between their scales. However, although one does explain for the apparent difference between the observed Planck scale and electroweak scale, a new problem arises. The problem of stabilizing the radius of the extra dimension. The size of the extra dimension cannot be explained. Experimental bounds on the radius of the extra dimensions can be seen in [12].

1.1.4 Warped Extra Dimensions models

A similar approach is that of the warped extra dimensions models. We will briefly describe the Randall-Sundrum model [13]. This model assumes a five-dimensional space-time, $M_{1,3} \times S^1/\mathbb{Z}_2$, where the fifth dimension is compactified on a circle, while one also imposes the symmetry $y \to -y$. Thus one is limited to only a part of the fifth dimension $y \in [0, \pi R_c]$. A cosmological constant Λ is also assumed in the bulk and on the two boundaries, Λ_0 for $y = 0$ and $\Lambda_{\pi R_c}$ for $y = \pi R_c$. The action reads

$$S_5 = -\int d^5x \left[\sqrt{-g}\frac{M^3_{\text{Pl}(5)}}{2}R + \Lambda + \sqrt{-g_0}\delta(y)\Lambda_0 + \sqrt{-g_{\pi R_c}}\delta(y-\pi R)\Lambda_{\pi R_c} \right] , \qquad (1.1.14)$$

where g_0 and $g_{\pi R_c}$ are the induced metrics on the two branes at $y = 0$ and $y = \pi R_c$ respectively. The metric reads

$$ds^2 = a(y)^2 dx^\mu dx^\nu \eta_{\mu\nu} + dy^2 \, , \quad a(y) = e^{-ky} \, ,$$

where $k = \sqrt{-\Lambda/6M^3_{\text{Pl}(5)}}$ and $a(y)$ is the so called warp factor which defines how the scales vary on the four-dimensional branes. So we see that the energies will scale with a factor of $e^{-k\pi R_c}$ on the brane at $y = \pi R_c$, with respect to the brane at $y = 0$. The brane at $y = 0$ is referred to as the infrared brane, while the brane $y = \pi R_c$ is referred to as the ultraviolet brane. We also note that $\Lambda_0 = -\Lambda_{\pi R_c} = -\Lambda/k$.

Once the four-dimensional KK reduction of the five-dimensional fields is performed, the apparent, four-dimensional Planck mass M_{Pl} ia given by

$$M^2_{\text{Pl}} = \int_0^{\pi R_c} dy e^{2ky} M^3_{\text{Pl}(5)} = \frac{M^3_{\text{Pl}(5)}}{2k} \left(1 - e^{-2k\pi R_c}\right) \qquad (1.1.15)$$

As in the ADD model, one can take $M_{\text{Pl}} \sim m_{\text{EW}}$ and for proper values of R_c and k obtain the apparent M_{Pl} to be at the observed value. We note here that while there was no (natural) mechanism to stabilize the radius in the ADD case, mechanisms have been proposed for the Randall-Sundrum model [15; 16].

The standard model fields will be localized on the IR-boundary. Another model has been proposed, where $R_c \to \infty$. This model is named Randall - Sundrum II [14]. The Planck mass, remains finite in this model. Also models where the Standard Model fields are all free to propagate in the bulk, with the exception of the Higgs boson [17; 18; 19].

1.1.5 Universal Extra Dimensions models

We finally turn to the Universal Extra Dimensions (UED) models [20; 21; 22; 23]. The main characteristic of these models is that some, or all, the standard model fields can propagate through the bulk, along with gravity. We will review the simplest UED model, namely the Minimal Universal Extra Dimensions (MUED)[20].

The space-time this model lives in is $M_{1,3} \times S_1/\mathbb{Z}_2$. Both the SM fields and gravity are free to propagate in all 5 dimensions. The symmetry of identifying two opposite points on the S_1 circle, $y = 0$ and $y = \pi R_c$ is imposed. This implies that the fields should be either even, or odd. Even fields will obey Neumann boundary conditions at the points $y = 0$ and $y = \pi R_c$, while odd fields will obey Dirichlet boundary conditions.

The fields are decomposed as

$$\begin{aligned}
A_\mu(x,y) &= \frac{1}{\sqrt{\pi R_c}}\left[A_{\mu 0}(x) + \sqrt{2}\sum_{n=1}^{\infty} A_{\mu n}(x)\cos\left(\frac{ny}{R_c}\right)\right] \\
A_4(x,y) &= \sqrt{\frac{2}{\pi R_c}}\sum_{n=1}^{\infty} A_{4\,0}(x)\sin\left(\frac{ny}{R_c}\right) \\
\psi_R^+(x,y) &= \frac{1}{\sqrt{2\pi R_c}}\psi_{R0} + \frac{1}{\sqrt{\pi R_c}}\sum_{n=1}^{\infty}\psi_{Rn}\cos\left(\frac{ny}{R_c}\right) \\
\psi_R^-(x,y) &= \frac{1}{\sqrt{\pi R_c}}\sum_{n=1}^{\infty}\psi_{Ln}\sin\left(\frac{ny}{R_c}\right) .
\end{aligned}$$

The zero modes of the even vector fields, will be identified with the gauge bosons of the Standard Model, while the zero modes of the right-handed fermions will be identified with the $SU(2)_W$ singlet of the SM. The $\psi_{Rn}(x)$ and $\psi_{Ln}(x)$ will combine to give a tower of KK Dirac fermions with mass $\frac{n}{R_c}$. The same will happen with the Left handed states, where the zero mode will be identified with the $SU(2)_W$-doublet. In this manner, the entire content of the SM is reproduced.

As mentioned above, this is only the minimal model, with one extra dimension. Phenomenological bounds for this model, as well as other UED models, appear here [12; 20].

This concludes our discussion of extra-dimensional models. All these models have had a common characteristic of decreased Planck mass, as low as $M_{\mathrm{Pl}} \sim$ TeV. If one of these models is in the correct direction, ultraplanckian energies will be accessible to the LHC and future colliders, thus giving experimental data on how gravity behaves at scales above the Planck scale.

1.2 Black Hole production and KK bremsstrahlung.

Large extra dimensions models that have gravity at the TeV scale are within grasp of the LHC and are thus being investigated. According to these models, gravity will be the dominant force at such energies. As will be discussed later, gravity will be classical. We are thus able to make predictions without computing in quantum gravity. One of the most interesting predictions of theories with Large extra dimensions is the possibility of black hole production in colliders [33].

This thesis is devoted to the study of bremsstrahlung radiation emitted during the collisions of ultrarelativistic particles. The estimation of the bremsstrahlung has attracted the attention of several papers. In a series of papers, D'Eath and Payne [36], have proposed the colliding waves model (CWM). In this model the gravitational field of the colliding particles, before the collision, is represented by two Aichelburg-Sexl [41] shockwaves. In their setup, the impact parameter is zero. They find a closed trapped surface and the radiation is estimated as the difference between the initial energy and the mass of the emerging black hole. This method has been generalized to extra dimensions and non-zero impact parameters (the maximal impact parameter studied in these papers is $b_{\max} = 3.219GE$) [37; 38]. However, this method does not take into account the back-reaction effects. Also the assumption that the two particles are described as colliding waves implies that the radiation is negligible, while the difference between the Black hole mass and the initial energy, identified as gravitational radiation, is of the order of the initial energy.

The same problem was studied in $D = 4$ by Amati, Ciafaloni and Veneziano in a series of papers [27; 28; 29]. They considered the collision of two strings in ultraplanck-lian energy. They use quantum string theory to study the problem of ultraplanckian collisions for massless particles.

On the other hand, bremsstrahlung itself represents the natural process to test the existence of extra dimensions and probe them. Colliding ultrarelativistic particles will radiate and the number of dimensions can easily be determined by the dependence of the radiated energy from the Lorentz factor $\gamma \gg 1$ of collision.

The drawbacks mentioned above, make another approach to the computation of bremsstrahlung desirable. Also, the regime where the impact parameter is larger than the Schwarzschild radius still remains unexplored. In this thesis, we will be using a different technique to compute the radiation, applicable to different values of the impact parameter.

1.3 Classicality of Gravity in transplanckian collisions

In order to begin our study of the behaviour of ultraplanckian gravity, we should define the relevant constants. By dimensional analysis, we relate the $4+d$-dimensional Newton's constant, G_{4+d}, to the $4+d$-dimensional Planck mass, $M_{\mathrm{Pl}(4+d)}$, restoring for this section the dependence on c and $\hbar$.

$$G_{4+d} = \frac{\hbar^{d+1}}{M_{\mathrm{Pl}(4+d)}^{d+2} c^{d-1}} \,. \tag{1.3.1}$$

Similarly we construct the $4+d$-dimensional Placnk length, $\lambda_{\mathrm{Pl}(4+d)}$,

$$\lambda_{\mathrm{Pl}(4+d)} = \left(\frac{\hbar G_{4+d}}{c^3}\right)^{\frac{1}{d+2}} \,. \tag{1.3.2}$$

Also the de Broglie wavelength λ_B associated with the colliding particles is

$$\lambda_B = \frac{\hbar c}{\sqrt{s}} \,. \tag{1.3.3}$$

It will also be useful to compute the Schwarzschild radius, r_S, of the given system [24] in $4+d$ dimensions

$$r_S = \frac{1}{\sqrt{\pi}} \left[\frac{8\Gamma\left(\frac{d+3}{2}\right)}{d+2}\right]^{\frac{1}{d+1}} \left(\frac{G_{4+d}\sqrt{s}}{c^4}\right)^{\frac{1}{d+1}} \,. \tag{1.3.4}$$

At this length scale, curvature effects become significant. If we know take the formal *classical limit*, $\hbar \to 0$, keeping G_{4+d} and $\sqrt{s}$ fixed, we obtain $M_{\mathrm{Pl}(4+d)} \to 0$. This shows us that at energies much higher than the Planck scale, we obtain the formal *classical limit*. We also see that at this limit, the Schwarzschild radius remains finite. The Planck length, as well as the de Broglie wavelength vanish. So we conclude that in transplanckian energies, classical mechanics will be applicable in the following regime,

$$\sqrt{s} \gg M_{\mathrm{Pl}(4+d)} \qquad r_s \gg \lambda_{\mathrm{Pl}(4+d)} \gg \lambda_b \,. \tag{1.3.5}$$

In a collision with impact parameter, b, we can see by dimensional analysis that the scattering angle θ, will be of order $\theta \sim G_{4+d}\sqrt{s}/b^{d+1}$. So we see that the quantum gravitational effects will not be important at high energies, so long as the impact parameter is large enough.

The fact of the classicality of ultraplanckian gravity has been discussed in several papers. It was first proposed by 't Hooft [25] approximated the field of the moving particle by a shockwave, obtaining a result similar to the Veneziano amplitude. It has also been shown that if the eikonal approximation is used in either string theory [27; 28; 29], or four-dimensional gravity [26], 't Hooft's result is reproduced. The classicality of gravity is also discussed in these papers [30; 31; 32].

1.4 Computational scheme

In order to study the collision and thus the bremsstrahlung, we will be employing a perturbative scheme within classical General Relativity. In chapters 2 and 3 we will be studying the collision of two massive particles, with masses m and m', one of which is charged. Since only one particle is charged, the interaction among the two particles is purely gravitational, this will be essential in the study of this collision. The computation scheme used, is based on the following.

To zeroth order, we assume a flat spacetime where the two particles are free. We will be working in the Lorentz frame where the charged particle is stationary, while the second particle is performing uniform linear motion towards it with some impact parameter b. We write down the trajectories of the two particles and assume the absence of any other fields. We compute the zeroth order energy - momentum tensors, $T_{\mu\nu}$ and $T'_{\mu\nu}$ of the two particles respectively.

Proceeding to the first order, we use the zeroth order energy - momentum tensors of the particles to compute the first order correction to the metric they produce $h_{\mu\nu}$ and $h'_{\mu\nu}$ respectively. Each of the two particles is now moving within the metric produced by the other. We write down the equations of motion for the two particles and compute their first order trajectories. We also write down the first order equation for the scalar or vector field.

Finally, to second order, we compute the second order correction to the scalar or vector field and their source. This is what contributes to the emitted momentum.

We then proceed to write down the emitted momentum from which we derive the formula for the radiated energy. While in the case of scalar radiation no polarizations are required, in the case of vector radiation, the polarization vectors are computed.

This method has been generalized to compute gravitational bremsstrahlung emitted by two massive particles [1].

The last chapter studies the same problem, for massless particles, in 4 dimensions. The scheme is essentially the same. The metric is expanded around flat Minkowski spacetime. The first order term in the metric, describes two massless shockwaves moving towards each other with the speed of light, with some impact parameter b. Finally the second order describes the interaction of the two pre-collision waves.

We note that this method also takes into account the back-reaction effects.

1.5 Results

The scheme described above has been used to study the collisions of ultraplanckian particles in three setups.

In chapter 2[1] we study the collision of two massive point-like particles with some large impact parameter $b \gg r_s$. The two particles interact gravitationally, while one of the two particles is charged under a massless scalar field Φ. The calculation is done within the ADD scenario. This setup is expected to capture all the essential features of gravitational bremsstrahlung, ignoring however the complications due to the tensor nature of the gravitational radiation.

In chapter 3[2] we proceed to study the collision of two massive point particles, again with impact parameter $b \gg r_s$ and interacting gravitationally. However now one of the two particles is charged under electromagnetism. We perform the calculation both in the ADD scenario, as well as in the UED scenario. The process of vector radiation emission from a charged particle due to acceleration represents a realistic problem, as the detectors of electromagnetic radiation are highly advanced. On the other hand, the problem of radiation reaction has not received a solution. The number of physical cases where an explicit solution has been given is quiet limited (see references in chapter 3). So the emission of vector bremsstrahlung due to the collision of a charged particle with another partner particle is of theoretical interest.

Chapter 4[3] is devoted to the study of the collision of two massless Aichelburg-Sexl shockwaves interacting gravitationally in four dimensions. Once more an impact parameter b is introduced, satisfying $EG \ll b \ll 1/p \equiv r_{\rm IR}$ and $r \in (0, 1/p)$, where E is the initial energy in the CM frame, G is Newton's constant, while $r_{\rm IR}$ is some infra-red cut-off that will be discussed in detail in 4. It thus gives as an insight in a region of the impact parameter not discussed in the previous chapters and also differing from

[1] The work in chapter 2 appeared in [48].
[2] The work in chapter 3 was published in [49].
[3] In chapter 4 we will present the work published in [50].

approaches in the literature for head-on or nearly head-on collisions. This collision takes place in flat, four-dimensional Minkowski space. We explicitly compute the second order correction to the metric in coordinate space.

In chapters 2 and 3, the scalar and vector bremsstrahlung emitted during the trans-planckian collision of two gravitating massive point particles in arbitrary dimensions was studied classically in the laboratory frame. The emitted momentum in the leading order of the Lorentz factor γ was computed in an arbitrary number of extra dimensions d.

The split of radiation into truly massless and massive modes was computed analytically and numerically. Our main results are summarised in the following.

The source of the emitted radiation composes of two pieces, the *local part*, due to the trajectory of the moving particle and the *non-local* part due to the non-linear terms of the vector or scalar field with gravity. We show that these two terms *interfere destructively* in the region $\frac{\gamma}{b} \lesssim \omega \lesssim \frac{\gamma^2}{b}$, that represents the pure effect of gravitational interaction. By this we mean that the two leading orders, in the ultra-relativistic expansion, of the local and non-local parts exactly cancel. The remainder is expressed as a sum of two terms j_z and $j_{z'}$, with frequency cut-offs at $\omega \leqslant \gamma^2/b$ and $\omega \leqslant \gamma/b$ respectively.

The destructive interference effect naturally specifies three frequency regimes, namely, $1/b$, γ/b and γ^2/b. The dominant contribution regime to the radiated energy was determined for the scalar case in the ADD model and was found to depend on the number of extra dimensions. It was also determined in the vector case for several extra-dimensional models. The ultra-low frequency regime of the radiation was dominated by the local part of the current in all dimensions. In the lab frame, most of the radiation was beamed in a narrow cone with angle $1/\gamma$ along the spatial direction of the moving particle's motion. In the high frequency regime, the local and non-local currents seem to be equally important.

In chapter 4 we studied the collision of two massless, point-like particles, boosted to the speed of light, colliding with an impact parameter b in 4 flat space-time dimensions.

Summarizing our results, a closed form formula for the first corrections of the metric and of the energy-momentum tensor were computed in the presence of an impact parameter, including the back-reactions.

It was shown that for zero impact parameter, the perturbative approximation breaks down and there is an instantaneous and point-like violation of the conservation of the energy momentum tensor, which however, is hidden behind a horizon. The introduction of an impact parameter regulates the mechanics in the absence of any other transverse scale.

The total energy momentum tensor was shown to be traceless before and after the collision up to the order computed in the expansion.

The energy emitted during a collision of gravitational waves was computed and argued that the result is exact to all orders.

In [1] the gravitational bremsstrahlung produced in ultra-planckian collisions by massive particles was computed. Although the computation there was more technically complex, our expectation that the analysis presented in chapter 2 would be able to capture the main features of the full problem was justified. The energy emitted was found to depend on the same powers of the Lorentz factors, up to a numerical coefficient, after redefining the couplings.

A comment regarding the massless limit in the four-dimensional case is in order. This limit can be taken in our treatment in chapters 2 and 3, as well as in [1], by taking the limit $m \to 0$ and $b \to \infty$ while keeping their product constant. The massless limit of the radiated energy, as shown in [1], is zero. Using the scheme of chapter 4, the result for the radiated energy seems to be inconclusive. However we do compute the radiation produced by gravitational waves and find it to be zero. This is analogue to taking the massless limit and the impact parameter to infinity. Thus we are in agreement with chapters 2 and 3, as well as [1]. On the other hand Eardley and Giddings have estimated the energy radiated to be approximately 55% of the center of mass energy for the maximal value of their impact parameter which is $b_{\max} = 3.219GE$.

This thesis is organized as follows:

- In chapter 2, we study the classical bremsstrahlung of a massless scalar field Φ in gravity mediated ultra-relativistic collisions with impact parameter b of two massive point particles in the presence of d non-compactor toroidal extra dimensions. The spectral and angular distribution of the scalar radiation are analyzed, while the total emitted $\Phi-$energy is found to be *strongly enhanced* by a $d-$dependent power of the Lorentz factor γ. The direct radiation amplitude from the accelerated particles is shown to *interfere destructively* (in the first two leading ultra-relativistic orders) with the one due to the $\Phi - \Phi - graviton$ interaction in the frequency regime $\gamma/b \lesssim \omega \lesssim \gamma^2/b$ in all dimensions.

- In chapter 3 a classical computation of vector bremsstrahlung in ultrarelativistic gravitational-force collisions of massive point particles is presented in an arbitrary number d of extra dimensions. The total emitted energy, as well as its angular and frequency distribution and characteristic values, are discussed in detail. The domain of validity of the classical result is discussed.

- Finally, in chapter 4 the collision of two massless, gravitationally interacting, point-like massless particles, boosted to the speed of light, colliding with an impact parameter b is being investigated. The collision takes place in flat four-dimensional space-time background. A perturbative scheme is employed and the corrections to the energy momentum tensor and to the metric are computed and closed form formulas are provided. This includes the back-reaction on the metric after the collision. Including such corrections suggests that the tracelessness of the initial stress tensors of the colliding particles is preserved during and after the collision. The necessity for introducing an impact parameter in the perturbative treatment is highlighted and the breaking of the underlying perturbative approach at $b = 0$ is motivated. In addition, the energy radiated in the form of gravitational bremsstrahlung radiation is discussed while an example from gravitational-waves collision is being studied.

Summarizing, we employ a classical, perturbative scheme to study the collisions of particles interacting gravitationally at CM energies greater than the Planck scale. We study this both in four-dimensional theories, as well as in several models with Large Extra Dimensions, namely the ADD model and the UED model. We particularly study the scalar and vector bremsstrahlung emitted in such a process. We find that in the frequency regime $\gamma^2/b > \omega \gg \gamma/b$ the local and non-local amplitudes are approximately equal and thus the total current $j(\omega)$ is suppressed by a factor of γ^2. We express this as

$$j(\omega) \sim j(\gamma/b) \left(\frac{\gamma/b}{\omega}\right)^2 . \tag{1.5.1}$$

The total emitted energy in the form of scalar or vector Bremsstrahlung was computed for several numbers of extra dimensions d. For $d = 0$ we have

$$E \approx C_0 \frac{\left(\alpha m' \varkappa_4^2\right)^2}{b^3} \gamma^3 , \tag{1.5.2}$$

while for $d = 1$

$$E = C_1 \frac{\left(\alpha m' \varkappa_5^2\right)^2}{b^6} \gamma^3 \ln \gamma , \tag{1.5.3}$$

and for $d \geq 2$

$$E \approx C_d \frac{\left(\alpha m' \varkappa_D^2\right)^2}{b^{3d+3}} \gamma^{d+2} , \tag{1.5.4}$$

where α is the scalar or the vector charge f and e respectively. C_0, C_1 and C_d are numerical coefficients differing for the scalar and vector radiation. C_0 and C_1 are computed numerically in chapters 2 and 3 for the scalar and vector cases respectively, while an analytical formula is given for C_d for each case. Moreover the spectral and angular characteristics of the frequency are analysed. These results could be used as a way to probe the number (and existence) and nature of extra dimensions, as well as to set bounds to them.

The above were computed for $b \gg r_s$. In chapter 4 we attempted to enlarge this range for smaller values of the impact parameter in four dimensions. The main accomplishment of this thesis is exactly this, the study of ultraplanckian collisions in a parameter region not studied before.

Important future prospects include but are not limited to the following:

- Complete and thorough treatment of the massless limit for scalar, vector and gravitational bremsstrahlung.

- Extending the area of validity to yet smaller impact parameters. In this manner one would be able to make contact with the current experiments.

- In chapter 4, we have found that the energy momentum tensor is traceless both before and after the collision up to second order. It is worth investigating whether this is true to all orders.

We note that while the mostly minus signature $(+,-,-,-)$ metric is used throughout chapters 2 and 3 mostly plus signature $(-,+,+,+)$ is used in chapter 4.

Bibliography

[1] D. Gal'tsov, P. Spirin and T. N. Tomaras, JHEP **1301**, 087 (2013) 14, 17

[2] T. Kaluza, *"On the Problem of Unity in Physics," Sitzungsber. Preuss. Akad. Wiss. Berlin (Math. Phys.)* **1921***, 966 (1921). 2, 3*

[3] O. Klein, "Quantum Theory and Five-Dimensional Theory of Relativity. (In German and English)," Z. Phys. **37**, 895 (1926) 2

[4] J. H. Schwarz, *"Introduction to superstring theory," NATO Sci. Ser. C* **566** *(2001) 143 [hep-ex/0008017]. 2*

[5] N. Arkani-Hamed and M. Schmaltz, Phys. Rev. D **61***, 033005 (2000) [hep-ph/9903417]. 2*

[6] K. R. Dienes, E. Dudas and T. Gherghetta, Phys. Lett. B **436** *(1998) 55 [hep-ph/9803466]. 2*

[7] I. Antoniadis, Phys. Lett. B **246** *(1990) 377. 3*

[8] A. Salam and J. A. Strathdee, "On Kaluza-Klein Theory," Annals Phys. **141**, 316 (1982)

[9] N. Arkani-Hamed, S. Dimopoulos and G. R. Dvali, *"The Hierarchy problem and new dimensions at a millimeter," Phys. Lett. B* **429***, 263 (1998) 8*

[10] I. Antoniadis, N. Arkani-Hamed, S. Dimopoulos and G. R. Dvali, "New dimensions at a millimeter to a Fermi and superstrings at a TeV," Phys. Lett. B **436**, 257 (1998)

[11] T. Han, J. D. Lykken and R. J. Zhang, Phys. Rev. D **59** (1999) 105006 [hep-ph/9811350].
G. F. Giudice, R. Rattazzi and J. D. Wells, *"Quantum gravity and extra dimensions at high-energy colliders,"* Nucl. Phys. B **544**, 3 (1999).

[12] J. Beringer *et al.* [Particle Data Group Collaboration], *"Review of Particle Physics (RPP),"* Phys. Rev. D **86**, 010001 (2012). 2, 8

[13] L. Randall and R. Sundrum, *"A Large mass hierarchy from a small extra dimension,"* Phys. Rev. Lett. **83**, 3370 (1999) 2, 8

[14] L. Randall and R. Sundrum, *"An Alternative to compactification,"* Phys. Rev. Lett. **83**, 4690 (1999).

[15] W. D. Goldberger and M. B. Wise, *"Modulus stabilization with bulk fields,"* Phys. Rev. Lett. **83**, 4922 (1999). 9
10, 11

[16] J. Garriga and A. Pomarol, *"A Stable hierarchy from Casimir forces and the holographic interpretation,"* Phys. Lett. B **560**, 91 (2003) 2, 10

[17] A. Pomarol, *"Gauge bosons in a five-dimensional theory with localized gravity,"* Phys. Lett. B **486**, 153 (2000). 11

[18] S. Chang, J. Hisano, H. Nakano, N. Okada and M. Yamaguchi, *"Bulk standard model in the Randall-Sundrum background,"* Phys. Rev. D **62**, 084025 (2000).

[19] T. Gherghetta and A. Pomarol, *"Bulk fields and supersymmetry in a slice of AdS,"* Nucl. Phys. B **586**, 141 (2000). 10

[20] T. Appelquist, H. -C. Cheng and B. A. Dobrescu, *"Bounds on universal extra dimensions,"* Phys. Rev. D **64**, 035002 (2001). 10

[21] F. J. Petriello, *"Kaluza-Klein effects on Higgs physics in universal extra dimensions,"* JHEP **0205**, 003 (2002). 11

[22] T. Flacke, D. Hooper and J. March-Russell, *"Improved bounds on universal extra dimensions and consequences for LKP dark matter,"* Phys. Rev. D **73**, 095002 (2006). 11

[23] I. Gogoladze and C. Macesanu, *"Precision electroweak constraints on Universal Extra Dimensions revisited,"* Phys. Rev. D **74**, 093012 (2006). 11

[24] R. C. Myers and M. J. Perry, *"Black Holes in Higher Dimensional Space-Times,"* Annals Phys. **172**, 304 (1986). 11
11

[25] G. 't Hooft, *"Graviton Dominance in Ultrahigh-Energy Scattering,"* Phys. Lett. B **198**, 61 (1987). 11

[26] D. N. Kabat and M. Ortiz, *"Eikonal quantum gravity and Planckian scattering,"* Nucl. Phys. B **388**, 570 (1992). 11

[27] D. Amati, M. Ciafaloni and G. Veneziano, *"Superstring Collisions at Planckian Energies,"* Phys. Lett. B **197**, 81 (1987). 13

[28] D. Amati, M. Ciafaloni and G. Veneziano, *"Planckian scattering beyond the semi-classical approximation,"* Phys. Lett. B **289**, 87 (1992). 14

[29] D. Amati, M. Ciafaloni and G. Veneziano, *"Effective action and all order gravitational eikonal at Planckian energies,"* Nucl. Phys. B **403**, 707 (1993). 14

[30] I. J. Muzinich and M. Soldate, *"High-Energy Unitarity of Gravitation and Strings,"* Phys. Rev. D **37**, 359 (1988). 12, 14

[31] T. Banks and W. Fischler, *"A Model for high-energy scattering in quantum gravity,"* hep-th/9906038. 12, 14

[32] G. F. Giudice, R. Rattazzi and J. D. Wells, *"Transplanckian collisions at the LHC and beyond,"* Nucl. Phys. B **630**, 293 (2002). 12, 14

[33] P. C. Argyres, S. Dimopoulos and J. March-Russell, *Black holes and sub-millimeter dimensions,* Phys. Lett. B **441** (1998) 96 [hep-th/9808138]; T. Banks and W. Fischler, [arXiv:hep-th/9906038]; S. B. Giddings and S. Thomas, *High energy colliders as black hole factories: The end of short distance physics,* Phys. Rev. D **65** (2002) 056010 [hep-ph/0106219]; S. Dimopoulos and G. Landsberg, *Black holes at the LHC,* Phys. Rev. Lett. **87** (2001) 161602 [hep-ph/0106295]; 14

[34] D. Ida and K.-i. Nakao, *Isoperimetric inequality for higher-dimensional black holes,* Phys. Rev. D **66** (2002) 064026 arXiv:gr-qc/0204082; C. Barrabes, V. P. Frolov and E. Lesigne, *Geometric inequalities and trapped surfaces in higher dimensional spacetimes,* Phys. Rev. D **69** (2004) 101501, [gr-qc/0402081]; C. M. Yoo, K.-i. Nakao and D. Ida, *Hoop conjecture in five-dimensions: Violation of cosmic censorship,* Phys. Rev. D **71** (2005) 104014 [gr-qc/0503008]. 14

[35] R. Penrose, 1974 (unpublished). 14

[36] P. D. D'Eath, *High Speed Black Hole Encounters And Gravitational Radiation,* Phys. Rev. D **18** (1978) 990; P. D. D'Eath and P. N. Payne, *Gravitational Radiation In High Speed Black Hole Collisions. 1. Perturbation Treatment Of The Axisymmetric Speed Of Light Collision*, Phys. Rev. D **46** (1992) 658; Phys. Rev. D **46** (1992) 675; Phys. Rev. D **46** (1992) 694; P. D. D'Eath, *Black holes: Gravitational interactions*, (Oxford mathematical monographs) *Oxford, UK: Clarendon* (1996), pg. 286. 12

[37] D. M. Eardley and S. B. Giddings, Phys. Rev. D **66**, 044011 (2002), [arXiv:gr-qc/0201034]; S. B. Giddings and V. S. Rychkov, Phys. Rev. D**70**, 104026 (2004), [arXiv:hep-th/0409131].

[38] F. S. Coelho, C. Herdeiro, C. Rebelo and M. Sampaio, arXiv:1206.5839 [hep-th].

[39] H. Yoshino and Y. Nambu, Phys.Rev. **D66**, 065004, (2002); Phys. Rev. **D67** (2003) 024009 [gr-qc/0209003]; H. Yoshino and V. S. Rychkov, Phys. Rev. **D71** (2005) 104028[hep-th/0503171]; H. Yoshino and R. B. Mann, Phys. Rev. **D74** (2006) 044003 [gr-qc/0605131]. 12

[40] S. B. Giddings, Beyond the Planck scale arXiv:0910.3140 [gr-qc]. I. Y. Aref'eva, Theor. Math. Phys. **161** (2009) 1647 arXiv:0912.5481 [hep-th]; M. Bleicher and P. Nicolini, arXiv:1001.2211 [hep-ph]; S. B. Giddings, M. Schmidt-Sommerfeld and J. R. Andersen, arXiv:1005.5408 [hep-th]. 12
12

[41] P. C. Aichelburg and R. U. Sexl, Gen. Rel. Grav. **2** (1971) 303.

[42] T. Dray and G. 't Hooft, Nucl. Phys. B **253** (1985) 173.

[43] C. Herdeiro, M. O. P. Sampaio and C. Rebelo, arXiv:1105.2298 [hep-th]. 12

[44] V. Cardoso, O. J. C. Dias and P. S. Lemos, Phys. Rev. D **67**, (2003) 064016, [hep-th/0212168]; V. Cardoso, P. S. Lemos and S. Yoshida, Phys. Rev. D **68** (2003) 084011 [gr-qc/0307104]; E. Berti, M. Cavaglià and L. Gualtieri, Phys. Rev. D **69** (2004) 124011 [hep-th/0309203]; B. Koch and M. Bleicher, JETP Lett. **87** (2008) 75, [hep-th/0512353]; V. Cardoso, M. Cavaglià and J. Q. Guo, Phys. Rev. D **75** (2007) 084020, [hep-th/0702138]; H. Yoshino, T. Shiromizu and M. Shibata, Phys. Rev. D **74** (2006) 124022,[gr-qc/0610110]; P. Lodone and S. Rychkov, JHEP **0912** (2009) 036; arXiv:0909.3519 [hep-ph].

[45] A. Mironov and A. Morozov, Pisma Zh. Eksp. Teor. Fiz. **85**, 9 (2007) [JETP Lett. **85** (2007)] 6, [hep-ph/0612074]; A. Mironov and A. Morozov, [hep-th/0703097].

[46] D. V. Gal'tsov, G. Kofinas, P. Spirin and T. N. Tomaras, Phys. Lett. B **683** (2010) 331, arXiv:0908.0675 [hep-ph].

[47] D. V. Gal'tsov, G. Kofinas, P. Spirin and T. N. Tomaras, JHEP **0905** (2009) 074 arXiv:0903.3019 [hep-ph].

[48] Y. Constantinou, D. Gal'tsov, P. Spirin and T. N. Tomaras, "Scalar Bremsstrahlung in Gravity-Mediated Ultrarelativistic Collisions," JHEP **1111** (2011) 118 [arXiv:1106.3509 [hep-th]]. 15

[49] Y. Constantinou and P. Spirin, "Vector Bremsstrahlung by Ultrarelativistic Collisions in Higher Dimensions," JHEP **1401** (2014) 111 [arXiv:1310.6065 [hep-th]]. 15

[50] Y. Constantinou and A. Taliotis, "Bremsstrahlung and black hole production from collisions of ultra-boosted particles at non-zero impact parameter," JHEP **1311** (2013) 175 [arXiv:1308.2544 [hep-th]]. 15

2

Scalar Bremsstrahlung in Gravity-Mediated Ultrarelativistic Collisions

2.1 Introduction and results

The idea of TeV scale gravity with large extra dimensions (LED) [1; 2; 3; 4] has triggered a lot of activity in particle physics and gravitation theory. One of the most interesting predictions is the possibility of black hole production in colliders [5]. According to Thorne's hoop conjecture (generalized to higher dimensions [6]), for energies of colliding particles higher than the D-dimensional Planck mass M_* (transplanckian regime) such black holes should be produced classically for impact parameters $b \lesssim R_S$, where R_S is the Schwarzschild radius associated with the center-of-mass collision energy. To establish the creation of a black hole in the collision of ultrarelativistic particles one has to find closed trapped surfaces in the corresponding space-time. To this aim, an idea due to Penrose [7] was put into the form of an elaborated model in $D = 4$ by D'Eath and Payne [8] and with extra dimensions by Eardley and Giddings [9] and further refined in [10] (see recent reviews [11] and references therein). In that model one is after a solution of Einstein's equations with a special metric ansatz generalizing the Aichelburg-Sexl metric [12] (see also [13]). The ansatz amounts to replacing the gravitational field of two ultrarelativistic particles before the collision by colliding shock waves, while the collision region is described by some linear differential equation for a metric function, which is amenable to construct exact or approximate solutions.

The closed trapped surface emerging in such a solution for appropriate initial energies and impact parameters leads to an estimate of the produced black hole mass and its difference from the initial energy is interpreted as the amount of gravitational radiation produced (see e.g. the recent paper [14] and references therein).

The colliding waves model (CWM) of black hole formation is certainly a very nice and perhaps the simplest possible one, designed to answer an intriguing question about the nature of transplanckian collisions. It gives the gravitational radiation loss for head-on and almost head-on collisions and also demonstrates that the black hole is indeed present in the collision region. However, we would like to discuss some subtle points concerning the applicability of this model to high energy particle scattering. In fact, various effects which were not taken into account in the simple version of CWM such as an extended nature of the colliding particles [15] and their parton structure [16], have already been discussed. It was shown by Meade and Randall [16] that taking the finite size into account leads to a substantial decrease of the cross-section predicted by the CWM. It was also emphasized [16] that an even more critical effect is the radiative energy loss of the colliding partons before their energy is trapped inside a black hole horizon. The CWM seems to be able to clarify these issues, but in a closer look it probably cannot. In fact, the Aichelburg-Sexl solution is the limiting form of the linearized gravitational field of ultrarelativistic particle moving with a *constant* velocity. Therefore, presenting colliding particles as plane waves implicitly assumes that their radiation is negligibly small, otherwise the particle trajectories should be modified substantially by radiation friction (for a discussion of radiation reaction in extra dimensions see [17]). Furthermore, the energy mismatch between the mass of the black hole and the initial energy of the colliding particles, interpreted in CWM as radiation loss, is found to be of the order of the initial energy [9], which is by no means small.

Therefore, alternative methods of computing radiation losses in transplanckian collisions seem to be desirable. One such approach is the one by Amati, Ciafaloni and Veneziano [18] relevant in four dimensions and based on the combination of string and quantum field theory techniques. Other recent work on this subject includes [19] using various analytical classical and semi-classical approaches. In the framework of purely classical $D = 4$ general relativity, numerical simulations were also performed of collision of two scalar field balls interacting gravitationally via exact Einstein equations [20]. Gravitational radiation was extracted imposing appropriate boundary conditions. Gravitational radiation in collisions of higher-dimensional black holes (with non-compact extra dimensions) was studied numerically in [21].

For the ultrarelativistic scattering in models with large extra dimensions a crucial question is whether radiation is enhanced due to the extended phase space associated with extra dimensions. It was argued by Mironov and Morozov [22] that in the case of synchrotron radiation the expected enhancement can be damped by beaming of radiation in the forward direction, suppressing the number of excited Kaluza-Klein modes. In the case of bremsstrahlung the situation is different, namely in [23] it was found, that the energy loss of ultrarelativistic particles under non-gravitational scattering at small angle contains an additional factor γ^d due to the emission of light massive KK modes. Qualitatively, this can be explained as follows. For non-gravitational scattering in flat space the impact parameter b, the radiation frequency ω and the angle of emission $\vartheta \ll 1$ with respect to the momentum of the fast particle in the rest frame of the other are related by

$$\omega b(\vartheta^2 + \gamma^{-2}) \lesssim 1. \tag{2.1.1}$$

Frequencies near the cut-off frequency $\omega \sim \gamma^2/b$ are emitted in the narrow $(D-1)$ dimensional cone $\vartheta \lesssim \gamma^{-1}$, while intermediate frequencies are emitted into a wider cone. The main contribution comes from the first region, and in this case the emitted momenta in directions transverse to the brane are of the order ω/γ. The number of such light modes is of the order $(R\omega/\gamma)^d \sim (R\gamma/b)^d$ (R being the size of the compact extra dimensions), giving an extra factor γ^d to the radiated power. Analogous enhancement was reported for gravitational bremsstrahlung in transplanckian collisions [24], compatible with the numerical study of [21].

Our approach amounts to solving the two-body field-mediated problem iteratively. In electrodynamics this is a well known method, allowing to calculate spectral-angular distributions of bremsstrahlung in the classical range of frequencies small with respect to the particle energy $\hbar\omega \ll E$. In general relativity this approach was suggested in [27] under the name of "fast-motion approximation scheme" and was further developed and called "post-linear formalism". It was applied to the gravitational bremsstrahlung most notably by Kovacs and Thorne [28]. We will use a momentum space version of this approach, developed in [29], which has the advantage that it allows a fully analytical treatment of the problem. In [23; 24] we extended this technique to models with extra dimensions either infinite or compact. In [23] we calculated scalar bremsstrahlung radiation in the collision of two ultrarelativistic point-like particles interacting via a scalar field in flat space-time. Here we consider the situation in which the particles interact gravitationally but emit scalar radiation. This is an intermediate step towards the full treatment of the gravitational bremsstrahlung presented briefly in [24]. The latter case has additional complications due to the tensor nature of the radiation field and it will be presented in full detail in a future publication. Here, we will assume that only one of the colliding particles is coupled to the scalar field, so that their interaction is purely gravitational. On the other hand, we will compute only the scalar radiation emitted by the system. The main novel feature is this case is that the system becomes non-linear due to scalar-scalar-graviton vertex. As a result, the effective source of radiation field in the flat space picture becomes non-local due to contribution of the field stresses.

In four dimensions, it was shown long ago [30], that the contribution from the high-frequency regime $\gamma/b \lesssim \omega \lesssim \gamma^2/b$ is *suppressed by a factor* γ^{-4} *due to destructive interference* between the local and the non-local amplitudes, the latter being due to the gravitational interaction of the mediating field. The remaining radiation is beamed inside the cone with angle $1/\gamma$, it has characteristic frequencies $\omega \sim \mathcal{O}(\gamma/b)$ and emitted energy of order $E \sim \gamma^3$. There is in addition a sub-leading component of emitted radiation with frequencies $\omega \sim \mathcal{O}(\gamma^2/b)$, which is also beamed and has $E \sim \gamma^2$.

In the higher dimensional case the situation is more complicated. The destructive interference is also present, but with growing d the relative contribution of $\omega \sim \gamma^2/b$ increases faster, than that of $\omega \sim \gamma/b$ due to competition of the angular integrals.

The powers of γ of the emitted radiation energy in all frequency and angular regimes in the presence of d extra dimensions are summarized in the Table below.

ϑ \ ω	$\omega \ll \gamma/b$	$\omega \sim \gamma/b$	$\omega \sim \gamma^2/b$	$\omega \gg \gamma^2/b$
γ^{-1}	negligible (phase space)	$E_d \sim \gamma^3$	$E_d \sim \gamma^{d+2}$	negligible radiation
1	negligible (phase space)	$E_d \sim \gamma^{d+1}$	negligible radiation	negligible radiation

In the special cases of $d = 1$ or 2 extra dimensions there is an extra $\ln\gamma$ in the expression for the energy emitted in the regime ($\omega \sim \gamma/b$, $\vartheta \sim 1/\gamma$). The energy is measured in units of $\varkappa_D^4 m'^2 f^2/b^{3d+3}$, with m' the mass of the target particle, $\varkappa_D$ the $D-$dimensional gravitational coupling, f the scalar coupling of m and b the impact parameter of the collision and the overall numerical coefficients can be found in the text.

2.2 The setup

2.2.1 The action

The goal here is to calculate within the ADD scenario classical spin-zero bremsstrahlung in ultra-relativistic gravity-mediated scattering of two massive point particles m and m'. The space-time is assumed to be $M_4 \times T^d$, the product of four-dimensional Minkowski space and a d-dimensional torus, with coordinates $x^M = (x^\mu, y^i)$, $M = 0, 1, \ldots, D-1, \mu = 0, \ldots, 3$, $i = 1, \ldots d$.

Particles move in M_4 (the brane) and interact via the gravitational field g_{MN}, which propagates in the whole space-time $M_4 \times T^d$. We also assume the existence of a massless bulk scalar field $\Phi(x^P)$, which interacts with m, but not with m'. The action of the model is symbolically of the form

$$S \equiv S_g + S_\Phi + S_m + S_{m'} \,,$$

and explicitly, in an obvious correspondence,

$$S = \int d^D x \sqrt{|g|} \left[-\frac{R}{\varkappa_D^2} + \frac{1}{2}\, g^{MN} \partial_M \Phi\, \partial_N \Phi \right] - \frac{1}{2} \int \left[e\, g_{MN} \dot{z}^M \dot{z}^N + \frac{(m+f\Phi)^2}{e} \right] d\tau - \\ - \frac{1}{2} \int \left[e' g_{MN} \dot{z}'^M \dot{z}'^N + \frac{m'^2}{e'} \right] d\tau' \tag{2.2.1}$$

with $16\pi G_D \equiv \varkappa_D^2$ relating $\varkappa_D$ to Newton's constant. Here the ein-beins $e(\tau)$ and $e'(\tau')$ are introduced, which lead to a somewhat unusual form of interaction with Φ, but it reduces to the standard non-derivative interaction once they are integrated out. The constant f is the scalar charge of m. To solve the corresponding coupled equations of motion we shall use perturbation theory with respect to the scalar and gravitational couplings. To zeroth order, both gravitational and scalar fields are absent and the two particles move along straight lines as determined by the initial conditions. In first order, one takes into account the (non-radiative Coulomb-like) gravitational and scalar fields produced by the particles in their zeroth order trajectories. Next, one computes the first order correction to their trajectories, due to their first order gravitational interaction (the scalar mutual interaction vanishes in our set-up). The leading contribution to the scalar radiation field, of interest here, emitted by the accelerated particle m is then obtained in the second order of perturbation theory. This approach allows us to compute consistently the lowest order radiation in the case of ultrarelativistic collision, when deviations from straight trajectories is small and the iterative solution of the coupled particle-field equations of motion is convergent. The resulting expression for the radiative energy loss will be therefore correct only in the leading ultrarelativistic order.

To carry out such a computation it is sufficient to restrict oneself to linearized gravity. One writes $g_{MN} = \eta_{MN} + \varkappa_D h_{MN}$ and replaces the Hilbert-Einstein action by its quadratic part

$$S_g = \int \left[-\frac{1}{4} h^{MN} \Box_D h_{MN} + \frac{1}{4} h \Box_D h - \frac{1}{2} h^{MN} \partial_M \partial_N h + \frac{1}{2} h^{MN} \partial_M \partial_P h^P_N \right] d^D x, \qquad (2.2.2)$$

where the Minkowski metric is $\eta_{MN} = \mathrm{diag}(1, -1, -1, ...)$, $\Box_D \equiv \eta^{MN} \partial_M \partial_N$, raising/lowering the indices is performed with η_{MN} and $h \equiv h^M_M$. To avoid classical renormalization (which in principle can be treated along the lines of [17]) we take into account only *mutual* gravitational interaction. At the linearized level the total gravitational field h_{MN} is the superposition of the fields h^m_{MN}, $h^{m'}_{MN}$ due to the particles m and m', respectively, and of the gravitational field generated by the bulk scalar Φ. Assuming that the scalar interaction is of the same order as the gravitational one, the latter contribution to h_{MN} is of higher order and will be neglected here. Therefore, to this order of approximation

$$h_{MN} = h^m_{MN} + h^{m'}_{MN} \, . \qquad (2.2.3)$$

For simplicity the superscripts m, m' will be omitted in what follows. Thus, h^m_{MN} and $h^{m'}_{MN}$ will be denoted as h_{MN} and h'_{MN}, respectively. Ignoring the self-interaction and the associated radiation reaction problem, we will consider each of the particles m' and m as moving in the other's metric

$$g_{MN} = \eta_{MN} + \varkappa_D h_{MN} \quad \text{and} \quad g'_{MN} = \eta_{MN} + \varkappa_D h'_{MN} \, , \qquad (2.2.4)$$

respectively. Correspondingly, the action for the particle m, which interacts with both gravity and Φ, takes the form

$$S_m = -\frac{1}{2} \int \left[e(\eta_{MN} + \varkappa_D h'_{MN}) \dot{z}^M \dot{z}^N + \frac{(m + f\Phi)^2}{e} \right] d\tau. \qquad (2.2.5)$$

Similarly, the action for m' is

$$S_{m'} = -\frac{1}{2} \int \left[e'(\eta_{MN} + \varkappa_D h_{MN}) \dot{z}'^M \dot{z}'^N + \frac{m'^2}{e'} \right] d\tau. \qquad (2.2.6)$$

Finally, the action for the scalar field, which propagates in the gravitational field h'_{MN} of the uncharged particle, expanded to linearized order of the gravitational field, is

$$S_\Phi = \frac{1}{2} \int \partial^M \Phi \, \partial^N \Phi \, \left[\left(1 + \frac{\varkappa_D}{2} h' \right) \eta_{MN} - \varkappa_D h'_{MN} \right] d^D x \, . \qquad (2.2.7)$$

In principle, Φ propagates in the full gravitational field $h_{MN}+h'_{MN}$ of both particles, but the singular product of h_{MN} and Φ generated by the same point particle m corresponds again to the self-action problem, which is ignored here. The products of h'_{MN} due to m' and Φ due to m does not lead to singularities and correctly describe the situation.

2.2.2 Equations of motion

Varying the action with respect to $z(\tau)$ and $z'(\tau)$ one obtains the linearized geodesic equations of each mass moving in the gravitational field of the other:

$$\frac{d}{d\tau}\left(eg'_{MN}\dot{z}^N\right) = \frac{e}{2}g'_{LR,M}\dot{z}^L\dot{z}^R, \qquad \frac{d}{d\tau}\left(e'g_{MN}\dot{z}'^N\right) = \frac{e'}{2}g_{LR,M}\dot{z}'^L\dot{z}'^R. \tag{2.2.8}$$

Variation with respect to the einbeins gives

$$e^{-2} = \frac{g'_{MN}\dot{z}^M\dot{z}^N}{(m+f\Phi)^2} \qquad e'^{-2} = \frac{g_{MN}\dot{z}'^M\dot{z}'^N}{m'^2} \tag{2.2.9}$$

Substituting this back into the particles' actions (2.2.5-2.2.6) one is led to their more familiar form

$$S_m = -\int (m+f\Phi)(g'_{MN}\dot{z}^M\dot{z}^N)^{1/2}d\tau, \qquad S_{m'} = -m'\int (g_{MN}\dot{z}'^M\dot{z}'^N)^{1/2}d\tau,$$

from which the scalar field equation is obtained

$$\Box_D\Phi = -\frac{\varkappa_D}{2}h'\Box_D\Phi + \varkappa_D h'_{MN}\Phi^{,MN} + f\int (g'_{MN}\dot{z}^M\dot{z}^N)^{1/2}\delta^D(x-z(\tau))\,d\tau, \tag{2.2.10}$$

Note, once again, that only the gravitational field due to the uncharged particle m' enters this equation.

Finally, the linearized Einstein equations for the metric deviation due to the two particles in the De Donder gauge

$$\partial_N h^{MN} = \frac{1}{2}\partial^M h$$

are obtained from (2.2.5, 2.2.6):

$$\Box_D h^{MN} = -\varkappa_D\left(T^{MN} - \eta^{MN}\frac{T}{D-2}\right), \quad T^{MN} = \int e\dot{z}^M\dot{z}^N\frac{\delta^D(x-z(\tau))}{\sqrt{-g'}}d\tau, \tag{2.2.11}$$

where $T = T^M_M$ and linearization of the metric factor is understood. Similarly,

$$\Box_D h'^{MN} = -\varkappa_D\left(T'^{MN} - \eta^{MN}\frac{T'}{D-2}\right), \quad T'^{MN} = \int e'\dot{z}'^M\dot{z}'^N\frac{\delta^D(x-z'(\tau))}{\sqrt{-g}}d\tau. \tag{2.2.12}$$

To ensure that the particles move on the brane, it is enough to choose the initial conditions $y^i(0)=0$, $\dot{y}^i(0)=0$ and similarly for m'. Then, using the equations of motion, it is easy to check that the entire world-lines will be $x^\mu = z^\mu(\tau)$, $x'^\mu = z'^\mu(\tau)$ and the energy-momentum tensors will only have brane components $T^{\mu\nu}, T'^{\mu\nu}$. However, the metric deviations h^{MN} and h'^{MN} will have in addition diagonal bulk components due to the trace terms in (2.2.11) and (2.2.12).

2.2.3 Iterative solution

Even in linearized gravity the relativistic two-body problem can not be solved exactly, so one has to use some approximation scheme. With the particle masses m, m' taken of the same order and eventually equal, the model is characterized by three classical length parameters. Namely, the classical radius of the scalar charge [23]:

$$r_f = \left(\frac{f^2}{m}\right)^{\frac{1}{d+1}}, \tag{2.2.13}$$

the D-dimensional gravitational radius of the mass m at rest

$$r_g = \left(\varkappa_D^2 m\right)^{\frac{1}{d+1}}, \tag{2.2.14}$$

and the Schwarzschild radius of the black hole, associated with the collision energy $\sqrt{s}$ [24]:

$$r_S = \frac{1}{\sqrt{\pi}}\left[\frac{8\Gamma\left(\frac{d+3}{2}\right)}{d+2}\right]^{\frac{1}{d+1}}\left(\frac{G_D\sqrt{s}}{c^4}\right)^{\frac{1}{d+1}}. \tag{2.2.15}$$

In the (initial) rest frame of the mass m' one has $\sqrt{s} = 2mm'\gamma$, where $\gamma = 1/\sqrt{1-v^2}$ is the Lorentz factor of the collision, v being the relative velocity of the colliding particles. So

$$r_S \sim r_g\gamma^\nu, \quad \nu = \frac{1}{2(d+1)}. \tag{2.2.16}$$

It will be assumed that the parameters r_g and r_f are of the same order, and both much smaller than the impact parameter b:

$$r_g \sim r_f \ll b\gamma^{-2\nu}, \tag{2.2.17}$$

or, in terms of r_S [24]:

$$b \gg r_S\gamma^\nu. \tag{2.2.18}$$

Under this condition, as will be shown below, the deviation of the metric from unity in the rest frame of m' is small, i.e. $\varkappa_D h_{MN}\dot{z}'^M\dot{z}'^N \ll 1$, which is necessary for the validity of the present perturbative treatment.

2.2.3.1 The formal expansion and zeroth order equations

The next step is to solve these equations iteratively. For the particle-m world-line one writes

$$z^M = {}^0z^M + {}^1z^M + \ldots, \qquad {}^0z^M = u^M\tau + b^M, \tag{2.2.19}$$

where the order is denoted by a left superscript and to zeroth order the particle moves in Minkowski space-time with constant velocity u^M, and with ${}^0z^M(0) = b^M$ another constant vector. Both vectors u^M, b^M will be assumed to lie on the brane, i.e. to have only μ-components and, in addition, to be orthogonal $b^\mu u_\mu$=0. It will be shown that as a consequence of the equations of motion ${}^1z^M$ also lies on the brane. However, it is convenient to keep D-dimensional notation in all intermediate steps.

For the particle-m' one writes similarly

$$z'^M = {}^0z'^M + {}^1z'^M + \dots, \qquad {}^0z'^M = u'^M\tau, \tag{2.2.20}$$

assuming that at $\tau = 0$ the particle is at the origin. We choose to work in the rest frame of m', and specify the coordinate axes on the brane so that $u'^\mu = (1,0,0,0)$, $u^\mu = \gamma(1,0,0,v)$, $\gamma = 1/\sqrt{1-v^2}$, and $b^\mu = (0,b,0,0)$, where b is the impact parameter. When needed, one may think of the brane-localized vectors as D-dimensional vectors with zero bulk components, e.g. $u^M = (u^\mu, 0, \dots, 0)$.

In a similar fashion, the bulk scalar is expanded formally as:

$$\Phi = {}^0\Phi + {}^1\Phi + \dots. \tag{2.2.21}$$

Substitute in (2.2.10) and set $\varkappa_D = 0$ to obtain for the leading contribution to Φ the equation

$$\Box_D\, {}^0\Phi = f \int \delta^D(x - u\tau - b)\, d\tau. \tag{2.2.22}$$

The ein-beins are also expanded

$$e = {}^0e + {}^1e + \dots, \qquad e' = {}^0e' + {}^1e' + \dots. \tag{2.2.23}$$

According to (2.2.9) one obtains in zeroth order

$${}^0e = m + f\ {}^0\Phi, \qquad {}^0e' = m'. \tag{2.2.24}$$

Finally, for the metrics one writes

$$h_{MN} = {}^0h_{MN} + {}^1h_{MN} + \dots, \tag{2.2.25}$$

and similarly for h'_{MN}. The leading order contributions to the metrics are then obtained from Eqs. (2.2.11, 2.2.12) with the zeroth order source on the right hand side, i.e. with

$${}^0T^{MN} = m \int \delta^D(x - {}^0z(\tau))\, u^M u^N d\tau, \qquad {}^0T'^{MN} = m \int \delta^D(x - {}^0z'(\tau))\, u'^M u'^N d\tau. \tag{2.2.26}$$

To calculate the leading order scalar bremsstrahlung it will be sufficient to know only the zeroth order term ${}^0h_{MN}$ of h_{MN}. So, in the sequel only ${}^0h_{MN}$ will appear and to simplify the notation, its left superscript will be omitted.

2.2.3.2 The first order equations

To derive the equations for the first order corrections to the particle world-lines one has to collect first order terms in the expansions of the embedding functions z^M, z'^M and the einbeins e, e' and choose suitable gauge condition to fix the τ, τ' reparametrization symmetries. From Eqs. (2.2.9) one finds for the first order corrections of the einbeins:

$$ {}^1e = -e_0 \left(\varkappa_D h'_{MN} u^M u^N + 2\, {}^1\dot{z}_M u^M \right), \qquad {}^1e' = -e'_0 \left(\varkappa_D h_{MN} u'^M u'^N + 2\, {}^1\dot{z}'_M u'^M \right). \tag{2.2.27} $$

The reparametrization freedom allows us to fix ${}^1e$ and ${}^1e'$ arbitrarily. We first substitute these expansions into Eq.(2.2.8), collect all the first order terms and then choose the gauge fixing conditions ${}^1e = {}^1e' = 0$, that is

$$ \varkappa_D h'_{MN} u^M u^N + 2\, {}^1\dot{z}_M u^M = 0 \tag{2.2.28} $$

in the equation for m, and

$$ \varkappa_D h_{MN} u'^M u'^N + 2\, {}^1\dot{z}'_M u'^M = 0 \tag{2.2.29} $$

in the equation for m'. The resulting equations for the first corrections to the particle trajectories read

$$ \Pi^{MN}\, {}^1\ddot{z}_N = -\varkappa_D \Pi^{MN} \left(h'_{NL,R} - \frac{1}{2} h'_{LR,N} \right) u^L u^R, \tag{2.2.30} $$

$$ \Pi'^{MN}\, {}^1\ddot{z}'_N = -\varkappa_D \Pi'^{MN} \left(h_{NL,R} - \frac{1}{2} h_{LR,N} \right) u'^L u'^R, \tag{2.2.31} $$

where the projectors onto the space transverse to the world-lines are

$$ \Pi^{MN} = \eta^{MN} - u^M u^N, \quad \Pi'^{MN} = \eta^{MN} - u'^M u'^N, \tag{2.2.32} $$

whose presence demonstrates explicitly that only the transverse perturbations of the world-lines are physical.

2.2.3.3 The second order equation for $\Phi-$radiation

The radiative component of the bulk scalar arises in the next order of iterations and is given by ${}^1\Phi$. With appropriate combination of terms on the right hand side, Eqn. (2.2.10) is written as:

$$ \Box_D\, {}^1\Phi(x, y) = j(x, y) \equiv \rho(x, y) + \sigma(x, y), \tag{2.2.33} $$

where the first term is localized on the world-line of the radiating particle m

$$\rho(x,y) = -f \int {}^1 z^\mu(\tau)\, \partial_\mu \delta^4(x - u\tau - b)\, \delta^d(\mathbf{y}) d\tau, \tag{2.2.34}$$

while the second is the non-local current

$$\sigma(x,y) = \varkappa_D\, \partial_M \left(h'^{MN}\, \partial_N\, {}^0\Phi - \frac{1}{2} h'\, \partial^M\, {}^0\Phi \right), \tag{2.2.35}$$

with both h'^{MN} and ${}^0\Phi$ having support in the bulk. This current arises from non-linear terms in (2.2.10) due to the interaction of the bulk scalar with gravity. It has to be emphasized that it is non-zero outside the world-line not only on the brane but also in the bulk. Note that the decomposition into the local and non-local parts is ambiguous in the sense that part of the non-local term can be cast into a local form using the field equations. But the total source j never reduces to a local form as a whole.

2.2.4 The solution for ${}^0\Phi$, h_{MN} and ${}^1z^M$ in $M_4 \times T^d$

Our notation and conventions for Kaluza-Klein decomposition and Fourier transformation as applied to the ADD scenario with the transverse directions being circles with radii equal to R, are given in section 2.6.1. It is important to stress at this point that in classical perturbation theory the interaction is described as an exchange of *interaction modes* (the classical analogs of virtual gravitons), but contrary to the Born amplitudes, where the simple pole diagrams diverge at high transverse momenta [3], here the sum over these modes contains an intrinsic cut-off. Therefore the classical elastic scattering amplitude is finite and, furthermore, it reproduces the result of the eikonal method, if the eikonal is computed in the stationary phase approximation [25]. In other words, classical calculations in ADD correspond to non-perturbative ones in quantum theory (the eikonal method is equivalent to summation of the ladder diagrams). As will be explicitly demonstrated in the present chapter, the same is true for bremsstrahlung. Specifically, it will be shown that the effective number of interaction modes is finite due to the cut-off and of order $(R/b)^d$. Also, the summation over the *emission modes* is cut-off to a finite effective number of order $(R\gamma/b)^d$, which leads to a large extra enhancement factor γ^d in ultrarelativistic collisions.

Straightforward Fourier transform of (2.2.22) gives

$$ {}^0\Phi^n(p) = -\frac{2\pi f \delta(pu)}{p^2 - p_T^2}. \tag{2.2.36}$$

Similarly, for the h_{MN} and h'_{MN}, it is enough to Fourier transform the source terms (2.2.26) and plug into (2.2.11) and (2.2.12). One then obtains

$$h^n_{MN}(p) = \frac{2\pi \varkappa_D\, m\, \delta(pu)}{p^2 - p_T^2} \mathrm{e}^{i(pb)} \left(u_M u_N - \frac{1}{D-2} \eta_{MN} \right), \tag{2.2.37}$$

where $p^2 = p_\mu p^\mu$, $pu = p_\mu u^\mu$ and $p_T^i = n^i/R$ is the quantized momentum vector in the transverse directions. To get $h'^n_{MN}(p)$, one has to replace $m \to m'$, $u^M \to u'^M, b \to 0$. Note that these fields do not describe radiation. They simply represent the scalar and gravitational potentials of the uniformly moving particles. Formally, this follows from the presence of the delta factors $\delta(pu)$ with $pu = \gamma(p^0 - p_z v)$, from which it follows that $p_\mu p^\mu = p_z^2(v^2 - 1) < 0$, while the mass-shell condition for the emitted wave is $p_\mu p^\mu = p_T^2 \geqslant 0$.

Substitution of (2.2.37) into (2.2.30) and integration of the resulting equation gives

$$ {}^1\!z^M(\tau) = -\frac{im'\varkappa_D^2}{(2\pi)^3 V}\sum_l \int d^4p \frac{\delta(pu')\,\mathrm{e}^{-i(pb)}}{(p^2 - p_T^2)(pu)} \left(\mathrm{e}^{-i(pu)\tau} - 1\right)\left(\gamma u'^M - \frac{1}{d+2}u^M - \frac{\gamma_*^2}{2(pu)}p^M\right), \tag{2.2.38}$$

with $\gamma_*^2 \equiv \gamma^2 - (d+2)^{-1}$ and the D-dimensional vector $p^M = (p^\mu, p_T^i = l^i/R)$. It is easy to check that the gauge condition (2.2.28) is satisfied. To ensure this *exactly* one has to keep the small second term in γ_*^2, which, however, will be dropped in what follows in view of our interest in $\gamma \gg 1$. We have chosen the initial value ${}^1\!z^M(0) = 0$ in order to preserve the meaning of b^μ as the impact parameter, namely $b^\mu = z^\mu(0) - z'^\mu(0)$. Note that the initial value of ${}^1\!\dot{z}^M(0)$ is non-zero and is computed from the gauge condition (2.2.28).

From (2.2.38) one can prove that the gravitational interaction does not expel the particles from the brane. Indeed, only the last p^M-term in the last parenthesis has non-zero components $p_T^i = l^i/R$ orthogonal to the brane. But the remaining expression is even under the reflection $l^i \to -l^i$ and the sum vanishes giving ${}^1\!z^i = 0$ [1].

The corresponding solution for the mass m' can be obtained by interchanging u^M and u'^M, replacing m by m' and omitting $\mathrm{e}^{-i(pb)}$.

2.2.5 $\Phi-$radiation - Basic formulae

Finally, $\Phi-$radiation is described by the wave equation (2.2.33), which in terms of Kaluza-Klein modes is

$$(\Box + k_T^2)\,{}^1\Phi^n(x) = j^n(x) \equiv \rho^n(x) + \sigma^n(x)\,, \tag{2.2.39}$$

where $k_T^i = n^i/R$, while $\rho^n(x)$ and $\sigma^n(x)$ are

$$\rho^n(x) = -f\int {}^1\!z^\mu(\tau)\,\partial_\mu\delta^4(x - u\tau - b)d\tau \tag{2.2.40}$$

[1] This is on the average true also quantum mechanically. The Φ-quanta emission is symmetric on the average under reflection from the brane and the brane stays on the average at rest. However, to guarantee transverse momentum conservation in single Φ emission in the bulk one should introduce brane position collective coordinates and deal also with the brane back reaction.

and

$$\sigma^n(x) = \frac{\varkappa_D}{V}\sum_l \partial_\mu \left(h'^{\mu\nu}_l(x)\, \partial_\nu\, {}^0\Phi_{n-l}(x) - \frac{1}{2} h'_l(x)\, \partial^\mu\, {}^0\Phi_{n-l}(x) \right), \tag{2.2.41}$$

respectively, with ${}^1z^\mu$, ${}^0\Phi$ and $h'_{\mu\nu}$ given in (2.2.38), (2.2.36) and (2.2.37). The rest of this chapter is devoted to the solution of (2.2.39) and the analysis of the spectral and angular distribution of the emitted $\Phi-$radiation.

Once the solution of these equations is available, one can compute the energy and momentum radiated away using the standard formulae of radiation theory. To compute the momentum loss due to scalar bremsstrahlung emitted during the collision one considers the world tube with topology $R^{1,3} \times T^d$, with boundary $\partial\Omega = \Sigma_\infty \cup \Sigma_{-\infty} \cup B$ consisting of two space-like hypersurfaces $\Sigma_{\pm\infty}$ in $R^{1,3}$ at $t = \pm\infty$ and the time-like hypersurface B at $r \to \infty$ and integrate the difference of the fluxes through $\Sigma_{\pm\infty}$ to obtain

$$P^\mu = \int\limits_V d^d y \Bigg(\int\limits_{\Sigma_\infty} - \int\limits_{\Sigma_{-\infty}} \Bigg) T^{\nu\mu} d^3\Sigma_\nu. \tag{2.2.42}$$

Here one makes use of the brane components of the energy-momentum tensor of the bulk scalar (it is easy to show that there is no radiation flux into the compact dimensions [23]). Start with

$$T^{MN} = \partial^M\Phi\partial^N\Phi - \frac{1}{2}\eta^{MN}(\partial\Phi)^2, \tag{2.2.43}$$

where only ${}^1\Phi$ has to be taken into account, since ${}^0\Phi$ is not related to radiation. The integral over B is zero due to fall-off conditions, so the difference of the surface integrals (2.2.42) can be transformed by Gauss' theorem to the volume integral [1]

$$P^\mu = \int\limits_V d^d y \int\limits_\Omega \partial_N T^{N\mu} d^4x = \int\limits_V d^d y \int\limits_\Omega \left(\partial^\mu\Phi\right)\, \Box_D\Phi\; d^4x. \tag{2.2.44}$$

Using (2.2.33) and the retarded Green's function of the $D-$dimensional D'Alembert operator to solve the wave equation

$$G_D(x-x', y-y') = \frac{1}{(2\pi)^4 V}\int d^4k\, \mathrm{e}^{-ik(x-x')} \sum_n \frac{\mathrm{e}^{ik_T(y-y')}}{k^2 - k_T^2 + i\epsilon k^0}, \tag{2.2.45}$$

one obtains

$$P^\mu = \frac{1}{16\pi^3 V}\sum_n \int \frac{d^3k}{k^0}\, k^\mu \left|j^n(k)\right|^2 \Big|_{k^0=\sqrt{\mathbf{k}^2+k_T^2}}, \tag{2.2.46}$$

where $j^n(k)$ is the Fourier-transform of $j^n(x)$ (for precise definition see section 2.6.1) and will be referred to as the *radiation amplitude*. With the parametrization $\mathbf{k} =$

[1] It was taken into account that T^d has no boundary

$|\mathbf{k}|(\sin\theta\cos\varphi,\ \sin\theta\sin\varphi,\ \cos\theta)$ one obtains for the spectral-angular distribution of the emitted energy $E = P^0$:

$$\frac{dE}{d|\mathbf{k}|d\Omega_2} = \frac{1}{16\pi^3 V}\sum_n \mathbf{k}^2|j^n(k)|^2, \quad d\Omega_2 = \sin\theta\, d\theta\, d\varphi. \tag{2.2.47}$$

Therefore, the leading order radiation loss is determined by the Fourier-transform $j^n(k)$ of the source in the four-dimensional wave equation (2.2.33) for ${}^1\Phi^n$ on the mass shell of emitted waves

$$k_\mu k^\mu = k_T^2. \tag{2.2.48}$$

If the impact parameter is small compared to the compactification radius ($b \ll R$), the summation over KK masses can be replaced by integration according to (2.6.9), with integration measure $d^d k_T = k_T^{d-1}\, dk_T\, d\Omega_{d-1}$. Since the radiation amplitude j^n depends only on $|k_T|$, integration over the angles is trivial and gives the volume Ω_{d-1} of the unit $d-1-$dimensional sphere. Therefore,

$$\frac{dE}{d|\mathbf{k}|d\Omega_2} = \frac{\Omega_{d-1}}{2(2\pi)^{D-1}}\int_0^\infty \mathbf{k}^2 k_T^{d-1}\, |j^n(k)|^2\, dk_T. \tag{2.2.49}$$

with n in j^n expressed in terms of k_T, and $k^0 \equiv \omega = \sqrt{\mathbf{k}^2 + k_T^2}$.

When the summation over KK emission modes is replaced by integration, one can compute the emitted energy using directly higher dimensional Minkowski coordinates. Take the coordinate system with angles on the $(D-2)-$dimensional sphere Ω_{D-2}, with ϑ the angle between the $(D-1)-$dimensional vectors $\mathbf{K} = (\mathbf{k}, k_T^i)$ and $\mathbf{u}$, ϕ the polar angle in the plane perpendicular to $\mathbf{u}$ varying from 0 (direction of $\mathbf{b}$) to 2π (see Figure 2.1) and integrate over the angles to obtain [23]

$$\frac{dE}{d\omega d\Omega_{d+2}} = \frac{\omega^{d+2}}{2(2\pi)^{d+3}}|j(k)|^2. \tag{2.2.50}$$

where $\omega \equiv (ku') = k^0 = \sqrt{\mathbf{k}^2 + k_T^2}$ is the higher-dimensional frequency.

2.3 The radiation amplitude

As we have seen, the radiation amplitude $j^n(k)$ is the sum of a local $\rho^n(k)$ and a non-local part $\sigma^n(k)$. These two parts have different dependence on the frequency and the angle θ of the emitted wave with respect to the direction of collision. Both have an intrinsic cut-off at some (angle-dependent) frequency, which in the ultrarelativistic case is high compared to the inverse impact parameter $1/b$. Typically, the two amplitudes cancel each other in some range of angles and frequencies. To obtain the correct expression for their sum one has to carefully take into account non-leading contributions.

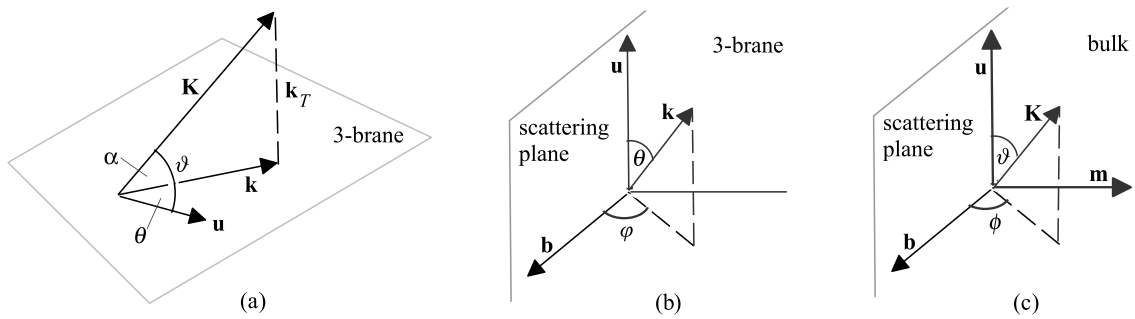

Figure 2.1: The angles in lab frame used in the text.

2.3.1 The local amplitude

Fourier-transformation of (2.2.40) gives

$$\rho^n(k) = i f e^{i(kb)} \int_{-\infty}^{\infty} \mathrm{e}^{i(ku)\tau} (k\,{}^1\!z)\, d\tau \tag{2.3.1}$$

where the scalar products are denoted as $(ab) \equiv a_\mu b^\mu$ and for simplicity the parentheses will also be omitted when it is not ambiguous. Substitution of ${}^1\!z^\mu$ from (2.2.38) and integration over τ gives [1]:

$$\rho^n(k) = \frac{\varkappa_D^2\, m' f \mathrm{e}^{i(kb)}}{4\pi^2 V (ku)^2} \sum_l \left[ku \left(\gamma k u' - \frac{ku}{d+2} \right) I_l - \frac{\gamma_*^2}{2} k_\mu I_l^\mu \right], \tag{2.3.2}$$

where the integrals I_l and I_l^μ are defined by

$$I_l = \int \frac{\delta(pu')\,\delta(ku - pu)\,\mathrm{e}^{-i(pb)}}{p^2 - p_T^2}\, d^4p, \quad I_l^\mu = \int \frac{\delta(pu')\,\delta(ku - pu)\,\mathrm{e}^{-i(pb)}}{p^2 - p_T^2}\, p^\mu\, d^4p, \tag{2.3.3}$$

The sum over l represents the sum over the interaction modes labeled by the set of integers l^i, while the dependence of the amplitude $\rho^n(k)$ on the vector index n, which labels the emission modes n^i, is hidden inside the k^0−component of the wave vector: $k^0 = \sqrt{\mathbf{k}^2 + k_T^2}$. The integrals are given in [23] and lead to Macdonald functions:

$$I_l = -\frac{2\pi}{\gamma v} K_0(z_l), \quad I_l^\mu = -\frac{2\pi}{\gamma v b^2} \left(bz K_0(z_l) \frac{\gamma u'^\mu - u^\mu}{\gamma v} + i \hat{K}_1(z_l)\, b^\mu \right), \tag{2.3.4}$$

with

$$z \equiv \frac{(ku)b}{\gamma v}, \quad z' \equiv \frac{(ku')b}{\gamma v}, \quad z_l \equiv (z^2 + p_T^2 b^2)^{1/2}, \tag{2.3.5}$$

[1] Note that the unity inside the first parenthesis of (2.2.38) corresponds to a constant ${}^1\!z$ and does not contribute to radiation. Formally, its contribution to ρ^n vanishes by symmetric integration [23].

and the hatted Macdonald functions defined by $\hat{K}_\nu(x) \equiv x^\nu K_\nu(x)$ and having for $\nu \neq 0$ a finite non-zero limit as $x \to 0$. Thus, in terms of Macdonald functions the local amplitude is:

$$\rho^n(k) = -\frac{\varkappa_D^2 m' f}{4\pi v V} \mathrm{e}^{i(kb)} \sum_l \left\{ \left[\left(2 - \frac{\gamma_*^2}{v^2\gamma^2} \right) \frac{z'}{z} - \frac{2}{\gamma} \left(\frac{1}{d+2} - \frac{\gamma_*^2}{2v^2\gamma^2} \right) \right] K_0(z_l) - i \frac{\gamma_*^2}{\gamma^2} \frac{(kb)}{v^2\gamma z^2} \hat{K}_1(z_l) \right\}. \tag{2.3.6}$$

2.3.1.1 The $\gamma \to \infty$ limit. Mode and frequency cut-offs.

In the ultrarelativistic limit $\gamma \to \infty$ the leading terms of ρ^n are

$$\rho^n(k) \simeq -\frac{\varkappa_D^2 m' f}{4\pi v V} \mathrm{e}^{i(kb)} \sum_l \left[\frac{z'}{z} K_0(z_l) - i \frac{(kb)}{\gamma z^2} \hat{K}_1(z_l) - \frac{d+1}{(d+2)\gamma^2} \left(\frac{z'}{z} - \frac{\gamma d}{d+1} \right) K_0(z_l) + ... \right] \tag{2.3.7}$$

This is a systematic ultra-relativistic expansion in powers of $1/\gamma$, modulo the coefficients of the various Macdonalds as well as the overall factor in front, which depend on the velocity v. However, as will become evident below, this form is adequate for the following discussion and the computation of the emitted energy to leading order.

Two important general remarks are in order here:

(a) *The effective number N_{int} of interaction modes.* The exponential fall-off of the Macdonald functions at large values of the argument z_l leads to an effective cut-off N_{int} of the number of interaction modes l in the sum. One can estimate the radius p_T^{int} of the sphere in the space of l^i, beyond which the modes can be neglected, by setting

$$(p_T^{\text{int}})^2 b^2 \sim 1, \tag{2.3.8}$$

from which

$$N_{\text{int}} \sim \left(\frac{R}{b} \right)^d \sim \frac{V}{b^d}. \tag{2.3.9}$$

For $N_{\text{int}} \gg 1$, which is the case of interest here, one may use (2.6.9) to obtain [23] $(Z > 0)$

$$\frac{1}{V} \sum_l \hat{K}_\lambda \left(\sqrt{Z^2 + p_T^2 b^2} \right) \simeq \frac{1}{(2\pi)^{d/2} b^d} \hat{K}_{\lambda + d/2}(Z) \tag{2.3.10}$$

and end up with

$$\rho^n(k) \simeq -\frac{\lambda \mathrm{e}^{i(kb)}}{v} \left[\frac{z'}{z} \hat{K}_{d/2}(z) - i \frac{(kb)}{\gamma z^2} \hat{K}_{d/2+1}(z) + \frac{1}{(d+2)\gamma} \left(d - \frac{(d+1)z'}{\gamma z} \right) \hat{K}_{d/2}(z) + ... \right], \tag{2.3.11}$$

where

$$\lambda \equiv \frac{\varkappa_D^2 m' f}{2(2\pi)^{d/2+1} b^d} \,. \tag{2.3.12}$$

(b) *Angular and frequency characteristics.* The local radiation amplitude above in the $b \ll R$ limit is expressed solely in terms of Macdonald functions with argument z. Later, it will be shown that the non-local amplitude contains also Macdonald functions but with argument z'. The exponential fall-off of these functions implies the effective cut-offs $z \sim 1$ and $z' \sim 1$ in the corresponding radiation amplitudes. These, in turn, translate into angular and frequency characteristics of the corresponding radiation.

Specifically, with θ, α and ϑ as shown in Fig. 2.1, define

$$\psi \equiv 1 - v\cos\theta\cos\alpha = 1 - v\cos\vartheta \,, \tag{2.3.13}$$

which satisfies

$$\frac{z}{z'} = \gamma\psi \,, \tag{2.3.14}$$

and in the ultrarelativistic limit varies in the interval $1/2\gamma^2 \simeq 1 - v \leqslant \psi \leqslant 1 + v \simeq 2$.

Consider the neighborhood of $z \sim 1$ which gives the dominant contribution of the local radiation amplitude. One has to distinguish various domains of the emission angles. For small emission angles θ, α one has

$$\psi \sim \frac{1}{2}(\gamma^{-2} + \theta^2 + \alpha^2) \,, \tag{2.3.15}$$

so that (i) inside the *small* cone $\theta^2 + \alpha^2 \lesssim 1/\gamma^2$ one obtains $\psi \sim 1/\gamma^2$, so that the characteristic frequencies $\omega \sim \gamma^2/b$. This angle-frequency regime will be called in the sequel *the z-region*. (ii) For $\psi \sim 1$, i.e. for $\alpha, \theta \sim \mathcal{O}(1)$, one obtains $z' \sim z/\gamma$, which implies a low frequency regime $\omega \sim 1/b$, whose contribution to the emitted energy is negligible in view of the relative smallness of the phase-space factor in (2.2.49).

To summarize, the above analysis of ρ^n combined with the phase space factors in (2.2.49), leads to the conclusion that the leading contribution of the radiation due to the local amplitude is *beamed*, i.e. directed inside the small cone $\theta^2 + \alpha^2 \lesssim 1/\gamma^2$ and has high frequencies $\omega \sim \gamma^2/b$. Radiation with these characteristics will occasionally be called *z-type*.

2.3.2 The non-local amplitude

The non-local amplitude obtained from (2.2.41) by Fourier transform is

$$\sigma^n(k) = \frac{\varkappa_D^2 m' f(ku')^2}{(2\pi)^2}\, \mathrm{e}^{i(kb)} J^n(k) \,, \quad J^n(k) \equiv \frac{1}{V}\sum_l J^{nl}(k) \,, \tag{2.3.16}$$

with

$$J^{nl}(k) = \int d^4p \frac{\delta(pu')\delta(ku - pu)e^{-i(pb)}}{(p^2 - p_T^2)\,[(k-p)^2 - (k_T - p_T)^2]}\,. \tag{2.3.17}$$

$k^0 = \sqrt{\mathbf{k}^2 + k_T^2}$ and $\mathbf{k}$ is a 3−dimensional vector lying on the 3−brane, where $k_T^i = n^i/R$ and $p_T^i = l^i/R$ with integers $\{n^i\}, \{l^i\}$ are d−dimensional discrete vectors corresponding to the emission and interaction modes, respectively.

Using Feynman parametrization J^{nl} takes the form:

$$J^{nl} = \int_0^1 dx\, e^{-i(kb)x} \int d^4p \frac{\delta[(pu') + (ku')x]\delta[(pu) - (1-x)(ku)]\,\mathrm{e}^{-i(pb)}}{[p^2 - (k_T x - p_T)^2]^2}.$$

Integrating over p^0 and splitting $\mathbf{p}$ into the longitudinal $p_{||}$ and transversal $\mathbf{p}_\perp$ parts, integrate over $p_{||}$. Then, introducing in $\mathbf{p}_\perp$ the spherical coordinates $d^2\mathbf{p}_\perp = |\mathbf{p}_\perp| d\Omega_1 d|\mathbf{p}_\perp|$ and integrating first over the angles and then over $|\mathbf{p}_\perp|$, one obtains

$$J^{nl} = \frac{\pi b^2}{\gamma v} \int_0^1 dx\, e^{-i(kb)x}\, \hat{K}_{-1}(\zeta_{nl})\,, \tag{2.3.18}$$

with

$$\zeta_{nl}^2(x) = {z'}^2 x^2 + 2\gamma z z' x(1-x) + z^2(1-x)^2 + b^2(k_T x - p_T)^2\,. \tag{2.3.19}$$

Again, the summation over l is performed trivially for $b \ll R$ using (2.3.10) [1]. The result is

$$J^n(k) = \Lambda_d \int_0^1 dx\, e^{-i(kb)x}\, \hat{K}_{d/2-1}(\zeta_n); \qquad \Lambda_d \equiv \frac{\pi b^{2-d}}{(2\pi)^{d/2}\gamma v}\,. \tag{2.3.20}$$

with

$$\zeta_n^2(x) = {z'}^2 x^2 + 2\gamma z z' x(1-x) + z^2(1-x)^2\,; \qquad \zeta_n(0) = z\,, \quad \zeta_n(1) = z'\,. \tag{2.3.21}$$

Writing ζ_n^2 successively in the form

$$\zeta_n^2(x) = -\xi^2 x^2 + 2\beta x + z^2 = a^2 - r^2\,, \tag{2.3.22}$$

[1] Using (2.6.9) the summation is converted to integration over $d^d l$. One then shifts the integration variable $p'_T = p_T - x k_T$ and applies (2.3.10). In the present case Z is not constant but depends on x. However, as it can also be checked numerically, (2.3.10) and the subsequent treatment is a good approximation for any $0 \leqslant x \leqslant 1$, because $Z(x) \gtrsim 1$ in all relevant frequency regimes.

with

$$\xi^2 \equiv 2\gamma z z' - z^2 - z'^2 = \omega^2 b^2 \sin^2\theta\cos^2\alpha + b^2 k_T^2 = z'^2\gamma^2 v^2 \sin^2\vartheta\,, \quad \beta \equiv \gamma z z' - z^2\,, \tag{2.3.23}$$

and

$$a \equiv \sqrt{\frac{\beta^2}{\xi^2} + z^2}\,, \quad r \equiv \xi\left(x - \frac{\beta}{\xi^2}\right)\,, \tag{2.3.24}$$

and using formula [36, 2.16.12-4]

$$\hat{K}_{\nu-1/2}\left(\sqrt{a^2-r^2}\right) = \frac{2^{1/2}}{\pi^{1/2}} a^{2\nu} \int_0^\infty \cosh(ry)\hat{K}_{-\nu}\left(a\sqrt{y^2+1}\right) dy\,, \quad \nu > -1 \text{ and } a > 0 \tag{2.3.25}$$

for $\mu = -1/2$, $\nu = (d-1)/2$ one may rewrite (2.3.20) in the form

$$J^n(k) = \Lambda_d \frac{2^{1/2} a^{2\nu}}{\pi^{1/2}} \int_0^\infty dy\, \hat{K}_{-\nu}\left(a\sqrt{y^2+1}\right) \int_0^1 dx\, e^{-i(kb)x} \cosh(ry). \tag{2.3.26}$$

Perform, next, the integration over x and introduce the additional angle ϕ, so that the generic $(D-1)$-dimensional unit vector $\mathbf{K}/|\mathbf{K}|$ (the *normalized* higher-dimensional emission vector $\mathbf{K}$) is decomposed as:

$$\frac{\mathbf{K}}{|\mathbf{K}|} = \frac{\mathbf{u}}{|\mathbf{u}|}\cos\vartheta + \frac{\mathbf{b}}{|\mathbf{b}|}\sin\vartheta\cos\phi + \mathbf{m}\sin\vartheta\sin\phi, \tag{2.3.27}$$

where $\mathbf{m}$ is a $D-1$ dimensional unit vector orthogonal to the collision plane (spanned by $\mathbf{u}$ and $\mathbf{b}$). Then $(k\cdot b) = -\gamma z' v \sin\vartheta\cos\phi = -\xi\cos\phi$ and $a = \omega b\psi/\sin\vartheta$. Substituting this into (2.3.26) we have

$$J^n(k) = \Lambda_d \frac{2^{1/2} a^{2\nu}}{\pi^{1/2}} \frac{1}{\xi} \sum_{j=0,1} (-1)^{j+1} e^{-ij(kb)} \times$$
$$\times \int_0^\infty dy\, \hat{K}_{-\nu}\left(a\sqrt{y^2+1}\right) \frac{y\sinh(\xi\delta_j y) - i\cos\phi\cosh(\xi\delta_j y)}{y^2+\cos^2\phi} \equiv J_0^n + J_1^n\,, \tag{2.3.28}$$

where $\delta_j = j - \beta/\xi^2$, $j = 0, 1$. [1] The convergence of these integrals is controlled by the competition of the exponential decay of the Macdonald function and the exponential growth of the hyperbolic functions. In all cases the first is faster, but when the difference

[1]Direct integration of (2.3.20) for $(\theta = 0, k_T = 0)$ gives $\int_0^1 \hat{K}_{d/2-1}(\sqrt{2\beta x + z^2})\, dx = \beta^{-1}[\hat{K}_{d/2}(z) - \hat{K}_{d/2}(z')]$. The constants of integration of the terms $j = 0, 1$ are chosen so that for $\theta = 0$ they satisfy $J_z^n|_{(\theta=0,k_T=0)} = \Lambda_d \beta^{-1}\hat{K}_{d/2}(z)$; $J_{z'}^n|_{(\theta=0,k_T=0)} = -\Lambda_d\beta^{-1}\hat{K}_{d/2}(z')$.

of the two arguments is small, the main contribution to the integral over y comes from large values of y.

Since $y^2+1 \geqslant 1$ and $0 \leqslant \sin^2\phi \leqslant 1$, one can equivalently write

$$J_j^n(k) = (-1)^{j+1} e^{-ij(kb)} \Lambda_d \frac{2^{1/2} a^\nu}{\pi^{1/2}\xi} \times \\ \times \sum_{k=0}^{\infty} \sin^{2k}\phi \int_0^\infty dy\, \frac{K_\nu\left(a\sqrt{y^2+1}\right)}{(y^2+1)^{\nu/2+1+k}} \left[y \sinh(\xi\delta_j y) - i\cos\phi \cosh(\xi\delta_j y)\right].$$

The y-integration for each value of k is performed by successive applications of the identity [34]

$$K_\nu(z) = K_{\nu+2}(z) - \frac{2(\nu+1)}{z} K_{\nu+1}(z) \tag{2.3.29}$$

in combination with

$$a^\nu \int_0^\infty dy\, \frac{K_{\nu+2}\left(a\sqrt{y^2+1}\right)}{(y^2+1)^{(\nu+2)/2}} \left\{ \begin{array}{c} y\sinh(\xi\delta_j y) \\ \cosh(\xi\delta_j y) \end{array} \right\} = \frac{1}{a^2} \left\{ \begin{array}{c} \xi\delta_j \hat{K}_{\nu+1/2}(z_j) \\ \hat{K}_{\nu+3/2}(z_j) \end{array} \right\} \tag{2.3.30}$$

obtained from (2.3.25), with argument $z_j = \sqrt{a^2 - \xi^2\delta_j^2}$, i.e. $z_0 = z, z_1 = z'$.

For example, using (2.3.29) the $k=0$ term leads to the integrals

$$a^\nu \int_0^\infty dy \left[\frac{K_{\nu+2}\left(a\sqrt{y^2+1}\right)}{(y^2+1)^{\nu/2+1}} - \frac{2(\nu+1)}{a} \frac{K_{\nu+1}\left(a\sqrt{y^2+1}\right)}{(y^2+1)^{(\nu+3)/2}} \right] \left\{ \begin{array}{c} y\sinh(\xi\delta_j y) \\ \cosh(\xi\delta_j y) \end{array} \right\}. \tag{2.3.31}$$

The first term in the square brackets is given by (2.3.30). The second is computed using again (2.3.29), which leads to two new integrals, the first of which is

$$a^{\nu-1} \int_0^\infty dy\, \frac{K_{\nu+3}\left(a\sqrt{y^2+1}\right)}{(y^2+1)^{(\nu+3)/2}} \left\{ \begin{array}{c} y\sinh(\xi\delta_j y) \\ \cosh(\xi\delta_j y) \end{array} \right\} = \frac{1}{a^4} \left\{ \begin{array}{c} \xi\delta_j \hat{K}_{\nu+3/2}(z_j) \\ \hat{K}_{\nu+5/2}(z_j) \end{array} \right\}, \tag{2.3.32}$$

suppressed for $a \gg 1$ compared to (2.3.30). Similarly, the second is further suppressed by two more powers of a. Terms with increasing k are evaluated in the same way and lead to further suppression by inverse powers of a^2.

The end result for $J_0^n(k)$ keeping terms up to $1/a^4$ is then

$$J_0^n(k) = \frac{\Lambda_d}{a^2\xi^2} \left(\beta\hat{K}_{d/2}(z) - i(kb)\hat{K}_{d/2+1}(z) - \frac{(d+1)\beta}{a^2}\hat{K}_{d/2+1}(z) + \frac{\beta\sin^2\phi}{a^2}\hat{K}_{d/2+2}(z) \right) + R_z\,. \tag{2.3.33}$$

Notice that $J_0^n(k)$ is a series of Macdonalds with argument z. Consequently, it is important mainly in the z-region, where $a = \omega b\psi/\sin\vartheta \sim \gamma \gg 1$, a self-consistency check of our approximations. The coefficients of all terms in (2.3.33) have expansions in powers of γ^{-1}. In the z-region the first term starts with $\mathcal{O}(\gamma^{-3})$, the second with $\mathcal{O}(\gamma^{-4})$, the third and fourth terms with order $\mathcal{O}(\gamma^{-5})$, while the remainder $R_z = \mathcal{O}(\gamma^{-6})$.

Following the same procedure $J_1^n(k)$ is written as a series of Macdonald functions with argument z', namely

$$J_1^n(k) \simeq \Lambda_d \, \mathrm{e}^{-i(kb)} \left(\frac{\delta_1}{a^2} \hat{K}_{d/2}(z') - i \frac{\cos\phi}{a^2 \, \xi} \hat{K}_{d/2+1}(z') \right) + R_{z'} \,, \tag{2.3.34}$$

whose main contribution comes from the region with $z' \sim 1$, i.e. $\omega \sim \gamma/b, \vartheta \sim 1$, in which indeed $a \sim \gamma \gg 1$.

The condition $a^2 \gg 1$ is not satisfied in the region with $\theta \sim 1/\gamma$. However, in that region both the exact expression and the approximate one have negligible contribution to the amplitude. Figure 2.2 displays graphically the maximal difference in the real part of $J_1^n(k)$ between the two expressions.

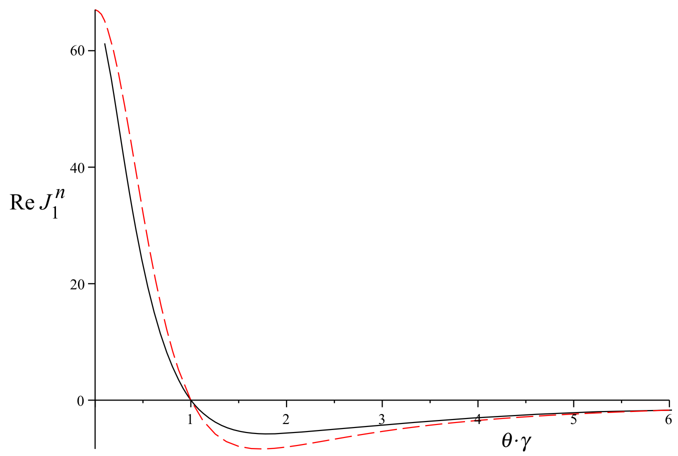

Figure 2.2: The real part of the amplitude J_1^n (solid line) in $D = 4$ dimensions, calculated numerically from the exact formula (2.3.28), compared with the approximation given by (2.3.34) (dashed) for $\gamma = 1000$ and for $\cos\phi = 1$, which gives the largest deviation between the two. For $\gamma\theta \gtrsim 4$ the deviation is negligible. For $\gamma\theta \lesssim 4$ the exact expression will be used numerically. The imaginary part has similar behavior, and furthermore is suppressed compared to the real part by inverse powers of γ.

Incidentally, notice that there is no strong anisotropy in ϕ in the z'−region: the real part of main terms of J_1^n (2.3.34) is independent on ϕ, while its imaginary part depends only by the overall factor $\cos\phi$. The same picture was obtained without any approximations in [23], where scalar mediated collisions were studied.

Going back to (2.3.16) one sees that $\sigma^n(k)$ is the sum of two sets of Macdonald functions, one with argument z and the other with argument z'. In analogy with ρ^n, the first sum contributes mainly in the z-region. Similarly, the leading contribution of the second set of Macdonalds comes from the region with $z' = \omega b/\gamma v \sim \mathcal{O}(1)$. In the ultrarelativistic limit this translates into angular and frequency characteristics of the emitted radiation. For generic values of the angles, this means $\omega \sim \gamma/b$ and defines what we will call the z'*−region* and, correspondingly, z'*−type* radiation. It is unbeamed radiation ($\vartheta \sim 1$) with characteristic frequency $\omega \sim \gamma/b$.

The non-local pieces $\sigma_0^n(k)$ and $\sigma_1^n(k)$. It is convenient to separate the two kinds of contributions to the non-local amplitude by writing

$$\sigma^n(k) \equiv \sigma_0^n(k) + \sigma_1^n(k)\,, \tag{2.3.35}$$

with the first (second) given by (2.3.16) with J_0^n (J_1^n) on the right hand side. Thus,

$$\sigma_0^n(k) = \lambda\, e^{i(kb)}\, \frac{\gamma v z'^2}{a^2\,\xi^2}\Big(\beta \hat{K}_{d/2}(z) - i(kb)\hat{K}_{d/2+1}(z) - \frac{(d+1)\beta}{a^2}\hat{K}_{d/2+1}(z) + \frac{\beta \sin^2\phi}{a^2}\hat{K}_{d/2+2}(z)\Big)\,, \tag{2.3.36}$$

and

$$\sigma_1^n(k) \simeq \lambda \frac{\gamma v z'^2}{a^2\,\xi^2}\left((\xi^2 - \beta)\,\hat{K}_{d/2}(z') + i(kb)\,\hat{K}_{d/2+1}(z')\right)\,, \tag{2.3.37}$$

respectively.

Correspondingly, the total radiation amplitude $j^n(k)$ is written as a sum of two terms, one function of z, and the other function of z'

$$j^n(k) \equiv j_z^n(k) + j_{z'}^n(k)\,,\;\; j_z^n(k) = \rho^n(k) + \sigma_0^n(k)\,,\;\; j_{z'}^n(k) = \sigma_1^n(k) \tag{2.3.38}$$

2.3.3 The part $j_z^n(k)$ of the radiation amplitude and destructive interference

2.3.3.1 j_z^n in the frequency range $\omega \gg \gamma/b$

Consider first the regime with $\vartheta \sim 1$. Here $z \sim \gamma$ and from (2.3.36) and (2.3.11) one obtains that $j_z^n \sim \exp(-\gamma)$ due to the Macdonald functions.

Now take the most interesting case of $\vartheta \sim 1/\gamma$, in which $z \sim 1$. Add $\rho^n(k)$ and $\sigma_0^n(k)$ given in (2.3.11) and (2.3.36), respectively, and use the ultra-relativistic expansions to obtain in leading order:

$$j_z^n(k) \simeq \frac{\lambda\,(d+1)\mathrm{e}^{i(kb)}}{\gamma\psi}\left[\frac{2\psi-\gamma^{-2}}{d+2}\hat{K}_{d/2}(z) - \frac{\cos^2\alpha}{\psi^2\omega^2 b^2}\left(\left(\sin^2\theta+\tan^2\alpha\right)\hat{K}_{d/2+1}(z) - \frac{\sin^2\theta\sin^2\varphi+\tan^2\alpha}{d+1}\,\hat{K}_{d/2+2}(z)\right)\right]. \quad (2.3.39)$$

All terms inside the square brackets are of $\mathcal{O}(\gamma^{-2})$. Given that in the z-region $1/\gamma\psi = z'/z \sim \mathcal{O}(\gamma)$, the leading contribution to j_z^n above is of $\mathcal{O}(\gamma^{-1})$. Higher order terms have been ignored. The terms of order $\mathcal{O}(\gamma)$ and $\mathcal{O}(1)$, both present in the ultra-relativistic expansions of $\sigma_0^n(k)$ and $\rho^n(k)$, have opposite signs and cancel in the sum. This is a general phenomenon of *destructive interference* related to the gravitational interaction. Thus, the two leading powers in the ultra-relativistic expansion of the direct $\Phi-$emission amplitude from the accelerated charged particle, cancel the ones coming from the indirect emission due to the $\Phi-\Phi-h$ interaction. As a consequence, the z-type (beamed and high frequency) part of the radiation is highly suppressed in the ultra-relativistic limit, compared to the naive expectation. One can check that destructive interference is valid also in the case of $\Phi-$radiation in arbitrary $D-$dimensional Minkowski space-time, which can be obtained as a limit of the present discussion. It was first observed for gravitational radiation in $D=4$ [30] (using a different approach) and it was recently generalized to arbitrary dimensions in [24] . For the system at hand, an alternative proof is presented in section 2.7, using a different approach also suitable to the frequency range $\omega \gg \gamma/b$.

The following comments are in order here: (a) As a check of the above series of approximations, one may consider the special case of $\theta=0$, for which $(kb)=-\xi=0$. In this case the exact value of J^n obtained from (2.3.20) coincides with the one obtained from the approximate expressions (2.3.33) and (2.3.34). (b) Furthermore, equation (2.3.39) can be shown to coincide with the corresponding quantity in the case of non-compactified $D=4+d-$dimensional Minkowski space. This generalizes to scattering and radiation processes in the relativistic case, the non-relativistic argument about the behavior of Newton's potential, i.e. that at distances $b \ll R$ a point particle generates the $D-$dimensional potential, while at $b \gg R$ its potential behaves as four-dimensional [35].

One may equivalently parametrize j_z^n using the angles ϑ and ϕ and write it in the form:

$$j_z^n(k) = \frac{\lambda\,\mathrm{e}^{i(kb)}}{\gamma\psi}\left[\frac{d+1}{d+2}\,(2\psi-\gamma^{-2})\hat{K}_{d/2}(z) - \frac{\sin^2\vartheta}{z^2}\left((d+1)\hat{K}_{d/2+1}(z) - \sin^2\phi\,\hat{K}_{d/2+2}(z)\right)\right]. \quad (2.3.40)$$

Note that in the computation of the emitted energy below both angles will be taken continuous; a sensible approximation for $N_{\rm int} \gg 1$ assumed here.

2.3.3.2 j^n_z in the frequency range $\omega \lesssim \gamma/b$

For $\omega \ll \gamma/b$ and $\vartheta \sim 1/\gamma$ using (2.3.11) for ρ^n and (2.3.16) and (2.3.20) for σ^n, one concludes that $|\rho^n| \gg |\sigma^n|$ and, therefore,

$$j^n(k)\Big|_{\omega\ll\gamma/b} \simeq \rho^n(k) \simeq -\lambda\left[\frac{1}{\gamma\psi}\hat{K}_{d/2}(z) + i\frac{\sin\vartheta\cos\phi}{\gamma\psi^2\omega b}\hat{K}_{d/2+1}(z)\right]. \qquad (2.3.41)$$

For $\vartheta \sim 1$, on the other hand, ρ^n, σ^n_0 and σ^n_1 are all of the same order, but suppressed compared to the previous case. In addition, the contribution of this regime to the emitted energy will be shown to be further suppressed by the integration measure.

More interesting is the case with $\omega \sim \gamma/b$. If $\vartheta \sim 1$, then $z \sim \gamma$ and using (2.3.11) and (2.3.36) one concludes that j^n_z is exponentially suppressed because of the Macdonald functions. However, for $\vartheta \sim 1/\gamma$, one may use (2.3.11) and (2.3.28) to obtain that $\rho^n \sim \gamma$ and $\sigma^n_0 \sim \gamma$, respectively [1].

2.3.4 The part $j^n_{z'}(k)$ of the amplitude

Equation (2.3.37) can equivalently be written in the form:

$$j^n_{z'} \simeq -\frac{\lambda}{\gamma\psi}\left[\left(\frac{1}{\gamma^2\psi} - 1\right)\hat{K}_{d/2}(z') + i\frac{\sin\theta\cos\alpha\cos\varphi}{\gamma z'\psi}\hat{K}_{d/2+1}(z')\right] \qquad (2.3.42)$$

Furthermore, using the angles ϑ and ϕ it becomes:

$$j^n_{z'} \simeq -\frac{\lambda}{\gamma\psi}\left[\left(\frac{1}{\gamma^2\psi} - 1\right)\hat{K}_{d/2}(z') + i\frac{\sin\vartheta\cos\phi}{\gamma z'\psi}\hat{K}_{d/2+1}(z')\right] \qquad (2.3.43)$$

First, for $\omega \gg \gamma/b$ one has $z' \gg 1$ and, consequently, $j^n_{z'}$ in (2.3.43) is exponentially suppressed. Next, for ($\omega \sim \gamma/b$, $\vartheta \sim 1$) $j^n_{z'}$ in (2.3.43) is dominated by its real part which is of order $\mathcal{O}(1/\gamma)$. For ($\omega \ll \gamma/b$, $\vartheta \sim 1$) one obtains $j^n_{z'} \sim \sigma^n_0 \sim 1/\gamma$. As will be shown below, however, this region contributes negligibly little to the emitted energy. Similarly, for ($\omega \ll \gamma/b$, $\vartheta \sim 1/\gamma$) on the basis of (2.3.11) and (2.3.20) one concludes that the amplitude $j^n_{z'} \sim \sigma^n_0 \ll \rho^n \sim \gamma^2$. Finally, based on numerical study and previous results in $D = 4$ [30] one obtains that (2.3.43) is valid also in the regime ($\omega \sim \gamma/b$, $\vartheta \sim 1/\gamma$) and gives $j^n_{z'} \sim \gamma$.

[1] Using the formulae of section 2.6.3 one gets in this kinematical regime $a = z'\gamma\psi/\sin\vartheta \sim 1$ and also $\xi \sim 1$ as well as $\beta \sim 1$. The integrand in (2.3.28) is independent of γ. All γ dependence comes from the overall coefficients in (2.3.28) and (2.3.16).

2.3.5 Summary

The behavior of the local and non-local currents in all characteristic frequency and angular regimes is summarized in the following Table I.

ϑ \ ω	$\omega \ll \gamma/b$	$\omega \sim \gamma/b$	$\omega \gg \gamma/b$
γ^{-1}	no destructive interference $j^n \sim \rho^n \gg \sigma_0^n \sim \sigma_1^n$	no destructive interference $j_z^n \sim \rho^n \sim \sigma_0^n \sim \gamma$ $j_{z'}^n = () \sim \gamma$	destructive interference $j_z^n = () \sim \rho^n/\gamma^2 \sim 1/\gamma$ $j_{z'}^n = () \sim \exp(-\gamma)$
1	no destructive interference $j^n \sim \rho^n \sim j_z^n \sim j_{z'}^n$	destructive interference $j_z^n = (\,+\,) \sim \exp(-\gamma)$ $j_{z'}^n = () \sim \gamma^{-1}$	destructive interference $j_z^n = (\,+\,) \sim \exp(-\gamma)$ $j_{z'}^n = () \sim \exp(-\gamma)$

2.4 The emitted energy - Spectral and angular distribution

The spectral and angular distribution of the emitted energy is obtained from (2.2.49) or (2.2.50). The integrand is the sum of three pieces proportional to $|j_z^n(k)|^2$, $|j_{z'}^n(k)|^2$ and $\overline{j_z^n} j_{z'}^n + j_z^n \overline{j_{z'}^n}$ (the bar denotes complex conjugation), so the total radiated energy splits into three parts

$$dE = dE^z + dE^{z'} + dE^{zz'} \,, \tag{2.4.1}$$

which will be called $z-$, $z'-$ and $zz'-$radiation, respectively. All terms contain a factor of λ^2 from the square of the amplitude, an explicit $1/2(2\pi)^{(d+3)}$ from the Fourier transform in (2.2.50), and a factor $b^{-(d+3)}$ from the corresponding power of ω in the integrand. This leads to a general expression for the total emitted energy of the form

$$E \sim \frac{1}{8(2\pi)^{2d+5}} \frac{\varkappa_D^4 m'^2 f^2}{b^{3d+3}} \gamma^{\#} \,, \tag{2.4.2}$$

with an overall coefficient expected to be of order one and the power of gamma depending on the particular type of radiation under discussion and which is easily determined as follows: As argued above and in [30] and also shown for example in Figure 2.3 (obtained numerically), the $\Phi-$radiation is emitted predominantly in well-defined relatively narrow frequency and angular windows, and with amplitudes shown in Table I. Thus, it is straightforward to estimate the powers of γ in the various components of its energy, using (2.2.50)

$$E \sim \int d\omega \int d\vartheta \, |j|^2 \, \omega^{d+2} \sin^{d+1} \vartheta \tag{2.4.3}$$

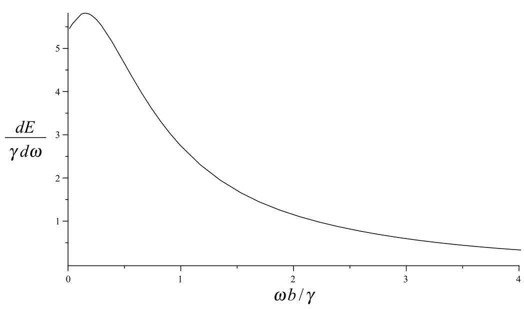

(a)

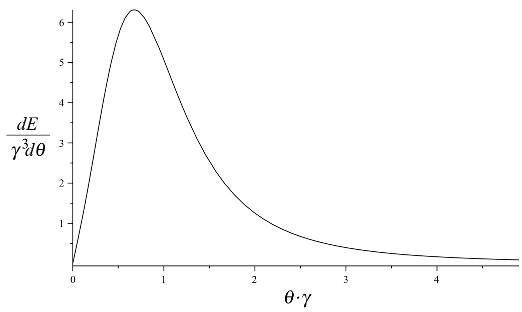

(b)

Figure 2.3: Frequency (a) and angular (b) distribution for $d = 0$ and $\gamma = 10^5$.

with $|j|^2$ being $|j_z^n|^2$ or $|j_{z'}^n|^2$ or $\overline{j_z^n} j_{z'}^n + j_z^n \overline{j_{z'}^n}$, and with the range of integration not contributing extra factors of γ. For example, the contribution of j_z^n, which is dominant in the regime $(\omega \sim \gamma^2/b, \vartheta \sim 1/\gamma)$ has $1/\gamma^2$ from $|j_z^n|^2$, $(1/\gamma)^{d+2}$ from the angular integration, and $(\gamma^2)^{d+3}$ from the integration over ω, with the final estimate being γ^{d+2}.

The result of this computation is the content of Table II below [1].

ϑ \ ω	$\omega \ll \gamma/b$	$\omega \sim \gamma/b$	$\omega \sim \gamma^2/b$	$\omega \gg \gamma^2/b$
γ^{-1}	negligible (phase space)	$E_d \sim \gamma^3$, from j_z^n and $j_{z'}^n$	$E_d \sim \gamma^{d+2}$, from j_z^n	negligible radiation
1	negligible (phase space)	$E_d \sim \gamma^{d+1}$, from $j_{z'}^n$	negligible radiation	negligible radiation

We proceed next to the detailed study of the various components of radiation with the frequency and angular characteristics of the three most important cells of Table II.

2.4.1 The $z-$type component of radiation with $\omega \sim \gamma^2/b$

According to Table II, the z-type radiation (due to $|j_z^n|^2$) is always beamed inside $\vartheta \sim 1/\gamma$. Furthermore, for $d \geqslant 2$ it is dominant with characteristic frequency $\omega \sim \gamma^2/b$. The cases $d = 0$ and $d = 1$ will be treated separately in another subsection.

[1] Note that in $D = 4$ it is found that all three types of radiation are of equal $\mathcal{O}(\gamma^3)$. This seems to disagree with [30], where it is stated that the leading $\mathcal{O}(\gamma^3)$ is due to $z'-$type alone.

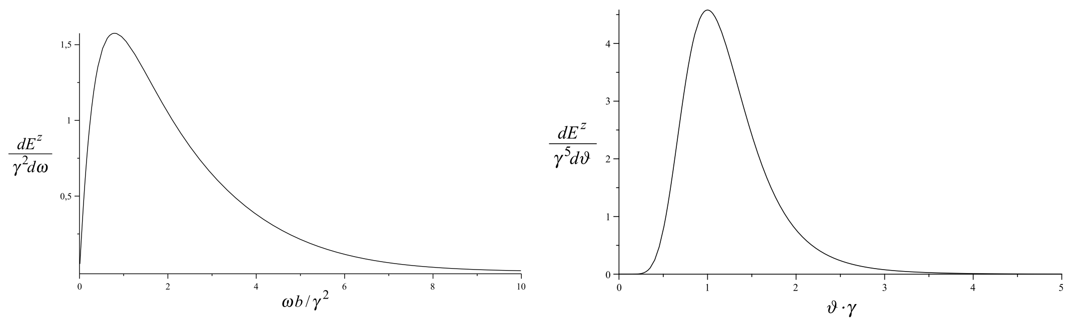

(a) (b)

Figure 2.4: Frequency (a) and angular (b) distribution of z-radiation for $d = 3$ and $\gamma = 10^3$.

It is convenient to write the current j_z (2.3.40) in the form

$$j_z^n = \mathrm{e}^{i(kb)} \sum_{s=0}^{2} {}^s j_z \tag{2.4.4}$$

$$ {}^0 j_z = \frac{\lambda}{\gamma} \frac{d+1}{d+2} \left(2 - \frac{1}{\gamma^2 \psi} \right) \hat{K}_{d/2}(z) \tag{2.4.5}$$

$$ {}^1 j_z = -\lambda \, (d+1) \frac{\sin^2 \vartheta}{\gamma \psi z^2} \hat{K}_{d/2+1}(z) \tag{2.4.6}$$

$$ {}^2 j_z = \lambda \, \frac{\sin^2 \vartheta \sin^2 \phi}{\gamma \psi z^2} \hat{K}_{d/2+2}(z) \tag{2.4.7}$$

Squaring and substituting into (2.2.50) one obtains

$$\frac{dE^z}{d\omega d\Omega_{d+2}} = \frac{\omega^{d+2}}{2(2\pi)^{d+3}} \sum_{a,b=0}^{2} {}^a j_z {}^b j_z \, . \tag{2.4.8}$$

To integrate over frequencies it is convenient to change variable from ω to z and define the quantities

$$C_{ab}^{(d)} = \int \hat{K}_{d/2+a}(z) \hat{K}_{d/2+b}(z) z^{d+2(\delta_{0a}+\delta_{0b}-1)} dz. \tag{2.4.9}$$

The integration over ϑ is performed using (2.6.11). Finally, the integration of $\sin^2\phi$ and $\sin^4\phi$ over the remaining angles of S^{d+1} is $\Omega_{d+1}/2$ and $3\Omega_{d+1}/8$, respectively. The angular and frequency profiles of this component of radiation in dimensions $d \geqslant 2$, for which it is dominant, were obtained analytically and numerically, respectively, and have the general form shown for $d = 3$ in Figure 2.4.

The end result for the total emitted energy in this component of radiation is

$$E^z = \frac{\lambda^2 \Omega_{d+1}}{2(2\pi\, b)^{d+3}}\, \gamma^{d+2} \sum_{a,b=0}^{2} C_{ab}^{(d)} D_{ab}^{(d)} \tag{2.4.10}$$

where

$$\begin{aligned}
D_{00}^{(d)} &= \frac{2^{d+1}(d+1)^2\,\Gamma^2\left(\frac{d+2}{2}\right)}{\Gamma(d+4)}, & D_{01}^{(d)} &= -\frac{2^{d+3}(d+1)^2\Gamma^2\left(\frac{d+4}{2}\right)}{(d+2)\Gamma(d+4)},\\
D_{02}^{(d)} &= -\frac{1}{2(d+1)} D_{01}^{(d)}, & D_{11}^{(d)} &= \frac{2^{d+4}(d+1)^2\Gamma\left(\frac{d+6}{2}\right)\Gamma\left(\frac{d+4}{2}\right)}{\Gamma(d+5)},\\
D_{12}^{(d)} &= -\frac{1}{2(d+1)} D_{11}^{(d)}, & D_{22}^{(d)} &= \frac{3}{8(d+1)^2} D_{11}^{(d)}\,.
\end{aligned} \tag{2.4.11}$$

When integrating over z in (2.4.9) one should remember that the expansion (2.3.40) is accurate in the high frequency domain, around and beyond $z \sim 1$. However, for $d \geqslant 2$ it can be checked both analytically and numerically that the integral from 0 to 1 of the difference of the exact energy density based on (2.3.11) and (2.3.28) and the approximate one based on (2.4.4) is negligible. Thus, one can conveniently expand the integration region in (2.4.9) from 0 to ∞ and evaluate $C_{ab}^{(d)}$ using (2.6.13).

Collecting all contributions one obtains for the energy of high frequency $z-$type radiation

$$E^z = C_d \frac{\varkappa_D^4 m'^2 f^2}{b^{3d+3}} \gamma^{d+2} \tag{2.4.12}$$

with $C_2 = 1.42 \times 10^{-6}$, $C_3 = 6.02 \times 10^{-7}$, $C_4 = 3.45 \times 10^{-7}$, $C_5 = 2.67 \times 10^{-7}$ and $C_6 = 2.76 \times 10^{-7}$.

2.4.2 The $z'-$type radiation with $\vartheta \sim 1$

According to Table II, wide angle radiation ($\vartheta \sim 1$) is mainly z'-type (due to $|j_{z'}^n|^2$) in all dimensions and has characteristic frequency $\omega \sim \gamma/b$. Also, for $d \geqslant 3$ radiation with $\omega \sim \gamma/b$ is predominantly emitted in wide angles.

Squaring (2.3.43), substituting into (2.2.50) and integrating over ω from 0 to ∞ and all angles except ϑ, one gets the angular distribution

$$\frac{dE^{z'}}{d\vartheta} = \frac{\varkappa_D^4 m'^2 f^2 \gamma^{d+1}}{b^{3d+3}} \frac{\Gamma\left(\frac{3d+3}{2}\right)\Gamma^2\left(\frac{2d+3}{2}\right)\Gamma\left(\frac{d+3}{2}\right)}{2^7 \pi^{3d/2+4}\Gamma\left(\frac{d+2}{2}\right)\Gamma(2d+3)} \frac{\sin^{d+1}\vartheta}{\psi^2}\,. \tag{2.4.13}$$

Formula (2.4.13) gives the dominant wide angle radiation in all dimensions $d \geqslant 3$. Figure 2.5 shows the angular and frequency profile of this component of radiation for $d = 3$. To compute the total energy of this type we integrate over ϑ making use of (2.6.12).

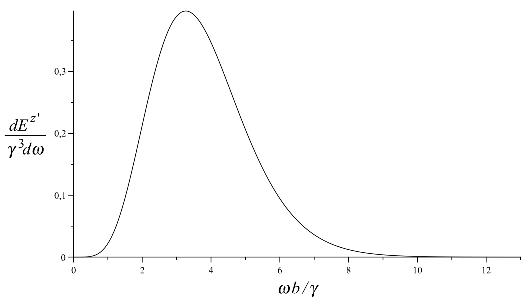

(a)

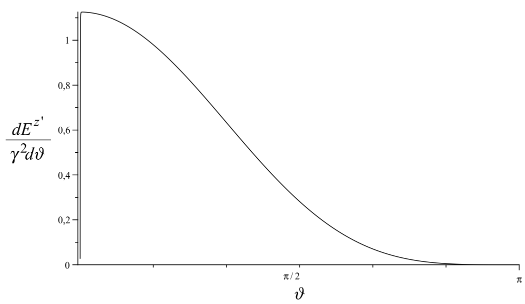

(b)

Figure 2.5: Frequency (a) and angular (b) distribution of z'-radiation for $d = 3$ and $\gamma = 10^4$. The angular distribution is actually smooth, but rises very steeply at this scale for $\vartheta \simeq 0$.

For $d \geqslant 3$ the emitted energy is given by

$$E^{z'} = C'_d \frac{\kappa_D^4 m'^2 f^2}{b^{3d+3}} \gamma^{d+1}, \qquad C'_d = \frac{2^{d-8}\Gamma\left(\frac{3d+3}{2}\right)\Gamma^2\left(\frac{2d+3}{2}\right)\Gamma\left(\frac{d+3}{2}\right)\Gamma\left(\frac{d-2}{2}\right)}{\pi^{3d/2+4}\Gamma(2d+3)\Gamma(d)} \tag{2.4.14}$$

For $d = 2$ one obtains

$$E^{z'} = \frac{105\varkappa_6^4 m'^2 f^2}{2^{16}(2\pi)^7 b^9}\gamma^3 \ln\gamma\,. \tag{2.4.15}$$

The cases $d = 0, 1$ have to be considered separately since for them z-, z'- and zz'-types of radiation are comparable and splitting the amplitude into j_z and $j_{z'}$ is not particularly useful.

2.4.3 The cases d=0, 1

According to Table II the emitted energy in 4D is concentrated in the region $\omega \sim \gamma/b$, $\theta \sim \gamma^{-1}$. In this case the exponent $e^{i\,x\,\omega b \sin\vartheta\cos\varphi}$ in the stress amplitude $\sigma(k)$ does not oscillate fast and the emitted energy may be easily computed numerically. The frequency and ϑ-distributions in this case are shown for $\gamma = 10^5$ in Figure 2.3, while the distribution over ϕ (which coincides with φ in 4D) is presented by Figure 2.6.

The total emitted energy is

$$E_0 = C_0 \frac{\varkappa_4^4 m'^2 f^2}{b^3}\gamma^3, \qquad C_0 \approx 8.3\times 10^{-5}\,. \tag{2.4.16}$$

The frequency distribution is non-zero at $\omega = 0$ (see Figure 2.3), in agreement with the analytically derived value

$$\left.\frac{dE_0}{d\omega}\right|_{\omega=0} = \frac{1}{3\times 2^6\times\pi^4}\frac{\varkappa_4^4 m'^2 f^2}{b^2}\gamma^2,$$

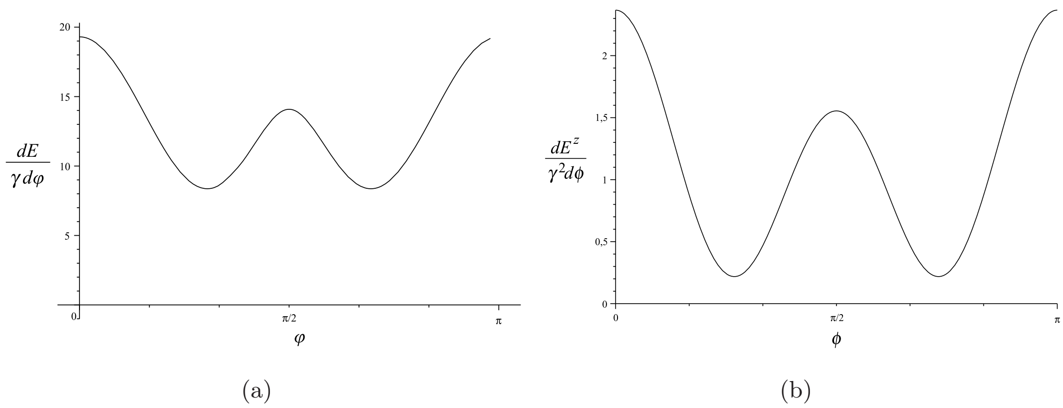

Figure 2.6: (a) The $\phi-$distribution in 4D for $\gamma = 10^4$ and (b) in 6D for $\gamma = 10^3$.

due mainly to the imaginary part of the $\rho-$amplitude.

The frequency distribution of the emitted energy E_1 in 5D for $\gamma = 10^4$ is shown in Figure 2.7. It is characterized by a long tail beyond the value $\omega \sim \gamma/b$, which as can also be argued analytically [1] leads to a behavior $dE_1/d\omega \sim 1/\omega$ (Figure 2.7(b)) all the way to $\omega \sim \gamma^2/b$, beyond which it falls-off exponentially. The integral of $dE_1/d\omega$ over the range $(\gamma/b, \gamma^2/b)$ gives an extra logarithm in the total emitted energy, which is computed numerically to be

$$E_1 = C_1 \frac{\varkappa_5^4 m'^2 f^2}{b^6} \gamma^3 \ln \gamma\,, \qquad C_1 \approx 1.64 \times 10^{-5}\,. \tag{2.4.17}$$

2.4.4 The estimate of the $zz'-$interference part of radiation

The purpose of this subsection is to estimate the contribution of the interference part $(j_z^n \, \overline{j_{z'}^n} + c.c.)$. It will be shown that it is subleading for $d \geqslant 2$ and of the same order as $z-$ and $z'-$ contributions for $d = 0, 1$.

The interference term $E^{zz'} \sim \int (j_z^n \, \overline{j_{z'}^n} + c.c.)\, \omega^{d+2}\, d\omega\, d\Omega_{d+2}$ contains the product of Macdonald functions $\hat{K}(z)\hat{K}(z')$. Thus, its value depends on the overlap of these functions in the domain ($z \lesssim 1$, $z' \lesssim 1$), or equivalently ($\omega \lesssim \gamma/b$, $\vartheta \lesssim 1/\sqrt{\gamma}$). The presence of the factor ω^{d+2} implies that most of the contribution to the integral comes from the large ω regime with $\omega \sim \gamma/b$, in which $z' \sim 1$.

For $z \ll 1/\gamma$ the integral is suppressed by the volume factor. Thus, the interesting regime of z is $\gamma^{-1} \lesssim z \lesssim 1$. In this regime one may estimate the contribution to the

[1] Notice from Table I that the total amplitude satisfies $j(\omega \sim \gamma/b) \sim \gamma^2 j(\omega \sim \gamma^2/b)$. This gives for $d = 1$ the estimate $|j|^2\omega^{d+2} \sim 1/\omega$.

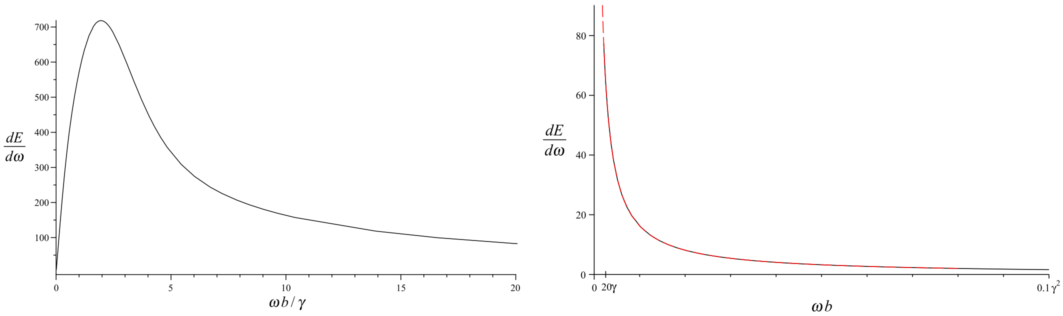

(a)

(b) Intermediate region $\omega b = 20\gamma - 0.1\gamma^2$: exact distribution (solid black) versus the approximate $dE/d\omega \sim 1/\omega$ (dashed red)

Figure 2.7: Frequency distribution for $d = 1$ and $\gamma = 10^4$: (a) for $\omega \lesssim \gamma/b$, (b) for $\gamma/b \lesssim \omega \lesssim \gamma^2/b$

interference integral using

$$j_z \sim \frac{\lambda e^{i(kb)}}{2} \frac{\sin^2\vartheta}{\gamma\psi z^2} \hat{K}_{d/2+1}(z)\,, \qquad j_{z'} \sim \frac{\lambda}{\gamma\psi} \hat{K}_{d/2}(z')\,, \tag{2.4.18}$$

since, it can be checked from (2.3.11), (2.3.36) and (2.3.43), that they are either dominant or of the same order as the remaining terms.

One then obtains for the interference part of the energy loss

$$\frac{dE^{zz'}}{d\Omega_{d+2}\, d\omega} \sim \frac{\lambda^2 \cos(\omega b \sin\vartheta \cos\phi)}{2(2\pi)^{d+3}\gamma^2\psi^2 z^2} \hat{K}_{d/2+1}(z)\hat{K}_{d/2}(z') \sin^2\vartheta\, \omega^{d+2}\,. \tag{2.4.19}$$

Integration over all angles except ϑ gives

$$\frac{dE^{zz'}}{d\vartheta\, d\omega} \sim \frac{\lambda^2}{2^{d+2}\pi^{(d+3)/2}\Gamma((d+1)/2)\gamma^2\psi^2 z^2} J_0(\omega\, b \sin\vartheta)\, \hat{K}_{d/2+1}(z)\, \hat{K}_{d/2}(z')\, \omega^{d+2} \sin^{d+3}\vartheta. \tag{2.4.20}$$

The value of the integral over ϑ and ω is controlled by J_0. For $\vartheta \sim 1/\sqrt{\gamma}$, z and z' are both of $\mathcal{O}(1)$, while the argument of J_0 is of $\mathcal{O}(\sqrt{\gamma}) \gg 1$. Using then the asymptotic expansion of J_0 and approximating the hatted Macdonalds by their values at $z \sim z' \sim 1$, one can estimate as in previous cases the power of γ in $E^{zz'}$ to be $\gamma^{d/2+3/4}$. This is negligible, compared to the other contributions in all dimensions.

One is left with the contribution from $\vartheta \sim 1/\gamma$, where $\omega\, b \sin\vartheta \sim 1$ and $z \sim 1/\gamma$. Substituting $J_0 \sim J_0(0) = 1$ and $\hat{K}(z) \simeq \hat{K}(z = 0)$ one estimates the integral to be of $\mathcal{O}(\gamma^3)$ in all dimensions. This is of the same dominant order as E^z and $E^{z'}$ for $d = 0$ and $d = 1$ and was included in the total energy evaluated in the previous subsection.

2.5 Summary of results

Scalar bremsstrahlung radiation during the transplanckian collision of two gravitating massive point particles in arbitrary dimensions was studied classically in the laboratory frame. The main goal was to compute the powers of the Lorentz factor γ and how they depend on the number of extra dimensions d.

We computed both analytically and numerically radiation into truly massless and massive (for the brane observer) modes. An essential difference with the previously considered case of scalar bremsstrahlung in flat space from particles interacting via a scalar field, is that in the latter the scalar field(s) is linear, while here the bulk scalar interacts non-linearly with gravity. Within the perturbation theory with respect to both scalar and gravitational coupling constants it was found that the radiation amplitude consists of a local and a non-local part. Furthermore, it was shown that in a certain range of angles and frequencies the leading terms of these two mutually cancel, while the remaining terms can be presented as the sum of two contributions (j_z, $j_{z'}$) which have frequency cut-offs at $\omega \leqslant \gamma^2/b$ and $\omega \leqslant \gamma/b$, respectively. Their contribution to the total radiated energy E_d depends on the phase-space in an intricate way, so that the resulting radiation does not have a simple universal expression. Specifically, it was found that in the absence of extra dimensions one obtains

$$E_0 = C_0\, m \left(\frac{r_g}{b}\right)^2 \left(\frac{r_f}{b}\right) \gamma^3, \qquad C_0 \approx 8.3 \times 10^{-5}, \tag{2.5.1}$$

with the "basic" relativistic enhancement factor γ^3. For one extra dimension one has

$$E_1 = C_1\, m \left(\frac{r_g}{b}\right)^4 \left(\frac{r_f}{b}\right)^2 \gamma^3 \ln\gamma, \qquad C_1 \approx 1.64 \times 10^{-5}\,, \tag{2.5.2}$$

with almost the same (up to the logarithm) enhancement factor. For $d \geqslant 2$ one finds

$$E_d = C_d\, m \left(\frac{r_g}{b}\right)^{2(d+1)} \left(\frac{r_f}{b}\right)^{d+1} \gamma^{d+2}\,, \tag{2.5.3}$$

with C_d are computed from (2.4.10), (2.4.9) and (2.4.11) and given above for $d = 2, \ldots, 6$. So the expected enhancement factor γ^{d+2} is regained, with each new dimension adding one power of γ to the radiation loss.

Another feature of interest is the spectral-angular distribution of radiation. It was shown that in the usual gravity theory without extra dimensions the partial cancelation of local and non-local amplitudes in the case of gravitational interaction can be attributed to the fact that in terms of a curved space picture the world lines of a massive ultrarelativistic radiating charge and the null geodesic of the emitted radiation stay close to each other, so that the formation length of the radiation emitted predominantly in the forward direction is γ times stronger than in flat space. In perturbation theory on a flat background this corresponds to cancelation of contributions at high frequencies. In the presence of extra dimensions the emitted radiation is predominantly massive from the brane observer point of view, so the trajectories do not stay close together. The resulting spectral distribution then has substantial remainder at high frequencies up to γ^2/b, as illustrated in Figs 2.4(a), 2.7(b).

2.6 Notation

2.6.1 KK mode decomposition and Fourier transformation - Notation and conventions

The Fourier decomposition of the bulk fields $h_{MN}(x^\mu, y^i)$, $h'_{MN}(x^\mu, y^i)$, $\Phi(x^\mu, y^i)$ all with periodic conditions e.g. $h_{MN}(x, y^k + 2\pi R) = h_{MN}(x, y^k)$ is of the form

$$h_{MN}(x, y) = \frac{1}{V} \sum_{n_1=-\infty}^{+\infty} \cdots \sum_{n_d=-\infty}^{+\infty} h^n_{MN}(x) \exp\left(i \frac{n_i y^i}{R}\right) \equiv \frac{1}{V} \sum_n h^n_{MN}(x) \mathrm{e}^{i n_k y^k / R}. \quad (2.6.1)$$

Using the representation of the delta-function

$$\frac{1}{V} \sum_n \mathrm{e}^{i n_k (y^k - y'^k)/R} = \delta^d(\mathbf{y} - \mathbf{y}'), \qquad \frac{1}{V} \int_V \mathrm{e}^{i n_k y^k} dy^d = \prod_{k=1}^{d} \delta_{n_k, 0}\,, \quad (2.6.2)$$

where $V = (2\pi R)^d$ is the volume of the torus, one obtains the inverse transformation:

$$h^n_{MN}(x) = \int_V h_{MN}(x, y) \mathrm{e}^{-i n_k y^k / R} d^d y\,. \quad (2.6.3)$$

Four-dimensional fields $h^n_{MN}(x)$ are then expanded as

$$h^n_{MN}(x) = \frac{1}{(2\pi)^4} \int \mathrm{e}^{-i(px)} h^n_{MN}(p)\, d^4 p, \quad (2.6.4)$$

where $(px) = px = q_\mu x^\mu$ is four-dimensional scalar product, and the final decomposition reads

$$h_{MN}(x, y) = \frac{1}{(2\pi)^4} \frac{1}{V} \sum_n \int h^n_{MN}(p) \mathrm{e}^{-i(px) + i n_k y^k / R} d^4 p\,, \quad (2.6.5)$$

while the inverse transformation is

$$h^n_{MN}(p) = \int_V d^d y \int_{R^4} h_{MN}(x, y) \mathrm{e}^{i(px) - i n_k y^k / R} d^4 x. \quad (2.6.6)$$

Occasionally we will also use another notation for the discrete transversal momenta: $p_T^i = n^i/R$, i.e.

$$h^n_{MN}(p) = \int h_{MN}(x,y) e^{i(px)-ip_T y} d^D x. \tag{2.6.7}$$

with $p_T\, y = p_T^i y^i$. From the four-dimensional point of view the zero mode $h^0_{MN}(x)$ ($n = 0$ means all $n^i = 0$) is massless, while the $n \neq 0$ modes are massive. Indeed, in the absence of the source term Eq. (2.2.11) reduces to

$$(\Box + p_T^2)\, h^n_{MN}(x) = 0, \quad p_T^2 = \frac{1}{R^2}\sum_{i=1}^{d}(n^i)^2\,, \tag{2.6.8}$$

where $\Box = \partial_\mu \partial^\mu$ is the four-dimensional D'Alembert operator, while the momenta transverse to the brane give rise to the mass term. In the standard scheme [3] one suitably combines polarization modes to get true massive gravitons with five spin states for each mass. For our purposes it will be easier to sum over modes using the original decomposition.

When the level spacing is small (e.g. when $R \gg b$), one can pass from summation over n to integration over p_T using

$$\frac{1}{V}\sum_n = \frac{1}{(2\pi)^d}\int d^d p_T. \tag{2.6.9}$$

Here it is implicitly assumed that both the sum and the integral converge. As pointed out in the text, and in contrast to quantum Born amplitudes, this is guaranteed in the framework of the classical perturbation approach presented here [25].

It is worth noting, that upon integration over modes in the case of small level spacing, one obtains the results expected in the uncompactified theory in $D = 4 + d-$dimensional Minkowski space.

In a similar fashion, expansion of $h'_{MN}(x,y)$ leads to the set of four-dimensional modes $h'^n_{MN}(x)$, and an expansion of the bulk scalar $\Phi(x,y)$ to the set $\Phi^n(x)$. These four-dimensional fields are further Fourier transformed to $h'^n_{MN}(p)$ and $\Phi^n(p)$, respectively.

2.6.2 Integration over angles and frequencies

In the main text the following integrals over the radiation angle θ were encountered

$$V^n_m = \int_0^\pi \frac{\sin^n\theta}{\psi^m} d\theta, \qquad \psi = 1 - v\cos\theta \tag{2.6.10}$$

with integers m, n.

For $2m > n+1$ one finds to leading order [23]

$$V_m^n = \frac{2^{m-1}}{\Gamma(m)} \Gamma\left(\frac{n+1}{2}\right) \Gamma\left(m - \frac{n+1}{2}\right) \gamma^{2m-n-1}. \tag{2.6.11}$$

For $n > 2m-1$ one obtains

$$V_m^n = \frac{2^{n-m}\Gamma\left(\frac{n+1}{2}\right)\Gamma\left(\frac{n+1}{2} - m\right)}{\Gamma(n-m+1)}. \tag{2.6.12}$$

In the case $2m = n+1$ the leading contribution to the integral is proportional to $\ln\gamma$. For example, one case needed in the text was $V_2^3 \simeq 4\ln\gamma$.

Calculation of the integrals over the frequency or over the impact parameter involving two Macdonald functions of the same argument is performed using the formula [36]:

$$\int_0^\infty K_\mu(cz)K_\nu(cz)z^{\alpha-1}dz = \frac{2^{\alpha-3}\Gamma\left(\frac{\alpha+\mu+\nu}{2}\right)\Gamma\left(\frac{\alpha+\mu-\nu}{2}\right)\Gamma\left(\frac{\alpha-\mu+\nu}{2}\right)\Gamma\left(\frac{\alpha-\mu-\nu}{2}\right)}{c^\alpha\Gamma(\alpha)}. \tag{2.6.13}$$

2.6.3 Useful kinematical formulae

The angles in the formulae below are defined in Figure 2.1.

$$\begin{aligned}
&u^\mu \equiv \gamma(1,0,0,v)\,, \quad u' \equiv (1,0,0,0)\,, \quad \psi \equiv 1 - v\cos\theta\cos\alpha = 1 - v\cos\vartheta\,, \\
&z' = \frac{(ku')b}{\gamma v} = \frac{\omega b}{\gamma v}\,, \quad z = \frac{(ku)b}{\gamma v} = \frac{\omega b}{v}\psi = z'\gamma\psi\,,\ 2\gamma z z' - z^2 - z'^2 = \omega^2 b^2 \sin^2\vartheta\,, \\
&\xi^2 \equiv 2\gamma z z' - z^2 - z'^2 = \omega^2 b^2 \sin^2\theta\cos^2\alpha + b^2 k_T^2 = (\gamma v z' \sin\vartheta)^2 \\
&-(kb) = \xi\cos\phi = \gamma z' v \sin\vartheta\cos\phi = \gamma z' v\cos\alpha\sin\theta\cos\varphi = \omega b\sin\theta\cos\varphi \\
&\beta \equiv \gamma z z' - z^2 = \frac{\omega^2 b^2\cos\vartheta(1 - v\cos\vartheta)}{v} = \gamma^2 z'^2\psi(1-\psi)
\end{aligned} \tag{2.6.14}$$

2.7 Destructive interference for $\gamma/b \lesssim \omega \lesssim \gamma^2/b$

An alternative proof of the destructive interference effect of the radiation amplitude in the $z-$region but with $\vartheta < 1/\gamma$ in higher dimensional Minkowski space will be presented here. In the main text we followed an approximation allowing to cover the full angular range. Here destructive interference in the restricted angular range will be demonstrated rigorously.

Start with (2.3.20), change variable x to ζ given by

$$\zeta\, d\zeta = f(x)\, dx\,, \quad f(x) = (z^2 + z'^2 - 2\gamma z z')\, x + \gamma z z' - z^2\,, \tag{2.7.1}$$

and integrate by parts twice using

$$\zeta \hat{K}_{\nu}(\zeta) = -\hat{K}'_{\nu+1}(\zeta)\,. \tag{2.7.2}$$

The first integration gives:

$$\int_0^1 dx\, e^{-ix(kb)} \hat{K}_{d/2-1}\left[\zeta(x)\right] = -\frac{\mathrm{e}^{-ix(kb)}}{f(x)}\,\hat{K}_{d/2}\left[\zeta(x)\right]\Big|_{x=0}^{x=1} + \int_0^1 dx\,\hat{K}_{d/2}(\zeta)\,\partial_x\left(\frac{\mathrm{e}^{-ix(kb)}}{f(x)}\right).$$

A second integration by parts leads to

$$\begin{aligned}\sigma(k) = \lambda_d \frac{\gamma\, v\, z'^2}{b^d}\Bigg[&\frac{e^{i(kb)}}{\gamma z z' - z^2}\left(\hat{K}_{d/2}(z) - i\, q_0 \frac{\hat{K}_{d/2+1}(z)}{\gamma z z' - z^2}\right) - \\ &- \frac{1}{z'^2 - \gamma z z'}\left(\hat{K}_{d/2}(z') - i\, q_1 \frac{\hat{K}_{d/2+1}(z')}{z'^2 - \gamma z z'}\right) + R\Bigg],\end{aligned} \tag{2.7.3}$$

where

$$q_0 = (kb) - i\frac{z^2 + z'^2 - 2\gamma z z'}{\gamma z z' - z^2}, \qquad q_1 = (kb) - i\frac{z^2 + z'^2 - 2\gamma z z'}{z'^2 - \gamma z z'}, \tag{2.7.4}$$

and

$$R = \int_0^1 dx\,\hat{K}_{d/2+1}(\zeta(x))\left[\left(\frac{\mathrm{e}^{-ix(kb)}}{f(x)}\right)'\frac{1}{f(x)}\right]'. \tag{2.7.5}$$

Continuing integration by parts further, one obtains an expansion in terms of $q_0\beta^{-1}$ and $q_1(\beta - \xi^2)^{-1}$. As we discussed before, in the $z-$region of interest here $\psi \sim 1/\gamma^2$, $z \sim 1$, $z' \sim \gamma$, so that $\xi^2 \sim \beta \sim \gamma^2 \sim (\beta - \xi^2)$, $q_0 \sim q_1 \sim \gamma$ and therefore the expansion parameters are: $q_0\beta^{-1} \sim \gamma^{-1} \ll 1$, $q_1(\beta - \xi^2)^{-1} \sim \gamma^{-1} \ll 1$. With this accuracy one can set $q_0 = q_1 = (kb)$, $\beta = \gamma z z'$ and write:

$$\sigma(k) \simeq \frac{\lambda_b}{b^d}\left[e^{i(kb)}\left(\frac{z'}{z}\hat{K}_{d/2}(z) - i\frac{(kb)}{\gamma z^2}\,\hat{K}_{d/2+1}(z)\right) + \left(\frac{z'}{z - z'/\gamma}\hat{K}_{d/2}(z') + i\,\frac{(kb)}{\gamma z^2}\,\hat{K}_{d/2+1}(z')\right)\right]. \tag{2.7.6}$$

The first parenthesis in σ cancels for $v = 1$ the leading terms of ρ (2.3.11), and the total amplitude $j(k) = \rho(k) + \sigma(k)$ contains only the second parenthesis in (2.7.6) plus the subleading terms mentioned above. Thus, the series obtained by integration by parts, converges inside $z-$cone $\vartheta < \arcsin\gamma^{-1}$ and establishes the effect of *destructive interference*.

Bibliography

[1] I. Antoniadis, C. Bachas, D. C. Lewellen and T. N. Tomaras, *On Supersymmetry Breaking In Superstrings,* Phys. Lett. B **207** (1988) 441; I. Antoniadis, *A Possible New Dimension At A Few Tev*, Phys. Lett. B **246** (1990) 377. 25

[2] N. Arkani-Hamed, S. Dimopoulos and G. Dvali, *The hierarchy problem and new dimensions at a millimeter, Phys. Lett.* **B429**(1998) 263[hep-ph/9803315]; I. Antoniadis, N. Arkani-Hamed, S. Dimopoulos and G. Dvali, *New dimensions at a millimeter to a fermi and superstings at a TeV, Phys. Lett.* **B436** (1998) 257[hep-ph/9804398]; N. Arkani-Hamed, S. Dimopoulos and G. Dvali, Phys. Rev. **D59**(1999) 086004 [hep-ph/9807344]. 25

[3] G. F. Giudice, R. Rattazzi and J. D. Wells, *Quantum gravity and extra dimensions at high-energy colliders,* Nucl. Phys. B **544** (1999) 3[hep-ph/9811291]; T. Han, J. D. Lykken and R. J. Zhang, Phys. Rev. D **59** (1999) 105006. 25, 35, 58

[4] L. Randall and R. Sundrum, Phys. Rev. Lett. **83** (1999) 3370 [hep-ph/9905221]; L. Randall and R. Sundrum, Phys. Rev. Lett. **83**(1999) 4690 [hep-th/9906064]. 25

[5] P. C. Argyres, S. Dimopoulos and J. March-Russell, *Black holes and sub-millimeter dimensions,* Phys. Lett. B **441** (1998) 96 [hep-th/9808138]; T. Banks and W. Fischler, [arXiv:hep-th/9906038]; S. B. Giddings and S. Thomas, *High energy colliders as black hole factories: The end of short distance physics,* Phys. Rev. D **65** (2002) 056010 [hep-ph/0106219]; S. Dimopoulos and G. Landsberg, *Black holes at the LHC,* Phys. Rev. Lett. **87** (2001) 161602 [hep-ph/0106295]; 25

[6] D. Ida and K.-i. Nakao, *Isoperimetric inequality for higher-dimensional black holes,* Phys. Rev. D **66** (2002) 064026 arXiv:gr-qc/0204082; C. Barrabes, V. P. Frolov and E. Lesigne, *Geometric inequalities and trapped surfaces in higher dimensional spacetimes,* Phys. Rev. D **69** (2004) 101501, [gr-qc/0402081]; C. M. Yoo, K.-i. Nakao and D. Ida, *Hoop conjecture in five-dimensions: Violation of cosmic censorship,* Phys. Rev. D **71** (2005) 104014 [gr-qc/0503008]. 25

[7] R. Penrose, 1974 (unpublished). 25

[8] P. D. D'Eath, *High Speed Black Hole Encounters And Gravitational Radiation*, Phys. Rev. D **18** (1978) 990; P. D. D'Eath and P. N. Payne, *Gravitational Radiation In High Speed Black Hole Collisions. 1. Perturbation Treatment Of The Axisymmetric Speed Of Light Collision*, Phys. Rev. D **46** (1992) 658; Phys. Rev. D **46** (1992) 675; Phys. Rev. D **46** (1992) 694; P. D. D'Eath, *Black holes: Gravitational interactions*, (Oxford mathematical monographs) *Oxford, UK: Clarendon* (1996), pg. 286. 25

[9] D. M. Eardley and S. B. Giddings, Phys. Rev. **D66** (2002) 044011, [gr-qc/0201034]. 25, 26

[10] H. Yoshino and Y. Nambu, Phys.Rev. **D66**, 065004, (2002); Phys. Rev. **D67** (2003) 024009 [gr-qc/0209003]; H. Yoshino and V. S. Rychkov, Phys. Rev. **D71** (2005) 104028[hep-th/0503171]; H. Yoshino and R. B. Mann, Phys. Rev. **D74** (2006) 044003 [gr-qc/0605131]. 25

[11] S. B. Giddings, Beyond the Planck scale arXiv:0910.3140 [gr-qc]. I. Y. Aref'eva, Theor. Math. Phys. **161** (2009) 1647 arXiv:0912.5481 [hep-th]; M. Bleicher and P. Nicolini, arXiv:1001.2211 [hep-ph]; S. B. Giddings, M. Schmidt-Sommerfeld and J. R. Andersen, arXiv:1005.5408 [hep-th]. 25

[12] P. C. Aichelburg and R. U. Sexl, Gen. Rel. Grav. **2** (1971) 303. 25

[13] T. Dray and G. 't Hooft, Nucl. Phys. B **253** (1985) 173. 25

[14] C. Herdeiro, M. O. P. Sampaio and C. Rebelo, arXiv:1105.2298 [hep-th]. 26

[15] S. B. Giddings and V. S. Rychkov, Phys. Rev. **D70** (2004) 104026 [hep-th/0409131]. 26

[16] P. Meade and L. Randall, JHEP **0805** (2008) 003, arXiv:0708.3017 [hep-ph]. 26

[17] B. P. Kosyakov, Theor. Math. Phys. **199** (1999) 493; D. V. Galtsov, Phys. Rev. D **66** (2002) 025016 [hep-th/0112110]; P. O. Kazinski, S. L. Lyakhovich and A. A. Sharapov, Phys. Rev. D **66** (2002) 025017, [hep-th/0201046]; D. V. Gal'tsov and P. A. Spirin, Grav. Cosmol. **13** (2007) 241. 26, 30

[18] D. Amati, M. Ciafaloni and G. Veneziano, Nucl. Phys. B **403** (1993) 707; E. Kohlprath and G. Veneziano, JHEP **0206** (2002) 057, [gr-qc/0203093]; D. Amati,

M. Ciafaloni and G. Veneziano, JHEP **0802** (2008) 049, arXiv:0712.1209 [hep-th]; G. Veneziano and J. Wosiek, arXiv:0804.3321 [hep-th]; arXiv:0805.2973 [hep-th]; M. Ciafaloni and D. Colferai, JHEP **0811** (2008) 047, arXiv:0807.2117 [hep-th]. 26

[19] V. Cardoso, O. J. C. Dias and P. S. Lemos, Phys. Rev. **D67**, (2003) 064016, [hep-th/0212168]; V. Cardoso, P. S. Lemos and S. Yoshida, Phys. Rev. **D68** (2003) 084011 [gr-qc/0307104]; E. Berti, M. Cavaglià and L. Gualtieri, Phys. Rev. **D69** (2004) 124011 [hep-th/0309203]; B. Koch and M. Bleicher, JETP Lett. **87** (2008) 75[hep-th/0512353]. V. Cardoso, M. Cavaglia and J. Q. Guo, Gravitational Larmor formula in higher dimensions, Phys. Rev. D **75** (2007) 084020, [hep-th/0702138]; H. Yoshino, T. Shiromizu and M. Shibata, Phys. Rev. **D72**, (2005) 084010[gr-qc/0508063]; H. Yoshino, T. Shiromizu and M. Shibata, Phys. Rev. **D74** (2006) 124022,[gr-qc/0610110]; P. Lodone and S. Rychkov, JHEP **0912** (2009) 036; arXiv:0909.3519 [hep-ph]. 26

[20] M. W. Choptuik, F. Pretorius, Phys.Rev.Lett. **104** (2010) 111101, arXiv:0908.1780v2. 26

[21] H. Witek, M. Zilhao, L. Gualtieri, V. Cardoso, C. Herdeiro, A. Nerozzi and U. Sperhake, Phys. Rev. D **82** (2010) 104014, arXiv:1006.3081 [gr-qc].

[22] A. Mironov and A. Morozov, Pisma Zh. Eksp. Teor. Fiz. **85**, 9 (2007) [JETP Lett. **85** (2007)] 6 [hep-ph/0612074]; A. Mironov and A. Morozov, [hep-th/0703097]. 26, 27

[23] D. V. Gal'tsov, G. Kofinas, P. Spirin and T. N. Tomaras, JHEP **1005** (2010) 055, arXiv:1003.2982 [hep-th]. 27

[24] D. V. Gal'tsov, G. Kofinas, P. Spirin and T. N. Tomaras, Phys. Lett. B **683** (2010) 331, arXiv:0908.0675 [hep-ph]. 27, 32, 37, 38, 39, 40, 45, 59

[25] D. V. Gal'tsov, G. Kofinas, P. Spirin and T. N. Tomaras, JHEP **0905** (2009) 074 arXiv:0903.3019 [hep-ph]. 27, 32, 47

[26] G. 't Hooft, Phys. Lett. B **198** (1987) 61. 35, 58

[27] B. Bertotti, Nuovo Cimento , **4** (1956) 898; J. N. Goldberg, Bull. Amer. Phys. Soc. Ser. II , **2** (1957) 232; P. Havas, Phys. Rev. **108** (1957) 1352; B. Bertotti, J. Plebansky, Ann. Phys. **11** (1960) 169; P. Havas, Bull. Amer. Phys. Soc., **6**

(1961) 346. J. N. Goldberg, in *Gravitation; An Introduction to the Current Reseach*, NY(1962) pg. 102; P. Havas, J. N. Goldberg , Phys. Rev. ,**B128** (1962) 495. 27

[28] K. S. Thorne and S. J. Kovacs, Astrophys. J. **200** (1975) 245; R. J. Crowley and K. S. Thorne, Astrophys. J. **215** (1977) 624; S. J. Kovacs and K. S. Thorne, Astrophys. J. **217** (1977) 252; S. J. Kovacs and K. S. Thorne, Astrophys. J. **224** (1978) 62. 27

[29] D. V. Gal'tsov, Yu. V. Grats, Gravitational Radiation under collision of relativistic bodies, in *Modern problems of Theoretical Physics*,Moscow State Univ. Publ. , Moscow(1976), pg. 258-273 (in Russian). 27

[30] D. V. Galtsov, Yu. V. Grats and A. A. Matyukhin, Sov. Phys. J. **23** (1980) 389. 28, 47, 48, 49, 50

[31] I. B. Khriplovich and E. V. Shuryak, Zh. Eksp. Teor. Fiz. **65** (1973) 2137; D. V. Gal'tsov and A. A. Matyukhin, (IN RUSSIAN), Yad. Fiz. **45** (1987) 894.

[32] R. A. Matzner and Y. Nutku, Proc. Roy. Soc. Lond. **336** (1974) 285.

[33] B. M. Barker, and S. N. Gupta, and J. Kaskas, Phys. Rev. **182**, (1969) 1391; B. M. Barker, and S. N. Gupta, Phys. Rev. **D9**, (1974) 334; B. M. Barker and O'Connell, Phys. Rev. D **12** (1975) 329.

[34] I.S. Gradshteyn and I.M. Ryzhik , Table of Integrals, Series and Products, Academic Press, (1965). 44

[35] A. Kehagias and K. Sfetsos, Phys. Lett. B **472** (2000) 39, [hep-ph/9905417]; E. G. Floratos and G. K. Leontaris, Phys. Lett. B **465** (1999) 95, [hep-ph/9906238]. 47

[36] A. P. Prudnikov, Yu. A. Brychkov and O. I. Marichev, Integrals and Series, Vol. 1, Elementary Functions, Gordon & Breach Sci. Publ., New York, (1986). 43, 59

3 Vector Bremsstrahlung by Ultrarelativistic Collisions in Higher Dimensions

3.1 Introduction

The first experiments of the Large Hadron Collider (LHC) at CERN have shown that creation of Black holes is much less than predicted by theorists. When the discovery of new physics at LHC associated with supersymmetry at low energies fails, the models of TeV-scale gravity become of particular interest. The LHC can be used to test models with Large Extra Dimensions (LEDs) and set bounds on their parameters [1; 2]. Initially proposed as an alternative to supersymmetry in solving the hierarchy problem, such models are motivated by string theory and open new interesting directions in cosmology. Inspired by earlier ideas of the Universe as a topological defect in higher-dimensional space-time and the TeV-scale supersymmetry breaking in heterotic string theory associated with compactification [3], they appeared in several proposals.

A conceptually and technically simple one is the Arkani-Hamed, Dimopoulos and Dvali (ADD) scenario [4], with the Standard Model particles living in the four-dimensional space-time and gravity propagating in the D-dimensional bulk with the $d = D - 4$ flat dimensions compactified on a torus. Gravity is strong with a corresponding Planck mass $M^*_{\rm Pl}$ at the (presumably) TeV scale.

Other LED scenaria include the warped compactification Randall-Sundrum (RS) models [5], which are based on an identification of the physical four-dimensional space-time with a 3-brane embedded into a five-dimensional bulk endowed with the cosmological constant, in which case the fifth dimension may be infinite. The model known as "Universal Extra Dimensions" [6] (UED) allows *all* fields to propagate through the bulk.

The common feature of all these models is the existence of a large (in Planck units) length L_{Pl}, which may appear either via a compactification radius, or via inverse powers of curvature of the infinite bulk. If the quantum gravity scale happens to be of order of TeV, the LHC, expected to reach center of mass energies one order of magnitude higher, will be able to study information about gravity at ultraplanckian energies [7]. The gravitational radius associated with the center of mass collision energy increases with energy, and in the transplanckian regime becomes larger than the Planck length, indicating that gravity behaves *classically* at least for some region of momentum transfers [8]. Thus the transplanckian gravity is believed to be adequately described by the classical Einstein equations [9]. This, presumably, allows one to make reliable theoretical predictions of gravitational effects without entering into the complications related to quantum gravity.

Black Hole production is arguably the most exciting inelastic process in the context of the TeV-gravity. Apart from the creation of black holes, another inelastic gravitational process is radiation. Bremsstrahlung itself represents the natural process to test the existence of extra dimensions and probe them. Colliding ultrarelativistic particles will radiate and the number of dimensions can easily be determined by the dependence of the radiated energy from the Lorentz factor $\gamma \gg 1$ of collision.

Bremsstrahlung is characterized by the only one length parameter of experiment – the impact parameter b. To keep gravity classical, it is expected to be much greater than the Schwarzschild radius r_S, associated with the energy $\mathcal{E} \simeq \sqrt{s}$, where s stands for the Mandelstam s-variable:

$$b \gg \gamma^{1/(d+1)} r_S \sim \left(\varkappa_D^2 \gamma \sqrt{s}\right)^{1/(d+1)} . \tag{3.1.1}$$

However, the calculation of classical ultraplanckian *gravitational* bremsstrahlung in the context of the ADD model [15] predicts strong enhancement of radiation losses as compared to theories without extra dimensions already for large values of the impact parameter. These extreme losses possibly originate from the large number of light Kaluza-Klein (KK) modes [10; 11]. Our estimate shows that transplanckian collisions should be heavily damped by radiation, and classical radiation reaction has to be taken into account in the study of gravitational collapse and BH production in colliders.

On the other hand, the theory of electromagnetic radiation (both classical and quantum) has been developed to much greater extent than gravitational radiation. The same applies to the corresponding *detectors of the emitted waves*. Thus it is natural to include vector bremsstrahlung among the realistic inelastic problems, where the force causing the acceleration may be either gravitational or non-gravitational.

Nevertheless the problem of radiation reaction is far from solved, even in electrodynamics. Inspired by the pioneering work of Dirac [19], it was developed by Rohrlich and Teitelboim in flat space-time [20; 21], adapted by de Witt and Brehme for curved background [22] and generalized to curved background in higher dimensions in [24].

Some attempts to include radiation reaction in QED have been made during the last thirty years [25; 27; 28]. However, the number of physical cases where these attempts have succeeded in producing a closed form result, is quite modest [23].

Thus electromagnetic bremsstrahlung in an external gravitational field (generated by the partner particle) represents a process of particular theoretical interest in the context of another application of tail appearance coming from the non-local part of the Green's function in curved background.

It actualizes the purposes of this chapter. Furthermore, the synchrotron radiation shows that within some region of parameters, the electromagnetic field can be also treated classically, accurately matching the result of quantum electrodynamics.

Thereby, in addition, to make the scheme self-consistent, one has to demand also the classicality of the particles' trajectory and *classicality* of the electrodynamics.

Perturbation theory over the gravitational constant $\varkappa_D$ will be of usage in the computation presented here. Given as a zeroth-order solution, Minkowski space-time will be used as an effective background for the wave propagation. The significance of such a choice is highlighted by the following facts: (i) it ensures the asymptotically flat space-time, (ii) one considers tensors and their variations as tensors in flat space with simple raise/lowering indices and (iii) it allows the freedom to use Fourier-transforms.

Thus one considers the Minkowski space-time as the background, while the direct nature of modes (Kaluza-Klein modes for toroidal extra dimensions or curvature-mediated modes in cosmological models with no compactification, like RS2) should be taken into account as a correction due to the curvature. Depending on the choice of model, the vector field can either propagate through the bulk, or not, even though the charges are confined on the 3-brane. Thus we generically consider Minkowski space-time as the background with *arbitrary* dimensionality $D \geqslant 4$, while all interesting cases can be obtained as limiting cases of the generic calculation.

This work continues a series of papers [12; 13; 14; 15]: pure gravitational trans-planckian bremsstrahlung is considered in [15], the classical scalar bremsstrahlung in [13], while [14] is devoted to the scalar emission in the gravity-mediated bremsstrahlung.

Mathematically, in the ADD model the Minkowski limit appears as the reduction of summation over KK-modes into the integration, as long as the restriction on the large size of extra dimensions holds. Therefore, one has to assume

$$b \ll R \tag{3.1.2}$$

to have large number of KK-quanta, for each model to be applied to.

Most of the previous works on classical bremsstrahlung were concerned with gravitational radiation: for reviews see [15] and references therein, and [17] among the most recent.

Among the previous works in four dimensions on the electromagnetic radiation caused by gravitational force, one emphasizes the papers by Peters [18], by Matzner and Nutku [29] and the work by Gal'tsov, Grats and Matyukhin [30]. In [18] the post-linear formalism is used in the coordinate space for Schwarzschild background, considering bremsstrahlung near the vicinity of black hole.

Some qualitative arguments and estimates are given in [32]. In [29] the equivalent-photons method was adapted for gravitons. This approach was criticized in [30], who found that this method is of limited range when the frequency range is decreased γ times, and thereby inappropriate.

In [30] the iteration scheme accompanied by the perturbation theory is used – as well as in the present work, while mathematical techniques are different: contour integration in [30] versus expansion of Macdonald functions here. The similar features are: (i) the damping of radiation amplitude at high frequencies $\omega \sim \gamma^2/b$ (at Lab frame), (ii) the significant frequency $\omega \sim \gamma/b$, coming from the partial cancelation of local and non-local currents, and (iii) the final power of Lorentz factor:

$$E_{\rm rad} \sim \frac{(Gem')^2}{b^3}\,\gamma^3\,.$$

The difference is related with the erroneous neglect of the local current (which turns out to be significant) at the dominant frequency $\omega \sim \gamma/b$ in [30], whereas it has the same magnitude as the non-local part which is retained. Because of this, the total coefficient is determined with an error, as well as the small- and medium-frequency behavior. Thus our answer in four dimensions corrects the overall coefficient obtained in [30], and generalizes it to the higher dimensions. Furthermore, we show that in higher dimensions the higher-frequency regime

$$\omega \sim \gamma^2/b$$

dominates over the domain $\omega \sim \gamma/b$, due to the volume factors in the momentum space.

Taking into account some similar features appearing in these works [14; 15], we minimize the derivations and refer to the previously derived ones, when it is possible. Meanwhile we would like to emphasize the features not observed in previous works: conservation of source (validity of the gauge condition), influence of self-action, the bremsstrahlung of two charges, the length of the emitted wave formation (coherence length), etc.

In order to distinguish vector radiation by gravitational scattering from pure electromagnetic bremsstrahlung (which is expected to represent much larger effect due to the values of couplings in 4D), we charge only one particle *in the most* of the chapter, while a subsection in the Discussion section is devoted to the radiation effects coming from the scattering of two charges.

The chapter is organized as follows: the model, approximation method and formulae necessary for subsequent computation of the emitted energy, including the polarization vectors, are described in the Section 3.2. The local and non-local amplitudes, their combination and the amplitude damping at high frequencies (the destructive interference effect) are derived in Section 3.3. Section 3.4 is devoted to the computation of total emitted energy. Some additional aspects (zero-frequency limits) are discussed. Particular attention is paid to the emission in the ADD model. Possible cut-offs, the comparison of electromagnetic bremsstrahlung by gravitational and non-gravitational forces, the conclusions and prospects are presented in the Discussion section. Finally, some necessary formulae for computation and the simple proof of the destructive interference phenomenon in the vector case, dealing with just the integration-by-parts technique, are given in the last three sections.

3.2 The model

We compute here a classical spin-one bremsstrahlung in ultra-relativistic gravity-mediated scattering of two massive point particles m and m'. The space-time is assumed to be $M_{1,D-1}$ with coordinates x^M, $M = 0, 1, \ldots, D-1$, with the mostly minus signature $(+, -, \ldots, -)$. The units we use are $c = \hbar = 1$.

Particles are localized on the observable 3-brane and interact via the gravitational field g_{MN}, which propagates in the whole space-time $M_{1,D-1}$. We also assume the existence of a massless bulk vector field A^M, which interacts with m, but not with m'. Thus only m has an electromagnetic charge e.

3.2.1 Setup and Equations of motion

The action of the model is symbolically of the form

$$S \equiv S_g + S_A + S_{m'} + S_m + S_{mA}\,,$$

and explicitly, in an obvious correspondence, in the reparametrization-invariant form

$$S = -\int d^D x \sqrt{|g|}\left[\frac{R}{\varkappa_D^2} + \frac{1}{4}\, g^{MN} g^{RS} F_{MR} F_{NS}\right] - \int m' \sqrt{g_{MN}\dot z'^M \dot z'^N}\, d\tau' \\ - \int \left[m\sqrt{g_{MN}\dot z^M \dot z^N} - eA_M \dot z^M\right] d\tau \tag{3.2.1}$$

with[1] $\varkappa_D^2 \equiv 16\pi G_D$ where G_D stands for the D-dimensional Newton's constant. F_{MN} is the field strength defined as usual: $F_{MN} = \nabla_M A_N - \nabla_N A_M$. Our convention for the Riemann tensor is $R^B{}_{NRS} \equiv \Gamma^B_{NS,R} - \Gamma^B_{NR,S} + \Gamma^A_{NS}\Gamma^B_{AR} - \Gamma^A_{NR}\Gamma^B_{AS}$, with $\Gamma^A_{NR} = (1/2)\, g^{AB}(g_{BR,N} + g_{NB,R} - g_{NR,B})$. Finally, the Ricci tensor and curvature scalar are defined as $R_{MN} \equiv \delta^B_A\, R^A{}_{MBN}$ and $R \equiv g^{MN}\, R_{MN}$, respectively.

In the sequel we deal with the affine parameter of the both particles' worldline, so $g_{MN}\dot z^M \dot z^N = g_{MN}\dot z'^M \dot z'^N = 1$. Thus we consider only that class of the worldline reparametrizations, which maintains the natural (affine) parametrization of the trajectory.

Variation of (3.2.1) with respect to z^M and z'^M gives the particles' equations of motion in the covariant form

$$m\, D\dot z^M = e\, F^{MN}\dot z_N\,, \qquad D'\dot z'^M = 0\,, \tag{3.2.2}$$

where the covariant derivative is defined as

$$D\pi^M \equiv \frac{\partial \pi^M}{\partial \tau} + \Gamma^M_{RS}\, \pi^R \dot z^S\,. \tag{3.2.3}$$

Variation over A^M leads to

$$\nabla_N F^{MN} = -J^M\,, \qquad J^M(x) = e\int \dot z^M(\tau)\, \frac{\delta^D\big(x - z(\tau)\big)}{\sqrt{|g|}}\, d\tau\,. \tag{3.2.4}$$

Finally, varying the action with respect to the metric g_{MN}, one obtains the Einstein equations

$$R^{MN} - \frac{1}{2}\, g^{MN}\, R = \frac{\varkappa_D^2}{2}\, T^{MN}\,, \tag{3.2.5}$$

[1] We do not deal with massless particles. Thus the Polyakov form of the mechanical action is not required.

where T^{MN} is a total matter of the system-at-hand.

In order to resolve the equations of motion we use perturbation theory with respect to the gravitational coupling and the electromagnetic coupling.

As was argued in the Introduction, one expands the metric as a perturbation on the Minkowski background:

$$g_{MN} = \eta_{MN} + \varkappa_D h_{MN}$$

and then finds the solution of equations of motion in each order iteratively. Respectively, all tensors are to be considered as tensors in flat space-time, as well as raising/lowering of their indices.

3.2.2 Approximation method

We intend to use an approximation technique that relies on the fact that the deviation from the Minkowski metric is small i.e. $\varkappa_D h_{MN} \ll 1$. In particular, we have to evaluate $\varkappa_D h_{MN}$ at the location of the charge, i.e. considering m' as the source of an external gravitational field. In what follows:

$$b \gg r_g\,, \qquad\qquad {r'_g}^{d+1} = \frac{8\Gamma\left(\frac{d+3}{2}\right)}{\pi^{(d+1)/2}(d+2)}\, G_D m'\,. \tag{3.2.6}$$

The possible restrictions due to the charge do not affect the perturbative approximation we use and their discussion is postponed to the Discussion section.

As mentioned above we will be solving the equations of motion iteratively. Therefore all fields and kinematical quantities are to be expanded as follows:

$$\phi = {}^0\phi + {}^1\phi + {}^2\phi + \dots\,, \tag{3.2.7}$$

where ϕ can be h_{MN}, T^{MN}, A_M, z^M and z'^M as well as their derivatives. Thus the left superscript is used to denote the order of iteration.

Next, to perform the iterations, it is more useful to work with a flat-derivative interpretation of the EoM (3.2.4):

$$\frac{1}{\sqrt{|g|}}\left(\sqrt{|g|}\, g^{ML} g^{NR} F_{LR}\right)_{,N} = -J^M\,, \qquad\qquad F_{MN} = \partial_M A_N - \partial_N A_M \tag{3.2.8}$$

and to rewrite it, introducing "new" current[1] $\tilde{J}^M$:

$$\partial_N\left(\sqrt{|g|}\, g^{ML} g^{NR} F_{LR}\right) = -\tilde{J}^M\,, \qquad\qquad \tilde{J}^M(x) = e\int \dot{z}^M(\tau)\,\delta^D\big(x - z(\tau)\big)\, d\tau\,. \tag{3.2.9}$$

[1] It represents the vector density with respect to the total metric, but each term of expansion of it will represent the vector in flat background.

Finally, one has to explicitly manifest the matter sources of the generic equations to vary them in the sequel: the mechanical energy-momentum tensor of two particles and the stress-tensor of the bulk vector field are given by corresponding action variation over the total metric g_{MN} and read (in the gauge $g_{MN}\dot{z}^M\dot{z}^N = 1$)

$$T^{MN}_{\rm m} = m\int \frac{\dot{z}^M\dot{z}^N\delta^D\big(x - z(\tau)\big)}{\sqrt{-g}}\,d\tau \qquad\qquad T^{MN}_{\rm m'} = m'\int \frac{\dot{z}'^M\dot{z}'^N\delta^D\big(x - z'(\tau')\big)}{\sqrt{-g}}\,d\tau', \tag{3.2.10}$$

and

$$T^{MN}_{\rm em} = F^{ML}F_L{}^N + \frac{1}{4}g^{MN}F_{LP}F^{LP}, \tag{3.2.11}$$

respectively[1].

Zeroth order. To zeroth order one expects the flat space with no fields in it:

$${}^0h_{MN} = 0\,, \qquad\qquad {}^0A^M = 0\,.$$

In what follows, to this order both particles move freely:

$${}^0\ddot{z}^M = {}^0\ddot{z}'^M = 0$$

with constant velocities ${}^0\dot{z}^M \equiv u^M$ and ${}^0\dot{z}'^M \equiv u'^M$.

Furthermore we will be working in the Lorentz frame where the uncharged particle m' is at rest (at zeroth order): in addition, we set the origin of coordinate system to coincide with its zeroth-order location.

$$u'^M = (1, 0, \dots 0)\,, \qquad\qquad {}^0z'^M = u'^M\,\tau'\,. \tag{3.2.12}$$

The charged particle m is ultra-relativistic and moves along the 3-brane with high-speed $v \lesssim 1$ and large Lorentz factor $\gamma \equiv (1 - v^2)^{-1/2} \gg 1$. We choose the spatial direction of zeroth-order motion as the $z-$axis, while the vector of closest proximity b^M between the two particles is chosen to coincide with the $x-$axis. Finally we choose the time of scattering to be zero. In what follows

$$u^M = \gamma(1, 0, 0, v, 0\dots 0)\,, \qquad\qquad {}^0z^M = {}^0u^M\,\tau + b^M\,, \qquad\qquad b^M = (0, b, 0, \dots, 0)\,. \tag{3.2.13}$$

Thus $\gamma = u\cdot u'$ represents the Lorentz factor of collision, $b > 0$ represents the impact parameter of this scattering, while both u^M and b^M lie on the brane and are mutually orthogonal.

[1] Raising/lowering of indices here is performed using the total metric, g_{MN}. Parallel displacement bi-vectors $\bar{g}^M{}_A(x,z)$ are assumed in (3.2.4,3.2.10) and omitted, due to the coincidence limit $\delta^D(x - z)$.

Finally, vectorial and tensorial sources coming from equations (3.2.9) and (3.2.10) are given by

$$ {}^0\tilde{j}^M(x) = e\,u^M \int \delta^D\big(x - {}^0z(\tau)\big)\, d\tau \tag{3.2.14}$$

and

$$ {}^0T^{MN} = m\,u^M u^N \int \delta^D\big(x - {}^0z(\tau)\big)\, d\tau\,, \qquad {}^0T'^{MN} = m\,u'^M u'^N \int \delta^D\big(x - {}^0z'(\tau)\big)\, d\tau\,, \tag{3.2.15}$$

respectively, while ${}^0T^{MN}_{\text{em}} = 0$.

First order. The zeroth-order sources produce corresponding first-order fields. Namely, from the Einstein equations (3.2.5) one expects to get the equation for ${}^1h_{MN}$.

Consecutively computing the first-order variations[1]

$$\begin{aligned}
& g^{(1)}_{MN} = h_{MN} && \Gamma^{(1)R}_{MN} = (h^R_{M;N} + h^R_{N;M} - h_{MN}{}^{;R})/2 \\
& g^{(1)MN} = -h^{MN} && R^{(1)}_{MN} = \frac{1}{2}\Big(h^R_{N;MR} + h^R_{M;NR} - \Box\, h_{MN} - h_{;MN}\Big) \\
& \xi^M \equiv \Gamma^{(1)M}_{NR}\eta^{NR} && R^{(1)} = -\Box\, h + h_{MN}{}^{;MN} - R^{(1)}_{MN}h^{MN} \\
& \Box \equiv \eta^{MN}\partial_M\partial_N && G^{(1)}_{MN} = \frac{1}{2}\left(-\Box\, h_{MN} + \frac{\Box h}{2}\,\eta_{MN} - \xi^{\;;L}_L\,\eta_{MN} + \xi_{M;N} + \xi_{N;M}\right),
\end{aligned} \tag{3.2.16}$$

one introduces

$$ \psi^{MN} = h^{MN} - \frac{1}{2}\,\eta^{MN}\,h, \qquad h \equiv h^P_P \tag{3.2.17}$$

and sets the flat de Donder gauge

$$ \partial_N \psi^{MN} = 0\,, \qquad \partial_N h^{MN} = \frac{1}{2}\,h^{,M}\,, \tag{3.2.18}$$

which leads to

$$ R^{(1)}_{MN} = -\frac{1}{2}\,\Box\, h_{MN}\,, \qquad R^{(1)} = -\frac{1}{2}\,\Box\, h\,, \qquad G^{(1)}_{MN} = -\frac{1}{2}\,\Box\, \psi_{MN}\,. \tag{3.2.19}$$

We note that the gauge fixation (3.2.18) implies

$$ \partial_N\, {}^k\psi^{MN} = 0\,, \qquad {}^k\psi^{MN} \equiv {}^kh^{MN} - \frac{{}^kh_{LP}\,\eta^{LP}}{2}\,\eta^{MN}\,. \tag{3.2.20}$$

Eventually, substituting $h_{MN} = {}^1h_{MN} + {}^2h_{MN} + \ldots$ and taking into account the gauge (3.2.20), one obtains the first-order variations corresponding to our iteration scheme:

$$ {}^1R_{MN} = -\frac{1}{2}\,\Box\, {}^1h_{MN}\,, \qquad {}^1R = -\frac{1}{2}\,\Box\, {}^1h\,, \qquad {}^1G_{MN} = -\frac{1}{2}\,\Box\, {}^1\psi_{MN}\,. \tag{3.2.21}$$

[1] Notice, here h_{MN} represents the entire tower of its iterations. In these notations with right superscript we follow Weinberg [36].

In what follows the first-order Einstein equation (3.2.5) reads

$$\Box\, {}^1\psi^{MN} = -\varkappa_D\, {}^0T^{MN}\,, \qquad \Box\, {}^1h^{MN} = -\varkappa_D \left({}^0T^{MN} - \eta^{MN}\, \frac{{}^0T}{D-2} \right), \tag{3.2.22}$$

where ${}^0T \equiv \eta_{LR}\, {}^0T^{LR}$.

Substituting the zeroth-order matter part (3.2.15) one obtains ${}^1h^{MN}$ as a sum

$${}^1h^{MN} = {}^1h^{MN}_{\mathrm{m}} + {}^1h^{MN}_{\mathrm{m}'} \tag{3.2.23}$$

due to linearity of the first order, where each term represents a solution of (3.2.22) with source by the corresponding particle separately.

Furthermore, the first order of (3.2.9) reads

$$\partial_N\, {}^1F^{MN} = -\, {}^0\tilde{j}^M \tag{3.2.24}$$

with source given by (3.2.14).

Impose the flat Lorentz gauge for all orders[1]

$$\partial_M\, {}^kA^M = 0\,, \qquad {}^kF_{MN} \equiv {}^kA^{N,M} - {}^kA^{M,N} \tag{3.2.25}$$

to derive

$$\Box\, {}^1A^M = {}^0\tilde{j}^M \tag{3.2.26}$$

as also a d'Alembert equation.

Now consider the first-order equations of motion for two particles: making use of (3.2.2), one derives the electromagnetic part of a force, acting on the charge as

$$m\, {}^1\ddot{z}^M_{\mathrm{em}} = e\, {}^1F^{MN} u_N\,. \tag{3.2.27}$$

Whereas ${}^1F^{MN}$ is produced by the same particle m, and one has to consider ${}^1F^{MN}$ as *external* field and omit the self-action of fields in this order[2].

In what follows, to first order, both particles move along the geodesics created by the gravitational field produced by the partner particle, that we denote schematically

$$g_{MN} = \eta_{MN} + \varkappa_D\, {}^1h^{MN}_{\mathrm{m}'} + \mathcal{O}(\varkappa_D^2)\,, \qquad g'_{MN} = \eta_{MN} + \varkappa_D\, {}^1h^{MN}_{\mathrm{m}} + \mathcal{O}(\varkappa_D^2)\,. \tag{3.2.28}$$

[1] Take into account, it differs from the originally covariant $\nabla_M A^M = 0$.

[2] The account of self-action in coordinate representation leads to the renormalization of mass, radiation and radiation reaction phenomena [19; 20; 21; 24] but these effects are proportional to $\ddot{z}^M$ and its derivatives, and do not appear in the first order of PT, because of ${}^0\ddot{z} = 0$ found above. The appearance of self-action terms in higher orders will be discussed below.

Thus only the gravitational part of force survives[1] and the total first-order EoMs for the acceleration (3.2.2) represent a motion in the external linearized gravitational field and read

$$
\begin{aligned}
{}^{1}\ddot{z}^{M} &= -\varkappa_D \left({}^{1}h^{ML,R}_{\mathrm{m}'} - \frac{1}{2}\, {}^{1}h^{LR,M}_{\mathrm{m}'} \right) u_L u_R \,, \\
{}^{1}\ddot{z}'^{\,M} &= -\varkappa_D \left({}^{1}h^{ML,R}_{\mathrm{m}} - \frac{1}{2}\, {}^{1}h^{LR,M}_{\mathrm{m}} \right) u'_L u'_R \,.
\end{aligned}
\tag{3.2.29}
$$

For a more complete derivation of this gravitational part see [15]. It justifies our model as ”radiation under gravity-mediated collisions”.

Second order equation for A–radiation. The solution of linear equation (3.2.26) is the field generated by an uniformly moving charge and represents the boosted Coulomb field. Hence it does not contribute to radiation. In four dimensions it explicitly follows from the Larmor formula for the electromagnetic radiation by an accelerated charge. In arbitrary dimension it implicitly follows from the Equivalence principle. We will discuss this more thoroughly later.

The second order of our scheme leads to the radiation. For the vector emission in the bremsstrahlung process it is enough to consider only the correction to electromagnetic field ${}^{2}A^{M}$ and its source.

Taking the next order of (3.2.9) together with the Lorentz gauge fixing, one obtains

$$
\Box\, {}^{2}A^{M} = j^{M}(x) \,, \qquad\qquad j^{M}(x) \equiv \rho^{M}(x) + \sigma^{M}(x) \,, \tag{3.2.30}
$$

where

$$
\rho^{M}(x) \equiv {}^{1}\tilde{J}^{M}(x) = e \int \left({}^{1}\dot{z}^{M} - u^{M}\, {}^{1}z^{N} \partial_N \right) \delta^{D}(x - {}^{0}z)\, d\tau \tag{3.2.31}
$$

and

$$
\sigma^{M}(x) = -\varkappa_D\, \partial_N \left({}^{1}h^{M}{}_{L}\, {}^{1}F^{LN} + {}^{1}h^{N}{}_{L}\, {}^{1}F^{ML} - \frac{1}{2}\, {}^{1}h\, {}^{1}F^{MN} \right) , \tag{3.2.32}
$$

respectively.

We will refer to the first term as the *local* term since it is fixed on the trajectory of particle m, while the second term will be referred to as the *non-local* current[2], as

[1] We remind that this phenomenon is a direct consequence of the fact that only one particle is charged in the model-at-hand.

[2] Note that there is some ambiguity with regard to the definition of the local and the non-local part: indeed, if both sides of (3.2.8) are not multiplied by the factor $\sqrt{|g|}$ and if vary it instead (3.2.9), the variation of this factor will remain in the RHS and will be identified as local. Nevertheless, for the source of 2nd-order field one needs the sum of ρ^{M} and σ^{N} and, of course when such a factor disappears from one term, it resurrects in another hand side variation – hence the sum is insensitive to such algebraical transformations.

it comes from the left-hand side of (3.2.9) and represents the non-linear terms of the vector field with gravity.

A note to be added: in fact, we use the perturbation theory only over the gravitational coupling $\varkappa_D$. This is achieved by the fact that only the gravitational force acts on the particles up to the first order. Because of this fact, both terms in (3.2.31) are proportional to $\dot{z}^M$ and z^M, respectively, and thus contain $\varkappa_D$ as a pre-factor.

3.2.3 The radiation formula

Here we highlight the basic steps to derive the momentum radiated in the form of an electromagnetic field. A flat space world tube W with a boundary of two space-like hypersurfaces, $\Sigma_{\pm\infty}$ defined at $t \to \pm\infty$, as well as a time-like cylindrical surface C located at infinite distance is considered. Spatially, both particles are located within the volume or order b^{D-1}, due to the small scattering angle, while with respect to time the process is restricted by the characteristic time of collision, where both fields in the source (3.2.32) are of equal significance. Thus one considers the source of emission to be restricted by the characteristic space-time volume $\mathcal{V}$. Integrating the flux through the two hypersurfaces with the time-positive normals, we write the emitted momentum P^M, using the flat-space background concept:

$$P^M = \int\limits_{\Sigma_{+\infty}} T^{MN}\, dS_N^+ - \int\limits_{\Sigma_{-\infty}} T^{MN}\, dS_N^+ = \int\limits_{\partial W} T^{MN}\, dS_N = \int\limits_{W} \partial^N T_{MN}\, d^D x = -\int\limits_{W} F^{MN} J_N\, d^D x \,, \tag{3.2.33}$$

where T^{MN} and J^M are flat analogues of (3.2.11) and (3.2.4), respectively. Here one uses the Gauß's theorem and the Maxwell equations and implies the cancelation of the surface integral over C due to the fact that it corresponds to the retarded moment $t \to -\infty$ of emission, where the motion was free.

Performing a Fourier-transformation[1], substituting F^{MN} by its retarded solution via the Green's function and making use of current transversality $(k \cdot j = 0)$ with the fact that $j^M(x)$ is a real-valued function, we obtain

$$P^M = \frac{i}{(2\pi)^D} \int d^D k\, k^M\, G_{\rm ret}(k)\, j^*(k) \cdot j(k) \,, \tag{3.2.34}$$

where $G_{\rm ret}(k) = -\mathcal{P}\left(1/k^2\right) + i\pi\, \mathrm{sgn}(k^0)\, \delta(k^2)$. The real part $-\mathcal{P}\left(1/k^2\right)$ does not contribute to the integral due to imparity over time integration. Finally, transforming the integral

[1] Our convention on the Fourier-transforms is

$$\varphi(x) = \frac{1}{(2\pi)^D} \int \varphi(k)\, e^{-ikx} d^D k \,, \qquad \varphi(k) = \int \varphi(x)\, e^{ikx} d^D x \,.$$

into positive values of k^0 and integrating over $|k|$ with $\delta(k^2)$, one finally obtains

$$P^M = -\frac{1}{2(2\pi)^{D-1}} \int \frac{k^M}{|\mathbf{k}|}\, j^*_N(k)\, j_L(k)\, \eta^{NL}\, d^{D-1}\mathbf{k}\,, \tag{3.2.35}$$

where $\mathbf{k}$ is an absolute value of $(D-1)$-dimensional spatial part of k^M. Taking into account the transversality and the on-shell condition $k^2 = 0$ of the emitted wave, one can replace the Minkowski metric in η^{MN} by

$$\Delta^{MN} \equiv \left({}_g\Pi^M{}_L\right)\left({}_{k'}\Pi^{LN}\right) = \eta^{MN} + \frac{k^M k^N - 2\,(kg)\,k^{(M}g^{N)}}{(kg)^2}\,, \tag{3.2.36}$$

with any time-like unit vector g, where ${}_g\Pi = 1 - g\otimes g$ and ${}_{k'}\Pi = 1 + k'\otimes k'/(kg)^2$ are projectors onto subspaces transverse to g and $k' \equiv {}_g\Pi k = k - (kg)\,g$, respectively. Since $k'\cdot g = 0$, the projectors ${}_g\Pi$ and ${}_{k'}\Pi$ commute. Their product Δ^{MN} is then a symmetric projector onto the subspace $M_{k,g}$, perpendicular to k and g. By construction, the projector Δ is idempotent ($\Delta^2 = \Delta$), thus it acts on $M_{k,g}$ as the unit operator. In what follows, we will conveniently choose $g_M = u'_M$ and calculate the flux in the Lorentz frame (referred to as the Lab frame further) with $u'_M = (1, 0, \ldots, 0)$.

We arbitrarily choose the orthonormal basis $\{\varepsilon^M_i\}$ on $M_{k,g}$ and set the resolution of identity

$$\Delta^{MN} = -\sum_i \varepsilon^M_i\, \varepsilon^N_i\,, \qquad \varepsilon^M_i\, \varepsilon_{jM} = -\delta_{ij}\,, \qquad i = 1, 2 ..., D-2\,.$$

Finally, setting $M = 0$ for the energy, the radiation formula reads

$$E_{\text{rad}} = \frac{1}{2\,(2\pi)^{D-1}} \sum_i \int\limits_0^\infty \omega^{D-2}\, d\omega \int\limits_{S^{D-2}} d\Omega\, |J\cdot\varepsilon_i|^2 \tag{3.2.37}$$

as sum over polarizations, where $\omega \equiv k^0$ while $d\Omega$ stands for the measure on unit sphere S^{D-2} in $\mathbb{R}^{D-1}$.

Polarization vectors. Polarization vectors are mutually orthogonal and satisfy $\varepsilon_i\cdot k = \varepsilon_i\cdot u' = 0$. It is convenient to choose the first $D-4$ vectors ε_α to be orthogonal to the collision space ({scattering plane} $\times$ {time}), defined by the linear shell of u^M, u'^M and b^M. Thereby they satisfy the relations $\varepsilon_\alpha\cdot k = \varepsilon_\alpha\cdot u' = \varepsilon_\alpha\cdot u = \varepsilon_\alpha\cdot b = 0$, where $\alpha = 3, \ldots, D-2$. Choosing the D-dimensional unit antisymmetric tensor to be $\epsilon^{0xyz3,\ldots(D-2)} = 1$, we define the remaining two polarization vectors as

$$\varepsilon^M_1 = N^{-1}\left[(ku)\,u'^M - (ku')\,u^M + \left(u\cdot u' - \frac{k\cdot u}{k\cdot u'}\right)k^M\right] \tag{3.2.38}$$

and

$$\varepsilon_2^M = N^{-1}\epsilon^{MM_1M_2\ldots M_{D-1}}\, u_{M_1}u'_{M_2}k_{M_3}\,\varepsilon_{3M_4}\ldots\varepsilon_{(D-2)M_{D-1}}\,, \tag{3.2.39}$$

respectively, where N is a normalization constant given by

$$N^2 = -\Big[(ku')\,u - (ku)\,u'\Big]^2 . \tag{3.2.40}$$

By construction, it is easy to verify that $\varepsilon_1 \cdot u' = \varepsilon_2 \cdot u = \varepsilon_2 \cdot u' = 0$ and $\varepsilon_1 \cdot k = \varepsilon_2 \cdot k = \varepsilon_1 \cdot \varepsilon_2 = 0$.

Introducing the angles according to Fig. 2.1 (for additional info see section 3.6), the normalization factor reads $N = \gamma v \sin\vartheta (ku')$ and the following products do not vanish: $(e_1 b)$, $(e_1 u)$ and $(e_2 b)$, respectively. The values of these contractions are given by

$$\varepsilon_1 \cdot b = -b\,\cos\vartheta\cos\phi\,, \qquad \varepsilon_1 \cdot u = \gamma v \sin\vartheta\,, \qquad \varepsilon_2 \cdot b = -b\,\sin\phi\,. \tag{3.2.41}$$

For the derivation, see [15]. Thus the "bulk" polarizations do not contribute into radiation; thereby in addition, one can introduce chiral polarization vectors in a usual way as

$$\varepsilon_\pm^M = \frac{\varepsilon_1^M \pm i\varepsilon_2^M}{\sqrt{2}}\,. \tag{3.2.42}$$

To summarize this Section: the formula for emitted radiation (3.2.37) and the appropriate polarization states of massless D-dimensional photon are derived, and for the problem-at-hand only two polarizations given in the covariant form (3.2.38, 3.2.39), contribute into the total emitted energy, as it is proper in four dimensions.

The source of the emitted field is to be computed within the iteration scheme based on the perturbation theory over gravitational constant $\varkappa_D$.

Notice, J^M in (3.2.37) represents the *total* source of the total A^M as a solution in *flat* space-time, and thus in our iteration scheme it is given by the series

$$J^M(k) = {}^0J^M(k) + j^M(k) + \ldots\,. \tag{3.2.43}$$

Here the ${}^0J^M$ given by (3.2.14) is a source of boosted Coulomb field, and its square does not contribute to the radiation. It will be shown below that the contribution of product ${}^0J^* \cdot j + {}^0J \cdot j^*$ also vanishes, and $\sum |j \cdot \varepsilon_i|^2$ becomes the first surviving order which contributes to the total emitted energy.

Thereby $j^M(k)$ (3.2.30) as well as its constituents becomes of particular significance and we concentrate on its evaluation. Looking at $\sigma^M(k)$ (3.2.32), it is enough to restrict ourselves on the first-order perturbation of the gravitational field ${}^1h^{MN} = {}^1h^{MN}_{\rm m} + {}^1h^{MN}_{\rm m'}$. Thus in order to simplify notations, we keep h^{MN} as a simplified notation of ${}^1h^{MN}_{\rm m}$ and denote, respectively, $h'^{MN} \equiv {}^1h^{MN}_{\rm m'}$.

3.3 The radiation amplitudes

The first-order fields, discussed above, in the momentum space are given by

$$\begin{aligned}
h_{MN}(q) &= \frac{2\pi\,\varkappa_D\,m}{q^2}\,\mathrm{e}^{iqb}\,\delta(qu)\left(u_M u_N - \frac{1}{d+2}\,\eta_{MN}\right),\\
h'_{MN}(q) &= \frac{2\pi\varkappa_D m'}{q^2}\,\delta(qu')\left(u'_M u'_N - \frac{1}{d+2}\,\eta_{MN}\right),\\
{}^1\!A^M(q) &= -\frac{2\pi\,e}{q^2}\,\mathrm{e}^{iqb}\,\delta(qu)\,u^M,\\
{}^1\!F^{MN}(q) &= i\,\frac{2\pi\,e}{q^2}\,\mathrm{e}^{iqb}\,\delta(qu)\left[q^M u^N - q^N u^M\right].
\end{aligned}\tag{3.3.1}$$

Respectively, the Fourier-transform of ${}^0\tilde{J}(x) = {}^0J(x)$ reads

$${}^0J^M(q) = 2\pi\,e\,\mathrm{e}^{iqb}\,\delta(qu)\,u^M\,. \tag{3.3.2}$$

Now we proceed to compute the two parts of the radiation amplitude.

3.3.1 Local amplitude

The Fourier transform of (3.2.31) reads

$$\rho^M(k) = e\,\mathrm{e}^{i(kb)}\int\left[{}^1\dot{z}^M + i\,(k\,{}^1z)\,u^M\right]\mathrm{e}^{i(ku)\tau}\,d\tau\,. \tag{3.3.3}$$

The first order correction to the trajectory is computed in 2 and we quote that result here.

$${}^1z^M(\tau) = -\frac{im'\varkappa_D^2}{(2\pi)^{D-1}}\int d^Dq\,\frac{\delta(qu')}{q^2(qu)}\,\mathrm{e}^{-iqb}\left(\mathrm{e}^{-i(qu)\tau}-1\right)\left[\gamma u'^M - \frac{1}{d+2}\,u^M - \frac{\gamma_*^2}{2\,(qu)}\,q^M\right], \tag{3.3.4}$$

where $\gamma_*^2 \equiv \gamma^2 - (d+2)^{-1}$. We drop all the terms containing u'^M since they are transverse to the polarization vectors and thus will not contribute to the radiation. After integrating with respect to τ we obtain

$$\rho^M(k) = -\frac{em'\varkappa_D^2\,\mathrm{e}^{i(kb)}}{(2\pi)^{D-2}}\left[\gamma\,I\left(u'^M - \frac{ku'}{ku}\,u^M\right) - \frac{\gamma_*^2}{2\,(ku)}\,I^M + \frac{\gamma_*^2\,k\cdot I}{2\,(ku)^2}\,u^M\right], \tag{3.3.5}$$

where the integrals I and I^M are defined by

$$I = \int\frac{\delta(pu')\,\delta(ku-pu)\,\mathrm{e}^{-i(pb)}}{p^2}\,d^Dp\,,\qquad I^M = \int\frac{\delta(pu')\,\delta(ku-pu)\,\mathrm{e}^{-i(pb)}}{p^2}\,p^M\,d^Dp\,. \tag{3.3.6}$$

These integrals have been computed in [13] in terms of Macdonald functions (modified Bessel functions of 3rd kind):

$$I = -\frac{(2\pi)^{d/2+1}}{\gamma v\, b^d}\, \hat{K}_{d/2}(z)\,, \qquad I^M = \frac{(2\pi)^{d/2+1}}{\gamma v\, b^{d+1}} \left[z\, \hat{K}_{d/2}(z)\, \frac{u^M - \gamma u'^M}{\gamma v} - i\hat{K}_{d/2+1}(z)\, \frac{b^M}{b} \right], \tag{3.3.7}$$

with

$$z \equiv \frac{(ku)b}{\gamma v}\,, \qquad z' \equiv \frac{(ku')b}{\gamma v}\,, \tag{3.3.8}$$

where we use the more economic, non-conventional notation $\hat{K}_\nu(x) \equiv x^\nu K_\nu(x)$, in order to simplify the explanation of estimates making use of slowly altering at $[0, \mathcal{O}(1)]$ function.

Substituting (3.3.7) into (3.3.5) one obtains

$$\rho^M(k) = \frac{\lambda\, \mathrm{e}^{i(kb)}}{v} \left[\left(1 - \frac{\gamma_*^2}{2\gamma^2 v^2} \right) \left(u'^M - \frac{z'}{z}\, u^M \right) \hat{K}_{d/2}(z) + \right. \\ \left. + \frac{i\gamma_*^2}{2\gamma^2 v z} \left(\frac{(kb)}{\gamma v z}\, u^M - \frac{b^M}{b} \right) \hat{K}_{d/2+1}(z) \right], \tag{3.3.9}$$

with

$$\lambda \equiv \frac{e m' \varkappa_D^2}{(2\pi)^{d/2+1}\, b^d}\,. \tag{3.3.10}$$

Here we have restored the dependence on u'^M in order to make obvious the conservation of the current (Subsection 3.3.5).

The local current $\rho^M(k)$ contains Macdonald functions $K_\nu(z)$ and, combined with the volume factor $\omega^{d+2} \sin^{d+1}\vartheta$, gives dominant contribution in the region $\omega \sim \gamma^2/b$, $\vartheta \sim \gamma^{-1}$ (i.e. $z \sim 1$), as was argued in [13] and will be discussed later in Subsection 3.5.1. In this region for the usage below we expand $\rho^M(k)$ in powers of γ:

$$\rho^M(k) = \frac{\lambda\, \mathrm{e}^{i(kb)}}{2} \left[-\frac{z'}{z}\, \hat{K}_{d/2}(z)\, u^M - i \left(\frac{z' \sin\vartheta \cos\phi}{z}\, u^M + \frac{b^M}{b} \right) \frac{\hat{K}_{d/2+1}(z)}{z} + \right. \\ \left. + \frac{d+1}{d+2}\, \frac{z'}{\gamma^2 z}\, \hat{K}_{d/2}(z)\, u^M + \mathcal{O}(\gamma^{-2}) \right], \tag{3.3.11}$$

where the first term in the parenthesis is of order $\mathcal{O}(\gamma)$, the square-bracket-term has order $\mathcal{O}(1)$, while the last term is of order $\mathcal{O}(\gamma^{-1})$ and the rest represents all subleading terms.

3.3.2 Non-local (stress) amplitude

The Fourier transform of (3.2.32) is given by

$$\sigma^M(k) = \frac{\varkappa_D^2\, e\, m'\, \mathrm{e}^{i(kb)}}{(2\pi)^2}\left[(ku')\left((ku')\,u^M - (ku)\,u'^M\right)J + \left(\gamma\,(ku') - \frac{(ku)}{d+2}\right)J^M + \right.$$
$$\left. + \left(\frac{u^M}{d+2} - \gamma u'^M\right) k\cdot J + \left((ku)\,u'^M - (ku')\,u^M\right) u'\cdot J\right], \qquad (3.3.12)$$

where[1]

$$J(k) \equiv \int \frac{\delta(pu')\,\delta(ku-pu)\,\mathrm{e}^{-i(pb)}}{p^2\,(k-p)^2}\, d^Dp\,, \qquad J^M(k) \equiv \int \frac{\delta(pu')\,\delta(ku-pu)\,\mathrm{e}^{-i(pb)}}{p^2\,(k-p)^2}\, p^M\, d^Dp\,, \qquad (3.3.13)$$

which have been computed in [15] as integrals over Feynman parameter x. We keep (3.3.12) for the proof of gauge conservation and further suppress terms proportional to u'^M, as they do not contribute to the radiation. From this definition (3.3.13) it follows that $u'\cdot J = 0$, thus $\sigma^M(k)$ reads:

$$\sigma^M(k) = \frac{\lambda\,\mathrm{e}^{i(kb)}}{2\gamma v}\int_0^1 dx\,\mathrm{e}^{-i(kb)\,x}\left\{ i\left[\frac{(kb)}{d+2}\,u^M + \left(\gamma^2 v z' - \frac{\gamma z v}{d+2}\right)\frac{b^M}{b}\right]\hat{K}_{d/2}(\zeta) + \right.$$
$$\left. + \left[\frac{\beta - x\xi^2}{d+2} - \left(\gamma z' - \frac{z}{d+2}\right)\left((1-x)\,z + \gamma z' x\right) + \gamma^2 v^2 z'^2\right]\hat{K}_{d/2-1}(\zeta)\,u^M\right\}, \qquad (3.3.14)$$

with

$$\xi^2 \equiv 2\gamma z z' - z^2 - z'^2\,, \qquad \beta \equiv \gamma z z' - z^2\,, \qquad \zeta^2(x) \equiv z'^2 x^2 + 2\gamma z z' x\,(1-x) + z^2\,(1-x)^2.$$

The non-local amplitude has now been written in terms of three scalar integrals of the following type:

$$J_{(\sigma,\tau)} \equiv \int_0^1 x^\sigma\,\mathrm{e}^{-i(kb)x}\,\hat{K}_{d/2+\tau}(\zeta)\,dx\,, \qquad (\sigma,\tau) = (0,-1),(0,0) \text{ and } (1,-1)\,. \qquad (3.3.15)$$

These integrals have been studied in details in [15]: introducing parameter $\varrho \sim \omega b \vartheta$, (3.3.15) is expanded as series over $1/\varrho$. Thus in the high-frequency region (or z−region, for brevity) $\omega \sim \gamma^2/b$, $\vartheta \sim \gamma^{-1}$ the dominant contribution comes from small $x = 0\ldots\mathcal{O}(\gamma^{-2})$ and all integrals (3.3.15) are to be expanded in terms of Macdonald functions with argument $\zeta(0) = z$, with expansion parameter $1/\gamma$. In the large-angle region

[1] We denote these double-propagator Fourier integrals as J and J^M, the same letter as vectorial source introduced in the Section 3.2, in order to keep notation and contact with [15], so we hope, this will not bring a reader to some misleading.

(or $z'-$region) $\omega\sim\gamma/b$, $\vartheta\sim 1$ the dominant contribution comes from the values of x near 1: $x = 1-\mathcal{O}(\gamma^{-2})\ldots 1$ and all such integrals are to be expanded in terms of Macdonald functions with argument $\zeta(1) = z'$.

In the transition region ($\omega\sim\gamma/b$, $\vartheta\sim\gamma^{-1}$) the exponential in (3.3.14) does not oscillate rapidly and the whole domain $x = [0,1]$ contributes equally. The series with Macdonald functions $K_\nu(z)$ and $K_{\nu'}(z')$ is also valid (see section 3.8) but converges very slow since no small factor is available: $\varrho\sim 1$. Finally, in the ultimate region ($\omega\sim\gamma^2/b$, $\vartheta\sim 1$) the whole integral is exponentially suppressed by $\mathcal{O}(\mathrm{e}^{\gamma})$.

Next we consider more thoroughly the high-frequency behavior of local and non-local amplitudes.

3.3.3 Destructive interference

We now proceed to demonstrate the cancelation of the two leading orders of σ^M and ρ^M in powers of γ in the $z-$region, which leads to the strong damp of the amplitude by $\mathcal{O}(\gamma^2)$ and the emitted energy by four orders of γ. We will refer to this effect as destructive interference. The same effect for gravity was described in [14; 15] by means of the same representation via Macdonald functions. In another representation it appeared in [30] dealing with only four dimensions.

We follow [15] and sketch the procedure for showing this: in the $z-$region ($z\sim 1, z'\sim\gamma$) the integral $J_{(1,-1)}$ is suppressed by two orders of γ with respect to the $J_{(0,-1)}$ and $J_{(0,0)}$ as it was implicitly mentioned in the previous Subsection and proved in [15, eqn.(3.28)]. We now keep only the terms that will give us the first three orders of (3.3.14):

$$\sigma^M(k)\approx\frac{\lambda\,\mathrm{e}^{i(kb)}z'\gamma}{2}\int\limits_0^1 dx\,\mathrm{e}^{-i(kb)\,x}\left[z'\hat{K}_{d/2-1}(\zeta)\,u^M+\frac{i}{b}\,\hat{K}_{d/2}(\zeta)\;b^M-\right.$$
$$\left.-\left(\frac{d+1}{d+2}\,\frac{z}{\gamma}+\frac{z'}{\gamma^2}+z'x\right)\hat{K}_{d/2-1}(\zeta)\,u^M\right].\qquad(3.3.16)$$

Finally we substitute the approximation [15, eqn.(B.10)], appropriately simplified here neglecting the exponentially suppressed Macdonalds $K_{\nu'}(z')$ ($a\equiv z/\sin\vartheta$):

$$\int\limits_0^1 dx\,\mathrm{e}^{-i(kb)\,x}\hat{K}_{\nu-1}(\zeta)\approx\frac{\beta}{a^2\xi^2}\left[\hat{K}_\nu(z)-i\frac{kb}{\beta}\,\hat{K}_{\nu+1}(z)-\frac{2\nu+1}{a^2}\,\hat{K}_{\nu+1}(z)+\frac{\sin^2\!\phi}{a^2}\,\hat{K}_{\nu+2}(z)\right]\approx$$
$$\approx\frac{\hat{K}_\nu(z)}{\gamma zz'}-i\frac{(kb)\,\hat{K}_{\nu+1}(z)}{(\gamma zz)^2}+\frac{1-\gamma^2\psi}{\gamma^3z'z}\,\hat{K}_\nu(z)-\frac{\sin^2\vartheta}{\gamma z^3z'}\left[(2\nu+1)\hat{K}_{\nu+1}(z)-\sin^2\!\phi\,\hat{K}_{\nu+2}(z)\right].$$
$$(3.3.17)$$

For $J_{(1,-1)}$-type integral [15, eqn.(3.28)] we retain only the leading terms:

$$\int_0^1 dx\, x\, \mathrm{e}^{-i(kb)\,x}\, \hat{K}_{\nu-1}(\zeta) \approx -\frac{1}{(\gamma z')^2}\, \hat{K}_{\nu}(z) - \frac{(2\nu+1)}{(\gamma z z')^2}\, \hat{K}_{\nu+1}(z) + \frac{1}{(\gamma z z')^2}\, \hat{K}_{\nu+2}(z)\,.$$

Thus upon substitution of the latter two into (3.3.16) and retaining the first three orders, one obtains:

$$\sigma^M \approx \frac{\lambda\, \mathrm{e}^{i(kb)}}{2\gamma} \left[\frac{\gamma z'}{z}\, \hat{K}_{d/2}\,(z)\, u^M + i\left(\gamma \frac{b^M}{b} - \frac{(kb)}{z} u^M\right) \frac{\hat{K}_{d/2+1}(z)}{z} - \frac{d+1}{d+2}\, \hat{K}_{d/2}(z)\, u^M - \right.$$
$$\left. -(d+1)\left(1 - \frac{\sin^2\vartheta}{\psi}\right) \frac{\hat{K}_{d/2+1}(z)}{z^2}\, u^M + \left(\left(\frac{\sin^2\vartheta\, \sin^2\phi}{\psi} - 1\right) u^M + \frac{(kb)}{z'} \frac{b^M}{b}\right) \frac{\hat{K}_{d/2+2}(z)}{z^2} \right].$$

The first two orders of this expression exactly cancel with the first two orders of (3.3.11), leaving us with

$$j^M \approx \frac{\lambda\, \mathrm{e}^{i(kb)}}{2\gamma} \left[\frac{d+1}{d+2} \left(\frac{1}{\gamma^2\psi} - 1\right) \hat{K}_{d/2}(z)\, u^M - (d+1)\left(1 - \frac{\sin^2\vartheta}{\psi}\right) \frac{\hat{K}_{d/2+1}(z)}{z^2}\, u^M + \right.$$
$$\left. + \left(\left(\frac{\sin^2\vartheta\, \sin^2\phi}{\psi} - 1\right) u^M + \frac{(kb)}{z'} \frac{b^M}{b}\right) \frac{\hat{K}_{d/2+2}(z)}{z^2} \right]. \tag{3.3.18}$$

We note that even though the current will finally be projected on the two polarization vectors, this will not change our conclusion, as the contractions (3.2.41) add no powers of γ *at the region of interest*.

3.3.4 The total radiation amplitude

In order to compute the total radiation energy, we will need to study the following three regions. The z-type radiation emitted for angles $\vartheta \sim 1/\gamma$ and $\omega \sim \gamma^2/b$, the region with frequency $\omega \sim \gamma/b$ again for small angles and finally the radiation at angles $\vartheta \sim 1$ at medium-frequencies.

High frequency regime. The radiation amplitude in $z-$regime after the destructive interference was derived in the previous Subsection. Projecting (3.3.18) on (3.2.42), the chiral amplitudes $j_\pm \equiv j \cdot \varepsilon_\pm$ read:

$$j_\pm(k) \approx \frac{\lambda\, \mathrm{e}^{i(kb)} \sin\vartheta}{2\sqrt{2}} \left[\frac{d+1}{d+2} \frac{1-\gamma^2\psi}{\gamma^2\psi}\, \hat{K}_{d/2}(z) - \frac{d+1}{z^2}\left(\frac{\sin^2\vartheta}{\psi} - 1\right) \hat{K}_{d/2+1}(z) + \right.$$
$$\left. + \frac{\sin^2\phi}{z^2}\left(\frac{\sin^2\vartheta}{\psi} - 1\right) \hat{K}_{d/2+2}(z) \pm i\, \frac{\sin 2\phi}{2\, z^2}\, \hat{K}_{d/2+2}(z) \right]. \tag{3.3.19}$$

All terms in the parenthesis (3.3.19) are of order $\mathcal{O}(1)$ (in $\lambda = 1$ units) within $z-$regime, hence the whole amplitude goes like $\mathcal{O}(\gamma^{-1})$ due to the common pre-factor $\sin\vartheta$.

Large angle regime. In this region of the parameters (z'–regime) z is of order $\mathcal{O}(\gamma)$, so the Macdonald functions that have z as their argument are exponentially suppressed. Thus we ignore the local part of the current and consider only the non-local part. To repeat, in this regime the main contribution of the integrals with respect to x comes from the area near $x = 1$, and the integrals $J_{0,\tau} - J_{1,\tau}$, which are of the form $1 - x$, are suppressed by a factor of $\mathcal{O}(\gamma^{-2})$ with respect to both $J_{0,\tau}$ and $J_{1,\tau}$. We rewrite (3.3.14) in a way where we are expanding both with respect to γ but also with respect to $1-x$. Taking also into account that u^M is perpendicular to the second projection, while it gives us an order of γ when projected on the first polarization, while b^M gives no additional powers of γ when projected on either polarization, we write the two leading orders:

$$j^M(k) \approx \frac{\lambda\, \mathrm{e}^{i(kb)}}{2\gamma} \int_0^1 dx\, \mathrm{e}^{-i(kb)\,x} \left\{ \left[\left(\gamma^2 z'^2 - \frac{d+1}{d+2} \gamma z z' \right) (1-x) + \frac{z'^2}{d+2} \right] \hat{K}_{d/2-1}(\zeta)\, u^M + \right.$$
$$\left. + i \left[\frac{(kb)}{d+2} u^M + \left(\gamma^2 z' - \frac{\gamma z}{d+2} \right) \frac{b^M}{b} \right] \hat{K}_{d/2}(\zeta) \right\} . \quad (3.3.20)$$

Since no destructive interference is expected, we retain only the leading terms of integrals, and set $x = 1$ inside the integrand of (3.3.20). These integrals have been computed in [15] and give, to the leading order,

$$\int_0^1 \mathrm{e}^{i(kb)x}\, \hat{K}_\tau(\zeta)\, dx \approx \frac{\mathrm{e}^{-i(kb)}}{z'^2 \gamma^2 \psi}\, \hat{K}_{\tau+1}(z') . \quad (3.3.21)$$

Eventually, the entire first line in (3.3.20) turns out to be subleading with respect to the second one, and, upon substitution (3.3.21) j^M reads:

$$j^M(k) \approx \frac{\lambda\, i}{2\gamma\psi} \left[\frac{(kb)}{\gamma^2 z'^2 (d+2)} u^M + \left(\frac{1}{z'} - \frac{z}{\gamma z'(d+2)} \right) \frac{b^M}{b} \right] \hat{K}_{d/2+1}(z') . \quad (3.3.22)$$

Finally projecting on $\varepsilon_\pm$ (3.2.42) the two significant radiation amplitudes in z'–region are given by

$$j_\pm(k) \approx \frac{\lambda\, i}{2\sqrt{2}\gamma\psi} \left[-\frac{\sin^2\vartheta\, \cos\phi}{z'(d+2)} + \left(\frac{\psi}{d+2} - \frac{1}{z'} \right) \cos\vartheta \cos\phi \pm \right.$$
$$\left. \pm i \left(\frac{\psi}{d+2} - \frac{1}{z'} \right) \sin\phi \right] \hat{K}_{d/2+1}(z') . \quad (3.3.23)$$

In what follows, the amplitudes are of order $\mathcal{O}(\gamma^{-1})$.

Transition regime. In this region, the projection of the current on the polarization vectors will once more not add any powers of γ. We have $z \sim 1/\gamma$ and $z' \sim 1$. Looking at expressions (3.3.9) and (3.3.14) we see that they are of the same order $\mathcal{O}(\gamma)$ in any dimension in units $\lambda = 1$.

3.3.5 Conservation of current and validity of gauge fixation

In the above analysis, the following gauges were fixed:

- the affine parametrization of the trajectories along the worldlines of the scattered particles:

$$g_{MN}\dot{z}^M\dot{z}^N = g_{MN}\,\dot{z}'^{\,M}\,\dot{z}'^{\,N} = 1\,; \tag{3.3.24}$$

- the de Donder gauge on the gravitational field:

$$\partial_M\,{}^k\psi^{MN} = 0, \qquad\qquad k = 1, 2, \ldots\,; \tag{3.3.25}$$

- the Lorentz gauge on the vector field:

$$\partial_M\,{}^kA^M = 0, \qquad\qquad k = 1, 2, \ldots\,. \tag{3.3.26}$$

To verify self-consistency of our scheme (at least to the lowest orders of interest), we show it explicitly.

To zeroth order, (3.3.24) degenerates into $u^2 = 1$ and $u'^2 = 1$ which is trivially satisfied.

In the first order, variation of (3.3.24) reads

$$\varkappa_D h'_{MN}(\,{}^0z)\,u^M u^N + 2\,(\,{}^1\dot{z}\cdot u) = 0\,, \qquad\qquad \varkappa_D h_{MN}(\,{}^0z')\,u'^M u'^N + 2\,(\,{}^1\dot{z}'\cdot u') = 0\,, \tag{3.3.27}$$

respectively. From (3.3.1) the value of $h'_{MN}(x)$ at the location of $m-$particle $x = {}^0z(\tau)$ reads

$$h_{MN}(\,{}^0z) = \frac{\varkappa_D\,m'}{(2\pi)^{D-1}}\int d^Dq\frac{\delta(qu')}{q^2}\left(u'_M u'_N - \frac{1}{d+2}\,\eta_{MN}\right)\,\mathrm{e}^{-iqz_0}. \tag{3.3.28}$$

Contracting it with $u^M\,u^N$ and substituting ${}^0z^M(\tau) = u^M\,\tau + b^M$ one obtains

$$h_{MN}(\,{}^0z)\,u^M\,u^N = \frac{\varkappa_D\,m'}{(2\pi)^{D-1}}\int d^Dq\frac{\delta(qu')}{q^2}\left(\gamma^2 - \frac{1}{d+2}\right)\,\mathrm{e}^{-iq\,\cdot(u\tau+b)}. \tag{3.3.29}$$

Differentiating (3.3.4) and contracting with u^M one obtains

$$(\,{}^1\dot{z}(\tau)\cdot u) = -\frac{m'\varkappa_D^2\,\gamma_*^2}{2(2\pi)^{D-1}}\int d^Dq\,\frac{\delta(qu')}{q^2}\,\mathrm{e}^{-iqb}\,\mathrm{e}^{-i(qu)\tau}\,. \tag{3.3.30}$$

Multiplying it by 2 and combining with (3.3.29) one gets the cancelation and thereby verifies (3.3.27) to the first order. The gauge on the trajectory of $m'-$particle is checked similarly.

Next, proceeding to the de Donder gauge on ${}^1\psi_{MN}$: one rewrites (3.3.1):

$$ {}^1\psi^{MN}(q) = \frac{2\pi\,\varkappa_D\,m}{q^2}\,\mathrm{e}^{iqb}\,\delta(qu)\,u^M u^N \,. $$

The divergence in Fourier space reads

$$ q_N\,{}^1\psi^{MN}(q) = \frac{2\pi\,\varkappa_D\,m}{q^2}\,\mathrm{e}^{iqb}\,(qu)\,\delta(qu)\,u^M = 0\,, $$

by virtue of distributional identity $x\,\delta(x) = 0$.

The divergence of ${}^1A^M$ (the first order of (3.3.26)) vanishes due to the same reason:

$$ q_M\,{}^1A^M(q) = -\frac{2\pi\,e}{q^2}\,\mathrm{e}^{iqb}\,\delta(qu)\,(qu) = 0\,. \tag{3.3.31} $$

Let also verify the gauge on ${}^2A^M$: in the momentum space

$$ {}^2A^M(k) = -\frac{{}^2j^M(k)}{k^2}\,, $$

where $j^M(k)$ is the full Fourier-transform taken off-shell $k^2 = 0$ and with no terms neglected due to polarizations. Thus Lorentz gauge of ${}^2A^M$ is equivalent to $k\cdot j = 0$.

The constituents of $j^M(k)$ are given by (3.3.5,3.3.9) and (3.3.12). Projecting both on k^M one concludes $k\cdot\rho(k) = 0$ and $k\cdot\sigma(k) = 0$. Thus both

$$ \partial_M\,\rho^M(x) = 0\,, \qquad\qquad \partial_M\,\sigma^M(x) = 0 $$

conserve separately, as well as their sum.

Finally, one has to point out, that the conservation of ${}^2A^M$ on flat background represents the same effect as conservation of J^M (3.2.4) (continuity equation) in the curved background:

$$ \nabla_M J^M(x) = 0\,. \tag{3.3.32} $$

Explicitly the latter reads

$$ \nabla_M J^M = \partial_M J^M + \Gamma^N_{N,M}\,J^M\,. \tag{3.3.33} $$

The zeroth-order variation coincides with the conservation of ${}^0J^M = {}^0\tilde{J}^M$ discussed above. The first-order variation of (3.3.33) is given by

$$ {}^1\big[\nabla_M J^M\big] = \partial_M\,{}^1J^M + {}^1\Gamma^N_{N,M}\,{}^0J^M\,. \tag{3.3.34} $$

These terms read

$$ \begin{aligned} \partial_M\,{}^1J^M &= e\,\partial_M \int \Big({}^1\dot{z}^M - u^M\,{}^1z^N\partial_N - \frac{\varkappa_D}{2}\,h\,u^M\Big)\,\delta^D\big(x - {}^0z\big)\,d\tau \\ {}^1\Gamma^N_{N,M}\,{}^0J^M &= \frac{e\,\varkappa_D}{2}\,h_{,M}\int u^M\,\delta^D\big(x - {}^0z\big)\,d\tau\,, \end{aligned} \tag{3.3.35} $$

thus their sum equals

$$e\int\left({}^{1}\dot{z}^{M}-u^{M}\,{}^{1}z^{N}\partial_{N}\right)\partial_{M}\,\delta^{D}\left(x-{}^{0}z\right)\,d\tau=e\int d\left({}^{1}z^{M}\,\partial_{M}\,\delta^{D}\left(x-{}^{0}z\right)\right)=0 \qquad (3.3.36)$$

as a total derivative. The latter represents the proof in coordinate-space of the property $\partial_M\,{}^{1}\tilde{J}^{M}(x)=\partial_M\,\rho^{M}(x)=0$, discussed above.

Thus the iteration scheme we use is compatible with the gauge we fix, and gives the apparent way to compute radiation amplitude and, eventually, the flux of emitted momentum.

3.4 The emitted energy

In order to compute the emitted energy, we take the zeroth component of the emitted momentum (3.2.37):

$$E=\frac{1}{2\left(2\pi\right)^{d+3}}\sum_{i}\int_{0}^{\infty}\omega^{d+2}d\omega\int d\Omega\,\left|j_{i}(k)\right|^{2}, \qquad (3.4.1)$$

First we summarize the radiation amplitudes derived in the previous Section and overview the corresponding contributions to the total flux. In Table 3.1 we present the energy emitted in the several relevant regimes of frequency and angle, where the estimates of contribution to the total emitted energy are deduced from (3.4.1) with the estimate of $j_i(k)$ and the characteristic value of ϑ and ω following immediately from the corresponding Table's entry.

Now we illustrate qualitatively the effects described above and based on the derivation in previous Section.

On Fig.3.1 we plot a characteristic picture of the behavior of local and non-local amplitudes and their sum (the radiation amplitude) for the case $d=0$ at characteristic value of ϑ and some common value of ϕ.

The qualitative features deserving attention are the following:

- At $\omega\to 0$ $\mathrm{Im}\,\rho(k)$ goes like $1/\omega$ and dominates in total j, in Fig. 3.1 it corresponds to the asymptote with tangent -1 on green (dot-dashed) curve. This property is valid for all $d\geqslant 0$ and will be of usage further, when the zero-frequency limit is to be computed;

ϑ \ ω	$\omega \lesssim 1/b$	$\omega \sim \gamma/b$	$\omega \sim \gamma^2/b$	$\omega \gg \gamma^2/b$
γ^{-1}	$j \sim \mathrm{Im}\,\rho$ $E_{\mathrm{rad}} \sim \gamma^2$ (subleading by phase space)	$j \sim \mathcal{O}(\gamma)$, from ρ and σ $x \in [0, 1]$, medium regime no destructive interference $E_{\mathrm{rad}} \sim \gamma^3$	$j \sim \mathcal{O}(\gamma^{-1})$, from $\rho + \sigma(z)$ $x \in [0, \mathcal{O}(\gamma^{-2})]$ z − regime destructive interference $E_{\mathrm{rad}} \sim \gamma^{d+2}$	negligible radiation – exponential fall-off
1	$j \sim \rho$ $E_{\mathrm{rad}} \sim \gamma^0$ (subleading by phase space)	$j \sim \mathcal{O}(\gamma^{-1})$, from $\sigma(z')$ $x \in [1 - \mathcal{O}(\gamma^{-2}), 1]$ z' − regime $E_{\mathrm{rad}} \sim \gamma^{d+1}$	negligible radiation – exponential fall-off	negligible radiation – exponential fall-off

Table 3.1: The behavior of radiation amplitudes and contribution to the emitted energy of each of the several characteristic regions of angle and frequency. The values are normalized as $\lambda = b = 1$.

- At $x \to -\infty$ $(\omega \to 0)$ $|\mathrm{Re}\,\sigma| \ll |\mathrm{Re}\,\rho|$ hence $\mathrm{Re}\,j \approx \mathrm{Re}\,\rho$. At this limit $\omega \to 0$ $|\mathrm{Re}\,\sigma|$ goes like ω^0 (black, dotted line in Fig. 3.1) for $d = 0$, like ω^1 for $d = 1$ and like ω^2 for $d \geqslant 2$, as it follows directly from (3.3.14) and behavior of hatted Macdonald functions.

- At $x > 2$ each curve has rapid fall-off at $y = -\infty$, corresponding to the strong exponential decay of an amplitude at $\omega \gtrsim \gamma^2/b$;

- At $x > 1$ $\mathrm{Re}\,\sigma \approx -\mathrm{Re}\,\rho$, so their sum (difference of absolute values in the plot) $\mathrm{Re}\,j$ (cyan, solid) is much smaller. At $x \approx 2$ the difference of $\mathrm{Re}\,j$ and $\mathrm{Re}\,\rho$ is $\Delta y \approx 2$, so j is damped by γ^2 with respect to $\mathrm{Re}\,\rho$. This illustrates the destructive interference at $\gamma^2/b > \omega \gg \gamma/b$, that can be rewritten as

$$j(\omega) \sim j(\omega_0)\,\frac{\omega_0^2}{\omega^2}\,, \qquad \omega_0 \sim \frac{\gamma}{b}\,;$$

- At $x \approx 2$ the values of logarithms of $\mathrm{Re}\,\rho > \mathrm{Im}\,\rho > \mathrm{Re}\,j$ differ by $\Delta y \approx 1$, that confirms the expansion in power of γ made in (3.3.11);

- In the region $x = (1, 2)$ $\log_\gamma |\mathrm{Re}\,j|$ represents straight-line piece with tangent -2, what corresponds to the destructive interference region $\omega = (\gamma/b, \gamma^2/b)$. Thus the radiation amplitude itself goes like ω^{-2} at this region. Being averaged over angles (with some average angle $\bar{\vartheta} = \mathcal{O}(\gamma^{-1})$), the same is valid for the frequency distribution. For higher dimensions the corresponding behavior of the latter $dE/d\omega \equiv F$

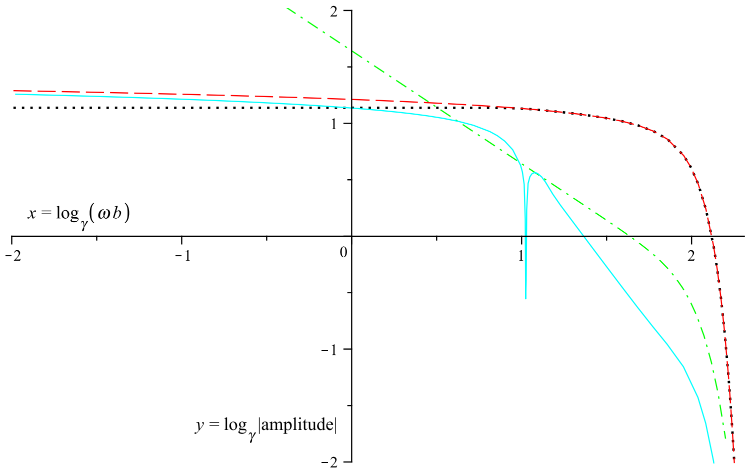

Figure 3.1: Radiation amplitudes of first polarization for $d = 0$ and $\gamma = 10^3$ in logarithmic scales $x = \log_\gamma \omega b$ and $y = \log_\gamma |\text{amplitude}|$, evaluated at $\vartheta = 1/\gamma$, $\phi = \pi/4$. The plots are given for $-\text{Re}\,\rho(k)$ (red, dashed), $\text{Im}\,\rho(k)$ (green, dot-dashed), $\text{Re}\,\sigma$ (black, dotted) and $\text{Re}\,j$ (cyan, solid). The common phase factor $\mathrm{e}^{i(kb)}$ is neglected. At $x \approx 1$ the curve $\log_\gamma |\text{Re}\,j|$ in logarithmic scale has discontinuity $y = -\infty$ related with the fact that corresponding original amplitude $\text{Re}\,j$ changes its sign.

is

$$F(\omega) \sim (\omega\bar{\vartheta})^{d+2} j^2(\omega) \sim \frac{j^2(\omega_0)\,\omega_0^4}{\gamma^{d+2}}\,\omega^{d-2} \sim \gamma^{4-d}\,\omega^{d-2}, \tag{3.4.2}$$

in this region $(\gamma/b < \omega < \gamma^2/b)$;

- $|\text{Im}\,\rho|$ is subleading with respect to $|\text{Re}\,\sigma|$ but larger than $|\text{Re}\,j|$ (at $x > 1$) on this plot. It is damped by $|\text{Im}\,\sigma|$ not presented here, so their sum $|\text{Im}\,j|$ becomes much smaller than $|\text{Re}\,j|$.

Thus in fact, we have two radiation amplitudes instead of a single one in 2, with obvious identification $f \to e, f' \to e'$. In other words our primary problem now is to derive the final overall coefficient.

3.4.1 Total radiated energy

As can be seen from Table 3.1, the dominant radiation comes from different regimes depending on the number of extra dimensions, d. Indeed, as it follows from (3.4.2),

$$E \sim \int\limits_{\sim\gamma/b}^{\sim\gamma^2/b} \frac{dE}{d\omega}\,d\omega \sim \frac{1}{\gamma^{d-4}} \int\limits_{\omega_0}^{\gamma\omega_0} \omega^{d-2}\,d\omega\,, \tag{3.4.3}$$

so the dominant contribution comes from the upper limit $\omega \sim \gamma^2/b$ for $d \geqslant 2$, from the lower limit $\omega_0 \sim \gamma/b$ for $d = 0$ and from the whole domain for $d = 1$, respectively.

According to this argument, we need to consider separately the cases where the number of extra dimensions are $d = 0$, $d = 1$ and $d \geqslant 2$. We start with studying the $d \geqslant 2$ case.

$d \geqslant 2$. In this case, as can be seen in the table, the radiation with frequency in the area of $\omega \sim \gamma^2/b$ dominates. In the case of interest here, $R \gg b$, we can replace the summation by integration and use the uncompactified formula for the emitted energy.

The next step is to substitute the expression we have already found for (3.2.42), which will give the dominant contribution in this case. We notice that when squaring the two amplitudes we will have products of the Macdonald functions. In order to perform the integration over ω, we will change variable to z and the radiated energy will take the following form:

$$\frac{dE}{d\Omega} = \frac{\lambda^2 \sin^{d+3}\vartheta}{8\,(2\pi)^{d+3}\, b^{d+3}\psi^{d+3}} \sum_{a,b=0}^{2} C_{ab}^{(d)} D_{ab}^{(d)}(\vartheta,\phi)\,, \tag{3.4.4}$$

with[1] $C_{ab}^{(d)} \equiv \int \hat{K}_{d/2+a}(z)\hat{K}_{d/2+b}(z)\, z^{d+2(\delta_{0a}+\delta_{0b}-1)}\, dz$. We are now left with the integration over ω. The expressions for $j_\pm(k)$ (3.3.19) are accurate for high frequencies, however it has been shown 2 that for $d \geqslant 2$ it is possible to expand the integration domain $z = (\sim 1/\gamma, \infty)$ up to $z = (0, \infty)$, with the relative error $\mathcal{O}(\gamma^{-1})$. Computing $C_{ab}^{(d)}$ with help of [37]

$$\int_0^\infty K_\mu(z)K_\nu(z)\, z^{\alpha-1}\, dz = \frac{2^{\alpha-3}\Gamma\left(\frac{\alpha+\mu+\nu}{2}\right)\Gamma\left(\frac{\alpha+\mu-\nu}{2}\right)\Gamma\left(\frac{\alpha-\mu+\nu}{2}\right)\Gamma\left(\frac{\alpha-\mu-\nu}{2}\right)}{\Gamma(\alpha)}\,, \tag{3.4.5}$$

$(\alpha > \mu + \nu)$ and summing up the contributions of two chiral polarizations, the angular part reads

$$\begin{aligned}
D_{00}^{(d)} &= \left(\frac{d+1}{d+2}\right)^2 \left(\frac{1}{\gamma^4\psi^2} - \frac{2}{\gamma^2\psi} + 1\right), & D_{11}^{(d)} &= (d+1)^2 \left(\frac{\sin^2\vartheta}{\psi} - 1\right)^2, \\
D_{22}^{(d)} &= \sin^4\phi \left(\frac{\sin^2\vartheta}{\psi} - 1\right)^2 + \frac{\sin^2 2\phi}{4}, & D_{01}^{(d)} &= -\frac{(d+1)^2}{d+2}\left(\frac{\sin^2\vartheta}{\psi} - 1\right)\frac{1-\gamma^2\psi}{\gamma^2\psi}, \\
D_{02}^{(d)} &= \frac{d+1}{d+2}\left(\frac{\sin^2\vartheta}{\psi} - 1\right)\frac{1-\gamma^2\psi}{\gamma^2\psi}\sin^2\phi\,, & D_{12}^{(d)} &= -(d+1)\left(\frac{\sin^2\vartheta}{\psi} - 1\right)^2 \sin^2\phi\,.
\end{aligned} \tag{3.4.6}$$

[1] We omit overall pre-factors $v \simeq 1$ where it is unambiguous.

By virtue of summation, we can integrate each $D_{ab}^{(d)}(\vartheta,\phi)$ separately. The integration over the ϕ is trivial using the following relations

$$\int\limits_{S^{d+1}} d\Omega_{d+1} = \Omega_{d+1}\,, \qquad \int\limits_{S^{d+1}} \sin^2\!\phi \; d\Omega_{d+1} = \frac{1}{2}\,\Omega_{d+1}\,, \qquad \int\limits_{S^{d+1}} \sin^4\!\phi \; d\Omega_{d+1} = \frac{3}{8}\,\Omega_{d+1}\,. \tag{3.4.7}$$

with the volume of unit sphere of dimensionality $n-1$ (in Euclidean $\mathbb{R}^n$) given by

$$\Omega_{n-1} = \frac{2\,\pi^{n/2}}{\Gamma(n/2)}\,. \tag{3.4.8}$$

Making use of

$$\int\limits_0^{\pi} \frac{\sin^n\vartheta}{\psi^m}\, d\vartheta = \frac{2^{m-1}\Gamma\left(\frac{n+1}{2}\right)\Gamma\left(m-\frac{n+1}{2}\right)}{\Gamma\left(m\right)}\, \gamma^{2m-n-1}\,, \tag{3.4.9}$$

(valid for $2m > n+1$, for derivation see section 2.6.2), we integrate over ϑ to end up with the expression

$$E = \frac{e^2 m'^2 \varkappa_D^4 \gamma^{d+2}}{2^{\,2d+8}\pi^{(3d+7)/2}\Gamma\left(\frac{d+5}{2}\right)} \sum_{a,b=0}^{2} C_{ab}^{(d)} D_{ab}^{(d)}\,, \tag{3.4.10}$$

where now

$$D_{00}^{(d)} = \left(\frac{d+1}{d+2}\right)^2, \qquad D_{11}^{(d)} = (d+1)^2\,, \qquad D_{22}^{(d)} = \frac{d+6}{8}\,,$$
$$D_{01}^{(d)} = \frac{(d+1)^2}{d+2}\,, \qquad D_{02}^{(d)} = -\frac{d+1}{d+2}\,, \qquad D_{12}^{(d)} = -\frac{d+1}{2}\,.$$

and summing up in (3.4.10), we arrive at the following expression:

$$E \approx C_d \frac{\left(em'\varkappa_D^2\right)^2}{b^{3d+3}}\, \gamma^{d+2}\,. \tag{3.4.11}$$

We give here the values of C_d for several values of the number of extra dimensions: $C_2 = 4.39\times10^{-6}$, $C_3 = 1.12\times10^{-6}$, $C_4 = 5.63\times10^{-7}$, $C_5 = 4.35\times10^{-7}$ and $C_6 = 4.62\times10^{-7}$, respectively.

***d* = 1.** We now focus our attention to the cases $d = 0, 1$. Here we also can use the high-frequency approximation as for $d \geqslant 2$, but it does not represent the main contribution now. On the other hand, in the transition region $\omega \sim \omega_0$ the phase of an exponential in the integrand is of order $\mathcal{O}(1)$, thereby the integrand does not strongly oscillate and can be easily computed numerically. So we revert to numerical methods.

The radiated energy will mostly come from the small angle regime, i.e. $\theta \lesssim 1/\gamma$. As mentioned, in 5D the frequency distribution of the emitted energy falls as $1/\omega$ in the regime between $\mathcal{O}(\gamma/b)$ and $\mathcal{O}(\gamma^2/b)$. Thus the dependence on γ following from (3.4.3), is determined by

$$E \sim \gamma^3 \int\limits_{\omega_0}^{\gamma\omega_0} \frac{d\omega}{\omega} \sim \gamma^3 \ln\gamma \,.$$

We have computed this result numerically[1] to deduce:

$$E = C_1 \frac{\left(em'\varkappa_5^2\right)^2}{b^6}\, \gamma^3 \ln\gamma\,, \qquad\qquad C_1 = 1.34 \cdot 10^{-4}\,. \tag{3.4.12}$$

***d* = 0.** As can be seen from the tables, the radiation mainly comes from the transition regime ($\theta \lesssim 1/\gamma$ and $\omega \sim \gamma/b$). As it follows from (3.4.2), at higher frequencies the frequency-distribution curve decays as $1/\omega^2$, and according to (3.4.3), the estimate of emitted energy reads:

$$E \sim \gamma^4 \int\limits_{\omega_0}^{\gamma\omega_0} \frac{d\omega}{\omega^2} \sim \frac{\gamma^4}{\omega_0} \sim \gamma^3\,,$$

in agreement with the Table 3.1.

Hence we once more use numerical methods to compute the energy:

$$E \approx C_0 \frac{\left(em'\varkappa_4^2\right)^2}{b^3}\, \gamma^3\,, \qquad\qquad C_0 = 1.36 \cdot 10^{-4}\,. \tag{3.4.13}$$

The frequency distribution in four dimensions is given in Fig. 3.3(b).

Spectral-angular characteristics. The frequency distribution curves in logarithmic $x-$scale are presented in Fig. 3.2: in linear scale of $dE/d\omega$ (a) and, to illustrate the rate of growth/fall, in logarithmic $y-$scale (b). Curves at the destructive-interference region $x \in (1,2)$ on the subfigure (b) represent straight lines with integer tangents $d-2$, confirming the general idea (3.4.2), while at low frequencies ($x < 0$) any curve has an asymptote with integer tangent d, to confirm an idea of (3.4.21).

The angular distribution $dE/d\vartheta$ curves are presented on Fig. 3.3(a).

3.4.2 The ADD bremsstrahlung

Among the higher-dimensional scenarios the models with direct Kaluza-Klein modes, where the bulk represents compactification on a torus T^d, are of particular history and significance. Here the transformation between $D-$dimensional couplings and their four-dimensional colleagues can be established directly, via the dimensional reduction of an action.

[1] Numerical computation is performed for following values of γ: 10^3, $5 \cdot 10^3$, 10^4, $5 \cdot 10^4$, 10^5. The relative error in 90%-level of confidence probability is 5%.

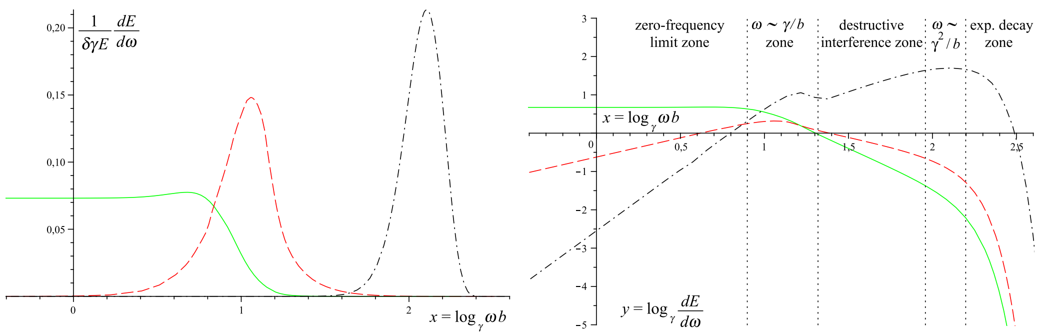

(a) (b)

Figure 3.2: Frequency distribution of emitted energy in linear (a), normalized by a factor $\delta = \Gamma^4\left(\frac{d+1}{2}\right)$, and logarithmic (b) y-scale as function of $\log_\gamma(\omega b)$ for $\gamma = 10^3$. The dimensions are: $d = 0$ (green, solid), $d = 1$ (red, dashed), $d = 3$ (b) and $d = 5$ (a) (both – black, dot-dashed).

The $D-$dimensional propagator is split on the corresponding tower of KK modes:

$$\frac{1}{q_M q^M} \to \frac{1}{V}\sum_{l\in\mathbb{Z}^d} \frac{1}{q_\mu q^\mu - l^2/R^2} \qquad \mu = 0\ldots 3\,,$$

where R stands for the compactification radius and $V = (2\pi R)^d$ is a volume of extra dimensions.

Thus, concerning our computation, the momentum integrals I, I^M, J and J^M introduced above, arise as a sum over integer-valued momentum inside the argument of the Macdonald functions. The summand represents (3.3.7) with $d = 0$ and the argument of the Macdonald functions $z_l = \left(z^2 + l^2 b^2/R^2\right)^{1/2}$, both divided by a normalizing factor V. Thus upon the transfer from summation to integration according to the Euler – Maclaurin rule

$$\frac{1}{V}\sum_{l\in\mathbb{Z}^d} \hat{K}_\lambda\left(\sqrt{z^2 + l^2 b^2/R^2}\right) \to \frac{1}{V}\int \hat{K}_\lambda\left(\sqrt{z^2 + l^2 b^2/R^2}\right)\, d^d l = \frac{1}{(2\pi)^{d/2} b^d}\,\hat{K}_{\lambda+d/2}(z) \tag{3.4.14}$$

(for derivation see [13]) in the final result one restores the expression (3.3.7) with ”actual” d.

Apart from the features common to higher-dimensional models, the ADD scenario has some particular properties:

- the SM fields and massive particles live on the 3-brane, while gravity is essentially higher-dimensional;

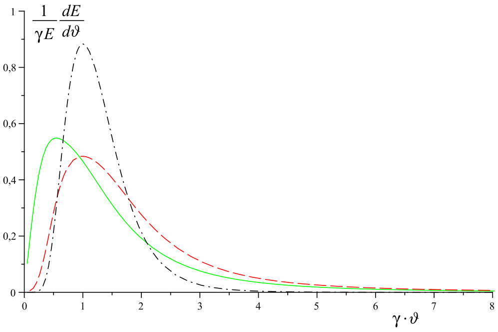

(a) Angular distribution $dE/d\vartheta$ of the emitted energy ($\gamma = 10^3$) for $d = 0$ (green, solid), $d = 1$ (red, dashed) and $d = 5$ (black, dot-dashed), normalized by the total emitted energy E.

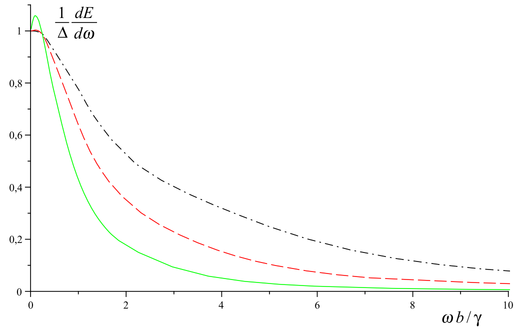

(b) Frequency distribution plots for ADD-bremsstrahlung for $d = 0$ (green, solid), $d = 2$ (red, dashed) and $d = 5$ (black, dot-dashed) ($\gamma = 10^3$), normalized by the ZFL factor $\Delta = \Gamma^2(d/2+1)/(3 \cdot 2^5 \pi^{d+4})$.

Figure 3.3: Angular and frequency distributions.

- ADD is initially proposed as linearized theory of gravity.

Thus in order to evaluate electromagnetic bremsstrahlung by gravity-mediated collisions we can not apply some special cases among those derived before: indeed, $D = 4$ does not allow for gravity to propagate in the bulk, while $D > 4$ does allow for the vector field to live in the bulk.

Meanwhile, the linearized action for gravitational part

$$S_g = \int \left[-\frac{1}{4} h^{MN} \Box h_{MN} + \frac{1}{4} h \Box h - \frac{1}{2} h^{MN} h_{,MN} + \frac{1}{2} h^{MN} h^{P}_{N,MP} \right] d^D x \,, \qquad (3.4.15)$$

and corresponding spin-zero (spin-one) field lead to the essentially same picture after KK-summation, as initially D-dimensional gravity with $D-$dimensionally massless photon (graviton), as it was shown in [14; 15].

In what follows we have to take a $D-$dimensional source j^M and substitute it into the radiation formula (3.2.37) for $d = 0$, where we vanish the bulk components $M = 4 \ldots D-1$. Thus the photon wave vector is parametrized by $k^M = (k^\mu, 0, \ldots, 0)$, with

$$k^\mu = \omega \left(1, \sin\theta \cos\varphi, \sin\theta \sin\varphi, \cos\theta\right) \,. \qquad (3.4.16)$$

Thereby, two KK propagators, corresponding to the interaction in a source, sit inside the $D-$dimensional amplitudes j and j^*, while a third propagator from the Green's function in (3.2.34) appears with normalization factor. Meanwhile, the model allows for the emitted photon to propagate only along the brane, that implies only zeroth emitted mode. Thus the sum degenerates into a single term while the normalizing factor survives. Eventually, the formula for the emitted energy via the electromagnetic field in ADD reads

$$E_{\text{ADD}} = -\frac{1}{16\pi^3 V}\int\limits_0^\infty \omega^2\, d\omega \int\limits_{S^2} d\Omega\, j^*_\mu(k)\, j^\mu(k) = \frac{1}{16\pi^3 V}\sum_{i=1,2}\int\limits_0^\infty \omega^2\, d\omega \int\limits_{S^2} d\Omega\, \left|j_\mu(k)\, \varepsilon_i^\mu\right|^2 . \tag{3.4.17}$$

In other words, we take the four-dimensional formula for radiation (normalized by V) and put a $D-$dimensional source projected on the four-dimensional sector: $j^\mu(k^\nu) = j^M(k)\,\delta^M_\mu\big|_{k^i=0}$.

Thus we use the four-dimensional coordinate system (Fig. 2.1, b) (with angles θ, φ) for parametrization of the emitted photon and keep $D-$dimensional angles ϑ, ϕ (Fig. 2.1, c) for the parametrization of interaction graviton.

The on-shell condition now reads $k_\mu k^\mu = 0$; taking into account, that basis vectors u^M, u'^M and b^M do not contain bulk components, it is enough to take higher-dimensional amplitudes $\rho(k)$ and $\sigma(k)$ and two polarization vectors (3.2.38) and (3.2.39)

$$\varepsilon_1^\mu = \frac{1}{\gamma v z' \sin\theta}\left[z\, u'^\mu - z' u^\mu + \left(\gamma - \frac{z}{z'}\right)\frac{b\, k^\mu}{\gamma v}\right], \qquad \varepsilon_2^\mu = \frac{b}{\gamma^2 v^2 z' \sin\theta}\, \epsilon^{\mu\nu\lambda\rho}\, u_\nu u'_\lambda k_\rho\,, \tag{3.4.18}$$

where in addition, contractions (3.2.41) hold under appropriate substitutions $\vartheta \to \theta, \phi \to \varphi$.

To iterate, one takes $\rho(k)$ by (3.3.9) plus $\sigma(k)$ in the integral representation (3.3.14), square and integrate with measure ω^2. Thus all notes on the destructive interference are *still valid*. Eventually, multiplying by ω^2 leads to the same behavior as in four dimensions, due to the hatted Macdonald function $\hat{K}_\nu(x)$ goes like $\mathcal{O}(1)$ at the range $x = 0 \ldots \mathcal{O}(1)$ for any non-negative index ν. So the four-dimensional behavior of the frequency distribution is reproduced, with some numerical corrections. Respectively, we repeat the strategy of computation in 4D presented above.

Thus the characteristic frequency and angle are given by

$$\omega_{\text{ADD}} \sim \omega_0 = \frac{\gamma}{b}\,, \qquad \theta \sim \bar{\vartheta} = \frac{1}{\gamma}\,, \tag{3.4.19}$$

i.e. one has beaming in forward direction with respect to the charged particle's motion. The total emitted energy reads

$$E_{\text{ADD}} = \bar{C}_d\, \frac{(em'\varkappa_D^2)^2}{b^{2d+3} V}\, \gamma^3\,, \tag{3.4.20}$$

with coefficient $\bar{C}_d$ to be defined numerically. The results of numerical computation (overall coefficients $\bar{C}_d$) are listed here: $\bar{C}_1 = 4.90\cdot 10^{-5}$, $\bar{C}_2 = 2.54\cdot 10^{-5}$, $\bar{C}_3 = 1.77\cdot 10^{-5}$, $\bar{C}_4 = 1.52\cdot 10^{-5}$, $\bar{C}_5 = 1.55\cdot 10^{-5}$, $\bar{C}_6 = 1.85\cdot 10^{-5}$, while the frequency distribution plots are shown in Fig. 3.3(b).

ZFL of the frequency distribution. Given that the stress part (3.3.14) of the radiation amplitude is finite (for $d = 0$) and vanishes for $d > 0$ at the limit $\omega \to +0$, the zero-frequency limit of $dE_{\rm ADD}/d\omega$ is determined by the imaginary part of the local amplitude (3.3.11): indeed

$$j^\mu(k) = -i\,\frac{\lambda\, e^{i(kb)}}{2}\left(\frac{z'\sin\theta\cos\varphi}{z}\,u^\mu + \frac{b^\mu}{b}\right)\frac{\hat{K}_{d/2+1}(z)}{z} \sim \frac{1}{\omega}, \tag{3.4.21}$$

while the other terms are regular or diverge logarithmically (for $d = 0$) at $\omega \to 0$. Such a behavior in ω is reminiscent of the infrared divergence of the corresponding Feynman diagrams. However, upon multiplication by ω^2 from the measure of integration, it contributes a finite amount to the radiation loss.

Taking the finite limit of hatted Macdonald $\hat{K}_n(z) = 2^{n-1}\Gamma(n)$ (for $n > 0$) and omitting the phase factors

$$j^\mu(k) \simeq \frac{\lambda\,\Gamma(d/2+1)}{2^{1-d/2}\omega\, b\,\psi}\left(\frac{\sin\theta\,\cos\varphi}{\gamma\psi}\,u^\mu + \frac{b^\mu}{b}\right), \tag{3.4.22}$$

with $\psi \equiv 1 - v\cos\theta$ now.

Squaring it and substituting into the first formula (3.4.17), one has

$$\left.\frac{dE_{\rm ADD}}{d\omega}\right|_{\omega=0} = \frac{(em'\varkappa_D^2)^2\,\Gamma^2(d/2+1)}{2^8\pi^{d+5}b^{2d+2}V}\int d\theta\, d\varphi\,\frac{\sin\theta}{\psi^2}\left(1 - \frac{\sin^2\theta\,\cos^2\varphi}{\gamma^2\psi^2}\right), \tag{3.4.23}$$

Consecutively integrating over φ with help of (3.4.7), and over θ via (3.6.9), the ZFL in ADD bremsstrahlung reads

$$\left.\frac{dE_{\rm ADD}}{d\omega}\right|_{\omega=0} = \frac{\Gamma^2(d/2+1)}{3\cdot 2^5\pi^{d+4}}\,\frac{(em'\varkappa_D^2)^2}{b^{2d+2}V}\,\gamma^2\,. \tag{3.4.24}$$

Notice, that this formula is still valid in four dimensions.

Going back and taking into account that destructive interference suppresses not only the radiation amplitude at frequencies $\omega > \mathcal{O}(\gamma/b)$ – but also the flux, one concludes that frequency

$$\omega_{\rm ADD} \sim \omega_0 = \frac{\gamma}{b}$$

gives the effective cut-off for all cases of ADD, as well as to four-dimensional bremsstrahlung. Thereby the realistic estimate is

$$E_{\rm ADD} \sim \left.\frac{dE_{\rm ADD}}{d\omega}\right|_{\omega=0}\times\,\omega_{\rm ADD} = \frac{\Gamma^2(d/2+1)}{3\cdot 2^5\pi^{d+4}}\,\frac{(em'\varkappa_D^2)^2}{b^{2d+3}V}\,\gamma^3\,. \tag{3.4.25}$$

Such an approach is used by Smarr [31] to estimate four-dimensional gravitational bremsstrahlung.

Therefore, the vector bremsstrahlung in ADD case repeats the four-dimensional picture, up to numeric coefficient.

3.4.3 The UED bremsstrahlung and average number of Kaluza-Klein modes

Through the entire text we implied that (3.1.2) is satisfied and one has large number of KK-modes, that allows to pass from KK-summation to the continuous integration and that eventually leads to the enhancement of $\gamma-$factor power.

Meanwhile, for the UED models, where the vector field can propagate through the bulk, the contemporary constraints [6] on the size of the extra dimensions, coming from the experimental data (including the recent ATLAS and CMS experiments), give the following bound:

$$1/R_{\text{UED}} \sim 300 - 3000\,\text{GeV}\,, \qquad\qquad R_{\text{UED}} \sim 10^{-16}\,\text{cm}\,. \tag{3.4.26}$$

In this case the inequality $b < R$ (3.1.2), combined with $b \gg r_{\text{cl}}$, to have a charge point-like, does not hold. Does it imply that the whole derivation presented above, fails?

Consider the situation more thoroughly: we first restore the original KK-summations, before switching to integration. The analogue of (3.2.37) reads:

$$E = \frac{1}{16\pi^3 V} \sum_i \sum_{n\in\mathbb{Z}^d} \int\limits_0^\infty \varpi^2\, d\varpi \int\limits_{S^2} d\Omega\; |j_i(k)|^2 \Big|_{k^0=\sqrt{\varpi^2+n^2b^2/R^2}} \qquad\qquad \varpi^2 = \sum_{a=1}^{3} (k^a)^2, \tag{3.4.27}$$

with $\varpi = |\mathbf{k}|$ being a continuous frequency in four-dimensional sector.

The local current is given by (3.3.5), after the corresponding change of the integrals I and I^M in (3.3.6), given in 2, to:

$$I = -\frac{2\pi}{\gamma v V} \sum_{l\in\mathbb{Z}^d} K_0(z_l)\,, \qquad\qquad I^M = -\frac{2\pi}{\gamma v\, b^2 V} \sum_{l\in\mathbb{Z}^d} \left(b\, z\, K_0(z_l)\, \frac{\gamma u'^M - u^M}{\gamma v} + i\hat{K}_1(z_l)\, b^M \right), \tag{3.4.28}$$

respectively, with $z_l^2 \equiv z^2 + l^2 b^2/R^2$. A similar summation arises in the stress integrals.

When $b \gg R$, one passes in (3.4.28) to integration according to (3.4.14), and the expressions (3.3.7) are restored. The stress amplitude is split into the KK-sum in a similar way.

Such a summation appears inside the amplitude $j^M(k)$ and corresponds to the KK-compactification of the interaction graviton. So the effective number of KK-modes of interaction is determined by the exponential decay of Macdonald function ($l^2b^2/R^2 \lesssim 1$) and reads

$$N_{\rm int} \equiv l_{\rm max} = [L/b] + 1\,, \tag{3.4.29}$$

independent of the value $0 \leqslant z \lesssim 1$.

In the ADD-case the bound on the compactification radius is $R_{\rm ADD} \sim 10^{-2}\,{\rm cm}$ (for $d = 2$), and (3.1.2) is well satisfied, thus one has a large number of the interaction KK-modes.

In the case of UED, one has $R_{\rm UED} < l_C$ and one has to revisit the computation. The above condition implies that the interaction has only *zeroth* KK-mode.

Thus the sum in (3.4.28) degenerates into

$$I = -\frac{2\pi}{\gamma v V}\,K_0(z)\,, \qquad\qquad I^M = -\frac{2\pi}{\gamma v\, b^2 V}\left(b\, z\, K_0(z)\,\frac{\gamma u'^M - u^M}{\gamma v} + i\hat{K}_1(z)\, b^M\right), \tag{3.4.30}$$

plus exponentially-suppressed terms, and the radiation amplitude represents the expressions derived in Section 3.3 for $d = 0$, but normalized by the factor V.

Therefore, the emission modes are determined by the exponential decay of Macdonalds $K_0(z)$ and $K_1(z)$. In the original KK-treatment the argument z becomes dependent upon the number of emission KK-quantum as

$$z \equiv \frac{(ku)b}{\gamma v} \simeq \sqrt{\varpi^2 b^2 + n^2 b^2/R^2} - \varpi b\, v\cos\theta \tag{3.4.31}$$

In the total absence of emission KK-modes, the characteristic frequency is given by its $d = 0$–value $\varpi \sim \omega_0$ (3.4.19), thus the typical value of ϖb is at least $\varpi b \gtrsim \gamma$. Assume that

$$b < R\gamma\,, \tag{3.4.32}$$

that is reasonable for R given by (3.4.26) and $\gamma \sim 10^{14}$. Then the first massive KK-mode is available, and some number $n < N_{\rm emit}$ of first KK-modes satisfy $nb/R < \gamma$. In this case one expands the radical in (3.4.31) to obtain

$$z \approx \varpi b + \frac{n^2 b}{2\,\varpi R^2} - \varpi b\, v\cos\theta = \varpi b\psi + \frac{n^2 b}{2\,\varpi R^2} \tag{3.4.33}$$

Thus the effective number of emission KK-modes

$$N_{\rm emit} \equiv n_{\rm max}(\varpi) = \sqrt{\frac{2\varpi R^2}{b}}\,, \tag{3.4.34}$$

becomes dependent on the frequency. In the most favorable case the maximal frequency is determined from the first term of the RHS of (3.4.33), which should be less than unity independently [13]: $\varpi \sim \psi^{-1}/b \sim \gamma^2/b$. Thus

$$N_{\rm emit} \sim \frac{\gamma R}{b} > 1\,, \tag{3.4.35}$$

according to the necessary condition (3.4.32).

In addition, now assume the stronger condition[1]:

$$\frac{\gamma R}{b} \gg 1\,, \tag{3.4.36}$$

Then $N_{\rm emit} \gg 1$, so the modes are quasi-continuous, and we combine quasi-continuous momenta with continuous ϖ into single ω, shift angles $(\theta,\varphi) \to (\vartheta,\phi)$ and we return to the case (3.4.1), where we integrate the square of radiation amplitude with volume measure

$$\mathcal{V}_d = \frac{1}{2(2\pi)^{d+3}}\,\omega^{d+2}\,\sin^{d+1}\!\vartheta\, d\omega\, d\vartheta\, d\Omega_{d+1}\,. \tag{3.4.37}$$

Given that the hatted Macdonald function $\hat{K}_\nu(z)$ alters slowly with the change of index $\nu \geqslant 0$, the integration should be performed along the same lines as in Subsection 3.4.1. Namely, for $d \geqslant 2$ the high-frequency regime dominates, and for the radiation amplitudes one has instead (3.3.19) and (3.3.10), the following one:

$$\begin{aligned} j_\pm(k) \approx \frac{\lambda_0\,{\rm e}^{i(kb)}\sin\vartheta}{2\sqrt{2}} \Bigg[&\frac{d+1}{d+2}\,\frac{1-\gamma^2\psi}{\gamma^2\psi}\,K_0(z) - \frac{1}{z^2}\left(\frac{\sin^2\!\vartheta}{\psi}-1\right)\hat{K}_1(z) + \\ &+\frac{\sin^2\!\phi}{z^2}\left(\frac{\sin^2\!\vartheta}{\psi}-1\right)\hat{K}_2(z) \pm i\,\frac{\sin 2\phi}{2\,z^2}\,\hat{K}_2(z)\Bigg]\,, \end{aligned} \tag{3.4.38}$$

with[2] $\lambda_0 \equiv e m' \varkappa_D^2/2\pi V$.

Again, we split the integrals on frequency and angular parts, as in (3.4.4):

$$\frac{dE_{\rm UED}}{d\Omega} = \frac{\lambda_0^2\sin^{d+3}\!\vartheta}{8\,(2\pi)^{d+3}\,b^{d+3}\psi^{d+3}} \sum_{a,b=0}^{2} \tilde{C}^{(d)}_{ab}\,\tilde{D}^{(d)}_{ab}(\vartheta,\phi)\,, \tag{3.4.39}$$

where $\tilde{C}^{(d)}_{ab} \equiv \int \hat{K}_a(z)\hat{K}_b(z)\, z^{d+2(\delta_{0a}+\delta_{0b}-1)}\,dz$. As before, these integrals are to be computed with help of (3.4.5).

Comparing (3.4.38) with (3.3.19), one concludes that the angular coefficient functions $\tilde{D}^{(d)}_{ab}$ have the corresponding changes with respect to those ones $D^{(d)}_{ab}$ given in

[1] We will return to the validity of this condition in the Subsection 3.5.3.

[2] The numeric coefficient before $\hat{K}_1(z)$ is related with the index of Macdonald function in the series (3.3.17) and corresponds to the same expression as in (3.3.19), with $d=0$ is fixed. The numeric coefficient before $K_0(z)$ is coming from the D-dimensional h'_{MN} and keeps $d-$dependence inside itself.

(3.4.6):

$$\tilde{D}^{(d)}_{01} = \frac{D^{(d)}_{01}}{d+1}\,, \qquad \tilde{D}^{(d)}_{11} = \frac{D^{(d)}_{11}}{(d+1)^2}\,, \qquad \tilde{D}^{(d)}_{12} = \frac{D^{(d)}_{12}}{d+1}\,.$$

The same relations exist for the integrated over all angles constants. Combining them all and substituting to (3.4.39), one obtains the energy loss

$$E_{\mathrm{UED}} \approx \tilde{C}_d \frac{\left(em'\varkappa_D^2\right)^2}{V^2 b^{d+3}}\,\gamma^{d+2}\,. \tag{3.4.40}$$

The values of $\tilde{C}_d$ for small values of the number of extra dimensions are listed as: $\tilde{C}_2 = 7.8\times 10^{-6}$, $\tilde{C}_3 = 1.5\times 10^{-6}$, $\tilde{C}_4 = 4.5\times 10^{-7}$, $\tilde{C}_5 = 1.7\times 10^{-7}$.

$\boldsymbol{d=1}$**.** Repeating the same arguments, we compute the total radiation numerically:

$$E = \tilde{C}_1 \frac{\left(em'\varkappa_5^2\right)^2}{V^2 b^4}\,\gamma^3 \ln\gamma\,, \qquad \tilde{C}_1 = 2.74\cdot 10^{-5}\,. \tag{3.4.41}$$

The spectral characteristics in UED bremsstrahlung are the same as in higher-dimensional case (Subsection 3.4.1), while the angular characteristics are similar to all cases considered above.

A summary. In Table 3.2 we summarize the ultimate cases of an ultrarelativistic bremsstrahlung from the viewpoint of average numbers of the Kaluza-Klein modes excited in the bremsstrahlung process.

3.5 Discussion

According to the computation presented above, we overview possible effects and give the estimates on them.

3.5.1 Scattering of two charges

When both particles are charged by the vector field A^M then the direct electromagnetic interaction is expected to be the dominant force. Then the acceleration (and, being integrated, the trajectory deflection) represents (to first order of PT) the sum of two contributions of electromagnetic and gravitational nature, respectively. In turn, these addenda to trajectory may lead to radiation via vector and tensor fields. We do not consider gravitational waves in this work, and thus focus here to the pure vector bremsstrahlung.

A similar approach (i.e. bremsstrahlung without accounting for gravity) was considered in [13] for the scalar bremsstrahlung, so it is not necessary to reproduce that

N_{emit} \ N_{int}		$N_{\text{int}} \lesssim 1$	$N_{\text{int}} \gg 1$
$N_{\text{emit}} \lesssim 1$	space-time model =	$M_{1,3}$	ADD
	characteristic frequency =	$\omega \sim \omega_0$	$\omega \sim \omega_0$
	radiation amplitude =	$j = j_0$	$j = j_d$
	phase volume =	$\mathcal{V} = \mathcal{V}_0$	$\mathcal{V} = \mathcal{V}_0/V$
	KK modes =	$N_{\text{int}} = N_{\text{emit}} = 1$	$N_{\text{emit}} = 1$
	emitted energy =	γ^3	γ^3/V
$N_{\text{emit}} \gg 1$	space-time model =	UED	$M_{1,d+3}$
	characteristic frequency =	$\omega \sim \gamma\omega_0$	$\omega \sim \gamma\omega_0$
	radiation amplitude =	$j = j_0/V$	$j = j_d$
	phase volume =	$\mathcal{V} = \mathcal{V}_d$	$\mathcal{V} = \mathcal{V}_d$
	KK modes =	$N_{\text{int}} = 1$	$N_{\text{emit}} = \gamma N_{\text{int}}$
	emitted energy =	γ^{d+2}/V^2	γ^{d+2}

Table 3.2: The qualitative relation between the cases of gravity-mediated vector bremsstrahlung from viewpoint of number of KK-modes. The values are normalized as $\lambda = b = e = 1$. $N = 1$ implies that only the zeroth KK-mode is actual. The measure of the phase volume integration is defined by (4.37).

computation in details. Instead of the detailed computation, we highlight the main steps and overview the results.

Making use of perturbation theory over e and considering (3.2.2) on the flat background with F_{MN} (3.3.1) generated by charge e', the acceleration on trajectory reads:

$$ {}^1\ddot{z}^M_{\rm em}(\tau) = i\,\frac{e'e}{(2\pi)^{d+3}m}\int d^Dq\frac{\delta(qu')}{q^2}\,e^{-iqb}e^{-i(qu)\tau}\left[\gamma q^M-(qu)\,u'^M\right]. \tag{3.5.1} $$

The scattering angle, computed along the same lines as in [12], is given by

$$ \alpha_{\rm em}\sim\frac{e\,e'}{m\,\gamma\,b^{d+1}}\sim\left[\frac{\sqrt{r_{\rm cl}r'_{\rm cl}}}{b}\,\frac{\sqrt{m'}}{\sqrt{m}}\right]^{d+1}\frac{1}{\gamma}<\frac{(m'/m)^{\frac{d+1}{2}}}{\gamma}\,. \tag{3.5.2} $$

Performing the perturbation-theory scheme (with the obvious restriction $b>r_{\rm cl}$), one obtains the following second-order source valid in *all* frequency regimes:

$$ j^M(k)\sim i\,{\rm e}^{i(kb)}\,\frac{e^2\,e'}{m\gamma b^d}\left(\frac{\sin\vartheta\cos\phi}{\gamma\psi}\,u^M+\frac{b^M}{b}\right)\frac{\hat{K}_{d/2+1}(z)}{z}\,. \tag{3.5.3} $$

It is produced by the fast particle, while the corresponding terms due to the target and the interference give subleading in γ contribution.

As was mentioned above, such an argument of the Macdonald function leads to the dominance of $z-$region in the entire spectrum. Thus in the Lab frame the characteristic spectral-angular values are:

$$ \omega_{\rm em}\sim\frac{\gamma^2}{b}\,,\qquad\qquad \vartheta_{\rm em}\sim\frac{1}{\gamma}\,, \tag{3.5.4} $$

On the other hand we see that such a behavior at low frequencies leads to the finite ZFL of frequency distribution, which for the case of non-compactified extra dimensions reads

$$ \left(\frac{1}{\omega^d}\frac{dE}{d\omega}\right)_{\omega=0}\sim\frac{(e^2\,e')^2}{b^{2d+2}}\,\gamma^{-d}\,. \tag{3.5.5} $$

Here no process which drastically changes the amplitude (like destructive interference) occurs in the whole frequency domain $\omega\in[0,\omega_{\rm em}]$, and one applies ZFL-approximation with maximal frequency given by (3.5.4):

$$ E_{\rm em}\sim\left(\frac{1}{\omega^d}\frac{dE}{d\omega}\right)_{\omega=0}\times\,\omega^{d+1}_{\rm em}\sim\frac{e^4\,e'^2}{m^2b^{3(d+1)}}\,\gamma^{d+2}\,. \tag{3.5.6} $$

Roughly speaking, the total emitted energy carried by the vector field is twice that of the scalar situation due to the two polarization states, after making the identifications

$f \to e, f' \to e'$, respectively. Therefore most of emitted waves are beamed into the cone with characteristic angle $1/\gamma$.

The efficiency is given by

$$\epsilon_{\rm em} \sim \left(\gamma \frac{r_{\rm cl}^3}{b^3}\right)^{1+d}. \tag{3.5.7}$$

Taking into account that when interacting gravitationally, the charge emits $E_{\rm rad} \sim \gamma^3$ in four dimensions, while only $E_{\rm em} \sim \gamma^2$ in Coulomb-field collision, it seems intriguing to derive that value of γ, for which the two contributions become comparable.

Correction to gravity-mediated vector bremsstrahlung. The acceleration of both particles in the first order of PT represents the sum of gravitational and Lorentz-force parts. The electromagnetic part causes $e^2 e'-$contribution to the vector current and leads to the pure electromagnetic bremsstrahlung reviewed above in this Subsection.

The appearance of a second charge e' (with mass m') adds some terms to the radiation amplitudes: namely, local (3.3.11) and non-local (3.3.12) parts will acquire addenda $\rho'(k)$ and $\sigma'(k)$, based on the integrals (3.3.6) and (3.3.13) where primed and unprimed quantities are mutually interchanged. These terms also can be derived in the same way in the Lorentz frame associated with $e-$charge (comoving frame), and then Lorentz-transformed into the Lab frame. With e and e' to be of the same order, in the comoving frame the emission is dominant due to these new terms, and governed by Macdonald function $K_\nu(z')$. Hence in this frame the emission is beamed inside the cone $\vartheta' \lesssim 1/\gamma$ with respect to $\mathbf{u}'$. Being transformed to the Lab frame, these terms remain to be $K_\nu(z')$ since z' is a Lorentz-scalar (3.3.8). Thus these addenda are not important in higher frequencies and represent subleading, by an order of γ terms (with respect to the terms we keep) due to the Lorentz transformation, with a corresponding interchange of primed and unprimed couplings in (3.4.11).

The conservation of these terms is easily verified using the same strategy as for the basic terms. The self-action terms appearing here, are discussed in section, 3.7.

3.5.2 Coherence length

In this subsection we consider qualitatively the effects arising in the bremsstrahlung process, and the spectrum of emitted waves, from the viewpoint of coherence length, coming from consideration of the particle's equation of motion in the presence of external field.

While accelerating, the particle emits radiation. Its spectral characteristics are translated from the corresponding temporal ones, related with the duration of accelerated motion, and with the value of acceleration and type of external force.

Apart from the formulae for the total energy loss on radiation in the coordinate and momentum representations given in subsection 3.2.3, the intensity of electromagnetic emission can be characterized by the square of the incomplete Fourier-transform of $A^M(x)$ considered as an integral over the particle's classical trajectory $z^M(\tau)$:

$$A^M(\omega, \mathbf{r}) \sim \frac{e}{\rho} \int u^M(\tau)\, \mathrm{e}^{i(\omega t - \mathbf{kz})}\, d\tau\,, \qquad \rho \equiv |\mathbf{r} - \mathbf{z}|\,.$$

Being squared, the combination $|A^M(\omega, \mathbf{r})|^2$ contains a double integral over $\tau_1 \tau_2$ with $\mathrm{e}^{ik\cdot\Delta z}$ in the integrand.

Expanding $\Delta z^M = u^M + \ddot{z}^M \tau + \dddot{z}^M \tau^2/2 + \ldots$, where $\tau \equiv \tau_2 - \tau_1$, the difference in the phases of the two waves emitted by a charge in the same direction $\mathbf{n}$ at close moments τ_1 and τ_2 of proper time, is determined by

$$\Delta\varphi = k \cdot \Delta z = \omega \left[t - \mathbf{n}\, \Delta\mathbf{z}(t)\right]\,, \qquad t \equiv \tau_2 - \tau_1\,.$$

In addition, in ultrarelativistic motion the transverse component of the force acts much more effectively than the longitudinal one. Because of this, one can transit from $D-$dimensional expansions to their spatial sector, and the latter equation can be rewritten as

$$\Delta\varphi = \omega t \left(1 - \mathbf{nv} - \frac{t}{2}\, \mathbf{n\dot{v}} + \frac{t^2}{6}\, \dot{\mathbf{v}}^2 + \ldots\right)$$

Thus to the leading order $\Delta\varphi \approx \omega t(1 - \mathbf{nv}) = \omega t(1 - v\cos\vartheta) = \omega t\psi$. When $\Delta\varphi$ becomes of order $\mathcal{O}(1)$, the waves with antiphase are present in the spectrum, so they annihilate and decoherence happens.

Thus the maximal duration of coherence is given by

$$t_{\mathrm{coh}} \sim \frac{1}{\omega\psi}\,, \qquad \tau_{\mathrm{coh}} \sim \frac{t_{\mathrm{coh}}}{\gamma} \sim \frac{1}{\omega\gamma\psi}\,. \tag{3.5.8}$$

Let us consider the wave formed within the coherence length (during the coherence time) and emitted in the angle ϑ with respect to $\mathbf{u}$. The characteristic duration of this signal in the Lab frame is determined by the difference of distances covered by two waves, emitted at the start and finish of the coherence interval and received far from the particle's location. Computing it, one obtains $t_{\mathrm{Lab}} = (1 - v\cos\vartheta)\, t_{\mathrm{coh}} = \psi\, t_{\mathrm{coh}}$. Going back to all cases of bremsstrahlung, most of the emitted radiation is beamed inside the cone $\vartheta \lesssim \bar{\vartheta} = 1/\gamma$, that is confirmed by the curves in Fig. 3.3(a).

Given that at coherence interval the deflection angle should be $\alpha < \gamma^{-1}$, the Lab-frame duration is estimated as

$$t_{\rm Lab} \simeq \frac{\vartheta^2 + \gamma^{-2}}{2}\, t_{\rm coh}\,. \tag{3.5.9}$$

Finally, using (3.5.8) one has:

$$\omega_{\rm com} \sim \frac{1}{t_{\rm coh}}\,, \qquad\qquad \omega \sim \frac{1}{t_{\rm coh}\psi} \sim \frac{1}{t_{\rm Lab}} \sim \gamma^2 \omega_{\rm com}\,. \tag{3.5.10}$$

The frequency in the Lab frame is, thereby, γ^2 larger than the frequency in the comoving frame, according to the Doppler effect.

Therefore we analyze the average time of accelerated motion.

Classical electrodynamics. Expanding (3.5.1) near $\tau = 0$ one deduces that the acceleration is determined by the transverse component ${}^1\ddot{z}^{\,x}_{\rm em}$ with characteristic value

$${}^1\ddot{z}^{\,x}_{\rm em}(0) \sim \frac{ee'}{m}\,\frac{\gamma}{b^{d+2}}\,. \tag{3.5.11}$$

The duration of the accelerated motion is characterized by that interval, for which the trajectory is deflected on an angle, comparable to the total deflection angle $\alpha_{\rm em}$ given by (3.5.2):

$$\tau_{\rm em} \sim \frac{b}{\gamma}\,, \qquad\qquad t_{\rm em} \sim b\,. \tag{3.5.12}$$

For details, see [42]. Next, consider the radiative part of the Lorentz-Dirac force in higher dimensions: it is determined by averaging over angles of the corresponding part of energy-momentum tensor, the latter reads $T^{\rm emit}_{\rm em} \sim e^2/r^{d+2}$, where r stands for the retarded Lorentz-invariant distance parameter (for construction see [38]).

For instance, in four dimensions it represents well-known (relativistic) Larmor formula for the emission intensity (in the units we use)

$$\frac{dE_{\rm rad}}{dt} = -\frac{1}{6\pi}\, e^2 \ddot{z}^{\,2}_{\rm em}\,, \qquad\qquad \dot{E}_{\rm rad} = -\frac{1}{6\pi}\, e^2 \ddot{z}^{\,2}_{\rm em} \dot{z}^0\,.$$

In even higher dimensions the analogue of the Larmor formula can be computed in a closed form and reads schematically (in the gauge $\dot{z}^2 = 1$)

$$\dot{E}_{\rm rad} \sim e^2\gamma \left[B_{\underbrace{(2,2;2\ldots 2)}_{d+2}} \left(\ddot{z}^{\,2}_{\rm em}\right)^{d/2+1} + \ldots + B_{(D/2,D/2)} \left(z^{(D/2)}_{\rm em} \cdot z^{(D/2)}_{\rm em} \right) \right]. \tag{3.5.13}$$

with some positively defined form in the parenthesis. Here $B_{(\alpha_{k\ldots})}$ is a constant with list of orders of derivatives, constituting the corresponding scalar products, while dots represent all intermediate scalar terms with the same dimensionality of mass ($[m] = \text{cm}^{-1}$).

Taking into account that for higher derivatives

$$\frac{d^{D/2}}{d\tau^{D/2}}\, {}^1z^M_{\text{em}} \sim {}^1z^x_{\text{em}}{}^{(D/2)} \sim {}^1\ddot{z}^x_{\text{em}}\,\frac{\gamma^{d/2}}{b^{d/2}}\,,$$

that follows from (3.5.1), and substituting (3.5.11), one obtains the estimate

$$ {}^1z^x_{\text{em}}{}^{(D/2)} \sim \frac{ee'}{m}\,\frac{\gamma^{d/2+1}}{b^{3d/2+2}}\,. \tag{3.5.14}$$

Given that all terms in the parenthesis have the same total dimensionality $\text{cm}^{-(d+2)}$, and that each derivative adds γ/b, one concludes that all terms have the same order of $\gamma-$factor. In what follows, the leading term is determined by the perturbation theory, and given by the term with minimal number of scalar products, namely, the last term in (3.5.13)[1]. From the dimensional analysis it is easy to see that all other terms contain more than two first-order kinematical quantities.

Thus the total emitted energy during the whole bremsstrahlung process is given by

$$E_{\text{em}} \sim e^2\left[{}^1z^x_{\text{em}}{}^{(D/2)}\right]^2 t_{\text{em}} \sim \frac{e^4e'^2}{m^2}\,\frac{\gamma^{d+2}}{b^{3d+3}}\,, \tag{3.5.15}$$

in agreement with (3.5.6). Thus the estimate of vector bremsstrahlung as induced emission of a charge in the external Coulomb field is valid within the same perturbation theory.

Finally, (3.5.12) represents the coherence length of emitted waves in the comoving Lorentz frame – the characteristic length of the trajectory, where the signal is formed. Applying (3.5.12) to (3.5.10), one obtains

$$\omega_{\text{em}} \sim \frac{1}{t_{\text{em}}\psi} \sim \frac{\gamma^2}{b}\,, \tag{3.5.16}$$

in agreement with (3.5.4).

Classical electrodynamics in external curved background. The deflection angle in a static gravitational potential in D dimensions is given by [12]

$$\alpha_{\text{gr}} \sim \frac{r_g'^{\,d+1}}{b^{d+1}} \ll 1\,, \tag{3.5.17}$$

[1] According to the affine parametrization, (i) one can exclude velocity from such scalar products and (ii) terms with scalar products of the form, for instance $\left(z^{(D/2+1)}, z^{(D/2-1)}\right)$, are equivalent to the retained $\left(z^{(D/2)}, z^{(D/2)}\right)$ by virtue of relation

$$\left(z^{(D/2+1)}, z^{(D/2-1)}\right) = \frac{d}{d\tau}\left(z^{(D/2)}, z^{(D/2-1)}\right) - \left(z^{(D/2)}, z^{(D/2)}\right),$$

where the full derivative does not contribute to the radiation and can be dropped. The same concerns the other scalar products $\left(z^{(D/2+k)}, z^{(D/2-k)}\right)$.

and, according to the Equivalence principle, does not depend upon the energy of the scattered particle.

Double-differentiating (3.3.4) one obtains the estimate of the transverse component of an acceleration caused by the gravitational force:

$$ {}^{1}\ddot{z}^{x}_{\rm gr}(0) \sim \frac{{r'_g}^{\,d+1}\gamma^2}{b^{\,d+2}}\,, \tag{3.5.18} $$

while the characteristic time of acceleration is governed, essentially, by the same factors as before and reads

$$ \tau_{\rm gr} \sim \frac{b}{\gamma}\,, \qquad\qquad t_{\rm gr} \sim b\,. \tag{3.5.19} $$

Nevertheless, the dominant contribution into $\ddot{z}^{\,2}(\tau)$ is given by domains $\tau \sim b/\gamma$ and $\tau \sim -b/\gamma$ where $|\,{}^{1}\ddot{z}^{0}_{\rm gr}|$ reaches its maximum[1], despite the fact that at $\tau = 0$ it vanishes:

$$ {}^{1}\ddot{z}^{0}_{\rm gr}(\pm\tau_{\rm gr}) \sim \frac{{r'_g}^{\,d+1}}{b^{\,d+2}}\,\gamma^2\,, \qquad\qquad {}^{1}\dot{z}^{0}_{\rm gr}(\pm\tau_{\rm gr}) \sim \frac{{r'_g}^{\,d+1}}{b^{\,d+1}}\,\gamma\ {}^{*2}. \tag{3.5.20} $$

If the space-time had been flat, the direct application of estimate (3.5.15) would lead to the result

$$ E_{\rm em/curve} \sim e^2\left[{}^{1}z^{x\,(D/2)}_{\rm gr}\right]^2 t_{\rm gr} \sim e^2 G^2 {m'}^2\,\frac{\gamma^{d+4}}{b^{3d+3}}\,. \tag{3.5.21} $$

However, not only is this result overestimated – it totally vanishes due to the following reasoning.

The analogue of Larmor formula in four dimensions in a *fixed* curved space-time is given by the finite part of formula by de Witt and Brehme [22], corrected by Hobbs [26][3]:

$$ f^{0}_{\rm em}(\tau) = \frac{e^2}{4\pi}\left[\Pi^{0\nu}\left(\frac{2}{3}\,D^2\dot{z}_\nu + \frac{1}{3}\,R_{\nu\lambda}\,\dot{z}^{\lambda}\right) + \dot{z}^{\nu}(\tau)\int\limits_{-\infty}^{\tau}\left({v^{0}}_{\lambda';\nu} - {v_{\nu\lambda'}}^{;0}\right)\dot{z}^{\lambda'}(\tau')\,d\tau'\right], $$

$$ \Pi^{\mu\nu} \equiv g^{\mu\nu} - \frac{\dot{z}^{\mu}\dot{z}^{\nu}}{\dot{z}^2}\,, \tag{3.5.22} $$

Here $v^{\nu\alpha}$ represents the non-local part of the vectorial Green's function in a curved background in terms of bi-tensor quantities, evaluated at points $z^{\mu}(\tau)$ and $z^{\mu'}(\tau')$.

[1]In four dimensions see (3.5.33) for the components of velocity and its derivatives.

[2]In what follows the validity of perturbation theory to this order: $\sup\,{}^{1}\dot{z}^{0}_{\rm gr} \ll u^0$ if $b \gg r'_g$ holds.

[3]Here and below the lower-case Greek indices emphasize the fact, that contraction of indices is performed in the curved background.

In flat background one has $g_{\mu\nu} \to \eta_{MN}\delta^M_\mu \delta^N_\nu$, $D\dot{z}^\mu \to \ddot{z}^M \delta^\mu_M$, $D^2\dot{z}^\mu \to \dddot{z}^M \delta^\mu_M$ etc., and (3.5.22) passes into the Lorentz-Dirac equation, there the radiative part is constituted from the radiation part $\sim \ddot{z}^2\, \dot{z}^M$ and radiation-reaction ("Schott") part $\sim \dddot{z}^M$.

The "Larmor" part here is given by

$$\frac{1}{6\pi}\, e^2\, \Pi^{0\nu}\, D^2 \dot{z}_\nu = \frac{1}{6\pi}\, e^2 \left[D\dot{z}_\nu D\dot{z}^\nu\, \dot{z}^0 + D^2 \dot{z}^0 \right] . \tag{3.5.23}$$

But the charge is moving across the geodesics, hence the covariant acceleration $D\dot{z}^\mu$ and its covariant derivatives vanish. The local term with Ricci-tensor of the *exact* metric also vanishes outside the source. Thus in the total-metric description all radiation effects come from the *tail* term in (3.5.22). The same structure of tail term appears in any dimensionality.

First we check that $D\dot{z}^M$ is still zero in the first order: indeed, as it follows from (3.2.3), the flat derivative ${}^1\ddot{z}^M$ is given by double derivative of (3.3.4), while the Christoffel part is given by (3.2.16) and (3.3.1). Roughly speaking, their sum is (3.3.27,b) contracted with u'^N and thus vanishes. The next orders do not affect on the order $(r'_g/b)^2$ we need. The same concerns the covariant derivatives of covariant acceleration in higher dimensions.

Next, proceed to the last, tail, term in (3.5.22): it comes from the modification of the self Coulomb field of a particle, by the weak curved background. Instead of derivation of tail integral according to the total metric, we consider the perturbation theory and give a direct correspondence to reconcile with what we do. In fact, we have been computing the lower orders of constituents of equation (3.5.22).

Now one has to estimate the tail function in (3.5.22) as tensor in Minkowski space-time, for the weak Newton field. The basic step in four dimensions was made in [23], and applied to the non-relativistic motion. The first order of this expression:

$${}^1\dot{E}_{\text{tail}}(\tau) = \frac{e^2}{4\pi}\, u^\nu u^{\lambda'} \int\limits_{-\infty}^{\tau} \left[{}^1 v_{\nu\lambda',0} \left({}^0 z(\tau),\, {}^0 z(\tau') \right) - {}^1 v_{0\lambda',\nu} \left({}^0 z(\tau),\, {}^0 z(\tau') \right) \right] d\tau' \tag{3.5.24}$$

represents the full derivative over τ and, being integrated further from $\tau = -\infty$ to $\tau = +\infty$, vanishes. A more detailed derivation is to be given in [43]. The second-order

(m'^2) is given by six terms

$$\frac{4\pi}{e^2}\,{}^2\dot{E}_{\rm tail}(\tau) = u^\nu \int\limits_{-\infty}^{\tau} \left({}^1v_{\nu\lambda',0} - {}^1v_{0\lambda',\nu}\right) {}^1\dot{z}^{\lambda'}(\tau')\,d\tau' + {}^1\dot{z}^\nu(\tau)\,u^{\lambda'} \int\limits_{-\infty}^{\tau} \left({}^1v_{\nu\lambda',0} - {}^1v_{0\lambda',\nu}\right) d\tau' +$$
$$+ u^\nu u^{\lambda'}\,{}^1z^\sigma(\tau) \int\limits_{-\infty}^{\tau} \left({}^1v_{\nu\lambda',0\sigma} - {}^1v_{0\lambda',\nu\sigma}\right) d\tau' + u^\nu u^{\lambda'} \int\limits_{-\infty}^{\tau} \left({}^1v_{\nu\lambda',0\sigma'} - {}^1v_{0\lambda',\nu\sigma'}\right) {}^1z'^{\sigma'}(\tau')\,d\tau' +$$
$$+ u^\nu u^{\lambda'} \int\limits_{-\infty}^{\tau} \left({}^2v_{\nu\lambda',0} - {}^2v_{0\lambda',\nu}\right) d\tau' - u^\nu u^{\lambda'} \int\limits_{-\infty}^{\tau} \left({}^1\Gamma^0_{\sigma\nu}\,{}^1v^\sigma{}_{\lambda'} + {}^1\Gamma^\sigma_{\nu 0}\,{}^1v_{\sigma\lambda'}\right) d\tau' \qquad (3.5.25)$$

where the integrals are to be evaluated on the *unperturbed* trajectory. The first line represents the variation of $\dot{z}^\nu \dot{z}^{\lambda'}$, the second one is a first term of Taylor expansion of ${}^1v_{\mu\nu',\lambda}$ while the third line is constituted from second-order $v_{\mu\nu',\lambda}$ and $\Gamma-$terms from covariant differentiation of $v_{\mu\nu'}$, respectively.

Among these terms after the substitution of exact expressions, we can rearrange terms according to leading power of γ and ability to be integrated over τ'. Namely, some terms of ${}^2v$ correspond to the second-order expansion of Ricci tensor in whole space (i.e. with a source and thereby non-vanishing) plus another quadratic on ${}^1h$ combination, to be integrated over volume with the flat-space Green's functions ${}^DG$. Denote such a combination as $\tilde{R}$: $\tilde{R} = \mathcal{O}(h^2)$.

Below we show (3.5.31) that by virtue of symmetry, the differentiations ∂_μ and $\partial_{\mu'}$ ($\mu = t, z$), with x, x' taken on the unperturbed trajectory, add $u_\mu(\tau-\tau')/|\tau-\tau'|^2$. Using the de Witt – de Witt coordinates [23, eqn. A.1] and integrating by parts over volume and over τ', these terms in the force read schematically

$$\tilde{R}_{\nu\alpha;\underbrace{\beta\gamma\delta\ldots}_{d}}\,\underbrace{u^0 u^\nu u^\alpha u^\beta u^\gamma\ldots}_{d+3}\,.$$

Looking at the second-order-expansion of Ricci-tensor (see e.g. [15, eqn. A.4]), one notices that these terms correspond to the quadratic on ${}^1h$ part and not to the $\Box\,{}^2h-$part.

In other words, if one takes the first-order post-linear metric as exact and computes Ricci-tensor according to it, then Ricci-tensor of this *fictitious* metric well survives and schematically reads

$$R_{\lambda\lambda}\left[\eta_{\mu\nu} + \varkappa_D\,{}^1h_{\mu\nu}\right] = \mathcal{O}\left(r_g'^{\,2}/r^4\right)\,.$$

Going back to (3.5.22) one concludes that such a term corresponds to the Ricci-term if consider such incomplete metric, with a significant note that it comes purely from tail and does not come from the true Ricci-tensor, since the latter vanishes in all orders.

The analogue of (3.5.22) in six dimensions is given in [24]. One can show directly, that radiative part in even dimensionality coincides with its flat-space analogue, with obvious generalization of derivatives from common to the covariant. Thereby on the geodesic motion this part vanishes by the same reason.

The curved local part (constituted from the single Ricci-term in four dimensions) comes from the derivative of the Heaviside of Synge function, accompanying the $v_{\mu\nu'}$, and from the coinciding-point limit of the covariant expansions of bi-tensor quantities [34]. Given that the dimensionality of e^2 is $[e^2] = \text{cm}^d$, the curved local in D dimensions ($D = $ even) is constituted from combinations of Ricci- and Riemann tensors with $D^k \dot{z}^\nu$ of total dimensionality $\text{cm}^{-(d+2)}$. Among these terms, taking into account ${}^0\ddot{z}^\mu = 0$, the maximal in γ order has a term of the following type:

$$\Pi^{0\nu} R_{\nu\alpha;\underbrace{\beta\gamma\delta\ldots}_{d}} \dot{z}^\alpha \dot{z}^\beta \dot{z}^\gamma \ldots \sim R_{\nu\alpha;\beta\gamma\delta\ldots} \underbrace{\dot{z}^0 \dot{z}^\nu \dot{z}^\alpha \dot{z}^\beta \dot{z}^\gamma \ldots}_{d+3},$$

with *positive* coefficient of proportionality in even d, coming from the construction of curved Green's functions.

Given that for Newton field in first non-vanishing order $R_{\lambda\lambda} \sim (r'_g)^{2d+2}/r^{2d+4}$ (for $b \gg r'_g$) and that $\dot{z}^0$ and $\dot{z}^z$ give $\gamma-$factor each, the local curvature term is of order

$$\dot{E}_{\text{curv}}(\tau) \equiv -f^0_{\text{curv}}(\tau) \sim -e^2 R_{\nu\alpha;\underbrace{\beta\gamma\delta\ldots}_{d}} \underbrace{u^0 u^\nu u^\alpha u^\beta u^\gamma \ldots}_{d+3} \tag{3.5.26}$$

Since the metric is static and spherically-symmetric, only the radial derivatives of Ricci-tensor appear. Finally among R_{00} and R_{rr} the latter is dominant:

$$R_{rr} \sim -\frac{{r'_g}^{2(d+1)}}{r^{2(d+2)}} + \mathcal{O}\left({r'_g}^{3(d+1)}/r^{3d+5}\right), \qquad r = \sqrt{b^2 + \gamma^2 v^2 \tau^2}\,.$$

Substituting it into (3.5.26) and taking care of the sign, one has:

$$\dot{E}_{\text{curv}}(\tau) \sim -e^2 R_{rr;\underbrace{rrrr\ldots}_{d}} u^0 \underbrace{u^z u^z u^z u^z \ldots}_{d+2} \sim \frac{{r'_g}^{2(d+1)}}{r^{3d+4}} \gamma^{d+3} > 0\,. \tag{3.5.27}$$

The characteristic spatial distance, where the curvature alters significantly across the particle's trajectory, is of order $\mathcal{O}(b)$, thus the mean time and mean proper time are given by (3.5.19), in what follows that $r \sim b$ and the relative contribution reads

$$E_{\text{curv}}(\tau) \sim \dot{E}_{\text{curv}}(\tau)\, \tau_{\text{gr}} \sim \frac{e^2 m'^2 G_D^2}{b^{3d+3}} \gamma^{d+2}\,. \tag{3.5.28}$$

The characteristic times (3.5.19) find a reflection in the characteristic frequencies for this partial process. These frequencies are given by $\omega \sim \gamma^2/b$ as a full analogy with (3.5.16).

Looking at the Table 3.1, one concludes that this sub-process corresponds to the high-frequency entry, with the proper estimate of partial contribution into the total emitted energy. To repeat, the local curvature terms coming from tail, structurally correspond to Ricci-tensor term constructed from incomplete metric, considered as *exact*.

A tail. Now consider the terms which can not be converted to the local ones. Direct application of the PT gives ${}^1v_{\mu\nu'}$ as some combination of the second-order derivatives of generic integral

$$I(x,x') = \int \delta^{(d/2)}\left((x'-x'')^2\right)\delta^{(d/2)}\left((x-x'')^2\right)\frac{d^Dx''}{r''^{d+1}}\,, \qquad x''=(t'',\mathbf{r}'')\,, \qquad (3.5.29)$$

which can be interpreted as a matrix element of Newtonian potential from initial state $|\text{in}\rangle = {}^DG|x\rangle$ to the final $|\text{out}\rangle = {}^DG|x'\rangle$, with ${}^DG$ is a Green's function in flat $D-$dimensional space-time.

In particular, the consistent account of the non-relativistic limit leads to the Smith –Will force in higher dimensions[1]. The discussion of all terms in (3.5.25) and all derivatives of (3.5.29) goes beyond our primary goal here. We will highlight here the four-dimensional estimate, with generalization to be done in forthcoming publication: the integral $I(x,x')$ in (3.5.29) is computed in [23] and reads

$$I(x,x') = \frac{1}{|\mathbf{r}-\mathbf{r}'|}\left[\theta(r+r'-t+t')\,\ln\frac{r+r'+|\mathbf{r}-\mathbf{r}'|}{r+r'-|\mathbf{r}-\mathbf{r}'|} + \right.$$
$$\left. + \,\theta(t-t'-r-r')\,\ln\frac{t-t'+|\mathbf{r}-\mathbf{r}'|}{t-t'-|\mathbf{r}-\mathbf{r}'|}\right]. \qquad (3.5.30)$$

The third-order derivatives over t and z have maximal value only if one keeps $\theta(t-t'-r-r')$ and differentiates the logarithm, otherwise for $\tau, t' \gg b/\gamma v$ $\delta^{(k)}(t-t'-r-r')$ contains γ inside an argument and γ goes to denominator.

Thereby

$$v_{\mu\nu',\lambda}(x,x') \sim r_g'\,\theta(t-t'-r-r')\,\frac{(x-x')_\mu (x-x')_{\nu'}(u_\lambda/\gamma)}{[(x-x')^2]^3}. \qquad (3.5.31)$$

[1] In fact, Smith and Will [33] have shown that the four-dimensional result by de Witt and de Witt for newtonian (weak) field [23] is still exact in the total Schwarzschild metric even for the case of strong field.

For x and x' are taken on the unperturbed trajectory, $(x-x')_\mu = u_\mu(\tau-\tau')$ contains γ (for $\mu = 0, z$), while $(x-x')^2 = (\tau-\tau')^2$ – does not, thus the typical term reads

$$v_{\mu\nu',\lambda}(x,x') \sim r'_g \, \frac{\theta(t-t'-r-r')}{\gamma} \, \frac{u_\mu u_{\nu'} u_\lambda}{(\tau-\tau')^4} \sim \gamma^2 \, \frac{\theta(t-t'-r-r')}{(\tau-\tau')^4} . \tag{3.5.32}$$

The solution for ${}^1\!z^0$ coming from (3.3.4) is given by

$${}^1\!\dot{z}^0(\tau) = \frac{m'\varkappa_4^2}{8\,\pi^2} \frac{\gamma}{\sqrt{b^2+(\gamma v\tau)^2}} \,, \qquad {}^1\!\dot{z}^z(\tau) = -\frac{d+4}{2\,(d+1)} \; {}^1\!\dot{z}^0(\tau) \tag{3.5.33}$$

According to $\theta(t-t'-r-r')$, $t-t' = \gamma(\tau-\tau') \equiv \gamma\xi$ is larger than $r + r' > 2b$. Thus $\xi > 2b/\gamma$. Substituting $r = \sqrt{b^2+\gamma^2 v^2 \tau^2}$ and $r' = \sqrt{b^2+\gamma^2 v^2 (\tau-\xi)^2}$, such an argument of Heaviside function has a solution only if $\tau\xi > b^2$. Taking into account the double $\tau\xi$-integration and that integration ranges of both ξ and τ are equally important, one expects the domination from the range

$$|\tau| \sim \xi \sim b \,. \tag{3.5.34}$$

Therefore the typical term of the total energy associated with a tail, reads

$${}^2E_{\text{tail}} \sim e^2\,(r'_g)^2 \gamma^4 \int\limits_{-\infty}^{\infty} d\tau \int\limits_{b^2/\tau}^{\infty} \frac{d\xi}{\xi^4} \frac{1}{\sqrt{b^2+(\gamma v\tau)^2}} \tag{3.5.35}$$

Substituting the estimate (3.5.34), one obtains finally

$${}^2E_{\text{tail}} \sim e^2\,(r'_g)^2 \gamma^4 \, \frac{\tau\xi}{\xi^4} \frac{1}{\sqrt{b^2+(\gamma v\tau)^2}} \bigg|_{\tau\sim\xi\sim b} \sim \frac{e^2\,(r'_g)^2}{b^3} \, \gamma^3 \,, \tag{3.5.36}$$

in agreement with (3.4.13)[1].

Thus, despite the rapid decrease of ${}^1\!\dot{z}^M$ at $\tau > b/\gamma$, the main contribution comes from $\tau \sim b$ due to the fact that ${}^1\!v$ alters slowly.

According to (3.5.34), the characteristic duration in the comoving and in the Lab frames, due to the Doppler effect, are given by

$$\tau_{\text{tail}} = b = \gamma\tau_{\text{em}} \qquad t_{\text{tail}} = \gamma\,\tau_{\text{tail}} = \gamma\, b \qquad t_{\text{Lab,tail}} \sim \frac{t_{\text{em}}}{\gamma^2} \sim \frac{b}{\gamma} \,, \tag{3.5.37}$$

[1] From the consideration made above we can say nothing about a sign of this expression. The main goal of this subsection is to qualitatively explain the spectral characteristic of this process arising to the tail. However, giving the direct correspondence to the positively-defined expression in the text, we hope that a consistent accounting of all terms in (3.5.25) will lead to the conclusion concerning the sign.

respectively, while applying the same deduction as in (3.5.10) one obtains the characteristic frequencies of this tail effect:

$$\omega_{\text{com,tail}} \sim \frac{1}{t_{\text{tail}}} \sim \frac{1}{\gamma b}\,, \qquad\qquad \omega_{\text{tail}} \sim \frac{1}{t_{\text{Lab,tail}}} \sim \frac{\gamma}{b} = \omega_0\,, \tag{3.5.38}$$

in agreement with (3.4.19), taken for $d = 0$.

Thus we arrive at the conclusion, that, at least in four dimensions, the transition region in the Table 3.1 corresponds to the tail effects of non-linearity in de Witt−Brehme sense. The generalization into higher dimensions represents the goal of forthcoming work.

Comparing with the bremsstrahlung by non-gravitational force, we conclude that in gravity the Lorentz transformation of frequency is determined not only by simple ultrarelativistic consideration of Doppler effect, but also by curved geometry and non-linear effects.

Thus we arrive at the following scheme:

$$\begin{aligned} \text{tail in curved space} \to & \text{ local curvature-term in fictitious first-order metric} \,(\omega_{\text{curv}} \sim \gamma^2/b) \\ & + \text{non-local tail terms for } v \text{ treated perturbatively} \,(\omega_{\text{tail}} \sim \gamma/b)\,. \end{aligned}$$

Thereby, to conclude: the contribution coming from a tail in the curved-space concept reappears as local curvature terms. This phenomenon is directly related with PT over Minkowski background, and with ultrarelativistic character of a motion. In our scheme it represents the same effect as the effective delocalization of the second-order-field source in the flat space.

The analogy of such a resurrection was proposed by [23] for the opposite ultimate case of non-relativistic motion along a bounded orbit, where originally-tail contribution (with respect to the total metric) reappeared as non-conservative non-relativistic Larmor energy.

3.5.3 Restrictions and possible cut-offs

Here we assume that $m\gamma \gg m'$ and the emitted energy is determined by those values obtained in the Section 3.4. Thereby the total initial energy is essentially the energy of the fast particle: $\mathcal{E}_0 \approx m\gamma$. Our goal here is to set bounds on the minimal value of an impact parameter b and to confirm the validity of the classical approach applied above.

The condition on the weakness of gravitational field, $b \gg r'_g$, has been discussed in (3.2.6). The condition $b \ll R$ (3.1.2) is related with the treatment of space-time as higher-dimensional. Additionally, in the ADD model, it is directly related to the pass from KK-mode-summation to the quasi-continuous integration. Finally, the condition on the classicality of the emitted vector field obviously reads

$$b > r_{\rm cl} = (e^2/m)^{d+1}. \qquad (3.5.39)$$

Next consider the conditions which do not follow from the classical theory but are necessary for the classical result to fit the quantum one.

The simple quantum-mechanical restrictions

$$\omega_{\max} \ll E_{\rm rad}\,, \qquad E_{\rm rad} < \mathcal{E}_0 \approx m\gamma \qquad (3.5.40)$$

reflect the fact that the particle can not lose energy more than it had initially (being free at infinity). The ultimate situations of hard bremsstrahlung, when the charge emits almost all its energy, are admissible in QED [16]. Next, for the treatment of the emitted photons as classical, we need a large number of their quanta, which implies the weak particle-recoil. For the radiation problem at hand, the weak particle-recoil condition due to the emission of photons with frequency ω is satisfied if the momenta of the emitted photons are much smaller than the momentum transfer of the elastic collision. For the hard-photon emission with $\omega < \mathcal{E}$ the latter condition is satisfied if the emission angle ϑ is less than the deflection angle $\alpha_{\rm gr}$, while for $\omega \ll \mathcal{E}$ this condition can be relaxed.

Substituting the characteristic emission angle $\vartheta \sim \bar{\vartheta} = 1/\gamma$ into (3.5.17) one obtains

$$b > r'_g \gamma^{\frac{1}{d+1}}\,.^{*1} \qquad (3.5.41)$$

This condition differs from the one, (3.1.1), given in the Introduction for gravitational bremsstrahlung. It is stronger than the weak-field condition (3.2.6) but weaker than (3.1.1).

Indeed, according to the iteration scheme, the ultrarelativistic charge emits the energy after its trajectory is gravitationally perturbed, so we do not need to accounting for the back-reaction of the gravitational field due to the fast charge, on the uncharged, target, particle.

Moreover, the experience from analogous computations of the total energy of synchrotron radiation shows that this condition can be relaxed and replaced, instead, by the weaker $\omega \ll \mathcal{E}_0$ without restriction on the angles of the emitted photon. When

[1] The latter quantity coincides with the energy-associated Schwarzschild radius r'_S of m' in the comoving (with m) Lorentz frame and approximately equals r_S (of m) in the Lab frame for comparable $m \sim m'$.

the emitted energy E is of order $\mathcal{E}_0$, this condition also guarantees a large number of emitted quanta, and justifies further the description of radiation with a classical field.

Estimating the efficiency of the emitted energy in four dimensions according to (3.4.13), one gets

$$\epsilon_0 \equiv \frac{E_{\rm rad}}{\mathcal{E}_0} \sim \frac{e^2\, m'^2 G_4^2}{mb^3}\, \gamma^2 \sim \frac{r_{\rm cl}}{b} \left(\frac{\gamma r'_g}{b} \right)^2 < 1\,, \tag{3.5.42}$$

by virtue of restrictions (3.5.39,3.5.41).

For the ADD bremsstrahlung (3.4.20), with the same characteristic frequency $\omega \sim \gamma/b$, the efficiency reads

$$\epsilon_{\rm ADD} \sim \frac{e^2\, m'^2 G_D^2}{mVb^{2d+3}}\, \gamma^2 \sim \left(\frac{r_{\rm cl}}{b} \right)^{d+1} \left(\frac{b}{R} \right)^d \left(\frac{\gamma^{\frac{1}{d+1}} r'_g}{b} \right)^{2(d+1)} < 1\,, \tag{3.5.43}$$

if one also takes into account (3.1.2).

In higher dimensions with characteristic frequency $\omega \sim \gamma^2/b$ the direct application[1] of the above estimates gives $\epsilon_d \ll \gamma^{d-1}$. Thereby this might lead to the efficiency catastrophe for $d > 1$.

The possible resolutions of this paradox may be related with:

- A small pre-factor, of order of $C_d \sim 10^{-5}$, in (3.4.11);
- Frequency $\omega \sim \gamma^2/b$ is incompatible with the requirement $m < M_*$. Thereby one needs a cut-off on the frequency;
- The possible Vainshtein limit of the process in a space with compactified radii;
- Combination of (3.5.39) with (3.5.41) gives

$$b > \max \left\{ (e^2/m)^{d+1}, r'_g \gamma^{\frac{1}{d+1}} \right\}.$$

Let us consider the latter possibility in practice.

For instance, for the scattering of protons on neutrons with $\gamma = 10^{14}$, available at the LHC, the classical radius of a proton and $\gamma r'_g$ for neutron are given ($d = 0$) by

$$r_{\rm cl} = 1.53 \cdot 10^{-16}\, \text{cm}, \qquad \gamma r'_g = 2.48 \cdot 10^{-38}\, \text{cm}, \tag{3.5.44}$$

respectively, while in higher dimensions the ratio $r_{\rm cl}/r'_g \gamma^{1/(d+1)}$ is even larger. Thus the restriction on b is determined, essentially, by $r_{\rm cl}$. Moreover, the latter is less than the actual size of a proton l_p and its Compton wavelength l_C of it:

$$l_p = 0.84 \cdot 10^{-13}\, \text{cm}, \qquad l_C = 2.10 \cdot 10^{-14}\, \text{cm}.$$

[1] We neglect here the $\ln \gamma$ in (3.4.12).

The scattering of nuclei present similar features.

On the other hand, the radiated energy efficiency coming from (3.4.11) can be presented as

$$\epsilon_d \sim \frac{e^2\, m'^2 G_D^2}{m b^{3d+3}}\, \gamma^{d+1} \sim \left(\frac{r_{\rm cl}}{b}\right)^{d+1} \left(\frac{\sqrt{\gamma}\, r'_g}{b}\right)^{2(d+1)} , \tag{3.5.45}$$

and, by virtue of $b > r_{\rm cl} > \gamma\, r'_g > \sqrt{\gamma}\, r'_g$, easily becomes smaller than unity. This practically resolves the efficiency paradox. The same argument makes the dominance of gravitational radiation over the electromagnetic, almost impossible, an issue raised above according to the naive comparison of the power of γ.

For the scattering of electrons one takes the Compton length. Thereby there is no the efficiency catastrophe in the problem-at-hand, but one sets the following bound on the value of the impact parameter:

$$l_C < b\,. \tag{3.5.46}$$

In UED, from (3.4.40) one obtains:

$$\epsilon_{\rm UED} \sim \frac{\left(e m' \varkappa_D^2\right)^2}{m V^2 b^{d+3}}\, \gamma^{d+1} \sim \left(\frac{b}{R}\right)^{2d} \left(\frac{r_{\rm cl}}{b}\right)^{d+1} \left(\frac{\sqrt{\gamma}\, r'_g}{b}\right)^{2(d+1)} . \tag{3.5.47}$$

Taking into account $b > l_C > R_{\rm UED}$ (3.4.26), one rewrites (3.5.47) as

$$\epsilon_{\rm UED} < \left(\frac{b}{R}\right)^{2(d+1)} \left(\frac{r_{\rm cl}}{b}\right)^{d+1} \left(\frac{\sqrt{\gamma}\, r'_g}{b}\right)^{2(d+1)} \sim \left(\frac{r_{\rm cl}}{b}\right)^{d+1} \left(\frac{\sqrt{\gamma}\, r'_g}{R}\right)^{2(d+1)} \ll 1\,, \tag{3.5.48}$$

if directly compare $\sqrt{\gamma}\, r'_g \ll \gamma\, r'_g \ll R_{\rm UED}$ by values (3.4.26) and (3.5.44).

Now return to the large-modes condition (3.4.36): substituting $R_{\rm UED}$ by (3.4.26) and comparing with (3.5.46) one concludes that for $\gamma = 10^{14}$ the condition

$$\gamma R \sim 10^{-2}\,{\rm cm} \gg b > 10^{-14}\,{\rm cm} \sim \lambda_C\,, \tag{3.5.49}$$

is well satisfied and a large number of the emission modes are excited, that gives the enhancement of the bremsstrahlung radiation.

Going back to the spectrum we see that if $b > 1/m$ holds, then

$$\omega_{\rm max} = \mathcal{E}_0 = m\gamma > \frac{\gamma}{b} = \omega_0\,.$$

Thus the maximal value of the frequency lies inside the domain $(\gamma/b, \gamma^2/b)$, so the part of destructive interference region, the main point of our computation, can be detected in practice in all kinds of the extra dimensions and corresponding gravity models.

Despite the radiation efficiency being tiny, one can expect that absolute amounts of the emitted radiation, due to the relatively large $r_{\rm cl}$ with respect to r_g, can be determined (for instance, for heavy nuclei) and can give information on the (possible) size and number of extra dimensions.

3.5.4 Results and conclusions

A detailed study of classical electromagnetic (vector) radiation emitted in ultra-relativistic collisions of massive point-like particles was presented. The space-time was assumed to have an arbitrary number of toroidal or non-compact extra dimensions and the post-linear approximation scheme of General Relativity was employed for the computation. The angular and frequency distributions of radiation, as well as the total emitted energy were studied in detail up to leading ultra-relativistic order.

Three characteristic frequency regimes ($1/b$, γ/b and γ^2/b) of the emitted radiation were identified and the characteristics of the dominant contribution was determined in various dimensions, depending on the gravity model.

In particular, in any number of dimensions the soft component of radiation is mainly due to the scattered particles, with negligible contribution coming from the cubic graviton-graviton-photon interaction term[1]. In all cases of bremsstrahlung most of the emitted waves are beamed (in the Lab frame) inside a narrow cone with angle $1/\gamma$ and along the spatial direction of fast-particle's motion.

Among the notable features we would like to mention, are the following:

- The radiation amplitude is damped by the factor $(\omega_0/\omega)^2$ at the frequency region $\gamma/b \lesssim \omega \lesssim \gamma^2/b$:
$$j(\omega) \sim j(\omega_0)\,\frac{\omega_0^2}{\omega^2}\,, \qquad\qquad \omega_0 \sim \frac{\gamma}{b}\,;$$
Thus at $\omega \sim \gamma^2/b$ the amplitude $j(\omega)$ is suppressed by γ^2 with respect to $j\,(\mathcal{O}(\gamma/b))$, that represents the destructive interference (DI) effect;

- The frequency distribution goes like
$$\frac{dE_{\rm rad}}{d\omega} \sim \gamma^{4-d}\,\omega^{d-2}$$
inside this frequency regime. Hence for $d = 0$ and in the ADD-case most of the radiation has characteristic frequency $\omega \sim \omega_0$, for $d \geqslant 1$ the dominant frequency is $\omega \sim \gamma\omega_0$ while in the transition case $d = 1$ the entire domain $\gamma/b \lesssim \omega \lesssim \gamma^2/b$ contributes equally to add a logarithm of γ into the total emitted energy;

- ZFL gives qualitatively adequate result for the ADD bremsstrahlung (where DI happens beyond $\omega_{\rm ADD} \sim \gamma/b$) and for pure electromagnetic bremsstrahlung (where no DI occurs and the amplitude has the same behavior up to $\omega_{\rm em} \sim \gamma^2/b$) in the small-angle region;

[1] In four dimensions this is a well-known fact, verified easily also in the context of Feynman diagram infrared graviton summation.

- No efficiency catastrophe for reasonable values of the Lorentz factor and charges;
- The applicability of perturbation theory is essentially determined by the Compton length of a charge:
$$b \gg l_C \,;$$
- The coherence length argument gives an adequate explanation of the frequency-angular characteristics of the radiation amplitude but does not predict which frequencies will dominate in spectrum.

However, in contrast to the four-dimensional case, in any number of extra dimensions $d > 0$ the frequency spectrum of the emitted radiation vanishes as $\omega \to 0$ and the total emitted energy in soft gravitons is negligible.

Also, contrary to what happens with soft radiation emission, the cubic graviton-graviton-photon interaction and the scattered particles themselves are equally important as sources of radiation with high frequency. In fact it was shown that in any dimension they lead to partial cancelation (*destructive interference*) of the total beamed radiation amplitude in the high frequency domain, as a result of which the emitted energy in the $\gamma^2/b-$frequency regime is reduced by two powers of the Lorentz factor γ in the Lab frame.

The relevance of the classical analysis to the full *quantum radiation* problem was also discussed. The *classicality conditions*, necessary for the classical treatment to be a good approximation to the full quantum problem were derived and the radiation efficiency ϵ, i.e. the fraction of the initial energy which is emitted in gravitational radiation, was computed for values of the parameters within the region of validity of our classical computation.

Thus one concludes that the gravitational scattering of charges and corresponding bremsstrahlung, at least classically, is a more reliable scheme to detect extra dimensions already in contemporary colliders, though, of course the quantum-field treatment of this process (at least for the vector field) is necessary and represents the direct prospect of further study.

Finally, the spectral characteristics are qualitatively discussed in the context of coordinate-space equation of a charge in dimensions of the even space-time dimensionality (Lorentz−Dirac and deWitt−Brehme−Hobbs types of equations). The pure vector bremsstrahlung is qualitatively described by the radiative part of the higher-dimensional Lorentz−Dirac equation in flat space. For the vector bremsstrahlung under the gravity-mediated collision it was found that the observable competition of frequencies originates from the different terms of the de Witt−Brehme−Hobbs equation, describing the motion of a charge in the fixed external curved background.

Thus one concludes that as qualitative argument, the concept of coherence length is valid and directly corresponds to the similar behavior of amplitudes at ultrarelativistic characteristic frequency regimes $\omega \sim \gamma/b$ and $\omega \sim \gamma^2/b$. Nevertheless, as a quantitative argument, coherence length is much less useful when the total physical process is split into some sub-processes. Coherence length consideration does not predict which frequency will dominate in the spectrum, since it does not take into consideration inside itself the possible competition between the spectral-angular characteristics of a source and volume factor in the integration measure when the flux is computed.

However, the implementation of this interpretation and the proper treatment of this classical computation have to be confirmed by the corresponding quantum approach. Meanwhile, even low- and medium-frequency parts of the spectral distribution, which are definitely in agreement with the quantum case, contain some distinctive features for the possible presence of extra dimensions to be detected.

3.6 Useful kinematical formulae

3.6.1 Notations

The angles in the formulae below are defined in Fig. 2.1.

$$u^\mu \equiv \gamma(1,0,0,v)\,, \quad u' \equiv (1,0,0,0)\,, \qquad \psi \equiv 1 - v\cos\vartheta\,,$$

$$z' \equiv \frac{(ku')b}{\gamma v} = \frac{\omega b}{\gamma v}\,, \qquad z \equiv \frac{(ku)b}{\gamma v} = \frac{\omega b}{v}\,\psi = z'\gamma\psi\,,$$

$$\xi^2 \equiv 2\gamma z z' - z^2 - z'^2 = (\gamma v z' \sin\vartheta)^2\,, \qquad \beta \equiv \gamma z z' - z^2 = \gamma^2 z'^2 \psi(1-\psi)\,,$$

$$(kb) = -\gamma z' v \sin\vartheta\cos\phi = -\omega b \sin\theta\cos\varphi\,, \qquad a \equiv z/\sin\vartheta\,.$$

3.6.2 Beaming angular integrals

In the main text the following angular integrals over ϑ were needed for integer m and n

$$V_m^n \equiv \int\limits_0^\pi \frac{\sin^n\vartheta}{(1 - v\cos\vartheta)^m}\, d\vartheta\,. \tag{3.6.1}$$

Consider small-angle contribution, corresponding to the beaming of emitted quanta. For $\gamma \gg 1$ and $\vartheta \lesssim \gamma^{-1}$ the numerator and denominator go like

$$\sin^n\vartheta \simeq \gamma^{-n}\,, \qquad (1 - v\cos\vartheta)^m \simeq \gamma^{-2m}\,, \tag{3.6.2}$$

respectively, thus if $2m > n+1$ one expects the dominance of small-angle region over the other integration domain.

Expanding

$$\sin\vartheta = \vartheta + \mathcal{O}(\vartheta^2)\,, \qquad\qquad 1 - v\cos\vartheta = \frac{\vartheta^2 + \gamma^{-2}}{2} + \mathcal{O}(\vartheta^4)\,, \tag{3.6.3}$$

the integral (3.6.1) reads

$$V_m^n = 2^m \int\limits_0^{\sim 1/\gamma} \frac{\vartheta^n}{(\vartheta^2 + \gamma^{-2})^m}\, d\vartheta\,. \tag{3.6.4}$$

Rescaling $\vartheta \to \vartheta/\gamma$ leads to

$$V_m^n = 2^m \gamma^{2m-n-1} \int\limits_0^{\sim 1} \frac{\vartheta^n}{(\vartheta^2 + 1)^m}\, d\vartheta\,. \tag{3.6.5}$$

This integral (without pre-factor) is of order $\mathcal{O}(1)$. Due to the integrand in (3.6.5) falls rapidly at $\vartheta \gg 1$ one expands the upper-limit to infinity. Indeed, for any $a \gg 1$ the contribution

$$\int\limits_a^{\infty} \frac{\vartheta^n}{(\vartheta^2 + 1)^m}\, d\vartheta \simeq \int\limits_a^{\infty} \vartheta^{n-2m}\, d\vartheta \sim a^{-(2m-n-1)} \ll 1\,. \tag{3.6.6}$$

Thus both the initial integral (3.6.1) and modified one (3.6.5) have subleading contribution from large values of an integration argument due to the rapid fall of integrands.

Thus

$$V_m^n = 2^m \gamma^{2m-n-1} \int\limits_0^{\infty} \frac{\vartheta^n}{(\vartheta^2 + 1)^m}\, d\vartheta\,. \tag{3.6.7}$$

Introducing new integration variable y according to $1+\vartheta^2 = 1/y$, the (3.6.7) is presented as

$$V_m^n = 2^{m-1} \gamma^{2m-n-1} \int\limits_0^{1} (1-y)^{\frac{n-1}{2}}\, y^{\frac{2m-n-3}{2}}\, d\vartheta\,, \tag{3.6.8}$$

that is exactly the Euler's Beta-function $\mathrm{B}\big(\frac{n+1}{2}, \frac{2m-n-1}{2}\big)$. Rewriting it via Gamma-functions, we finally arrive at

$$V_m^n = \frac{2^{m-1}\,\Gamma\big(\frac{n+1}{2}\big)\,\Gamma\big(\frac{2m-n-1}{2}\big)}{\Gamma(m)}\,\gamma^{2m-n-1}\,. \tag{3.6.9}$$

In [13], with another derivation of the above integral via Legendre functions, it was shown that first correction to the (3.6.9) is of relative order $\mathcal{O}(\gamma^{-2})$.

In the case $2m = n+1$ an expansion of the integral is logarithmic.

3.7 Self-action account

We have already discussed the reason we do not consider the self-action as far as radiation is concerned. It is however useful to show that including the self-action leads to a conserved current.

When one includes the self-action, the equations of motion change are of the same form but we should substitute h and h' with $h+h'$. This produces some extra terms in the local and non-local currents. We write here the extra terms in the local current:

$$\rho^M_{\rm self}(k) = -\frac{e\,m\,\varkappa_D^2\,{\rm e}^{i(kb)}}{(2\pi)^2}\int \frac{\delta(qu)\,\delta(ku-qu)}{q^2}\left[\frac{d+1}{2\,(d+2)}\frac{(kq)u^M}{(qu)} - \frac{d+1}{2\,(d+2)}\frac{q^M}{(qu)}\right]d^Dq \tag{3.7.1}$$

Making use of delta function and contracting with k_M, one obtains zero in what immediately follows that the above expression is a conserved quantity.

Similarly for the non-local part,

$$\sigma^M_{\rm self}(k) = \frac{e\varkappa_D^2 m}{(2\pi)^2}\int\left[\frac{ku}{d+2}\,q^M - \frac{ku}{d+2}\,u^M + \frac{d+1}{2\,(d+2)}\,\left(kq\,u^M - ku\,q^M\right)\right]\times$$
$$\times\,\frac{\delta(qu)\,\delta(ku-qu)\,{\rm e}^{-i(q\cdot b)}}{q^2(k-q)^2}\,d^Dq \tag{3.7.2}$$

Integration of both (3.7.1) and (3.7.2) over q^0 gives

$$\rho^M_{\rm self}(k) \sim \delta(ku)\int\frac{1}{(q^z)^2/\gamma^2+q_\perp^2}\left[\frac{d+1}{2\,(d+2)}\frac{(kq)u^M}{(qu)} - \frac{d+1}{2\,(d+2)}\frac{q^M}{(qu)}\right]dq^z\,d^{D-2}\mathbf{q}_\perp\,. \tag{3.7.3}$$

Thus the account of self-terms leads to the terms proportional to $\delta(ku)$. These terms are analogous to the Fourier-transforms of Coulomb field which does not contribute to the radiation.

The conservation of additional terms concerned with the appearance of second charge and the self-action terms is analogous to the proof presented in the Subsection 3.3.5.

3.8 An alternative proof of destructive interference

We provide another proof for destructive interference in the $z-$region, with $\vartheta < 1/\gamma$. This differs from the method followed in the main part of a chapter, which covered the full angular range. In angular region discussed here, we show the destructive interference effect rigorously, by the integration-by-parts technique.

We begin with (3.3.14). First of all we will perform a variable change from x to ζ, where

$$dx = \frac{\zeta(x)}{f(x)}\, d\zeta\,, \qquad f(x) = \left(z^2 + z'^2 - 2\gamma z z'\right) x + \gamma z z' - z^2\,. \tag{3.8.1}$$

We will also be using the identity

$$\zeta \hat{K}_\nu(\zeta) = -\hat{K}'_{\nu+1}(\zeta)\,. \tag{3.8.2}$$

Integrating the expression (3.3.14) by parts we obtain the following:

$$\begin{aligned}
\sigma^M(k) = \frac{\lambda}{2\gamma v}\Bigg\{&\left(\frac{\hat{K}_{d/2}(z)}{\gamma z z' - z^2}\,\mathrm{e}^{i(kb)} - \frac{\hat{K}_{d/2}(z')}{z'^2 - \gamma z z'} + \int_0^1 \hat{K}_{d/2}(\zeta)\left(\frac{\mathrm{e}^{i(kb)(1-x)}}{f(x)}\right)' dx\right) u^M \times\\
&\times\left[\frac{\beta}{d+2} - \gamma z' + \frac{z^2}{d+2} + \gamma^2 v^2 z'^2\right] + i\left[\frac{(kb)}{d+2}\, u^M + \left(\gamma^2 v z' - \frac{\gamma z v}{d+2}\right)\frac{b^M}{b}\right]\times\\
&\times\left(\frac{\hat{K}_{d/2+1}(z)}{\gamma z z' - z^2}\,\mathrm{e}^{i(kb)} - \frac{\hat{K}_{d/2+1}(z')}{z'^2 - \gamma z z'} + \int_0^1 \hat{K}_{d/2+1}(\zeta)\left(\frac{\mathrm{e}^{i(kb)(1-x)}}{f(x)}\right)' dx\right) +\\
&+\left[\frac{\xi^2}{d+2} + \left(\gamma z' - \frac{z}{d+2}\right)(\gamma z' - z)\right]\left(\frac{\hat{K}_{d/2}(z')}{z'^2 - \gamma z z'} + \int_0^1 \hat{K}_{d/2}(\zeta)\left(\frac{x\,\mathrm{e}^{i(kb)(1-x)}}{f(x)}\right)' dx\right) u^M\Bigg\}\,.
\end{aligned}$$

Further integration by parts gives

$$\begin{aligned}
\sigma^M(k) = \frac{\lambda}{2\gamma v}\Bigg\{&\left(\frac{\hat{\boldsymbol{K}}_{d/2}(z)}{\gamma z z' - z^2} - \frac{\hat{K}_{d/2}(z')}{z'^2 - \gamma z z'} - i\,q_0\frac{\hat{\boldsymbol{K}}_{d/2+1}(z)}{(\gamma z z' - z^2)^2} + i\,q_1\frac{\hat{K}_{d/2+1}(z')}{\left(z'^2 - \gamma z z'\right)^2} + R_0\right) u^M \times\\
&\times\left[\frac{\beta + z^2}{d+2} - \gamma z\, z' + \gamma^2 v^2 z'^2\right] + i\left[\frac{(kb)}{d+2}\, u^M + \left(\gamma^2 v z' - \frac{\gamma z v}{d+2}\right)\frac{b^M}{b}\right]\times\\
&\times\left(\frac{\hat{\boldsymbol{K}}_{d/2+1}(z)}{\gamma z z' - z^2} - \frac{\hat{K}_{d/2+1}(z')}{z'^2 - \gamma z z'} + i\,q_0\frac{\hat{\boldsymbol{K}}_{d/2+2}(z)}{\beta^2} - i\,q_1\frac{\hat{K}_{d/2+2}(z')}{\left(z'^2 - \gamma z z'\right)^2} + R_0\right) + \left[\frac{\xi^2}{d+2} +\right.\\
&\left.+\left(\gamma z' - \frac{z}{d+2}\right)(\gamma z' - z)\right]\left(\frac{\hat{K}_{d/2}(z')}{z'^2 - \gamma z z'} - \frac{\hat{\boldsymbol{K}}_{d/2+1}(z)}{(\gamma z z' - z^2)^2} + (i q_1 + 1)\frac{\hat{K}_{d/2+1}(z')}{\left(z'^2 - \gamma z z'\right)^2} + R_1\right) u^M\Bigg\}\,.
\end{aligned}$$

with notations $\hat{\boldsymbol{K}}_\tau(z) \equiv \mathrm{e}^{i(kb)}\,\hat{K}_\tau(z)$ and

$$q_0 = (kb) - i\frac{z^2 + z'^2 - 2\gamma z z'}{\gamma z z' - z^2}\,, \qquad q_1 = (kb) - i\frac{z^2 + z'^2 - 2\gamma z z'}{z'^2 - \gamma z z'}$$

and residues

$$R_\sigma \equiv \int_0^1 dx\, \hat{K}_{d/2+1}(\zeta(x))\left[\left(x^\sigma\frac{\mathrm{e}^{-ix(kb)}}{f(x)}\right)'\frac{1}{f(x)}\right]'.$$

Thus the boldface hatted Macdonald functions emphasize the fact that after each iteration of integration by parts, Macdonalds of z come with phase $e^{i(kb)}$ from boundary $x = 0$, while those ones with argument z' come with phase 1 from boundary $x = 1$.

If keep on integrating by parts, we will obtain an expansion. In the region that we are interested in, i.e. the $z-$region, we have $z \sim 1$, $z' \sim \gamma$, so that $\xi^2 \sim \beta \sim \gamma^2 \sim (\beta - \xi^2)$, $q_0 \sim q_1 \sim \gamma$. From this we see that the expansion parameters are: $q_0\beta^{-1} \sim \gamma^{-1} \ll 1$, $q_1(\beta - \xi^2)^{-1} \sim \gamma^{-1} \ll 1$. With this accuracy one can set $q_0 = q_1 = (kb)$, $\beta = \gamma z z'$ the leading part is then:

$$\sigma^M(k) = \frac{\lambda}{2\gamma}\left[\gamma\frac{z'}{z}\,\hat{K}_{d/2}(z)\,u^M - i\left(\frac{(kb)}{z} - \gamma\frac{b^M}{b}\right)\frac{\hat{K}_{d/2+1}(z)}{z}\right], \tag{3.8.3}$$

which exactly cancels with the leading part of (3.3.9), leaving only the subleading terms. The series converges thus establishing further the effect of destructive interference.

Bibliography

[1] P. C. Argyres, S. Dimopoulos and J. March-Russell, Phys. Lett. B **441** (1998) 96, [hep-th/9808138]; T. Banks and W. Fischler, [arXiv:hep-th/9906038]; S. Dimopoulos and G. Landsberg, Phys. Rev. Lett. **87** (2001) 161602 [hep-ph/0106295]; P. Meade and L. Randall, JHEP **0805** (2008) 003, arXiv:0708.3017 [hep-ph]. 65

[2] M. Bleicher and P. Nicolini, arXiv:1001.2211 [hep-ph]; S. B. Giddings, M. Schmidt-Sommerfeld and J. R. Andersen, arXiv:1005.5408 [hep-th]. 65

[3] I. Antoniadis, C. Bachas, D. C. Lewellen and T. N. Tomaras, Phys. Lett. B **207** (1988) 441; I. Antoniadis, Phys. Lett. B **246** (1990) 377. 65

[4] N. Arkani-Hamed, S. Dimopoulos and G. Dvali, Phys. Lett. B **429**, 263 (1998); [arXiv:hep-ph/9803315]; I. Antoniadis, N. Arkani-Hamed, S. Dimopoulos and G. Dvali, Phys. Lett. B **436**, 257 (1998); [arXiv:hep-ph/9804398]. 65

[5] L. Randall and R. Sundrum, Phys. Rev. Lett. **83** (1999) 3370 [hep-ph/9905221]; L. Randall and R. Sundrum, Phys. Rev. Lett. **83** (1999) 4690, [hep-th/9906064]. 65

[6] T. Appelquist; H.-C. Cheng, B. A. Dobrescu, Phys. Rev. D **64** (2001) 035002, [hep-ph/0012100], F. J. Petriello, JHEP **0205** (2002), 003, hep-ph/0204067; T. Flacke, D. Hooper, and J. March-Russell, Phys. Rev. D **73** (2006), 095002, hep-ph/0509352; I. Gogoladze and C. Macesanu, Phys. Rev. D **74** (2006), 093012, hep-ph/0605207 . 66, 97

[7] C. M. Harris, M. J. Palmer, M. A. Parker, P. Richardson, A. Sabetfakhri and B. R. Webber, JHEP **0505**, 053 (2005), [arXiv:hep-ph/0411022]; L. Lönnblad, M. Sjödahl and T. Åesson, JHEP **0509**, 019 (2005), [arXiv:hep-ph/0505181]; B. Koch, M. Bleicher and S. Hossenfelder, JHEP **0510**, 053 (2005), [arXiv:hep-ph/0507138]; L. Lönnblad and M. Sjödahl, JHEP **0610**, 088 (2006), [arXiv:hep-ph/0608210]; B. Koch, M. Bleicher and H. Stoecker, J. Phys. G **34**, S535 (2007), [arXiv:hep-ph/0702187]. 66

[8] G. 't Hooft, Phys. Lett. B **198** (1987) 61. 66

[9] G. F. Giudice, R. Rattazzi and J. D. Wells, Nucl. Phys. B **630**, 293 (2002); R. Emparan, M. Masip and R. Rattazzi, Phys. Rev. D **65**, 064023 (2002). 66

[10] V. Cardoso, O. J. C. Dias and P. S. Lemos, Phys. Rev. D **67**, (2003) 064016, [hep-th/0212168]; V. Cardoso, P. S. Lemos and S. Yoshida, Phys. Rev. D **68** (2003) 084011 [gr-qc/0307104]; E. Berti, M. Cavaglià and L. Gualtieri, Phys. Rev. D **69** (2004) 124011 [hep-th/0309203]; B. Koch and M. Bleicher, JETP Lett. **87** (2008) 75, [hep-th/0512353]; V. Cardoso, M. Cavaglià and J. Q. Guo, Phys. Rev. D **75** (2007) 084020, [hep-th/0702138]; H. Yoshino, T. Shiromizu and M. Shibata, Phys. Rev. D **74** (2006) 124022,[gr-qc/0610110]; P. Lodone and S. Rychkov, JHEP **0912** (2009) 036; arXiv:0909.3519 [hep-ph]. 66

[11] A. Mironov and A. Morozov, Pisma Zh. Eksp. Teor. Fiz. **85**, 9 (2007) [JETP Lett. **85** (2007)] 6, [hep-ph/0612074]; A. Mironov and A. Morozov, [hep-th/0703097]. 66

[12] D. V. Gal'tsov, G. Kofinas, P. Spirin and T. N. Tomaras, JHEP **0905** (2009) 074, arXiv:0903.3019 [hep-ph]. 67, 102, 106

[13] D. V. Gal'tsov, G. Kofinas, P. Spirin and T. N. Tomaras, JHEP **1005** (2010) 055, arXiv:1003.2982 [hep-th]. 67, 80, 93, 99, 100, 120

[14] Y. Constantinou, D. Gal'tsov, P. Spirin and T. N. Tomaras, JHEP **1111**, 118 (2011), arXiv:1106.3509 [hep-th]. 67, 69, 82, 94

[15] D. Gal'tsov, P. Spirin and T. N. Tomaras, JHEP **1301**, 087 (2013), arXiv:1210.6976 [hep-th]; D. V. Gal'tsov, G. Kofinas, P. Spirin and T. N. Tomaras, Phys. Lett. B **683** (2010) 331, arXiv:0908.0675 [hep-ph]. 66, 67, 68, 69, 75, 78, 81, 82, 83, 84, 94, 109

[16] V. B. Berestetskii, L. P. Pitaevskii and E. M. Lifshitz, Quantum Electrodynamics, 2nd edition: (Course of Theoretical Physics by L. D. Landau and E. M. Lifshitz, vol. 4), *Butterworth-Heinemann*, 1982; V. N. Bayer, V. M. Katkov and V. S. Fadin, Radiation by Relativistic Electrons, *Atomizdat*, Moscow, 1973 [on Russian]. 114

[17] Y. Constantinou and A. Taliotis, arxiv: 1308.2544 [hep-th]. 68

[18] P. C. Peters, Phys. Rev. D **7** (1973) 368. 68

[19] P. Dirac. Classical theory of radiating electrons. Proc. Roy. Soc.(London) A **167** (1938) 148. 67, 74

[20] F. Rohrlich, Nuovo Cimento **21** (1961) 811; F. Rohrlich, Classical charged particles, *Addison-Wesley, Reading, Mass.* 1965; 2nd edition: *Redwood City, CA*, 1990; T. Fulton and F. Rohrlich, Ann. Phys. **9** (1960) 499. 67, 74

[21] C. Teitelboim, Phys. Rev. D **1** (1970) 1572. 67, 74

[22] B. S. de Witt and R. W. Brehme, Ann. Phys. **9** (1960) 220. 67, 107

[23] C. Morette-de Witt and B. S. de Witt, Physics, **1** (1964) 3. 67, 108, 109, 111, 113

[24] D. V. Gal'tsov and P. A. Spirin, Grav. Cosmol. **13** (2007) 241, arXiv:1012.3085v1[hep-th]. 67, 74, 110

[25] B. S. de Witt, Phys. Rept. **19** (1975) 295. 67

[26] J. M. Hobbs, Ann. Phys. **47** (1968) 141. 107

[27] V. S. Krivitsky and V. N. Tsytovich, Sov.Phys.Usp. **34** (1991) 250; Usp. Fiz. Nauk **161** (1991) 125; V. I. Ritus, Sov. Phys. JETP **48** (1978) 788, Zh. Eksp. Teor. Fiz. **75** (1978) 1560. 67

[28] A. Higuchi and G. D. R. Martin, Phys. Rev. D **74** (2006) 125002, arXiv: gr-qc/0608028; A. Higuchi and P. J. Walker, Phys. Rev. D **79** (2009) 105023, arXiv:0903.1777 [gr-qc]; A. Higuchi and P. J. Walker, Phys. Rev. D **80** (2009) 105019, arXiv:0908.2723 [hep-th]. 67

[29] R. A. Matzner and Y. Nutku, Proc. Roy. Soc. Lond. **336** (1974) 285. 68

[30] D. V. Galtsov, Yu. V. Grats and A. A. Matyukhin, Sov. Phys. J. **23** (1980) 389, arXiv: 0112110v1 [hep-th]. 68, 82

[31] L. Smarr, Phys. Rev. D **15**, 2069 (1977). 97

[32] I. B. Khriplovich and E. V. Shuryak, Zh. Eksp. Teor. Fiz. **65** (1973) 2137. 68

[33] A. G. Smith and C. M. Will, Phys. Rev. D **22** (1980) 1276. 111

[34] S. M. Christensen, Phys. Rev. D **14** (1976) 2490. 110

[35] I. S. Gradshteyn and I. M. Ryzhik, Table of Integrals, Series and Products, *Academic Press*, 1965.

[36] S. Weinberg, Gravitation and Cosmology: Principles and Applications of the General Theory of Relativity, *Wiley*, 1972. 73

[37] A. P. Prudnikov, Yu. A. Brychkov and O. I. Marichev, Integrals and Series, Vol. 1, Elementary Functions, *Gordon & Breach Sci. Publ.*, New York, (1986). 90

[38] P. Spirin, Grav. Cosmol. **15** (2009) 82. 105

[39] D. M. Eardley and S. B. Giddings, Phys. Rev. D **66** (2002) 044011, [gr-qc/0201034].

[40] H. Yoshino and V. S. Rychkov, Phys. Rev. D **71** (2005) 104028, [hep-th/0503171]; S. B. Giddings and V. S. Rychkov, Phys. Rev. D **70** (2004) 104026, [hep-th/0409131].

[41] B. P. Kosyakov, Theor. Math. Phys. **199** (1999) 493.

[42] P. Spirin, in preparation. 105

[43] P. Spirin, Classical Relativistic Bremsstrahlung in Higher Dimensions: an overview, in preparation. 108

4

Bremsstrahlung and black hole production from collisions of ultra-boosted particles at non-zero impact parameter

4.1 Introduction

Gravitational ultra-relativistic collisions of two black holes, boosted to ultrarelativistic [1] speeds in flat backgrounds have been discussed in several contexts, [2; 3; 4; 5; 6; 7; 8; 9; 10; 11; 12; 13]. In fact, recently with the application of AdS/CFT in heavy ions, the interest in a numerical or an analytical approach to this problem has been growing rapidly [14; 15; 16; 17; 18; 19; 20] but in AdS backgrounds however.

The novel features of the present work are

- The usage of a different pertrurbative scheme[1] than the one employed in earlier works in the literature [2; 3; 4; 5; 13; 21; 22; 23; 24; 25].
- The inclusion of a non-zero impact parameter b.
- The computation of the corrections to the energy-momentum tensor due to the back-reaction effects in the presence of b. In particular, the present approach allows us to follow the collided particles either in the case where they will get trapped inside a horizon or if a horizon is not formed at all.

[1] The expansion parameter will be defined below.

- The first corrections of the metric including the back-reaction contribution of the above point.

Summarizing our results we have:

1. Derived a closed form formula for the first corrections of the metric and of the energy-momentum tensor[1] in the presence of an impact parameter, including the back-reactions.

2. Showed that the metric dependence on space and time is according to the ordering between the proper-time τ and the transverse distance $r = \sqrt{(x^1)^2 + (x^2)^2}$ from the center of the shocks. In particular, according to fig. 4.6, in the $b = 0$ limit there appears a $\tau \leftrightarrow r$ symmetry. A similar result has been observed in shock-wave collisions in AdS backgrounds applied to heavy ions [26]. Remarkably, the same observation has been made in [27] using completely different methods and in particular a hydro-approach. The analogies between the problem studied in this work and heavy ions/Quark Gluon Plasma is further discussed in conclusion ii of sec. 4.9.

3. Showed that for zero impact parameter, the perturbative approximation breaks down and there is an instantaneous and point-like violation of the conservation of the energy momentum tensor, which however, is hidden behind a horizon.

4. Have highlighted the importance of introducing an impact parameter which regulates the produced radiation in the absence of any other transverse scale.

5. Found that the total energy momentum tensor before the collision is traceless and remains traceless after the collision up to the order we have computed in our expansion. This could suggest that it is traceless to all orders and that tracelessness is conserved; a conjecture that is worth investigating further.

6. Calculated the energy emitted during a collision of gravitational waves and argued that the result is exact to all orders.

7. Finally, we have examined the problem of shock-wave collision, in the spirit of the trapped surface analysis, produced by extended sources [28]. The results show that for dilute enough concentration of energy a black hole is not formed. This result seems as a manifestation of the Hoop Conjecture proposed by K. Thorn.

[1] The corrections of the stress-tensor are quite general as they apply for any longitudinal profile of the colliding particles.

This chapter is organized as follows.

In section 4.2.1 we set-up the problem, specify the conventions and write the form of the metric that describes the superposition of the shockwaves before and after the collision.

In the next section 4.3, we compute the corrections to the energy-momentum tensor. These corrections are caused by the interaction of the shockwaves and are only present for positive times. We also discuss the region of applicability of our approach and we make connections with the time scales that a black-hole needs to be formed and equilibrate.

In section 4.4, we show the tracelessness and conservation of the stress tensor, modulo an instantaneous-point-like violation of conservation for zero impact parameter which, is hidden behind a horizon.

Sections 4.5 and 4.6 specify the gauge choice and state the field equations, up to second order taking into account the back-reactions found in section 4.4.

Section 4.7 deals with the solution of the field equations obtaining the second-order corrections to the metric.

A dimensional analysis argument is presented in section 4.8 and yields the dependence of the total energy radiated in the form of gravitational waves from, the energy that is available and, the only other meaningful dimension-full parameter, the impact parameter. In fact, it is shown that for massless particles carrying positive definite energy, the perturbative scheme that computes radiation fails. The origin of this result is identified and the total radiation for zero energy shock-waves is calculated.

We conclude, section 4.9, with a summary and some comments of our main results.

Section 4.10 contains a brief derivation/discussion of trapped surfaces formation from colliding extended matter distributions.

In section 4.11 we give the explicit forms of the polarization tensors.

4.2 Setting up the problem

4.2.1 Single Shockwave Solution

We choose light cone coordinates for the longitudinal direction as these are the most natural for the problem at hand. They are defined by

$$x^\mu = (x^+, x^-, x^1, x^2) \qquad x^\pm = \frac{x^0 \pm x^3}{\sqrt{2}} \tag{4.2.1}$$

where x^0 is the time axis and x^1, x^2, x^3 cover $\mathbb{R}^3$. We use the mostly plus convention for the metric and we raise and lower indices with the flat metric $\eta^{\mu\nu}$.

In order to set up the problem, we begin by writing the metric of a black hole which is boosted to the speed of light along the x^3 direction. This metric, the Aichelburg-Sexl solution [1], has the form

$$ds^2 = g_{\mu\nu} dx^\mu dx^\nu = -2dx^+ \, dx^- + t_1(x^+, x^1, x^2) dx^{+\,2} + dx_\perp^2 \tag{4.2.2}$$

where

$$t_1 = -4\sqrt{2} EG\delta(x^+) \log(pr) \,, \quad \vec{r} = (x^1, x^2) \,, \quad r = \sqrt{(x^1)^2 + (x^2)^2}. \tag{4.2.3}$$

The transverse part of the metric is flat, $dx_\perp^2 = (dx^1)^2 + (dx^2)^2$, while $\delta(x^+)$ is the Dirac delta function, E is the energy of the shockwave, G is the four-dimensional Newton's constant and p serves as an IR cutoff as explained in [1] and in section 4.3.3 below. The ansatz (4.2.2) reduces the generally non-linear field equations to a single linear equation. To see this we write Einstein's equations with out a cosmological constant in the form

$$R_{\mu\nu} = \kappa^2 \left(T_{\mu\nu} - \frac{1}{2} g_{\mu\nu} T \right) T = T^\mu_\mu = T_{\mu\nu} \, g^{\mu\nu} \quad , \kappa^2 = 8\pi G \,, \tag{4.2.4}$$

where $R^{\mu\nu}$ is the Ricci tensor and $T_{\mu\nu}$ is the Energy momentum tensor.

Substituting the ansatz (4.2.2) in Einstein's equations yields

$$R_{\mu\nu} = \delta_{\mu +} \delta_{\nu +} \left(4\sqrt{2} \pi EG \delta(x^+) \delta^{(2)}(\vec{r}) \right). \tag{4.2.5}$$

The presence of Kroenecker's delta, $\delta_{\nu +}$, shows that the only non zero component of the Ricci tensor is R_{++}. The T_{++} component on the right hand side of previous equation corresponds to a massless point-like particle moving along $x^+ = 0$ and so with the speed of light and, it is normalized such that the particle has energy E (see also (4.2.8)). Then t_1 of (4.2.2) is specified by solving the linear differential equation,

$$R_{++} = -\frac{1}{2} \nabla_\perp^2 t_1(x^+, x^1, x^2) = \kappa^2 T_{++} = 4\sqrt{2} \pi EG \delta(x^+) \delta^{(2)}(\vec{r}) \tag{4.2.6}$$

where $\nabla_\perp^2$ is the Laplace operator in two dimensions. Making use of

$$\nabla_\perp^2 \log(kr) = 2\pi \delta^{(2)}(\vec{r}) \tag{4.2.7}$$

one verifies that t_1 is given by equation (4.2.3).

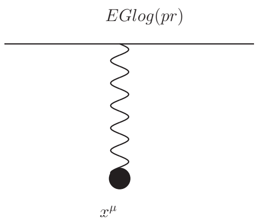

Figure 4.1: A pictorial description of the shockwave solution, that is an exact solution to Einstein's equation. The bulk source, represented by the straight line, emits a graviton, represented by the curly line, with a coupling constant $EG\log(pr)$. The filed is measured at the point x^μ.

In the next section we collide two such shockwaves with an impact parameter, b. We thus shift the origin along the x^1 axis and the stress-energy tensor is given by

$$T^{(1)}_{\mu\nu} = \frac{\sqrt{2}}{2}\delta_{\mu+}\delta_{\nu+}\left(E\delta(x^+)\delta(x^1 - b)\delta(x^2)\right). \tag{4.2.8}$$

The energy momentum tensor here describes a massless shockwave traveling at the speed of light along the x^- direction. One can check that this energy momentum tensor is covariantly conserved. We note that this quantity, as mentioned, has been normalized so as to satisfy $\int T_{++}d^3x = E$.

Figure 4.1 represents diagrammatically the configuration. It shows the gravitational field produced by a single graviton emission from the energy-momentum tensor of (4.2.8) with an effective coupling $EG\log(pr)$. The gravitational field is measured at the space-time point x^μ. The sketch provides a suggestive diagrammatic expression for the metric of equation (4.2.2).

4.2.2 Superimposing two Shockwaves

We assume that the background is a flat space-time with two shockwaves, t_1 and t_2 propagating in it.

In the language of the order counting, the background metric is described by terms of zeroth (flat piece of the metric) and of first order (the non interacting shocks) in the sources t_1 and t_2. The perturbations around this background, are considered second order in the sources and hence they involve products of t_1t_2. The next orders in this expansion, which we will not compute, have the form $t_1^2t_2$ and $t_1t_2^2$ etc.

Our calculation is an expansion under the energy E [1]. We use the superscripts $^{(n)}$ on the quantities $A^{(n)}$ to denote the n'th order of quantity A in the given expansion.

[1] Essentially the relevant dimensionless expansion parameter is $\frac{EG}{b}$ as section 4.8 suggests.

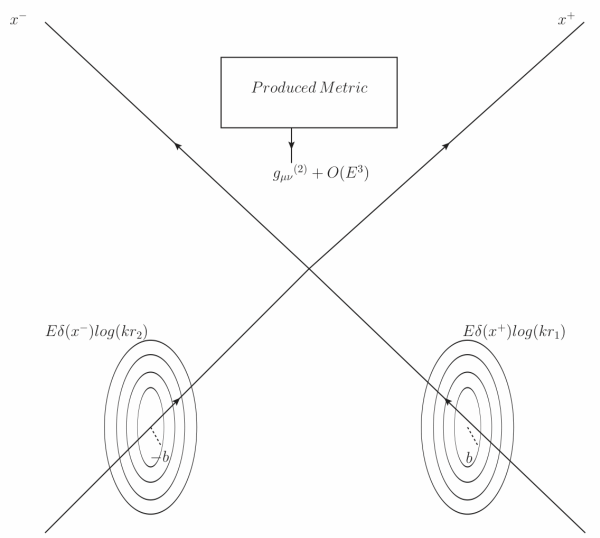

Figure 4.2: Presentation of the two shockwaves moving along the $x^{\pm}$ axis. Below the origin, time is negative and refers to pre-collision times. After the collision, the two shockwaves interact and produce a gravitational field in the forward light cone, described by the metric $g^{(2)}_{\mu\nu}$.

It is evident that essentially this corresponds to the number of times the source t_i $(i = 1, 2)$ is inserted as a (right hand side) source for the propagator corresponding to the d'Alembert operator (see for example equation (4.6.2)).

In what follows we collide two such shockwaves moving at the speed of light towards each other with an impact parameter, b. After the collision we will compute their trajectories taking into account the back-reaction of the metric. The problem is treated classically. We must add to the energy momentum tensor of (4.2.8) a second part, describing the second shockwave,

$$T^{(1)}_{--} = \frac{\sqrt{2}E}{2}\delta(x^-)\,\delta(x^1+b)\delta(x^2). \tag{4.2.9}$$

This collision is captured by fig. 4.2, where the two shockwaves are shown before the collision. Following [29; 30], the metric that describes the process should look like

$$\begin{aligned} ds^2 &= -2\,dx^+\,dx^- + dx_\perp^2 + t_1^{(1)}(x^+, x^1-b, x^2)\,dx^{+\,2} + t_2^{(1)}(x^-, x^1+b, x^2)\,dx^{-\,2} \\ &\quad + \theta(x^+)\theta(x^-)g^{(2)}_{\mu\nu}(x^\kappa, z)dx^\mu dx^\nu + \ldots, \\ t^{(1)}_{1,2}&(x^{\pm}, x^1 \mp b, x^2) = -4\sqrt{2}EG\log\left(k\sqrt{(x^1\mp b)^2+(x^2)^2}\right)\delta(x^{\pm}). \end{aligned} \tag{4.2.10}$$

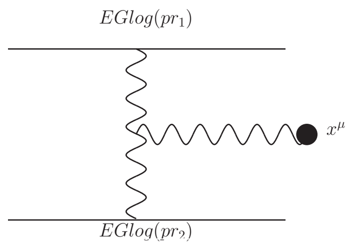

Figure 4.3: Schematic representation of the E^2 corrections to the metric. Along with the diagrams of figure 4.5, the present diagram consists of the first non-trivial correction to the metric (4.2.10). The interaction of the metrics produced by each of the shockwaves is shown at the point of intersection of the graviton propagators while the gravitational field is measured at the space-time point x^μ.

A few explanations are in order: (a) The first two terms of this metric describe a flat Minkowski spacetime. The next two terms describe the two point particles that are moving on a collision course at the speed of light along the x^3 coordinate, with an impact parameter of $2b$, as shown in figure 4.4. These terms are of first order in E, since they describe the two shockwaves and not their interactions so far. Each of them is schematically described as a vertex diagram, shown in figure 4.1. One can check that the metric, in this ansatz, satisfies the de Donder gauge up to first order in our counting. (b) The next term, $g^{(2)}_{\mu\nu}$, is of second order in E (as we will see, it appears as a product of $t_1 t_2$) and describes the interactions of the two pre-collision metrics. Essentially this term represents the superposition of the two vertices (as in figure 4.3) and only exists for times after the collision, a fact that is highlighted by the Heaviside theta function in (4.2.10). This is a consequence of retardation. For times before the collision where these corrections are zero, the remaining metric of the two shocks is an exact solution of the Einstein equations. (c) Our main result is the computation of the term that is quadratic in E, namely $g^{(2)}_{\mu\nu}$ which is presented schematically in fig. 4.3 and 4.5. (d) One might worry that in these coordinates the geodesics are discontinuous. As we will see in what follows, our approach applies for any profile of the shocks along $x^\pm$ and not only for $\delta(x^\pm)$ profiles. Hence, we implicitly assume that we deal with regularized smooth functions[1].

[1] In any case, the physics should not depend on the coordinate system.

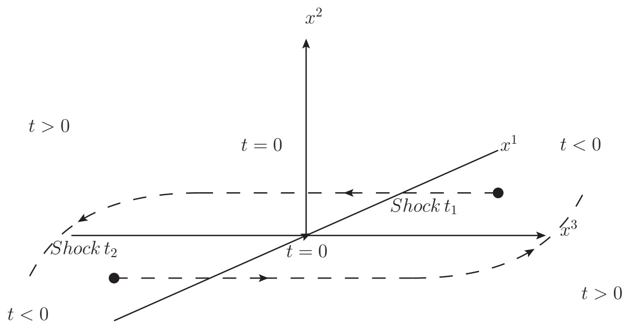

Figure 4.4: The two shockwaves, represented as black dots, move on the trajectories shown by the dashed lines. Before the collision, they move along straight lines while after the collision, occurring at at t=0, their trajectories are modified and follow what is pictorially shown as a curved path. This results to a change in the $T_{\mu\nu}$.

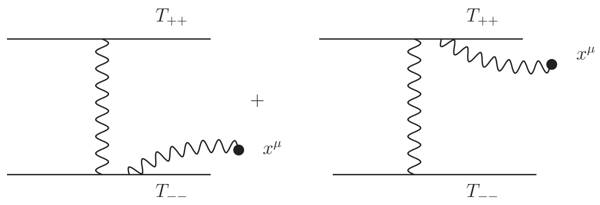

Figure 4.5: The diagrams representing the backreactions. The emission of gravitons, curly lines, due to the self corrections to $T_{\mu\nu}$ are shown. Each shockwave moves in the gravitational field produced by the other. The gravitational field is measured at the point x^μ.

4.3 Back-Reactions

4.3.1 Corrections to $T_{\mu\nu}$ and Geodesics

The energy momentum tensor of equation (4.2.8), $T^{(1)}_{++}$, is conserved in the metric described by equations (4.2.2) and (4.2.3). In fact, it is also conserved to all orders in E, even though in practice only terms linear in E will appear in the equations. This has an intuitive explanation in the context of figure 4.1. Gravity is linear in view of the metric (4.2.2) and the following equation

$$\nabla^\mu T_{\mu\nu} = 0 \tag{4.3.1}$$

is true to all orders.

It is also true that the combined energy momentum tensors $T^{(1)}_{++}$ and $T^{(1)}_{--}$ are conserved in the gravitational field of (4.2.10), when considering up to linear terms in E.

This is an exact result for negative times. Once quadratic terms are considered, i.e. at positive times, the metric needs to be corrected, because the trajectory of the particles responsible for the shockwaves is altered due to their mutual interaction. In figure 4.4 we show the trajectories of the two colliding shockwaves, while in figure 4.5 we show the self-corrections of the two energy momentum tensors. This occurs because for positive times each shockwave is moving in the gravitational field produced by the other. As a cross check the total energy-momentum tensor needs to be conserved up to the given order in E of the expansion.

4.3.2 Calculating the Corrections for $T_{\mu\nu}$

The two shockwaves are massless and are thus light-like. Papapetrou, [31], has rigorously proven that for particles moving on null geodesics, the energy momentum tensor conservation is guaranteed. The energy momentum tensor is a sum of point-like stress-tensors (particles) and is given by

$$T^{\mu\nu} = \frac{\pi E G}{\kappa^2} \sum_{(I=1)}^{2} \dot{x}^{\mu}_{(I)} \dot{x}^{\nu}_{(I)} \frac{1}{\sqrt{-g}} \delta^{(3)} \left(\vec{x}_{(I)} - \vec{x}_{(I)}(s_{(I)})\right). \tag{4.3.2}$$

The particle I $(I = 1, 2)$ entering (4.3.2) moves along the trajectory $\vec{x}_{(I)}(s_{(I)})$, where the trajectory has been parametrized by the variable $s_{(I)}$. The quantity $\sqrt{-g}$ refers to the determinant of the total metric. The dots denote differentiation with respect to the variable $s(I)$. The detailed calculation of the back-reaction was presented in detail in [26]. Here we will only outline the method and quote the result.

This is a two step process. In step (i) one should find the corrections to the geodesics of the one particle in the gravitational field of the other. In practice, the perturbative solution to the equations

$$\ddot{x}^{\mu}_{I} + \Gamma^{\mu}_{J;\nu\rho} \dot{x}^{\nu}_{I} \dot{x}^{\rho}_{I} = 0 \qquad I, J = 1, 2 \qquad I \neq J \tag{4.3.3}$$

is required. These are interpreted as the motion of particle I in the gravitational field of the particle J (due to $\Gamma^{\mu}_{J;\nu\rho}$ where Γ are the Christoffel symbols) and vice versa; this is precisely the meaning of the subscripts I and J. Step (ii) makes use of the result of step (i) by substituting the corrections of the initial trajectories x^{μ} from (4.3.3) inside (4.3.2). Expanding all the functions to the order that is consistent with the perturbation yields the result.

Second order corrections to the total $T_{\mu\nu}$

We present here the quadratic (in E) corrections to the total energy momentum tensor:

$$(T_{+-})^{(2)} = -(T^{+-})^{(2)} = \frac{1}{4}\frac{1}{\kappa^2}\left(t_2\nabla_\perp^2 t_1 + t_1\nabla_\perp^2 t_2\right) , \tag{4.3.4a}$$

$$(T_{++})^{(2)} = \frac{1}{4}\frac{1}{\kappa^2}\int dx^-\left(t_2\nabla_\perp^2 t_{1,x^+} + \nabla_\perp^2 t_{1,x^1}\int dx^- t_{2,x^1} + \nabla_\perp^2 t_{1,x^2}\int dx^- t_{2,x^2}\right), \tag{4.3.4b}$$

$$(T_{--})^{(2)} = \frac{1}{4}\frac{1}{\kappa^2}\int dx^+\left(t_1\nabla_\perp^2 t_{2,x^-} + \nabla_\perp^2 t_{2,x^2}\int dx^+ t_{1,x^2} + \nabla_\perp^2 t_{2,x^1}\int dx^+ t_{1,x^1}\right), \tag{4.3.4c}$$

$$(T_{+1})^{(2)} = \frac{1}{4}\frac{1}{\kappa^2}\nabla_\perp^2 t_1\int dx^- t_{2,x^1} \quad , \qquad (T_{-1})^{(2)} = \frac{1}{4}\frac{1}{\kappa^2}\nabla_\perp^2 t_2\int dx^+ t_{1,x^1} , \tag{4.3.4d}$$

$$(T_{+2})^{(2)} = \frac{1}{4}\frac{1}{\kappa^2}\nabla_\perp^2 t_1\int dx^- t_{2,x^2} \quad , \qquad (T_{-2})^{(2)} = \frac{1}{4}\frac{1}{\kappa^2}\nabla_\perp^2 t_2\int dx^+ t_{1,x^2} , \tag{4.3.4e}$$

$$(T_{11})^{(2)} = (T_{22})^{(2)} = (T_{12})^{(2)} = 0. \tag{4.3.4f}$$

It will prove to be useful to rewrite the first order energy momentum tensors of (4.2.8) and (4.2.9) using (4.2.7) yielding

$$T_{++}^{(1)} = \frac{1}{2\kappa^2}\nabla_\perp^2 t_1, \qquad T_{--}^{(1)} = \frac{1}{2\kappa^2}\nabla_\perp^2 t_2. \tag{4.3.5}$$

The expressions that will be most useful for the following analysis will be the compact expressions of equations (4.3.4). Nevertheless we also wish to show, for completeness, the energy momentum tensor explicitly in terms of the coordinates. Defining

$$\vec{r_1} = \vec{r} - \vec{b_1} \qquad \vec{r_2} = \vec{r} - \vec{b_2}. \tag{4.3.6}$$

and substituting (4.2.7) in (4.3.4) we obtain

$$(T_{+-})^{(2)} = \frac{16\pi E^2 G^2}{\kappa^2}\log(2p|b|)\delta(x^+)\delta(x^-)\times\left(\delta^{(2)}(\vec{r_1}) + \delta^{(2)}(\vec{r_2})\right) \tag{4.3.7a}$$

$$(T_{++})^{(2)} = \frac{16\pi E^2 G^2}{\kappa^2}\theta(x^-)\Bigg[\log(2p|b|)\delta'(x^+)\delta^{(2)}(\vec{r_1}) + \frac{x^-}{x^1+b}\delta(x^+)\delta'(x^1-b)\delta(x^2)$$
$$+ \frac{x^- x^2}{4b^2+(x^2)^2}\delta(x^+)\delta(x^1-b)\delta'(x^2)\Bigg] \tag{4.3.7b}$$

$$(T_{+1})^{(2)} = \frac{8\pi E^2 G^2}{\kappa^2|b|}\theta(x^-)\delta(x^+)\delta^{(2)}(\vec{r_1}) \tag{4.3.7c}$$

$$(T_{+2})^{(2)} = 0. \tag{4.3.7d}$$

The asymmetry between $T_{+1}^{(2)}$ and $T_{+2}^{(2)}$ is due to the fact that the impact parameter $\vec{b}$ has only an x^1 component by assumption. The other components of the energy momentum tensor are completely symmetric and are trivially obtained by exchanging simultaneously $+\leftrightarrow-$ and $b\leftrightarrow -b$ respectively.

The important feature of (4.3.4) is that all the corrections for $T_{\mu\nu}$ involve either a product of three delta and one theta functions or a product of four delta functions. This implies that equation (4.3.7) provides localized corrections that either apply only in the forward light cone or corrections that apply only at one point and only at one instant. Essentially this expresses the fact that the geodesics are discontinuous and as a result $T_{\mu\nu}$ experiences sudden changes as is to be expected. Using regularized functions would smooth out the underlying sudden "kicks" and it would introduce a finite interaction time.

4.3.3 Region of validity and the physical meaning of the IR cut-off

I. $b \to \infty$: One would expect that in this limit the particles would not interact. However, the single shock metric behaves as $\log(pr)$ (see (4.2.2) and (4.2.3)) where p is an IR cut-off resulting from the Aichelburg- Sexl ultrarelativistic boost[1]. Such a logarithmically large field at large distances away from the source creating it implies that a second source located very far from the first one, will feel that large field and vice versa[2]. This is clearly problematic. Therefore, combining this and the fact that p is an IR cut-off, we argue that the metric (4.2.2) and as a consequence the metric (4.2.10) makes sense for distances less than $\sim 1/p$. Thus, trusting the solution up to transverse distances of the order of $1/p$ we deduce that large b implies $pb \sim 1$ in which case $T^{(2)}_{\mu\nu} \to 0$ as should. On the other hand, the current set-up may be treated perturbatively when the inequality $EG/b \ll 1$ is valid (see section 4.8). This inequality can apply simultaneously with the inequality $b \ll 1/p$. Hence, our set-up is justified when

$$EG \ll b \ll 1/p \equiv r_{IR} \text{ and } r \in (0, 1/p). \tag{4.3.8}$$

We will see this necessity of placing an IR cut-off in more detail in section 4.8. It will become evident that in higher dimensions such a cut-off is not required and that this is an artifact of 4-dimensions.

Equation (4.3.7) suggests that there is another kinematical restriction for the applicability of our perturbative treatment. In particular the $T^{(2)}_{\pm\pm}$ components grow for large $x^{\pm}$. Obviously, we should expect that the corrections to $T_{\mu\nu}$ could not grow infinite

[1] Where in one of the intermediate steps of this large boost one has to integrate $1/\sqrt{r^2 + x_3^3}$ along the boost, that is along x_3, from $-\infty$ to $+\infty$. This obviously diverges logarithmically and an IR cut-off is placed at large $x_3 = 1/p$.

[2] Such an ambiguity arises as a result of the superposition of the two colliding metrics. One can check that the Riemann tensor of the single shock tends to zero as $r \to 0$. However, once the two metrics of the two shocks are superimposed, in the forward light-cone, this is no longer the case.

with time. Hence, restricting the expansion to lower orders is consistent if we restrict the kinematical region where we trust our result, that is from $x^{\pm} = -\infty$ up to $x^{\pm} \sim EG$.

Therefore, our expansion is an early times expansion close to the collision point $x^3 = 0$. It is expected that higher graviton exchanges, than those appearing in fig. 4.3 and 4.5, will unitarize the corrections to $T_{\mu\nu}$ as $x^{\pm} \to \infty$. In fact, the same restrictions on $x^{\pm}$ apply according to earlier works in the literature about gravitational-wave collisions in AdS_5 backgrounds [29; 30]. There, the set-up is similar to the one of this work. In fact, through resummations of multiple graviton exchanges in [29] , it is found that the shocks eventually will decay at large $x^{\pm}$ at times scales set by the energy of the shocks. Furthermore, it is found that the same time scale where the shocks stop sets also the thermalization time [32][1] . By the same analogy, one would expect that a similar result would apply here. That at times of the order of EG the remaining shocks that continue to move on the light-cone will be completely wiped out while a black hole will be formed[2]. Certainly, the final word on the metric evolution belongs to the numerical relativity community.

II. $b \to 0$: It seems that $T^{(2)}_{\mu\nu}$ diverges. As we will see, this is one of the many manifestations of the same fact: the problematic behaviour of the perturbative treatment in this limit.

4.4 Conservation, Tracelessness and Field Equations

We have so far computed the energy momentum tensor up to second order in E. Calculating the divergence of $T_{\mu\nu}$ up to second order in E, one finds

$$\begin{aligned}\Big((\nabla^{\mu})^{(0)} + (\nabla^{\mu})^{(1)}\Big)\Big((T_{\mu\nu})^{(1)} + (T_{\mu\nu})^{(2)}\Big) &= \delta_{\pm\nu}\nabla_{\perp}^2 t_1 \nabla_{\perp}^2 t_2 + O(E^3)\\ &\sim \delta_{\pm\nu}\delta^{(2)}(r)\delta^{(2)}(b)\delta(x^+)\delta(x^-) + O(E^3).\end{aligned} \tag{4.4.1}$$

The operator ∇ denotes the covariant derivative. In arriving to the second line of (4.4.1) it is not necessary to substitute the precise profiles of t_1 and t_2. Hence, this suggests that (4.3.4) has a rather general applicability. On the other hand, in arriving to the third line of (4.4.1), which shows conservation for non-zero impact parameter b, we had to use equation (4.2.7). We thus conclude that equation (4.3.4) is consistent

[1] Where thermalization time is estimated as $\sim E^{1/3}$ for these AdS_5 backgrounds.

[2] In this part of the discussion we assume assume $b \ll EG$ in which case the problem can only be studied numerically unless some resummations techniques, along the lines of [29], can be engineered.

with conservation and hence correct, for any longitudinal profile[1] provided that their transverse profile is localized and separated. To this end, one could argue that for zero impact parameter there exists an instantaneous violation of the conservation of $T_{\mu\nu}$ and hence of the Bianchi identities at the point $x^1 = x^2 = x^+ = x^- = 0$. However, on one hand, according to section 4.8, our perturbative treatment breaks down when $b = 0$ and on the other hand, as we know from [11], a black hole will be formed and the violation will be hidden behind the horizon.

One could imagine smoothening out the transverse distribution of the stress tensor of the initial point-like particles. For instance, one could use Gaussians instead of delta functions. Then at a first glance, the right hand side of equation (4.4.1) seems to be a product of Gaussians implying an instantaneous but non-localized violation of conservation. This would raise doubts about the validity of our calculation[2]. However, our present derivation for the corrections due to back reactions of $T^{(2)}_{\mu\nu}$ given by equation (4.3.4), is based on equation (4.3.2) which explicitly assumes point-like sources. In other words (4.3.4) is not applicable for extended sources and the derivation in such a case needs to be modified. Therefore, it is not a surprise that equation (4.3.4) for extended sources would invalidate conservation everywhere in space-time. Certainly, considering extended sources is an interesting generalization which we postpone for a future investigation. To this end, in section 4.10 we show, using a trapped surface criterion, that when the transverse distribution is dilute enough, a black-hole can not be formed [28]. This implies that under some circumstances, a horizon will not be formed and hence the non-local violation of conservation will not be hidden. Evidently, this is another indication that equation (4.3.4), despite its invariant-looking form, needs to be modified for extended sources along the transverse directions.

Calculating the trace of the stress-tensor to second order yields

$$T = g^{\mu\nu}T_{\mu\nu} = (g^{\mu\nu})^{(1)}(T_{\mu\nu})^{(1)} + (g^{\mu\nu})^{(0)}(T_{\mu\nu})^{(2)} = O\left(E^3\right) \tag{4.4.2}$$

up to quadratic order in E. This simplifies Einstein's equations as follows

$$R_{\mu\nu} = \kappa^2 T_{\mu\nu} + O(E^3) \qquad \kappa^2 = 8\pi G. \tag{4.4.3}$$

Equation (4.4.2) shows that the stress-tensor due to the "cross-talk" between the stress-tensor corresponding to the shock t_1 and the stress-tensor corresponding to the shock t_2, is precisely cancelled by the corrections due to the back-reaction contribution. As a result, we started with an energy momentum tensor that was traceless for negative

[1] Of $T_{\mu\nu}$ of the initial particles as a function of x^+ and x^-; not just for the $\delta(x^\pm)$ profiles.

[2] We thank S. Gubser and G. Horowitz for related discussions.

times and found that, up to second order, it is also traceless for positive times. This suggests that the energy momentum tensor could be traceless to all orders and all times, implying a conservation of tracelessness conjecture. This is worth investigating further.

4.5 Field Equations

4.5.1 Field Equations to $O(E^2)$

We now proceed to explicitly construct the field equations of (4.4.3) up to second order. The zeroth order terms satisfy the Einstein equations trivially since $R^{(0)}_{\mu\nu} = T^{(0)}_{\mu\nu} = 0$. The first order terms $R^{(1)}_{\mu\nu}$ from equation (4.2.10) satisfy the field equations with a right hand side given by $T^{(1)}_{\mu\nu}$, equations (4.2.8) and (4.2.9). Hence, we only require the second order terms to satisfy

$$R^{(2)}_{\mu\nu} = \kappa^2 T^{(2)}_{\mu\nu} \tag{4.5.1}$$

where the second order energy momentum tensor, $T^{(2)}_{\mu\nu}$, is given by (4.3.4) and it corresponds to the diagram of figure 4.5. We split the second order Ricci tensor in two parts. First, a known part that is due to the two shockwaves and is a product of the two vertices (see figure 4.1) of t_1 and t_2. We will use the notation $-S_{\mu\nu}$ for this part and it corresponds to the diagram of figure 4.3. The second part comes from the quadratic terms in E of the metric, $g^{(2)}_{\mu\nu}$ and we will use the notation $(R^{(2)}_{\mu\nu})_g$. We now proceed to expand (4.5.1) up to quadratic order in E thus obtaining

$$(R^{(2)}_{\mu\nu})_g - S^{(2)}_{\mu\nu} = \kappa^2 T^{(2)}_{\mu\nu}. \tag{4.5.2}$$

A more suggestive way of writing this expression is

$$(R^{(2)}_{\mu\nu})_g = \kappa^2 T^{(2)}_{\mu\nu} + S^{(2)}_{\mu\nu} \ , \tag{4.5.3}$$

where $S^{(2)}_{\mu\nu}$ is considered to be an effective energy momentum tensor, contributing to the total one. All terms in the right hand side of this equation are known. To simplify the notation we will be suppressing the superscripts denoting the order of the terms. We will restore them wherever it is necessary.

4.6 Choosing the Gauge and Field Equations

In this section we specify the gauge choice and present the field equations including the back-reacted contribution found in section 4.3.2. Working in the harmonic (de Donder) gauge

$$g_{\mu\nu},^{\mu} - \frac{1}{2} g^{\mu}{}_{\mu,\nu} = 0 \tag{4.6.1}$$

the Einstein's equations (4.5.3) in component form read

$$(++) \quad \Box g_{++} = -\frac{1}{2}\int dx^- \left(t_2 \nabla_\perp^2 t_{1,x^+} + \nabla_\perp^2 t_{1,x^1} \int dx^- t_{2,x^1} + \nabla_\perp^2 t_{1,x^2} \int dx^- t_{2,x^2} \right), \tag{4.6.2a}$$

$$(+-) \quad \Box g_{+-} = -\frac{1}{2}\left(t_2 \nabla_\perp^2 t_1 + t_2 \nabla_\perp^2 t_1 \right) - t_{1,x^1} t_{2,x^1} - t_{1,x^2} t_{2,x^2} + \frac{1}{2} t_{1,x^+} t_{2,x^-}\,, \tag{4.6.2b}$$

$$(+1) \quad \Box g_{+1} = -\frac{1}{2}\nabla_\perp^2 t_1 \int dx^- t_{2,x^1} + \frac{1}{2} t_{1,x^+} t_{2,x^1}, \tag{4.6.2c}$$

$$(11) \quad \Box g_{11} = t_{1,x^1} t_{2,x^1} + t_{1,x^1x^1} t_2 + t_1 t_{2,x^1x^1} = 0, \tag{4.6.2d}$$

$$(12) \quad \Box g_{12} = \frac{1}{2} t_{2,x^2} t_{1,x^1} + \frac{1}{2} t_{1,x^2} t_{2,x^1} + t_2 t_{1,x^1x^2} + t_1 t_{2,x^1x^2} = 0. \tag{4.6.2e}$$

The integration limits have been suppressed, as will be done in the rest of this chapter. For instance $\int t_{2,x^1} dx^+$ implies $\int_{-\infty}^{x^+} \partial_1 t_2(x'^+, x^1, x^2) dx'^+$ etc. The operator $\Box$ denotes the d'Alembert operator in flat space-time, i.e.

$$\Box \equiv \eta^{\mu\nu}\partial_\mu \partial_\nu = -2\partial_{x^+}\partial_{x^-} + \nabla_\perp^2. \tag{4.6.3}$$

In order to obtain equation (4.6.2), equation (4.3.4) was employed. We now have a set of differential equations, equations (4.6.2), which, we will proceed to solve in the next section utilizing the appropriate boundary conditions.

4.7 Solving the Field Equations and Causality

4.7.1 Green's Function and Boundary Conditions

We look for causal solutions of (4.6.2). The d'Alembert operator has a known retarded Green's function in light-cone coordinates

$$G(x^\mu - x'^\mu) = -\frac{1}{4\pi} \frac{\theta(x^+ - x'^+)\theta(x^- - x'^-)}{\frac{1}{\sqrt{2}}\left((x^+ - x'^+) + (x^- - x'^-)\right)} \times \delta\left(\sqrt{2(x^+ - x'^+)(x^- - x'^-)} - |\vec{r} - \vec{r}'| \right)\,, \tag{4.7.1}$$

where $\vec{r} = (x^1, x^2)$ as defined in (4.2.3), θ is the Heaviside theta function. The Green's function satisfies

$$\Box G(x^\mu - x'^\mu) = \delta(x^+ - x'^+)\delta(x^- - x'^-)\delta^{(2)}(\vec{r} - \vec{r}'). \tag{4.7.2}$$

4.7.2 Integrations

As usual, we integrate the product of the right hand side of (4.6.2), which plays the role of the source with (4.7.1) over all space-time. It will be useful to define the following vectors

$$\vec{b_1} = (b_{11}, b_{12}) \qquad \vec{b_2} = (b_{21}, b_{22}). \tag{4.7.3}$$

In the right hand side of (4.6.2) terms of the form $\partial_{x^i{}_a}(t_1t_2)$ and $\partial^2_{x^i{}_a x^j{}_c}(t_1t_2)$ appear. The subscript (a) refers to the source (taking the value 1 or 2) and the superscripts refer to the transverse coordinate (i) with respect to which the source is being differentiated (also taking values 1 and 2). It is simpler to exchange the differentiations over the spatial coordinates $x_{1,2}$ with derivatives over the vectors $b_{1,2}$, $\partial_{x^i_a} \to -\partial_{b_{ai}}$. At the end of the calculation the limits

$$\vec{b_1} \to (b, 0) \qquad \vec{b_2} \to (-b, 0) \tag{4.7.4}$$

must be taken.

Equations (4.6.2a)-(4.6.2e) involve the product t_1t_2 differentiated with respect to the transverse coordinates. We have already exchanged these differentiations with derivatives with respect to b's. As a result, one can verify that the transverse convolution of the sources with the Green's function, involves the following integral

$$\begin{aligned}\mathcal{J}(r_1, r_2, \tau) = \frac{1}{2\pi\tau}\int_0^\infty \int_0^{2\pi} r' dr' d\phi' \delta(\tau - r') \log(p|\vec{r'} + \vec{r_1}|) \log(p|\vec{r'} + \vec{r_2}|) \\ = \int \frac{d^2q d^2 l}{(2\pi)^2} \frac{e^{i\vec{q}\vec{r_1}} e^{i\vec{l}\vec{r_2}}}{q^2 l^2} J_0\left(\tau|\vec{l} + \vec{q}|\right)\end{aligned} \tag{4.7.5}$$

where we have introduced a new parameter, the proper time τ, defined as $\tau = \sqrt{2x^+x^-}$. The second equality comes from expanding the logarithms in Fourier space and performing the spatial integrations. Both of the momentum integrations have been performed in [26] and the result reads

$$\begin{aligned}\mathcal{J}(r_1, r_2, \tau) = \theta(r_1 - \tau)\theta(r_2 - \tau)\mathcal{J}_1(r_1, r_2, \tau) + \theta(\tau - r_2)\theta(r_1 - \tau)\mathcal{J}_2(r_1, r_2, \tau) \\ + \theta(\tau - r_1)\theta(r_2 - \tau)\mathcal{J}_3(r_1, r_2, \tau) + \theta(\tau - r_1)\theta(\tau - r_1)\mathcal{J}_4(r_1, r_2, \tau)\end{aligned} \tag{4.7.6}$$

where the $\mathcal{J}$'s are defined with the help of table 4.1 and the expression

$$\mathcal{J}(\tau, r_1, r_2) \equiv \ln(\xi_> k)\ln(\eta_> k) + \frac{1}{4}\left[Li_2\left(e^{i\alpha}\frac{\xi_<\eta_<}{\xi_>\eta_>}\right) + Li_2\left(e^{-i\alpha}\frac{\xi_<\eta_<}{\xi_>\eta_>}\right)\right], \tag{4.7.7a}$$

$$\xi_{>(<)} = max(min)(r_1, \tau) \quad \eta_{>(<)} = max(min)(r_2, \tau), \tag{4.7.7b}$$

$$\vec{r_1}.\vec{r_2} = r_1 r_2 \cos\alpha. \tag{4.7.7c}$$

Table 4.1: We defined $\vec{r}_{1,2} = \vec{r} - \vec{b}_{1,2}$

cases	$\xi_>$	$\eta_>$	$\xi_>\eta_>$	$\xi_<\eta_<$	$\mathcal{J}_i$	region (see figure 4.6)
1	r_1	r_2	$r_1 r_2$	τ^2	$\mathcal{J}_1$	I
2	r_1	τ	τr_1	τr_2	$\mathcal{J}_2$	II′
3	τ	r_2	τr_2	τr_1	$\mathcal{J}_3$	II
4	τ	τ	τ^2	$r_1 r_2$	$\mathcal{J}_4$	III

We denote the angle between $\vec{r}_1$ and $\vec{r}_2$ with α while Li_2 is the dilogarithm function. Notice that $\mathcal{J}$ is real as expected.

The value of $\mathcal{J}$ appears to depend on the ordering of r_1, r_2 and τ. There are six independent ways of ordering the three variables. One may observe that when $r_1, r_2 > \tau$ or/and $r_1, r_2 < \tau$ applies yields the same value for J regardless of the ordering of r_1 and r_2. This reduces the total number of independent orderings to four which are summarized in table 4.1 [1]. In particular, in the $b = 0$ limit there exist only two orderings $\tau > r$ and $\tau < r$ suggesting a $\tau \leftrightarrow r$ symmetry[2].

The integrations over $x^\pm$ are trivial since they involve Dirac delta functions. We now present all the components of the metric, and refer the reader to [26] for the details of the calculation.

The Formula for $g^{(2)}_{\mu\nu}$

Using the compact notation $\lim_{\vec{b}_{1,2}\to(\pm b,0)} \equiv \lim_{\vec{b}_2\to(-b,0)} \lim_{\vec{b}_1\to(b,0)}$ we finally have

$$g^{(2)}_{++} = \lim_{\vec{b}_{1,2}\to(\pm b,0)} \left\{ \frac{32}{\sqrt{2}} E^2 G^2 \theta(x^+)\theta(x^-) \left\{ \log\left(k|\vec{b}_2 - \vec{b}_1|\right) \partial_{x^+} \left(\frac{r_1}{r_1^2 + 2(x^\pm)^2} \theta(\tau - r_1) \right) \right.\right.$$
$$\left.\left. + \frac{1}{2x^+} \left[\frac{b_{11} - b_{21}}{|\vec{b}_2 - \vec{b}_1|^2} \theta(\tau - r_1) \partial_{x^1} \left(r_1 \frac{\tau^2 - r_1^2}{r_1^2 + 2(x^+)^2} \right) + (1 \leftrightarrow 2) \right] \right\} \right\}, \tag{4.7.8a}$$

$$g^{(2)}_{+-} = \lim_{\vec{b}_{1,2}\to(\pm b,0)} \left\{ 16 E^2 G^2 \theta(x^+)\theta(x^-) \operatorname{sech}\eta \left\{ \frac{1}{2\tau} \log\left(k|\vec{b}_2 - \vec{b}_1|\right) \delta(\tau - r_1) \right.\right.$$
$$\left.\left. + \left[\partial^2_{b_{11} b_{21}} - \frac{1}{4} \left(\frac{1}{\tau^2} \operatorname{sech}^2 \eta + \frac{1}{8} \tau \partial_\tau \left(\frac{1}{\tau} \partial_\tau \right) \right) \right] \mathcal{J}(r_1, r_2, \tau) + \left(1 \leftrightarrow 2\right) \right\} \right\}, \tag{4.7.8b}$$

$$g^{(2)}_{+1} = \lim_{\vec{b}_{1,2}\to(\pm b,0)} \left\{ \frac{32}{\sqrt{2}} E^2 G^2 \theta(x^+)\theta(x^-) \left\{ \frac{b_{11} - b_{21}}{|\vec{b}_2 - \vec{b}_1|^2} \frac{r_1}{r_1^2 + 2(x^\pm)^2} \theta(\tau - r_1) \right.\right.$$

[1] $\mathcal{J}_2$ for example is $\mathcal{J}(\xi_>\eta_> = \tau r_1, \xi_<\eta_< = \tau r_2)$ where $\mathcal{J}(\xi_>\eta_>, \xi_<\eta_<)$ is given in equation (4.7.7).

[2] In this case where $b = 0$ all order terms are required for calculating some quantities such as the radiation (see section 4.8). However, the argument for the $\tau \leftrightarrow r$ symmetry still applies.

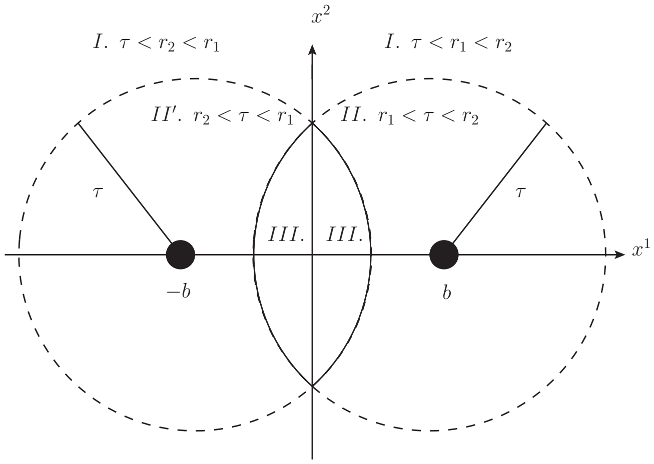

Figure 4.6: The metric after the collision on the transverse plane. The centres of the shocks are located at $x^1 = b$ and $x^1 = -b$. The two circles (dashed lines) have radius τ. At any given proper time τ, the metric evolves differently in the three regions I, II and III (there is an obvious $\mathbb{Z}_2$ symmetry under $x_1 \leftrightarrow -x_1$ for the other three regions). The evolution is determined according to equations (4.7.6), (4.7.7) and (4.7.8). Each region, determines whether the shocks have or have not enough proper time in order to propagate from the centers to the given region. For instance, region II defines the set of points where the shock with center at b has arrived but the shock with center at -b has not yet. Essentially, the evolution of the metric, according to this picture, is a manifestation of causality. In the $b = 0$ limit there is a $\tau \leftrightarrow r$ symmetry.

$$+\frac{1}{2}(\partial_{b_{21}})\left[\frac{1}{1+e^{\pm 2\eta}}\partial_\tau - \frac{1}{4\sqrt{2}\tau}\text{sech}^2\,\eta\right]\daleth(r_1,r_2,\tau)\Bigg\}\Bigg\}, \tag{4.7.8c}$$

$$g_{11}^{(2)} = \lim_{\vec{b}_{1,2}\to(\pm b,0)}\Bigg\{-16E^2G^2\theta(x^+)\theta(x^-)\text{sech}\,\eta\Big\{\partial^2_{b_{11}b_{21}} + \partial^2_{b_{11}b_{11}} + \partial^2_{b_{21}b_{21}}\Big\}\daleth(r_1,r_2,\tau)\Bigg\}, \tag{4.7.8d}$$

$$g_{12}^{(2)} = \lim_{\vec{b}_{1,2}\to(\pm b,0)}\Bigg\{-8E^2G^2\theta(x^+)\theta(x^-)\text{sech}\,\eta\Big\{\partial^2_{b_{22}b_{11}} + \partial^2_{b_{12}b_{21}} + 2\partial^2_{b_{11}b_{12}} + 2\partial^2_{b_{21}b_{22}}\Big\}\daleth(r_1,r_2,\tau)\Bigg\}. \tag{4.7.8e}$$

where

$$\tau = \sqrt{2x^+x^-}, \quad \eta = \frac{1}{2}\log\left(\frac{x^+}{x^-}\right) \text{ and } x^\pm = \frac{1}{\sqrt{2}}\tau e^{\pm\eta}. \tag{4.7.9}$$

It is remarked that the variables τ and η appearing in (4.7.8) should be thought as equal to their right hand side (see (4.7.9)) and not as a change of variables.

The reason for introducing the vector $\vec{b}_{1,2}$ should now be obvious. Apart from the simplification of the calculation, one can obtain the remaining components $g^{(2)}_{\mu 2}$ from $g^{(2)}_{\mu 1}$ by interchanging $1 \leftrightarrow 2$, before taking the limits of equation (4.7.4).

It is also simple to obtain the $(-\mu)$ components from the $(+\mu)$ components by exchanging $+ \leftrightarrow -$ and $\vec{b}_1 \leftrightarrow \vec{b}_2$. We have now computed entirely the metric up to quadratic order in E including back-reactions. This is the main result of our calculation.

In figure 4.6, we see a pictorial representation of the metric, described at the different regions, depending on the different values of the integral J (see (4.7.6)).

4.8 Bremsstrahlung Radiation

In section 4.3 we have computed the corrections to the stress-energy tensor of the two massless particles. This provides us the necessary information in order to compute the bremsstrahlung radiation. As in [12], one needs the polarization tensors and (the right hand side of) equations (4.6.2) in momentum space. Denoting with k the 4-momentum, the spectral-angular distribution then reads

$$\frac{dE_{rad}}{d\omega d\Omega} = \frac{G\omega^2}{2\pi^2}\sum_{pol}\left|J^{(2)}_{\mu\nu}\epsilon^{\mu\nu}(k)\right|^2 \quad , \quad J^{(2)}_{\mu\nu} \equiv T^{(2)}_{\mu\nu}(k) + S^{(2)}_{\mu\nu}(k)\,, \tag{4.8.1}$$

where $\omega \equiv \frac{k^+ + k^-}{\sqrt{2}}$ is the frequency and $\epsilon^{\mu\nu}(k)$ are the graviton polarization tensors. The polarization tensors are derived in section 4.11.

4.8.1 Estimating the radiated energy from dimensional analysis

In order to guess the dependence of the radiated energy from the impact parameter and the energy, we can use simple dimensional analysis.

The energy momentum tensor, $J_{\mu\nu}$, has dimensions of $[E]^4$, where $[E]$ denotes units of energy. Then the following is true

$$J^{(2)}_{\mu\nu}(x) \sim [E]^4 \sim E^2 G \frac{1}{[L]^4}. \tag{4.8.2}$$

where $[L]$ implies dimensions of length, while E is the energy of the shock. In the second proportionality we have used that $J^{(2)}_{\mu\nu}$ is of second order in E and first order in G, as explicitly shown in (4.3.7). The Fourier transformation of this quantity is

$$J^{(2)}_{\mu\nu}(k;b) \sim E^2 G f_{\mu\nu}(k;b)\,, \tag{4.8.3}$$

where $f_{\mu\nu}(k;b)$ is a set of dimensionless functions of k and the impact parameter, b, which is the only remaining length scale.

As a result of (4.8.1) the radiated energy behaves like

$$E^{(2)}_{rad} \sim G \int d\omega d\Omega \Big|\omega J_{\mu\nu}(k;b)\epsilon^{\mu\nu}(k)\Big|^2_{|\vec{k}|=\omega} \tag{4.8.4}$$

where the emitted radiation is taken on shell and thus must satisfy $|\vec{k}| = \omega$. Taking into account that the polarization tensors are dimensionless and performing the integrations, the emitted energy is completely determined by dimensional analysis. In particular, in the absence of any IR cut-offs we must formally have

$$E^{(2)}_{rad} \sim G \int d\omega d\Omega E^4 G^2 |\omega f(k;b)|^2_{|\vec{k}|=\omega} \sim \frac{E^4 G^3}{b^3}. \tag{4.8.5}$$

Therefore,

$$\frac{E^{(2)}_{rad}}{E} \sim \frac{E^3 G^3}{b^3}. \tag{4.8.6}$$

The question is whether the coefficient missing in (4.8.6) is finite. In particular, we would like to address the question where any possible divergences come from and whether there is a way to regulate them. We argue that the underlying coefficient is not well-defined in the absence of appropriate cut-offs and we will attempt to give an explanation.

The first step is to show that any rotationally symmetric physical shock-wave[1], grows as $\log(pr)$ at large $r = \sqrt{(x_1)^2 + (x_2)^2}$ where p is some transverse scale. Indeed, the radial part $\phi(r)$ of t_1 and of t_2 satisfy $\nabla^2_\perp \phi(r) \sim \rho(pr)$ where p is the transverse scale that fixes the width of ρ. Then, the slope of ϕ is $\phi' \sim 1/r \int_0^r r\rho dr \to 1/r$ as $r \to \infty$ because ρ is integrable by assumption. Since $\phi' \sim 1/r$ at large r it implies that $\phi \sim \log(pr)$.

The second step is to consider the quantity $J^{(2)}_{+-}$ from the right hand side of (4.6.2b) and in particular the term $\sim t_{1,x^+} t_{2,x^-}$. According to the previous statement the transverse part of this term grows as $t_{1,x^+} t_{2,x^-} \sim \log^2(pr)$ as $r \to \infty$. This term corresponds precisely to the components of the Riemann tensor, components, $R_{\pm\pm\mp\pm}$, that diverge as $r \to \infty$ (see discussion in section 4.3.3) when the two metrics are superimposed. The rest of the terms in $J^{(2)}_{+-}$ decay as $r \to \infty$.

The third step is to compute the Fourier transformation of $J^{(2)}_{+-}$ in order to apply (4.8.1). Evidently, such a Fourier transformation is not well defined because it suffers from an IR divergence at large r.

We thus conclude that using the perturbative expansion GE/b for such a geometrical configuration where the sources move with the speed of light in d=4 space-time dimensions is problematic when one attempts to compute the radiation of the any

[1] Which we define as the shock created by any positive, integrable rotational symmetric distribution $\rho(pr)$ which generalizes the point-like $\delta^{(2)}(r)$ distribution of the point-particle.

two gravitationally interacting sources. Since this statement applies for any physical transverse distribution, our conclusion is rather universal.

Relaxing one of the conditions could make the computation of the radiation feasible. For instance such a problematic behaviour for the Fourier transformation would not appear in higher dimensions[1] because the shocks at large distances fall of as $1/r^{d-4}$. Likewise, there are no issues appearing for particles moving with finite speed as the one's considered in [12; 34; 35; 36].

Another possibility to regulate the problem would be to put a sharp IR cut-off at some $r_{IR} = 1/p$ along the lines of section 4.3.3 and of equation (4.3.8). According to [37], the combined IR divergences arising from the quantum mechanical radiative corrections and from the classical Bremsstrahlung radiation are cancelled when a resummation procedure is performed. However, such a cancellation applies only for the collinear extremely soft photons and gravitons. It is thus unclear whether such a cancellation applies for our case.

Another related series of works to ours is found in [12; 34; 35; 36] where the authors study the radiation of massive particles that collide with an impact parameter. Their set-up allows them to take the massless limit provided the impact parameter is simultaneously taken to infinity. In this case, they find that the total radiated energy is zero. As we will see, this result is consistent with the example studied in section 4.8.2. It is pointed that the analysis of [12; 34; 35; 36] in the massless limit and finite impact parameter is rather inconclusive.

Our conclusions, methods and applicability region could be compared with the ones derived in [21; 23; 24; 25] where the authors consider a different avenue in organizing their perturbation scheme. They assume a strong and a weak shock and they expand along the light cone where the strong shock is located.

4.8.2 Example of radiation from gravitational waves

In this example, we consider the collision of gravitational waves which, by definition, correspond to a zero $T_{\mu\nu}$. For simplicity we consider homogeneous waves in the transverse direction[2]. It thus makes sense to compute the $E_{rad}/V_{x^1x^2}$ where $V_{x^1x^2}$ is the

[1] An attractive scenario would be a shock wave collision in the presence of extra dimensions along the lines of [33].

[2] One could argue that such shocks are a pure gauge. Indeed, when there is a single shock moving (say) along x^+, the transformation $x^+ \to x^+ + 1/2 \int t_1(x^-)dx^-$ removes the $t_1(x^-)(dx^-)^2$ component of the metric. However, when two shocks are superimposed such a transformation would not work in the forward light cone because there are mixing terms.

transverse volume. We expect that the total radiation will be zero as we collide zero energy shocks.

The only non trivial component of (4.6.2) is the (4.6.2b) component where only the last term in the right hand side remains. The second order solution is $g_{+-} = -1/4t_1(x^+)t_2(x^-)$ while $J^{(2)}_{+-} = 1/2t_{1,x^+}t_{2,x^-}$. The Fourier transformation of $J^{(2)}_{+-}(x^\mu)$ is $J^{(2)}_{+-}(k) \sim \delta^{(2)}(\mathbf{k}_\perp)$ where the proportionality constant depends on the details of the profile of $t_1(x^+)$ and $t_2(x^-)$.

The last step is to use (4.8.1) by contracting $J^{(2)}_{+-}(k)$ with $\epsilon^{+-}_{(i)} = -\frac{k_\perp^2}{2\sqrt{2}(k_\perp^2+1/2(k_+-k_-)^2)}$ for $i = I, II$ (see section 4.11) which, when the graviton is on shell, yields $\epsilon^{+-}_{(i)} = -\frac{k_\perp^2}{\sqrt{2}(k_++k_-)^2}$. Combining all the previous information and using (4.8.1) we finally obtain

$$E_{rad}/V_{x^1x^2} \sim E_{rad}/\delta^{(2)}(0) \sim \int dk_\perp k_\perp \frac{k_\perp^4\,\delta^{(2)}(\mathbf{k}_\perp)}{(k_+ + k_-)^4} = 0 \qquad (4.8.7)$$

where we used that the transverse volume is proportional to $\delta^{(2)}(0)$. Thus, we find that the total energy per transverse area radiated from gravitational waves is zero as expected.

In fact, it is not hard to argue that this is an all order result and hence an exact statement. The reason is that, since $J_{\mu\nu}$ in (4.8.1) has no transverse dependence, its Fourier transformation will be $\sim \delta^{(2)}(\mathbf{k}_\perp)$. Contracting then $J_{\mu\nu}(k)$ with any of the polarization tensors of (B5) and (B6) would yield zero because all the components are proportional to either k_1 or to k_2.

In order to make contact with [12; 34; 35; 36], one must consider the massless limit and in addition take the impact parameter to infinity. In this case, as already mentioned in last section, works [12; 34; 35; 36] yield a zero radiative energy. Likewise, if we start from the shocks (4.2.10) and take the $b \to \infty$ limit simultaneously with $p \to 0$ such that bp =fixed it implies that we collide the massless particles very far from each other while the IR cut-off is taken to zero[1].The resulting shocks when these two limits are taken correspond precisely into two transversally homogeneous gravitational waves with zero T_{++} and T_{--}. According to (4.8.7), these two waves radiate zero energy; exactly as in [12; 34; 35; 36].

4.9 Conclusions

We have studied the causal, purely gravitational, collision of two massless shockwaves, having a non-zero impact parameter taking into account back reactions following a

[1]The same occurs in [12; 34; 35; 36] where there is not an IR cut-off.

perturbative treatment. Our main conclusions as summarized as follows.

1. Our main computational result is the derivation of the second order corrections to the metric in the presence of an impact parameter b, taking into account the back-reaction. This has been presented in equation (4.7.8) and pictorially in fig. 4.6. Fig. 4.6 describes intuitively the manner which the metric evolves in time and how this evolution is in harmony with causality as it would be expected. In the $b = 0$ limit, equations (4.7.6), (4.7.7) and fig. 4.6 suggest a $\tau \leftrightarrow r$ symmetry. A similar symmetry has been observed in heavy ions in [26] and in [27] using different approaches.

2. In fact, it seems that the evolution of space-time soon after the collision is qualitatively similar as the situation with the expanding plasma in heavy ions in the following sense. During the first stages of the collision the plasma is thin in the longitudinal direction and due to the larger pressure, it has the tendency to expand and isotropize [38; 39]. Likewise, in the present set-up which, according to sec. 4.3.3 is an early times approximation, the metric is localized in the vicinity of $x^+ \sim x^- \sim 0$ due to the θ functions in equation (4.7.6). Another way to see the localization of the metric along the collision direction is from a trapped surface analysis perspective where the trapped surface at $t = 0^+$ is 2-dimensional [11; 28]. On the other hand, we expect that for sufficiently large energy, the final product will be a (spherically symmetric) Schwarzschild black hole showing that the produced metric will eventually isotropize, just like the produced medium in heavy ions.

3. For zero impact parameter, the perturbative treatment and consequently our approximation breaks down, since our expansion parameter, $\frac{EG}{b}$, diverges. When the impact parameter b is zero, the energy momentum tensor is no longer conserved and thus the Bianchi identities are also violated. We believe that this is a sign of non-perturbative effects that start to become dominant and that a perturbative treatment is no longer justified in this regime. It is pointed out that such a violation is point-like in space and instantaneous in time and is hidden behind a horizon that forms after the collision (see [11]).

4. We have shown that the trace of the energy momentum tensor is zero, not only up to first order (negative times), but also for up to second order (after the collision). This indicates that the energy momentum tensor could be traceless up to all orders, suggesting a sort of conservation of tracelessness: one starts with

a traceless energy momentum tenor at some initial time and this tracelessness continues to apply all the way during the time evolution. It is an interesting speculation which, certainly should be given further attention.

5. Our approach is perturbative and the region where it is valid is discussed in section 4.3.3. The discussion in that section extends beyond the analytical predictability of our perturbative approach. In particular, we guess that the equilibration time for a black hole to be formed at high energies must be given by $t_{eq} \sim EG$ which is the only available scale either in the $b = 0$ or in the $b \ll EG$ limit. This might seem counter-intuitive in the sense that in high energies one would expect things to be developed faster: for instance in [40], increasing the boost factor results in decreasing t_{eq}[1]. We argue that the set-up we have is different in the sense that the boost factor in our case is always infinite. We argue that by increasing the energy more, the process becomes more violent and it takes more time to equilibrate. Definitely, the numerical relativity approach which, unfortunately has limitations in taking large values of the boost-factor, is the most reliable avenue to explore such a question.

6. The estimation of the the gravitationally radiated energy with respect to the energy, E, and the impact parameter, b is discussed. As noted, positive energy transverse distributions create shocks with a universal behaviour: at large distances from the center of these sources, the shocks grow logarithmically instead of decaying. This implies that such shocks interact strongly for an infinite portion of space and this, in the present approach, would produce infinite radiation. We propose ways to regulate this issue and we show that this is a fact of fast moving, everywhere positive definite, transverse distributions in d=4 space-time dimensions. By relaxing one of these conditions, for example considering zero energy gravitational waves, we are able to compute the radiation. In this example we find that the total radiation produced is zero. We argued that such a result applies to all orders as it would be expected by conservation considerations.

7. We showed in section 4.10 that for dilute enough transverse distributions of the energy, a black hole can not be formed during head-on collisions. Equivalently, a black hole is formed when transversally-extended distributions are collided head-on only if the collision energy is sufficiently large compared to the width of the

[1]We thank F. Pretorious for a private communication on this issue and for discussing [40]. The set up used in [40] involves the gravitational collision coupled to a perfect fluid rather to point-like particles.

distributions. In other words, dense enough distributions are required in order to form a black hole and our analysis makes quantifies this statement

4.10 Trapped Surfaces from Extended Sources

In this section, we study the behaviour of shockwave collisions arising from extended sources on the transverse plane. This investigation has been carried out in great detail in [28] (see also [7]) where the author has generalized the investigation to any extended sources satisfying reasonably physical and quite mild constrains and for both, flat and *AdS* backgrounds[1].

Here, using a simple model, we show that when extended sources on the transverse plane are collided at zero impact parameter, two trapped surfaces (a small and a large one) are obtained for sufficiently large energy[2].

In order to see this, we replace the delta function localized matter distribution with an extended one and in particular we consider a transversally symmetric distribution ρ. Hence, we assume a $T_{++} \sim E\rho(kx_\perp)\delta(x^+)$ where $x_\perp^2 = (x^1)^2 + (x^2)^2$ and where k fixes the width of ρ which can be energy (E) depended or energy independent. The stress-tensor can be normalized such that when T_{++} is integrated to yield E. The corresponding transverse part, denoted by ϕ, of the shock satisfies $\nabla_\perp^2 \phi = \rho$. This yields

$$\phi \sim EG \int_0^r dr \left(\frac{\int_0^{r'} dr'' r'' \rho(r'')}{r'} \right). \tag{4.10.1}$$

The trapped surface consists of two pieces, S_+ and S_-. These are parametrized with the help of two functions, ψ_+ and ψ_-[3] which satisfy the following differential equation

$$\nabla_\perp^2 (\psi_\pm - \phi_\pm) = 0. \tag{4.10.2}$$

It is pointed out that $\nabla_\perp^2 \phi_\pm$ provides a source term for $\nabla_\perp^2 \psi_\pm$. The missing ingredient is the boundary conditions. Dropping the indices $\pm$ from $\psi_\pm$ from now on assuming a zero impact parameter and identical shocks we have $\psi_+ = \psi_- = \psi$. The boundary conditions then read

$$\psi\Big|_C = 0 \qquad \sum_{i=1,2} [\nabla_{x^i}\psi \nabla_{x^i}\psi]\Big|_C = 8 \tag{4.10.3}$$

[1] For AdS backgrounds on trapped surfaces there have been many interesting works including [32; 41; 42; 43]

[2] We thank G. Veneziano for a relevant discussion.

[3] For details we refer the reader to the appendices of [33; 44].

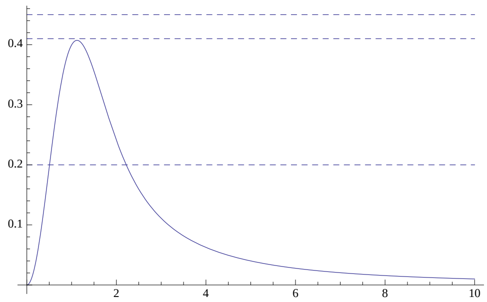

Figure 4.7: The function $\left((e^{-y^2}-1)/y\right)^2$ as a function of $y \equiv kx_\perp$.

for some curve C which defines the boundary of the trapped surface and where both, $S_+ = S$ and $S_- = S$ end.

The function ψ satisfying the left boundary condition in (4.10.3) is given by $\psi(x_\perp) = \phi(x_\perp) - \phi(x_\perp^c)$ which vanishes on the trapped surface defined by $x_\perp = x_\perp^c$. Imposing the right condition, allows one to specify $x_\perp^c$ in terms of the parameters of the problem, namely EG and k. Thus from $(\psi'(x_\perp))^2 \sim 1$ one obtains

$$(\psi'(x_\perp^c))^2 = (\phi'(x_\perp^c))^2 \sim 1 => \frac{\int_0^{y_c} dry\rho(y)}{y_c} \sim \frac{1}{EkG},\ y \equiv kx_\perp. \tag{4.10.4}$$

The last equation provides the condition of a trapped surface from colliding extended sources: for a given energy E and a transverse width k, a trapped surface exists if there is a y_c such that (4.10.4) has a solution. Taking for concreteness a Gaussian distribution $\rho = k^2 e^{-x_\perp^2 k^2}$ equation (4.10.4) yields

$$\left(\frac{e^{-k^2 x_\perp^2} - 1}{kx_\perp}\right)^2 \sim \left(\frac{1}{EkG}\right)^2 \Big|_{x_\perp = x_\perp^c}. \tag{4.10.5}$$

A few remarks are in order.

- The function $\left((e^{-y^2}-1)/y\right)^2$ for positive y becomes zero at $y=0$ and $y=\infty$ and is strictly positive with a maximum at $y \approx 1.12$ (see figure 4.7).
- The previous statement implies that for a given sufficiently large energy E there is a small trapped horizon and a large trapped horizon. In addition, according to figure 4.7, there is a critical value of the quantity EkG such that the small and the large apparent horizons merge. Finally, for smaller values of the quantity EkG, the trapped surface can not exist (see top dashed line in the figure). This implies that for small energies or for large widths (small k's; very dilute matter) the trapped surface can not be formed. This is an expected result.

- The full classification of all the distributions ρ and the kind of surfaces that they create has been performed in [28]. Here we briefly mention the basic features for completeness. There are three classes of trapped surfaces: (a) The ones created for energy no matter how small it is (k is assumed fixed). (b) Trapped surfaces with a single trapped horizon which are created only for sufficiently large energies. (c) Trapped surfaces with two trapped horizons which are created only for sufficiently large energies (see for example fig. 4.7). In all the cases, the shocks grow logarithmically at infinity while in the high energy limit $EkG \gg 1$, the entropy grows as $S_{trap} \sim E^2 G$. Such a growth applies for any distribution ρ and hence the result is universal.

4.11 Polarization tensors

We now proceed to derive the polarization tensors. There are two such tensors, $\epsilon^{\mu\nu}_{(1)}$ and $\epsilon^{\mu\nu}_{(2)}$. It is necessary to define two space-like unit vectors, e_1^M and e_2^M, that are both perpendicular among themselves and to the wave vector of the radiated gravitational radiation, k^μ, before one can derive the polarization tensors. These vectors satisfy the following relations

$$e^\mu_\alpha e_{\beta\mu} = \delta_{\alpha\beta} \qquad , \qquad e^\mu_\alpha k_\mu = 0\,. \tag{B1}$$

The two vectors explicitly written in light-cone coordinates read

$$e_1^\mu = \left(-\frac{k_\perp}{\sqrt{2}|\vec{k}|}, \frac{k_\perp}{\sqrt{2}|\vec{k}|}, \frac{k_1\,(k_+ - k_-)}{\sqrt{2}k_\perp|\vec{k}|}, \frac{k_2\,(k_+ - k_-)}{\sqrt{2}k_\perp|\vec{k}|}\right) \quad , \quad e_2^\mu \;=\left(0, 0, -\frac{k_2}{k_\perp}, \frac{k_1}{k_\perp}\right) \,, \tag{B2}$$

where we have defined $\vec{k} \equiv \left(k_1, k_2, \frac{k_+ - k_-}{\sqrt{2}}\right)$.

We can now proceed to construct the two polarization tensors. They should, by construction, be orthogonal to each other and traceless, i.e. satisfy the following relations

$$\eta_{\mu\nu}\epsilon_a^{\mu\nu} = 0 \qquad , \qquad \epsilon_a^{\mu\nu}\epsilon_{b\mu\nu} = \delta_{ab} \tag{B3}$$

One can easily see that the two polarization tensors can be written in terms of the polarization vectors as,

$$\epsilon^{\mu\nu}_{(I)} = \frac{e_1^\mu e_1^\nu + e_2^\mu e_2^\nu}{\sqrt{2}} \qquad , \qquad \epsilon^{\mu\nu}_{(II)} = \frac{e_1^\mu e_1^\nu - e_2^\mu e_2^\nu}{\sqrt{2}}\,. \tag{B4}$$

Writing the explicit form of the two tensors, we have

$$\epsilon^{\mu\nu}_{(I)} = \frac{1}{2\sqrt{2}|\vec{k}|^2} \begin{pmatrix} k_\perp^2 & -k_\perp^2 & k_1\left(k_- - k_+\right) & k_2\left(k_- - k_+\right) \\ -k_\perp^2 & k_\perp^2 & k_1\left(k_+ - k_-\right) & k_2\left(k_+ - k_-\right) \\ k_1\left(k_- - k_+\right) & k_1\left(k_+ - k_-\right) & 2k_2^2 + \left(k_+ - k_-\right)^2 & -2k_1k_2 \\ k_2\left(k_- - k_+\right) & k_2\left(k_+ - k_-\right) & -2k_1k_2 & 2k_1^2 + \left(k_+ - k_-\right)^2 \end{pmatrix}, \quad \text{(B5)}$$

$$\epsilon^{\mu\nu}_{(II)} = \frac{1}{2\sqrt{2}|\vec{k}|^2} \begin{pmatrix} k_\perp^2 & -k_\perp^2 & k_1\left(k_- - k_+\right) & k_2\left(k_- - k_+\right) \\ -k_\perp^2 & k_\perp^2 & k_1\left(k + -k_-\right) & k_2\left(k_+ - k_-\right) \\ k_1\left(k_- - k_+\right) & k_1\left(k + -k_-\right) & -\frac{2k_2^2|\vec{k}|^2 + k_1^2(k_+ - k_-)^2}{k_\perp^2} & \frac{2k_1k_2\left(k_\perp^2 + (k_+ - k_-)^2\right)}{k_\perp^2} \\ k_2\left(k_- - k_+\right) & k_2\left(k_+ - k_-\right) & \frac{2k_1k_2\left(k_\perp^2 + (k_+ - k_-)^2\right)}{k_\perp^2} & -\frac{2k_1^2|\vec{k}|^2 + k_2^2(k_+ - k_-)^2}{k_\perp^2} \end{pmatrix}. \quad \text{(B6)}$$

Bibliography

[1] P. C. Aichelburg and R. U. Sexl. On the Gravitational field of a massless particle. *Gen. Rel. Grav.*, 2:303–312, 1971. 128, 131

[2] P.D. D'Eath. High Speed Black Hole Encounters and Gravitational Radiation. *Phys.Rev.*, D18:990, 1978. 128

[3] P. D. D'Eath and P. N. Payne. Gravitational radiation in high speed black hole collisions. 1. Perturbation treatment of the axisymmetric speed of light collision. *Phys. Rev.*, D46:658–674, 1992. 128

[4] P. D. D'Eath and P. N. Payne. Gravitational radiation in high speed black hole collisions. 2. Reduction to two independent variables and calculation of the second order news function. *Phys. Rev.*, D46:675–693, 1992. 128

[5] P. D. D'Eath and P. N. Payne. Gravitational radiation in high speed black hole collisions. 3. Results and conclusions. *Phys. Rev.*, D46:694–701, 1992. 128

[6] D. Amati, M. Ciafaloni, and G. Veneziano. Effective action and all order gravitational eikonal at Planckian energies. *Nucl.Phys.*, B403:707–724, 1993. 128

[7] Emmanuel Kohlprath and Gabriele Veneziano. Black holes from high-energy beam-beam collisions. *JHEP*, 0206:057, 2002. 128, 152

[8] D. Amati, M. Ciafaloni, and G. Veneziano. Towards an S-matrix description of gravitational collapse. *JHEP*, 0802:049, 2008. 128

[9] G. Veneziano and J. Wosiek. Exploring an S-matrix for gravitational collapse. II. A Momentum space analysis. *JHEP*, 0809:024, 2008. 128

[10] M. Ciafaloni and D. Colferai. S-matrix and Quantum Tunneling in Gravitational Collapse. *JHEP*, 0811:047, 2008. 128

[11] Douglas M. Eardley and Steven B. Giddings. Classical black hole production in high-energy collisions. *Phys. Rev.*, D66:044011, 2002. 128, 140, 150

[12] Dmitri V. Gal'tsov, Georgios Kofinas, Pavel Spirin, and Theodore N. Tomaras. Transplanckian bremsstrahlung and black hole production. *Phys.Lett.*, B683:331–334, 2010. 128, 146, 148, 149

[13] Marco O. P. Sampaio. Radiation from a D-dimensional collision of shock waves: numerical methods. 2013. 128

[14] Jorge Casalderrey-Solana, Michal P. Heller, David Mateos, and Wilke van der Schee. From full stopping to transparency in a holographic model of heavy ion collisions. 2013. 128

[15] Paul Romatschke and J. Drew Hogg. Pre-Equilibrium Radial Flow from Central Shock-Wave Collisions in AdS5. 2013. 128

[16] Oliver DeWolfe, Steven S. Gubser, Christopher Rosen, and Derek Teaney. Heavy ions and string theory. 2013. 128

[17] Bin Wu. On holographic thermalization and gravitational collapse of tachyonic scalar fields. 2013. 128

[18] Bin Wu. On holographic thermalization and gravitational collapse of massless scalar fields. *JHEP*, 1210:133, 2012. 128

[19] Daniel Grumiller and Paul Romatschke. On the collision of two shock waves in AdS5. *JHEP*, 08:027, 2008. 128

[20] Bin Wu and Paul Romatschke. Shock wave collisions in AdS5: approximate numerical solutions. *Int.J.Mod.Phys.*, C22:1317–1342, 2011. 128

[21] F.S. Coelho, C. Herdeiro, C. Rebelo, and M.O.P. Sampaio. Radiation from a D-dimensional collision of shock waves: an insight allowed by the D parameter. 2013. 128, 148

[22] Wilke van der Schee, Paul Romatschke, and Scott Pratt. A fully dynamical simulation of central nuclear collisions. 2013. 128

[23] Flavio S. Coelho, Carlos Herdeiro, Carmen Rebelo, and Marco Sampaio. Radiation from a D-dimensional collision of shock waves: higher order set up and perturbation theory validity. *Phys.Rev.*, D87:084034, 2012. 128, 148

[24] Flavio S. Coelho, Carlos Herdeiro, and Marco O.P. Sampaio. Radiation from a D-dimensional collision of shock waves: a remarkably simple fit formula. *Phys.Rev.Lett.*, 108:181102, 2012. 128, 148

[25] Carlos Herdeiro, Marco O.P. Sampaio, and Carmen Rebelo. Radiation from a D-dimensional collision of shock waves: First order perturbation theory. *JHEP*, 1107:121, 2011. 128, 148

[26] Anastasios Taliotis. Heavy Ion Collisions with Transverse Dynamics from Evolving AdS Geometries. *JHEP*, 09:102, 2010. 129, 136, 143, 144, 150

[27] Steven S. Gubser. Symmetry constraints on generalizations of Bjorken flow. 2010. 129, 150

[28] Anastasios Taliotis. Extra dimensions, black holes and fireballs at the LHC. *JHEP*, 1305:034, 2013. 129, 140, 150, 152, 154

[29] Javier L. Albacete, Yuri V. Kovchegov, and Anastasios Taliotis. Asymmetric Collision of Two Shock Waves in AdS_5. *JHEP*, 05:060, 2009. 133, 139

[30] Javier L. Albacete, Yuri V. Kovchegov, and Anastasios Taliotis. Modeling Heavy Ion Collisions in AdS/CFT. *JHEP*, 07:100, 2008. 133, 139

[31] A. Papapetrou. Lectures on General Relativity. *D. Reidel Publishing Company*, First Edition, 1974. 136

[32] Yuri V. Kovchegov and Shu Lin. Toward Thermalization in Heavy Ion Collisions at Strong Coupling. *JHEP*, 03:057, 2010. 139, 152

[33] Anastasios Taliotis. Black Topologies Production in Extra Dimensions. 2012. 148, 152

[34] Yiannis Constantinou, Dmitry Gal'tsov, Pavel Spirin, and Theodore N. Tomaras. Scalar Bremsstrahlung in Gravity-Mediated Ultrarelativistic Collisions. *JHEP*, 1111:118, 2011. 26 pages, 7 figures. 148, 149

[35] Dmitry V. Galtsov, Georgios Kofinas, Pavel Spirin, and Theodore N. Tomaras. Classical ultrarelativistic bremsstrahlung in extra dimensions. *JHEP*, 1005:055, 2010. 148, 149

[36] Dmitry Gal'tsov, Pavel Spirin, and Theodore N. Tomaras. Gravitational bremsstrahlung in ultra-planckian collisions. *JHEP*, 1301:087, 2013. 148, 149

[37] Steven Weinberg. Infrared photons and gravitons. *Phys.Rev.*, 140:B516–B524, 1965. 148

[38] Yuri V. Kovchegov. Can thermalization in heavy ion collisions be described by QCD diagrams? *Nucl. Phys.*, A762:298–325, 2005. 150

[39] Yuri V. Kovchegov. Isotropization and thermalization in heavy ion collisions. *Nucl. Phys.*, A774:869–872, 2006. 150

[40] William E. East and Frans Pretorius. Ultrarelativistic black hole formation. *Phys.Rev.Lett.*, 110:101101, 2013. 151

[41] Steven S. Gubser, Silviu S. Pufu, and Amos Yarom. Entropy production in collisions of gravitational shock waves and of heavy ions. *Phys. Rev.*, D78:066014, 2008. 152

[42] I.Y. Arefeva, A.A. Bagrov, and E.O. Pozdeeva. Holographic phase diagram of quark-gluon plasma formed in heavy-ions collisions. *JHEP*, 1205:117, 2012. 152

[43] Alvaro Duenas-Vidal and Miguel A. Vazquez-Mozo. Noncentral collisions of Reissner-Nordstróm Shock Gravitational Waves in AdS. 2012. 152

[44] Elias Kiritsis and Anastasios Taliotis. Multiplicities from black-hole formation in heavy-ion collisions. 2011. 152

List of Figures

List of Tables